

**A VALUE PROPOSITION FOR LUNAR ARCHITECTURES
UTILIZING ON-ORBIT PROPELLANT REFUELING**

By

James Jay Young

In Partial Fulfillment
of the Requirements for the Degree of
Doctor of Philosophy in the
School of Aerospace Engineering

Georgia Institute of Technology

May 2009

Copyright © 2009 by James J. Young

A VALUE PROPOSITION FOR LUNAR ARCHITECTURES
UTILIZING ON-ORBIT PROPELLANT REFUELING

Approved by:

Dr. Alan W. Wilhite, Chairman
School of Aerospace Engineering
Georgia Institute of Technology

Dr. Douglas Stanley
School of Aerospace Engineering
Georgia Institute of Technology

Dr. Trina M. Chytka
Vehicle Analysis Branch
NASA Langley Research Center

Dr. Daniel P. Schrage
School of Aerospace Engineering
Georgia Institute of Technology

Dr. Carlee A. Bishop
Electronics Systems Laboratory
Georgia Tech Research Institute

Date Approved: October 29, 2008

ACKNOWLEDGEMENTS

As I sit down to acknowledge all the people who have helped me throughout my career as a student I realized that I could spend pages thanking everyone. I may never have reached all of my goals without your endless support. I would like to thank all of you for helping me achieve my goals. I would like to specifically thank my thesis advisor, Dr. Alan Wilhite, for his guidance throughout this process. I would also like to thank my committee members, Dr. Carlee Bishop, Dr. Trina Chytka, Dr. Daniel Scharge, and Dr. Douglas Stanley for the time they dedicated to helping me complete my dissertation. I would also like to thank Dr. John Olds for his guidance during my first two years at Georgia Tech and introducing me to the conceptual design field.

I must also thank all of the current and former students of the Space Systems Design Laboratory for helping me overcome any technical challenges that I encountered during my research. I would especially like to thank Bob Thompson for the hours he spent editing and reviewing drafts of my dissertation and Dr. Robert Braun and Dr. Joseph Saleh for mentoring me throughout my time at Georgia Tech.

Finally, I would like to thank my family for supporting me and encouraging me to strive for the best and to reach a future that I never thought possible, my grandparents for always pushing me and my sisters for their loving support. I especially want to thank my future wife, Michelle Kassner, for always being there for me and keeping me focused no matter how stressful and difficult life became. We have both completed our Ph.Ds and will be moving on with the rest of our lives together. Michelle I love you xx.

TABLE OF CONTENTS

ACKNOWLEDGEMENTS	IV
LIST OF TABLES	VIII
LIST OF FIGURES	X
NOMENCLATURE.....	XIV
SUMMARY	XVII
CHAPTER 1 INTRODUCTION	1
1.1 Motivation	1
1.1.1 NASA’s Shift in Design Strategies.....	2
1.1.2 A Summary of the Exploration Systems Architecture Study.....	4
1.2 Problem Statement.....	8
1.2.1 Introduction of Propellant Re-fueling as a Potential Solution	9
1.2.2 Understanding the Potential Value of Propellant Re-fueling	14
1.3 Research Objectives and Goals	16
1.4 Dissertation Overview	18
CHAPTER 2 BACKGROUND.....	21
2.1 Summary of ESAS Baseline Architecture	21
2.1.1 Baseline Lunar Concept of Operations.....	22
2.1.2 Cargo Launch Vehicle Summary.....	23
2.1.3 Lunar Surface Access Module (LSAM) Summary.....	25
2.1.4 Crew Launch Vehicle Summary.....	27
2.1.5 Crew Exploration Vehicle (CEV) Summary	30
2.2 Previous Propellant Refueling Design Studies	32
2.2.1 Propellant Refueling in Exploration Missions.....	33
2.2.2 Apollo Lunar Architecture	34
2.2.3 Refueling with Current Space Transportation System.....	37
2.2.4 Refueling with Reusable Launch Vehicles	38
2.2.5 Refueling in Destination Orbit for Return Maneuvers.....	41
2.2.6 Refueling with NASA Baseline Architecture	43
2.2.7 NASA’s Refueling Studies.....	45
2.2.8 Summary of Refueling Design Studies.....	47
2.3 Current Propellant Refueling Technology Development	50
2.3.1 In-space Propellant Transfer Technologies	51
2.3.2 Long Term Propellant Boiloff Mitigation Techniques	54
2.4 Commercial Launch Industry	57
2.4.1 Delta Family of Vehicles.....	58
2.4.2 Atlas Family of Vehicles	59
2.4.3 Orbital Sciences’ Family of Vehicles	60
2.5 International Commercial Launch Industry.....	60
2.5.1 Ariane Launch Vehicles	61
2.5.2 Russian Launch Vehicles	62
2.5.3 Asian Launch Vehicles.....	62
2.5.4 US Responsive Launch Vehicles.....	63
2.5.5 NASA Exploration Architecture Elements.....	64
2.5.6 Range of \$/LB Considered for Propellant Refueling Study.....	65
CHAPTER 3 PROPELLANT REFUELING DESIGN SPACE	70
3.1 Propellant Refueling Evaluation Methodology	70
3.2 Propellant Refueling Design Space	73

3.2.1	Additional Ascent Propellant.....	75
3.2.2	Boiloff Thermal Management System.....	76
3.2.3	LSAM Stage Re-fueled	77
3.2.4	Lander Propellant Quantity Re-fueled.....	79
3.2.5	LSAM Ascent Engine	79
3.2.6	LOI Maneuver.....	81
3.2.7	LEO Required Stay Time	82
3.2.8	Re-fuel Boiloff	83
3.2.9	TLI Propellant Offloaded from EDS, Scenario Two Only	84
CHAPTER 4 PROPELLANT REFUELING ANALYSIS AND SIMULATION ENVIRONMENT.....		87
4.1	Modeling and Simulation Environment.....	87
4.1.1	Launch Vehicle (CaLV) Model.....	91
4.1.2	Lunar Lander (LSAM) Model	104
4.1.3	Propellant Refueling Model.....	109
4.1.4	Life Cycle Cost Model	114
4.1.5	Reliability Model.....	126
4.1.6	Technology Risk Model	129
4.2	Validation of baseline Models	130
4.2.1	Cargo Launch Vehicle.....	131
4.2.2	Lunar Surface Access Module.....	133
CHAPTER 5 A PARETO FRONTIER FOR LUNAR SURFACE PAYLOAD CAPABILITY AND LIFE CYCLE COST: SCENARIO ONE		135
5.1	The Identifications of Non Dominated Solutions	136
5.1.1	Developing the Pareto Frontier.....	136
5.2	Baseline Improvements for Non Propellant Refueling Options	141
5.3	Design Trends in Non-Dominated Solutions.....	149
5.4	Cost per Pound of Delivering Payload to the Lunar Surface	165
5.5	Assumptions Affecting the Design Points Along the Frontier	172
5.5.1	The Effect of an Uncertain Propellant Price on the Pareto Frontier	173
5.5.2	The Effect of Launch Uncertainty on the Pareto Frontier.....	176
5.6	Summary of Non-Dominated Solutions	180
CHAPTER 6 A PARETO FRONTIER FOR LEO PAYLOAD CAPABILITY AND LIFE CYCLE COST: SCENARIO TWO		182
6.1	Development of a Pareto Frontier for Scenario Two.....	183
6.2	Design Trends in the Non Dominated Solutions	186
6.2.1	Design Points In Group Three	187
6.2.2	Design Points In Group Two	188
6.2.3	Design Points In Group One.....	191
6.3	Effect of Propellant Price on the Pareto frontier.....	195
6.4	Exploration of the Design Space Within the Frontier.....	201
6.5	Cost per Pound of Delivering Payload to LEO.....	206
6.6	Summary of Scenario Two Results	208
CHAPTER 7 VALUE PROPOSITION FOR PROPELLANT REFUELING		209
7.1	NASA's Propellant Refueling Value Proposition	209
7.1.1	Improvement in Architecture Capability	210
7.1.2	Reduction in Architecture Campaign Costs.....	221
7.1.3	Reduction in Architecture Development and Operational Risk.....	231
7.1.4	Improvement in Architecture Extensibility	243
7.2	Estimating the Value as the Total Effect on Life Cycle Cost	249
7.2.1	Life Cycle Cost Value for Mass Mitigation.....	250
7.2.2	Life Cycle Cost Value for Refueling Propellant Lost to Boiloff	255
7.2.3	Life Cycle Cost Value for an Increase in Payload Capability.....	257

7.2.4	Life Cycle Cost Value for Increasing Extensibility	259
7.3	The Value Proposition of Propellant Refueling for NASA	263
7.3.1	Increased Low Earth Orbit Payload Capability	264
7.3.2	Increased Lunar Surface Payload Capability	266
7.3.3	Decoupling Mission Reliability from Propellant Boiloff.....	269
7.3.4	Increasing the Functionality of the Earth Departure Stage	270
7.3.5	Decreasing the Size of the Architecture Elements.....	271
7.3.6	Summary of NASA Value Proposition.....	273
CHAPTER 8 CONCLUSIONS AND FUTURE WORK		274
8.1	Goals of the Dissertation	274
8.2	Hypotheses Discussed in this Dissertation	281
8.3	Contributions	283
APPENDIX A		285
APPENDIX B		286
APPENDIX C		293
REFERENCES.....		294

LIST OF TABLES

Table 1: CaLV Propulsion System Summary	24
Table 2: Comparison of Vehicle Concepts Considered.....	47
Table 3: Delta Family Launch Vehicle Summary].....	58
Table 4: Atlas V Launch Vehicle Summary [29]	59
Table 5: Orbital Sciences Launch Vehicle Summary [29]	60
Table 6: Ariane Family Launch Vehicle Summary [29]	61
Table 7: Russian Launch Vehicle Summary [29].....	62
Table 8: Asian Launch Vehicle Summary [29]	63
Table 9: Responsive Space Launch Vehicles	64
Table 10: Cargo Launch Vehicle Delivery Capability	65
Table 11: Summary of Potential Launch Vehicles	68
Table 12: CaLV Fairing Mass Estimates	78
Table 13: Summary of Ascent Engine Assumptions	81
Table 14: LSAM and EDS Propellant Boiloff Comparison	83
Table 15: Change in CaLV Dimensions as TLI Propellant is Offloaded	85
Table 16: Offloading LOX versus LH2	86
Table 17: Summary of Variables Passed Between Analyses.....	89
Table 18: Case 1 from the Morphological Matrix	90
Table 19: Summary of the Variables Passed between Analyses	92
Table 20: CaLV Reference Areas	94
Table 21: Cargo Launch Vehicle Mass Comparison	102
Table 22: Cargo Launch Vehicle Mass Comparison, Scenario 2	103
Table 23: LSAM Propellant Boiloff Comparison.....	105
Table 24. Summary of Ascent Engine Assumptions	106
Table 25. Lunar Lander Delta-V Table [ESAS, pg. 165]	106
Table 26: Lunar Surface Access Module Mass Comparison.....	109
Table 27. Summary of Depot Sizes for Various Propellant Mass	113
Table 28. Summary of System Acquisition Costs	116
Table 29. Summary and Description of NAFCOM Wraps.....	119

Table 30. Baseline Architecture Cost Summary.....	120
Table 31. Summary of Development Risk Assessment.....	130
Table 32. Summary of Trajectory Analysis.....	133
Table 33: Improvements in Baseline Design without Propellant of Refueling	143
Table 34: LSAM Ascent Stage Engine Complexity Factors	148
Table 35: Scenario One, Non-Dominated Solution Description, Points 1 - 14.....	153
Table 36: Scenario One, Non-Dominated Solution Description, Points 15- 27	154
Table 37: Description of the Changes between the Five Groups.....	164
Table 38: Summary of Pareto Frontier Changes as Propellant Price Increases.....	175
Table 39: Change in LCC with a Change in Launch Separation.....	179
Table 40: Relative Improvement in Groups 2 Design Points	189
Table 41: Summary of Pareto Frontier, Groups Two and Three	190
Table 42: Summary of Pareto Frontier, Group One	194
Table 43: Description of Changes between Groups	208
Table 44: Lunar Surface Payload Capability	211
Table 45: Lunar Surface Payload Capability for an Increase in the Ascent Burn	220
Table 46: Cost Values for Baseline Exploration Architecture.....	224
Table 47: Apollo Propellant Refueling Reliability []	232
Table 48: Comparative Cost for Mars Mission.....	247
Table 49: Summary of Propellant Refueling Value.....	273
Table 50: Summary of Preferred Refueling Strategies	279
Table 51: Lift Coefficients, without Solid Rocket Boosters.....	285
Table 52: Drag Coefficients, without Solid Rocket Boosters.....	285
Table 53: Drag Coefficients, with Solid Rocket Boosters	286
Table 54: Drag Coefficients, with Solid Rocket Boosters	286
Table 55: Lunar Architecture Reliability Estimation.....	293

LIST OF FIGURES

Figure 1: Historical NASA Budget and Percentage of Federal Budget [2].....	3
Figure 2: ESAS Baseline Lunar Architecture [6]	8
Figure 3: ESAS Baseline Lunar Architecture Concept of Operations.....	23
Figure 4: ESAS Baseline Launch Vehicles	29
Figure 5: ESAS Baseline Lunar Surface Access Module.....	29
Figure 6: ESAS Baseline CEV	31
Figure 7: Typical Lunar Concept of Operations	34
Figure 8: Apollo EOR Mission Mode]	35
Figure 9: Lunar Transportation System Options	39
Figure 10: Lunar Surface Payload using OOS and Return Depots.....	42
Figure 11: Cryogenic Fluid Management Key Concepts	51
Figure 12: Linear Acceleration Fluid Transfer Technique [24].....	53
Figure 13: Boiloff Management Concept Schematics [26]	56
Figure 14: Summary of \$/lb as a Function of Payload Capability.....	66
Figure 15: Summary of Demonstrated Reliability as a Function of \$/lb.....	67
Figure 16: Propellant Refueling Evaluation Methodology.....	72
Figure 17: Trade Study Morphological Matrix, Scenario One	74
Figure 18: Trade Study Morphological Matrix, Scenario Two	75
Figure 19. Lunar Architecture Simulation Environment	88
Figure 20. General Launch Vehicle Design Structure Matrix	92
Figure 21. Procedural Flow Chart for the Trajectory Meta-Model	95
Figure 22. Final CaLV Design Structure Matrix	97
Figure 23. Trajectory Meta-Model for CaLV 1 st Stage	97
Figure 24. Trajectory Meta-Model for the EDS	98
Figure 25. Additional EDS Propellant Meta-Model.....	100
Figure 26. Trajectory Comparison for Scenarios One and Two.....	100
Figure 27. LSAM Design Structure Matrix	104
Figure 28: LSAM Mass Sizing Flow Chart	108
Figure 29. Mass Sizing for LEO Propellant Depot.....	110

Figure 30. Depot Delivery Fairing Comparison	111
Figure 31. Notional Propellant Refueling Depot	113
Figure 32: Breakdown of Life Cycle Cost.....	115
Figure 33. Life Cycle Cost Analysis Flow of Information	124
Figure 34. Life Cycle Cost Spreading for Baseline Architecture	125
Figure 35. Reliability Model Fault Tree Analysis Structure.....	127
Figure 36: CaLV Altitude and Velocity Profile Comparison	132
Figure 37: CaLV Acceleration and Dynamic Pressure Profile Comparison	132
Figure 38: Trade Study Morphological Matrix.....	137
Figure 39: Pareto Frontier Creation Flow Chart	138
Figure 40: All Design Point with Fairing Constraint Applied.....	139
Figure 41: LSAM Volume Constraint Dimensions	140
Figure 42: Path for Establishing the Set of Non-Dominated Solutions, Scenario One ..	141
Figure 43: Improvements in Baseline Architecture	142
Figure 44: Total Mass of the Potential Thermal Management Systems	144
Figure 45: Loss of Mission effect on LCC	145
Figure 46: Engine Performance Values and Payload Capability.....	147
Figure 47: Propellant Refueling Pareto Frontier Groups	150
Figure 48: Total Thermal Management System Mass	152
Figure 49: Ascent Engine and Lander Refueling Pattern	156
Figure 50: Change in Payload for Difference Engine Performance Parameters	158
Figure 51: LSAM Gross Mass as a Function of Lunar Surface Payload.....	160
Figure 52: Change in Payload Capability as the Ascent Propellant is Increased	161
Figure 53: Effect of Propellant Refueling on Payload Capability, LCC and \$/lb	166
Figure 54: Regions of Different Rate of Change in the \$/lb.....	168
Figure 55: Effect of Propellant Refueling on Total Payload Capability.....	170
Figure 56: Marginal Cost of Increasing the Lunar Surface Payload	171
Figure 57: Changes to the Pareto Frontier with Increases in Propellant Cost	174
Figure 58: Effect of a Lower Launch Separation on Mission Success	176
Figure 59: Sensitivity to Assumptions in LEO Boiloff Refueling.....	178
Figure 60: Design Space Morphological Matrix, Scenario Two	184

Figure 61: Pareto Frontier and Design Points for Scenario Two.....	185
Figure 62: Scenario Two Pareto frontier Groups.....	187
Figure 63: The Effect of a Change in Propellant Price on the Pareto frontier.....	196
Figure 64: Propellant Price for the Elimination of Group One from the Frontier	197
Figure 65: The Effect on Group One of a Change in Propellant Price	198
Figure 66: The Effect on Group Two of a Change in Propellant Price	201
Figure 67: Lunar Orbit Injection Maneuver Breakdown	203
Figure 68: LEO Propellant Boiloff Refueling Breakdown	204
Figure 69: Breakdown of EDS Propellant Removal.....	205
Figure 70: Effect of Propellant Refueling on Payload Capability, LCC and \$/lb	206
Figure 71: Lunar Surface Payload Capability as a function of EDS Propellant.....	213
Figure 72: Lander Size Comparison as a function of Payload Capability	214
Figure 73: Change in Payload Capability as a function of Boiloff.....	217
Figure 74: Effects of LEO Stay Time on Overall Campaign Cost and Mission Success.....	218
Figure 75: Change in Payload Capability and the Ascent Propellant is increased	220
Figure 76: Baseline lunar Campaign Mission Summary].....	223
Figure 77: Improvement in the Lunar Surface Payload Capability	225
Figure 78: Improvement in the Lunar Surface Payload Capability	226
Figure 79: Budget Matching for the Propellant Refueling Option	227
Figure 80: Decrease in Length of Lunar Campaign, F/V: 80/20	229
Figure 81: Decrease in Length of Lunar Campaign, F/V: 60/40	230
Figure 82: Risk and Cost of a 2-Launch Solution.....	234
Figure 83: Improvement in LOM vs. Risk of Refueling Maneuver	236
Figure 84: The Effect of Vehicle Growth on Development Costs.....	238
Figure 85: Increase in Cargo Launch Vehicle Dimensions as a Function of Growth	239
Figure 86: Cost Comparison of Propellant Offloading vs. Increase in Vehicle Size	241
Figure 87: Max Payload Capability of ESAS Propulsive Stages	244
Figure 88: Payload Capability as a Function of Available Propellant.....	245
Figure 89: Increase in Mars Mission Payload Requirements	248
Figure 90: The Savings for Mitigating the Effects of Mass Growth	252
Figure 91: The Costs for Mitigating the Effects of Mass Growth	253

Figure 92: Value of Eliminating the LEO Boiloff LOM Scenario	257
Figure 93: Value of Increasing the Payload Capability of the Architecture.....	259
Figure 94: Value to Extending the Architecture to a Mars Mission.....	261
Figure 95: Total Value of Propellant Refueling	263
Figure 96: Propellant Refueling Design Space Simulation Environment	276
Figure 97: Trade Study Morphological Matrix, Scenario One	277
Figure 98: Trade Study Morphological Matrix, Scenario Two	277
Figure 99: Example Mass Breakdown of CaLV 1 st Stage	288
Figure 100: Example Mass Breakdown of CaLV 2 nd Stage	289
Figure 101: Example Mass Breakdown of LSAM Descent Stage.....	291
Figure 102: Example Mass Breakdown of LSAM Ascent Stage	292

NOMENCLATURE

Ae	Exit Area
APAS	Aerodynamics Preliminary Analysis System
CaLV	Cargo Launch Vehicle
CER	Cost Estimating Relationship
CEV	Crew Excursion Vehicle
CF	Complexity Factor
CLV	Crew Launch Vehicle
DDT&E	Design, Develop, Test and Evaluation
DRM	Design Reference Mission
DSM	Design Structure Matrix
EDS	Earth Departure Stage
EELV	Evolved Expendable Launch Vehicle
EOR	Earth Orbit Rendezvous
ESAS	Exploration Systems Architecture Study
ET	External Tank
EVA	Extra-Vehicular Activity
FOM	Figure of Merit
HTPB	Hydroxyl-terminated polybutadiene
ICBM	Inter-continental Ballistic Missile
IOC	Initial Operating Capability
ISCPD	In-space Cryogenic Propellant Depot
Isp	Specific Impulse
ISS	International Space Station
L1	First Lagrange Point
LCC	Life Cycle Cost
LEO	Low Earth Orbit
LH2	Liquid Hydrogen
LLO	Low Lunar Orbit
LOI	Lunar Orbit Insertion

LOM	Loss of Mission
LOR	Lunar Orbit Rendezvous
LOX	Liquid Oxygen
LSAM	Lunar Surface Access Module
LTV	Lunar Transfer Vehicle
MADM	Multi-Attributed Decision Making
MER	Mass Estimating Relationship
M_{inert}	Inert Mass
M_{initial}	Initial Mass
MLI	Multi-layer Insulation
MMH	Monomethylhydrazine
MR_{required}	Mass Ratio Required
MSFC	Marshall Space Flight Center
NAFCOM	NASA Air force Cost Model
NERVA	Nuclear Engine for Rocket Vehicle Application
NTO	Nitrogen tetroxide
NTP	Nuclear Thermal Propulsion
O/F	Oxidizer to Fuel Ratio
PBAN	Polybutadiene Acrylonitrile
PLM	Primary Living Module
POST	Program to Optimize Simulated Trajectories
SM	Service Module
SRB	Solid Rocket Booster
SSME	Space Shuttle Main Engine
STS	Space Transportation System
T/me	Thrust to Mass of the Engine
T/mi	Thrust to Mass Initial
TEI	Trans-Earth Injection
TFU	Theoretical First Unit
TLI	Trans-lunar Injection
TMI	Trans-Martian Injection

TRL Technology Readiness Level
VAB Vehicle Assembly Building

SUMMARY

In 2004, President Bush addressed the nation and presented NASA's new vision for space exploration. This vision included the completion of the International Space Station, the retirement of the Space Shuttle, the development of a new crew exploration vehicle, and the return of humans to the moon by 2020. NASA's Exploration Systems Architecture Study (ESAS) produced a transportation architecture for returning humans to the moon affordably and safely. This architecture requires the development of two new Shuttle-derived launch vehicles, an in-space transportation vehicle, a lunar descent and landing vehicle, and a crew exploration vehicle for human transportation. The development of an in-space propellant transfer capability could greatly improve the performance, cost, mission success, and mission extensibility of the overall lunar architecture, providing a more optimal solution for future exploration missions. The work done in this thesis will analyze how this new capability could affect the current NASA lunar architecture, and will outline the value proposition of propellant refueling to NASA.

A value proposition for propellant refueling will be provided to establish why an architecture that utilizes propellant refueling is better equipped to meet the goals of the Vision for Space Exploration than the current baseline design. The primary goal addressed in this research is the development of a sustainable and affordable exploration program. The value proposition will outline various refueling strategies that can be used to improve each of the architecture Figures of Merit. These include a decrease in the Life Cycle Cost of both the lunar and Mars exploration campaigns, the ability to more than double the mission payload that can be delivered to the lunar surface during cargo

missions, improving the probability of successfully completing each lunar mission, decreasing the uncertainty, and therefore risk, experienced during the development process, and improving the extensibility of the exploration architecture by utilizing a greater portion of the lunar program for future crewed mission. The ability to improve these Figures of Merit provides NASA with a more valuable architecture because NASA is able to achieve a greater return on its large initial investment.

CHAPTER 1

INTRODUCTION

The goal of this thesis is to present a comprehensive analysis of the potential value of a propellant depot in Low Earth Orbit for future space exploration. The use of this capability provides a means to mitigate the performance concerns with NASA's current exploration architecture design (circa 2008) by providing an improvement to near term and long term architecture payload capability, thus providing a more affordable and sustainable long term exploration program. The following sections will provide the reader with an understanding of NASA's current exploration goals and how the introduction of propellant refueling can help achieve these goals.

1.1 MOTIVATION

NASA's charter is "To understand and protect our home planet, To explore the universe and search for life, To inspire the next generation of explorers ...as only NASA can. [1]" In order to achieve the second goal, NASA has spent a large percentage of their budget in an attempt to develop a reliable and affordable space transportation system. To date, NASA has yet to demonstrate an exploration architecture that meets both of these goals. The Apollo program had few budget constraints with its \$150B budget but failed to produce a sustainable architecture, and the program was cancelled after the sixth moon landing. The goal of the current Space Transportation System was to provide reduced space access cost at greater reliability and safety, but even with its cost over runs, missed

both cost and safety goals by a order of magnitude. The latest exploration architecture for NASA's Vision for Space Exploration will attempt to bring together aspects of both designs: large payload capability, lower cost per pound and higher safety. The current design utilizes mostly expendable hardware similar to the Apollo architecture in order to lower the development cost. The design also utilizes Shuttle-derived components that help to lower the initial development cost and take advantage of proven and reliable systems. There is, however, much speculation as to whether this architecture can achieve the performance goals of future exploration programs while maintaining high reliability at a sustainable cost. This present analysis indicates that the introduction of Low Earth Orbit (LEO) propellant refueling can provide a greater payload capability and a lower Loss of Mission (LOM) probability. It may also be possible to lower the life cycle cost of the architecture by utilizing the increase in payload capability to decrease the required number of launches to perform a lunar mission.

1.1.1 NASA'S SHIFT IN DESIGN STRATEGIES

In order to truly understand the challenges that NASA faces with its current Visions for Space Exploration, one must understand how the priorities have changed since the last time NASA devoted itself to an exploration program of this magnitude. During the Apollo program, NASA's first priority was completing the task of landing a human on the lunar surface before the end of the 1960's, while cost was considered a secondary factor. During this period NASA had its highest annual operating budget, about 175% of its current funding levels [2]. The overall mission success for the Apollo architecture was predicted to be 0.4043 [3] while the demonstrated value was 0.857 [4],

not including missions prior to Apollo 11. The only mission failures were a malfunction of the fuel cell on the Service Module (SM) and a second stage engine failure during the Apollo 13 mission; the reliability of the remaining architecture components demonstrated a 100% reliability during these seven missions. The Apollo program reached its goal of landing a human on the lunar surface by the end of the 1960's, but the architecture cost was not sustainable as the NASA budget fell dramatically after its peak in 1964. NASA's yearly budget profile is provided in Figure 1. This budget profile shows that NASA's budget fell to 15 percent of its peak 1960's level in the years following the first human lunar landing. The last human lunar landing occurred at the end of 1972, [4] and NASA's budget has remained less than 1 percent of the total federal budget ever since. In order to re-establish NASA's human space presence beyond LEO, a more reliable and affordable architecture needs to be developed.

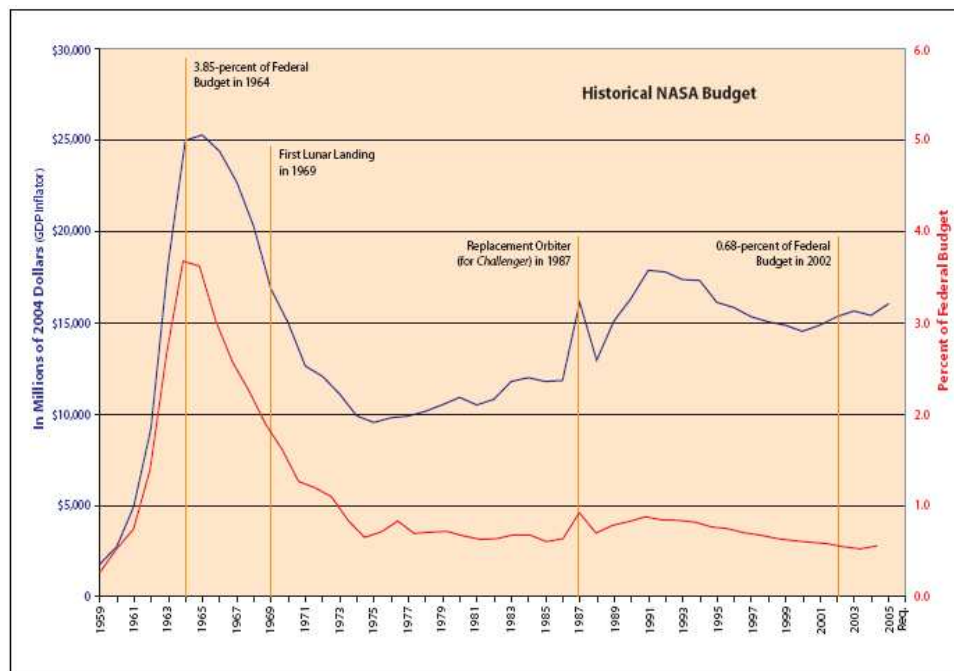


Figure 1: Historical NASA Budget and Percentage of Federal Budget [2]

In the post-Apollo era, NASA's design goals became more cost- and reliability-centric. NASA turned to the airline industry for this model, making the assumption that, if the system was designed to operate like an aircraft, then it would provide a more reliable and cost-effective solution. This idea gave birth to the Space Transportation Systems (STS). This system consists of the Space Shuttle Orbiter, the External Tank, and two Solid Rocket Boosters (SRB); the External Tank is the only aspect of the system that is not re-usable, though the SRBs are over-hauled after each launch, and the Orbiter is overhauled every six to eight flights. The Space Shuttle is launched vertically and returns via an un-powered glide. A draw back of the Space Shuttle is that it must go through an extensive series of repairs after each flight due to the extreme conditions that it experiences during each mission and lack of adequate performance margins. These inspections and repairs require a large work force and many months to complete. The full annual operations cost of the Space Shuttle are on the order of greater than \$4B, even when launched only a few times per year [5]. These repairs have kept the Space Shuttle from reaching its initial low cost operating estimate of \$8M - \$12M per flight. The Space Shuttle is scheduled to be retired in 2010 after the completion of the International Space Station (ISS). It will give way to a new expendable launch system which takes design aspects and lessons learned from both the Apollo and Space Shuttle programs to achieve NASA's goal of a long-term sustainable human space exploration program.

1.1.2 A SUMMARY OF THE EXPLORATION SYSTEMS ARCHITECTURE STUDY

In 2004, President George W. Bush announced a new Vision for Space Exploration in which he provided NASA with the goal of developing a new exploration

architecture to replace the current Space Transportation System. This new architecture would continue to meet the needs of the International Space Station in addition to providing a continuous human presence on the lunar surface and transportation for future exploration missions

The Space Shuttle will continue operation until the completion of the International Space Station in 2010, at which time it will be retired from operation. The new crew exploration vehicle must be operational by 2014 in order to continue its support the needs of the International Space Station. Initial lunar surface exploration missions should begin no later than 2020. This Vision marked the end of the Space Shuttle era and opened a new chapter in human exploration. The goal of this new architecture will be to accomplish a greater range of missions than the Apollo and Space Shuttle programs while achieving a higher reliability and remaining within NASA's planned budget profile, which may increase only at the rate of inflation. This is a difficult problem that will require the development of a very versatile and efficient architecture. The development and implementation of propellant refueling technologies may provide the architecture with the additional capability that it needs without a significant increase in the life cycle cost.

The Exploration Systems Architecture Study (ESAS) [6] was conducted in the summer of 2005 in response to the 2004 announcement by President George W. Bush that NASA would be redirecting its focus to returning humans to the moon by 2020. The study lasted approximately 90 days and established the initial baseline architecture for continued detailed studies to meet the needs of the Vision for Exploration. The goals of this study were to:

- Assess the top-level Crew Exploration Vehicle (CEV) requirements and plans that will enable the CEV to provide crew transport to the International Space Station, and that will accelerate the development of the CEV and crew launch system to reduce the gap between Shuttle retirement and CEV Initial Operational Capability (IOC).
- Define the top-level requirements and configurations for crew and cargo launch systems to support the lunar and Mars exploration programs.
- Develop a reference exploration architecture concept to support sustained human and robotic lunar exploration operations.
- Identify key technologies required to enable and significantly enhance these reference exploration systems, and reprioritize near and far-term technology investments.

The Exploration Systems Architecture Study team analyzed a variety of different launch vehicles and mission elements in an attempt to consider as many valid architecture options as possible. The different solutions were evaluated based on seven design reference missions (DRMs) and compared against five evaluation criteria called figures of merit (FOMs). The DRMs included three ISS crew and/or cargo missions, three lunar crew and/or cargo missions, and one Mars crew and cargo mission. The five FOMs

included: safety and mission success, affordability, performance, extensibility, and programmatic risk [6]. The first two criteria were considered most important in order to achieve a sustainable architecture while not exposing the astronauts to unnecessary risk.

The final architecture selection was a “one and a half” launch vehicle solution designed with the crew and cargo launching on separate launch vehicles. As shown in the lunar concept of operations in Figure 2. The mission mode selected for the lunar architecture was to use both a Lunar Orbit Rendezvous (LOR) and an Earth Orbit Rendezvous (EOR). In comparison, the Apollo architecture required only a LOR because it was capable of delivering all of the architecture elements in a single launch. The additional requirements on the current architecture (such as 4 crew, 7 day lunar mission, etc.) make use of a single launch vehicle very difficult using near-term technologies. The current baseline architecture requires the development of two new shuttle derived launch vehicles for delivering crew and cargo to LEO; the development of a two stage lunar lander to transfer the crew and cargo from low lunar orbit to the surface of the moon; and the development of a re-usable Crew Exploration Vehicle (CEV) that can provide safe transportation of the crew. The CEV is also tasked with the responsibility of transforming crew and cargo to the International Space Station. A more detailed description of the lunar concept of operations is provided in Chapter 2.

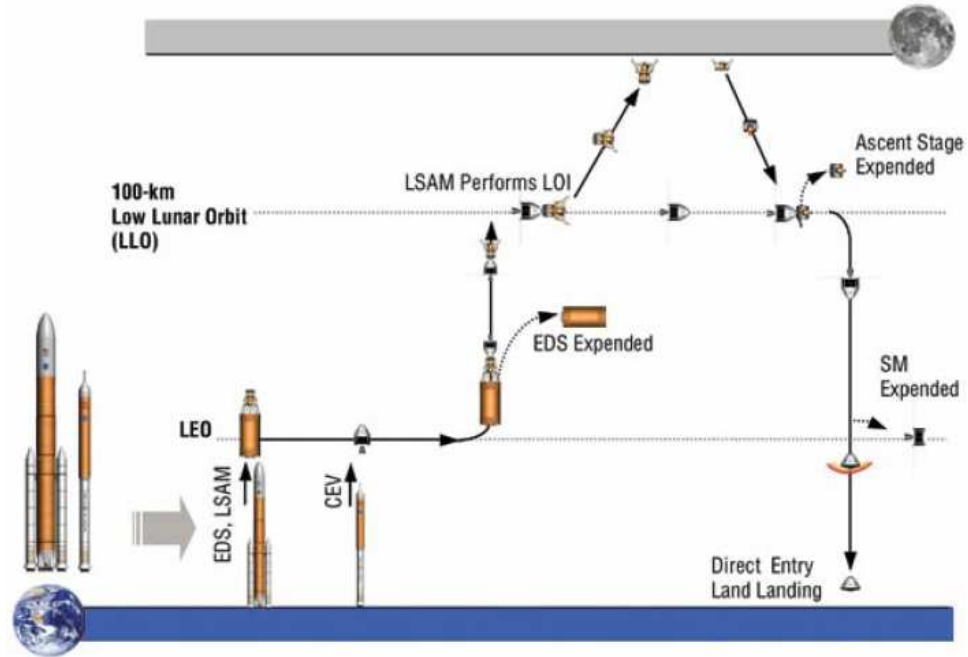


Figure 2: ESAS Baseline Lunar Architecture [6]

1.2 PROBLEM STATEMENT

Since humans began exploring space in the 1950s, the foundation of almost all exploration programs has been the use of high thrust chemical propulsion systems. The problem with chemical propulsion systems is that they have a relatively low specific impulse (I_{sp}), and therefore require large amounts of propellant to generate the required mission maneuvers resulting in vehicles that are up to 70 - 90 percent propellant mass. As an example, the ESAS cargo launch vehicle delivers 290,000 lbm of propellant to LEO while delivering less than 80,000 lbm of inert mass that includes the EDS, LSAM, and the lunar surface payload [6]. The propellant requirements for in-space transportation dominate the design of the launch vehicle more than any other aspect of the design and can significantly limit the design freedom of the architecture. With an in-space propellant

depot, the payload requirements of the launch vehicle are reduced by 70 to 90 percent or the payload of the in-space transpiration system can be improved by an order of magnitude. The trade is the cost of the developing the propellant depot and delivering the propellant to LEO versus building a “very large” launch vehicle or building a smaller launch vehicle that requires multiple launches. Developing a reliable and cost-effective means of providing propellant to LEO can help both reduce the cost of the overall lunar campaign and increase lunar surface and Mars payload capabilities.

1.2.1 INTRODUCTION OF PROPELLANT RE-FUELING AS A POTENTIAL SOLUTION

The concept of propellant refueling revolves around the idea that the performance of the architecture can be improved by developing a more efficient means of delivering propellant to LEO. In the architecture’s current form, the cargo launch vehicle is responsible for delivering the in-space propellant required to complete the mission. It is possible that a lower cost commercial operator could be tasked with providing this propellant to LEO and charging NASA based on the amount of propellant used. With this capability in place, a number of changes can be made to the baseline design that may provide an improvement to the exploration architecture.

There are a number of potential benefits that can be incorporated into the architecture elements when propellant refueling is introduced into the exploration architecture. One such improvement is the ability to reduce the payload requirement on the launch vehicles that are now being constrained in size because of current vehicle assembly and launch facilities. There are two resulting design strategies that can be employed when the Earth-to-orbit propellant requirements for in-space transportation are reduced. The first is an increase in the mission payload that can be delivered to LEO and

to the lunar surface. In this case the mass of the propellant is replaced by additional payload. The second design option is to reduce the size of the launch vehicles while achieving the same payload capability. A smaller launch vehicle would result in a smaller development and production cost. These improvements are both a result of the smaller total payload requirement. In addition to increasing the payload capability or decreasing the cost of the launch vehicle, propellant refueling can help reduce the concern that unexpected mass growth will push the size of the architecture elements beyond the limits of the current infrastructure. Any increase in mass can be offset by a corresponding decrease in the mass of propellant carried to LEO by the launch vehicles. These potential solutions will be evaluated to determine if they provide an increase in value to the exploration architecture.

Another potential benefit of propellant refueling is the ability to mitigate propellant boiloff by providing any lost propellant to the EDS and LSAM at the end of the LEO loiter, instead of carrying the additional propellant to orbit. With a propellant depot, the EDS and LSAM can remain in LEO indefinitely because there is no risk of losing the capability to perform the required mission maneuvers. The payload requirements on the launch vehicle are reduced because the architecture is no longer required to bring additional propellant to LEO to account for boiloff. The exploration architecture is also able to achieve a better loss of mission reliability because the maximum LEO loiter time is no longer dependent on the launch of the crew launch vehicle. The launch of the crew can now be considerably delayed without the risk of losing a mission.

The introduction of propellant refueling also allows an increased number of concepts of operation to be considered many of which are not possible with the current architecture. The availability of additional propellant in LEO allows the EDS to perform a greater variety of missions. As an example, the Lunar Orbit Rendezvous maneuver is currently performed by the Descent Stage of the LSAM. This scenario requires the lander to be sized to carry an additional 50,000 lbm of propellant. Allowing the EDS to perform the LOI in addition to the TLI maneuver reduces the size of the lander or greatly increases its payload capability because the lander can be sized to carry less propellant. This LOI maneuver capability using the EDS was not selected for the ESAS baseline design because the launch vehicle could not deliver the required propellant to allow the EDS to perform both maneuvers and because of T/W concerns with the EDS performing this maneuver. With the addition of propellant refueling, the additional propellant can be provided to the EDS once delivered to LEO. This allows the EDS to perform a wide range of mission maneuvers without altering the current vehicle configuration.

In the previous example, the capability of the EDS was expanded in order to accomplish both the TLI and LOI maneuvers. This was possible because sufficient propellant was available in LEO and because the EDS itself is a very large propulsive stage. The EDS doubles as the second stage of the cargo launch vehicle and is capable of holding 488,000 lbm of usable propellant. In the baseline design, this propellant is split between the ascent burn and the TLI maneuver, with approximately 225,000 lbm of propellant remaining once the EDS is delivered to LEO. A completely full EDS in LEO has the capability to deliver 400,000 lbm through TLI and in excess of 300,000 lbm of through TMI. The utilization of the EDS could eliminate the need for a new Nuclear

Thermal Propulsion (NTP) system and greatly reduce the number of launches needed, therefore decreasing the overall cost of large exploration missions. A large amount of propellant refueling is required to completely re-fuel the EDS once it reaches LEO and would require an efficient low cost propellant delivery method in order to become a viable architecture solution.

One of the goals established in the Vision for Exploration was to utilize commercial partners where possible. This could help improve the adorability and thus sustainability of NASA exploration architecture. The need to deliver propellant to LEO would allow commercial partners to play a larger role in NASA future exploration missions, and could help lower the cost of each mission. The other benefit of utilizing commercial launch providers to supply propellant to LEO is that it would increase the number of commercial launches completed each year. This would help drive down the launch costs to both NASA and to the rest of the commercial launch industry. The original low cost predictions for commercial launch vehicles have never been realized because the expected demand has never materialized. This demand has remained low because of the high cost of launching payload into orbit. This is a problem that cannot be solved without the introduction of an outside influence. The introduction of propellant refueling could solve this problem by supplying the demand needed to help reduce the current launch costs. This could then lead to an increase in demand throughout the rest of the launch market as the launch costs could be reduced to a more affordable level. The demand for propellant could also lead to the need for a much higher launch rate than can currently be provided by the launch industry. This could help pave the way for the

development of reusable launch vehicles that would ultimately provide the lowest cost for LEO payload delivery.

The final benefit of refueling that will be discussed is the ability to help mitigate the risk in developing complex systems which have large amounts of initial design uncertainty. During the development of most systems most of the major design decisions are made early in the design process where the least amount of knowledge is known about the final design. As a result a number of changes are often required during the design process. These changes lead to increases in cost and delays in schedule. Refueling can be used to help reduce the number of design changes needed or limit the impact they have on the system. This is accomplished by reducing the amount of propellant that is delivered to LEO. This provides an insurance policy for program managers to use when unexpected design changes occur that may require the addition advanced technologies or result in long program delays. Refueling reduces the risk by reducing the number design changes required throughout the development process.

The above discussion presented a number of potential improvements that could be incorporated into the exploration architecture if propellant refueling was available. There are however a number of potential concerns that may limit the value that can be achieved. A major concern is that the capability to refuel spacecraft in LEO is not a currently available technology. Chapter 2 provides a complete discussion of the current development effort for in-space propellant refueling. The second possible concern is the ability to provide a long term storage system that eliminates boiloff of the cryogenic propellants. A number of potential solutions exist, but again they have not been tested in a space environment. A truly zero-boiloff capability is not required but would aid in

reducing the price of propellant and the cost of the LEO propellant depot. The final concern is the ability to develop a low-cost propellant delivery system that can routinely deliver propellant to the storage system. The work in this thesis will look at how the price of propellant affects the value that propellant refueling provides the exploration architecture.

1.2.2 UNDERSTANDING THE POTENTIAL VALUE OF PROPELLANT RE-FUELING

The value of propellant refueling can be classified by understanding how the addition of this capability affects the design criteria and how well it address those issues facing the development of the architecture. A number of decision making methods can be used to look at the overall effects on the Figures of Merit. The tools utilized in this thesis will help define the cost and benefits of introducing propellant refueling and help establish which refueling strategies results in greatest improvement to the design of the architecture.

There are a number of ways to evaluate the potential benefits and cost of applying propellant refueling to the exploration architecture. The simplest method is to understand how the addition of this capability impacts each of the Figures of Merit. This approach allows the decision maker to evaluate a number of impacts on the architecture. While this method provides a more intuitive means to evaluate propellant refueling, it does not take into account the full multi-disciplinary nature of the problem. A Multi-Attributed Decision Making (MADM) method [7] is needed in order to evaluate the full impact of propellant refueling on the entire architecture. This type of method allows the utilization of various FOMs instead of a single decision making criteria and also provides a means

to weight the importance of each FOM. This additional information allows the decision maker to understand how impacts on each of the decision making criteria affect the selection of the final design point. The major concern with the implementation of a MADM method is the dependence on the use of weighting criteria to define the relative importance of the different figures of merit. An accurate estimation of these weights can be difficult, if not impossible, to determine. Therefore, various weighting scenarios are often considered to alleviate the uncertainty in these estimations. The result of this method is a ranking of the design points based on how well they perform across all of the Figures of Merit.

A Pareto frontier can be used to evaluate the value of various design options when more than one Figure of Merit is important to the decision maker. A Pareto frontier is also able to establish the solutions which naturally dominant a design space. As an example, if two design points are shown to have the same payload mass but design A has a lower cost than design B, it is said that design A is dominate because it achieves the same capability for a lower cost. Based on these two criteria point, B is always worse than point A and can be discarded as a potential solution. Using this logic, a curve of the solutions that bounds the decision space can be developed for a set of FOMs. The points along this frontier are considered Pareto-efficient, meaning that any improvement in one FOM requires a degradation of another. The decision maker can then make trade-offs to determine where in the design space the best solution exists. This method is similar to the MADM method and allows the decision maker to understand how the design changes as various weightings are applied. The benefit of this method is that it quickly reduces the size of the design, considering only the dominate solutions, therefore reducing the

amount of information that must be considered when making a final selection. The Pareto frontier also provides a relationship between the FOMs so that the decision maker can understand how the improvement in one FOM impacts another. However, when more than two FOMs are considered this concept becomes abstract and difficult to visualize.

A payload efficiency factor can also be used to show the potential value of introducing propellant refueling into the exploration architecture. This factor is defined by dividing the total cost of the lunar campaign by the total amount of payload delivered to the lunar surface. In some cases the addition of propellant refueling will increase the total cost of the architecture, but if the change in payload capability has a greater marginal improvement then the payload efficiency factor will decrease. This factor can also be used to help understand which architecture changes have the biggest impact and which have little to no impact on the baseline design. This helps to classify how propellant refueling can best be applied to the exploration architecture and potentially future exploration systems. The payload efficiency factor can not be the only FOM because NASA's yearly budget is constrained; thus a lower payload efficiency factor may be offset by an increase in annual cost over several years that must be considered; even though the total life cycle is less.

1.3 RESEARCH OBJECTIVES AND GOALS

The main objective of this research is to understand the effects of propellant refueling as it applies to the current NASA exploration architecture. This work will both investigate the propellant refueling design space within the current NASA lunar architecture and determine the cost and benefit of each point within the design space.

These results will then be compared against the ESAS baseline design to see if an improvement can be made to the architecture through the implementation of propellant refueling. While the results here will focus specifically on a lunar architecture, the overall trends should hold to other exploration missions. The following is a description of the main goals to be accomplished in this work.

- *Goal 1: Develop a lunar architecture model capable of utilizing various propellant refueling techniques.*

This model will be flexible enough to make trade-offs and measure the impact of various propellant refueling capability on NASA lunar architecture. It will also be able to model the baseline architecture and replicate the results of the ESAS within a few percentage points, providing accuracy and confidence for the model. The individual models must be able to calculate quickly so that Monte Carlo analysis can account for uncertainty in the model inputs.

- *Goal 2: Explore and understand the effects that propellant refueling have on NASA's baseline exploration architecture.*

A morphological matrix [8] will be used to characterize the different applications of propellant refueling and evaluate the design choices within each of these. This matrix encompasses the design space and provides the various inputs to the architecture model.

The results from these different combinations will give insight into the mass impacts that different applications of propellant refueling have on the architecture.

- *Goal 3: Determine the costs and benefits of adding propellant refueling to the lunar architecture and determine what approach has the greatest effect on the over all design of the architecture.*

The final results of this work will provide a guide to selecting the best application of propellant refueling as it applies to the lunar architecture. This guide will outline the trends observed along the Life Cycle Cost (LCC) and lunar surface payload capability Pareto frontier, examine where in the design space the most efficient design points are located, and determine how the addition of risk and extensibility considerations affect which designs have a greatest benefit to the architecture. The final selection will depend on the values of the decision maker, but design points that perform well within each of these analyses are likely candidates for the final architecture design. The differences and similarities between Scenarios One and Two will also be discussed to illustrate how different application of propellant refueling can significantly affect the design of the architecture. These two Scenarios will be fully discussed in Chapter 3.

1.4 DISSERTATION OVERVIEW

This dissertation will cover the entirety of the work completed during this study in an attempt to show the reader the benefits and costs of propellant refueling. This first chapter provides the motivation for the research conducted during this study. It provides

the reader with a historical view of NASA's exploration program, including the path leading up to the development of new exploration architecture. It then discusses how propellant refueling can potentially be used to improve the design of NASA baseline architecture. The chapter concludes with a discussion of the major goals to be accomplished.

The second chapter continues with a background discussion of propellant refueling and how it has been conceptually studied for exploration missions in the past. The limited work done utilizing this capability has led to the need to develop a more complete understanding of its effects on architecture design. A feasibility discussion will also be presented to provide the current status on the technology development of a long-term LEO propellant storage and cryogenic propellant transfer. A look at potential propellant suppliers will also be discussed.

Chapter 3 will outline the design space used in this thesis to explore the effects that propellant refueling has on the baseline architecture. A description of the design variables will be provided along with the ranges considered during this work. These design variables will provide the inputs to the modeling and simulation environment.

Chapter 4 will outline the development of the propellant refueling simulation environment. This outline will provide the reader with a complete understanding of the individual analyses and what interactions exist between each model, along with a discussion of the ModelCenter[®] [9] simulation environment used. The assumptions and limitations for each model will be provided. Chapters 3 and 4 should provide the reader with a clear understanding of the process for creating the results that will be discussed in Chapters 5, 6, and 7

Chapters 5 and 6 are very similar in structure and only differ because of the scenarios they discuss. Chapter 5 will define Scenario One, where the payload capability of the architecture is increased without changing the size of the different elements. Chapter 6 will define Scenario Two where the payload capability remains the same as the baseline architecture, but the individual elements are allowed to adjust their size. These chapters will discuss the results developed from the simulation environment and investigate the cost and benefits of each design point. A Pareto frontier will be used to establish the dominate design points and show the trade off that can be made between the cost and capability of the architecture.

The work in Chapter 7 will finalize the value proposition of propellant refueling to NASA. A detailed discussion will be presented to show the precise value that the introduction of this capability provides the architecture. In particular the effects of propellant refueling on each Figure of Merit will be presented.

The final chapter will be a concluding discussion outlining specific observations made during the study and a guide to the use of propellant refueling in exploration missions. A future work section will also be provided to discuss possible improvements, as well as additional work that can be made to improve the results provided.

CHAPTER 2

BACKGROUND

This chapter begins with a detailed discussion of the ESAS architecture which is the baseline for comparison in this thesis. Previous in-space propellant refueling design studies will be presented to provide the reader with what has been considered to date and what information is lacking. The basis for this research is to complete the understating of the benefits that propellant refueling can provide to exploration missions. A summary of the current technology development will also be included to provide the reader with the time frame needed to reach a technology Readiness Level (TRL) of 6 or higher. The commercial launch market is also discussed to provide the reader with a basis for the propellant deliver price estimations considered in developing the refueling model. The chapter will conclude with a discussion of the system engineering methods and practices used in this research.

2.1 SUMMARY OF ESAS BASELINE ARCHITECTURE

The results of the ESAS completed in 2005 provided the baseline architecture that NASA would used to complete the Vision for Space Exploration laid out by President George W. Bush. This architecture provided the baseline concept with which to begin developing NASA's new exploration architecture. This concept was not meant to be the final design but rather provide the foundation for further studies to build upon. This section will outline the baseline design, including all of the major architecture elements.

It will also provide a discussion as to which elements may be affected by the addition of propellant refueling to the architecture.

2.1.1 BASELINE LUNAR CONCEPT OF OPERATIONS

As seen in Figure 3, the ESAS architecture utilizes two launch vehicles to deliver the crew and cargo to Low Earth Orbit. The Crew Exploration Vehicle (CEV) rendezvous with the Earth Departure Stage (EDS) and Lunar Surface Access Model (LSAM) prior to trans-lunar injection (TLI), which is performed by the Earth Departure Stage. This represents the Earth Orbit Rendezvous portion of the architecture alluded to in Chapter 1. The EDS is expended once this maneuver is completed and the CEV, Service Module (SM), and LSAM continue on to the Moon. The descent stage of the LSAM performs a Lunar Orbit Injection maneuver to place the remaining architecture elements into a circular lunar orbit, often referred to as low lunar orbit (LLO). The crew then transfers from the CEV, which will remain in LLO, to the LSAM habitat; the LSAM then separates and descends to the lunar surface using descent stage of the LSAM. The LSAM is capable of supporting the four crew members up to seven days on the surface of the Moon. At the end of the lunar mission, the LSAM ascent stage separates and returns to LLO, leaving the descent stage on the lunar surface. Once in LLO, the ascent stage docks with the CEV/SM and the crew transfers back to the CEV. The ascent stage is expended, and the SM performs the Trans-Earth Injection (TEI) maneuver to provide the CEV with a direct Earth re-entry trajectory. After separation of the SM and re-entry, the CEV makes a land-based landing in the western United States.

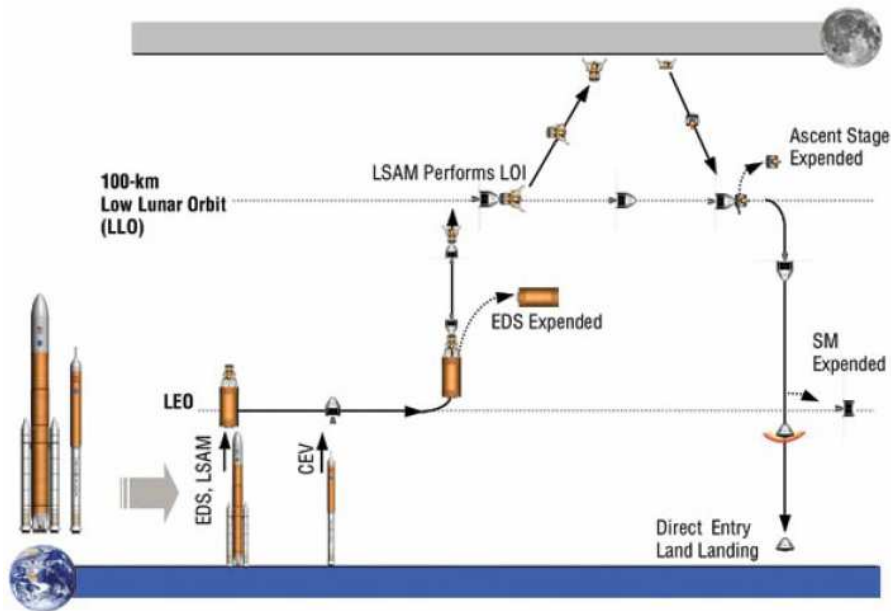


Figure 3: ESAS Baseline Lunar Architecture Concept of Operations

2.1.2 CARGO LAUNCH VEHICLE SUMMARY

The cargo launch vehicle (CaLV) is designed to provide reliable transportation of cargo, in particular the LSAM and EDS, from the Earth's surface to low earth orbit. The ESAS results favor the use of Shuttle-derived launch vehicles for the goals of supporting the proposed lunar exploration program. The CaLV (Figure 4) was designed as a space shuttle derived launch vehicle. The CaLV uses shuttle heritage components such as the reusable solid rocket boosters, though modified to include five segments instead of four, the Space Shuttle Main Engine (SSME), and an external diameter equal to the diameter of the Space Shuttle External Tank (ET) to both reduce overall development costs as well as take advantage of the significant effort already spent on increasing the reliability of the Shuttle components.

The CaLV consists of two and a half stages as shown in Figure 4. The core stage is a liquid oxygen (LOX) and liquid hydrogen (LH2) propulsion system powered by five SSMEs capable of generating 2,300,000 lbm of vacuum thrust with a vacuum specific impulse (Isp) of 452s. Two five segment solid rocket boosters are attached to each side of the core stage and are used to provide additional thrust at liftoff. The total vacuum thrust of the two SRBs is 7,600,000 lbm with a significantly lower Isp of 265s. The 2nd stage of the launch vehicle, which is also utilizes a LOX/LH2 system, is powered by two J-2Ss engines. These engines provide a total vacuum thrust of 550,000 lbm with a vacuum Isp of 451s. A summary of these values is provided in Table 1. The diameter of both stages is designed to be 27.5 ft to match the diameter of the External Tank of the Space Shuttle. The LSAM rests atop the EDS and is enclosed inside a 72 ft payload fairing. The CaLV is designed to carry the EDS and LSAM into a 30 X 100 nmi orbit prior to launch of the crew.

Table 1: CaLV Propulsion System Summary

	Vacuum Thrust [lb]	Vacuum Isp[s]	Propellant [lb]
Core Stage	2,300,000	452	2,200,000
5-Segment SRBs	7,600,000	265	2,800,000
2 nd Stage/ EDS	549,000	451	488,000

The upper stage of the CaLV doubles as the EDS which is responsible for performing the trans-lunar injection maneuver. Utilizing the 2nd stage for this maneuver instead of adding a third stage decreases the total mass of the vehicle because less engines and tanks are required. This stage is therefore designed to hold 488,000 lbm of

usable propellant of which only 264,000 lbm is used during 2nd stage ascent. The remaining propellant provides a significant in-space propulsive capability, but could be greatly increased if the full 488,000 lbm of propellant was available in LEO. The EDS tanks could be filled in LEO through propellant refueling. This additional propellant would allow the EDS to perform a wider range of missions including performing the LOI, originally performed by the LSAM, or proving large payloads to missions beyond the Moon.

There are a number of other potentially beneficial design changes on the CaLV that could be made to take advantage of propellant refueling. As discussed above, the EDS is a very large propulsive stage that could be utilized to perform a much wider variety of maneuvers than is possible with the baseline design. The immense size of the CaLV is partially due to the need to deliver the TLI propellant to LEO. Replacing the TLI propellant with propellant from the LEO depot would greatly reduce the size and mass of the launch vehicle. Also by not having to carry the TLI propellant to orbit, greater design margins could be achieved. It is also possible to increase the propellant burned during the 2nd stage ascent to provide a greater payload capability to LEO (although limited because of gravity losses). Much of the launch vehicle design revolves around the quantity of propellant that must be delivered to LEO for in-space maneuvers, with the introduction of propellant refueling this burden can be removed increasing the design flexibility of the exploration architecture.

2.1.3 LUNAR SURFACE ACCESS MODULE (LSAM) SUMMARY

The Lunar Surface Access Module (LSAM) provides both access to the lunar surface and a habitat for humans during exploration missions. Once in Low Lunar Orbit

(LLO), the crew transfers from the Crew Exploration Vehicle (CEV) to the LSAM for descent and landing on the surface. The crew utilizes the LSAM as a base of operations while on the surface. The Ascent Stage is used to return the crew to the CEV in LLO (Figure 3). The lander follows a similar design approach used during the Apollo program, though the ESAS baseline lander can reach a greater variety of locations on the Moon, support up to four crew, and remain on the surface for seven days. All of which are significant improvements over the Apollo program; however, more payload capability for the entire system architecture is required.

The LSAM is a two stage vehicle design (Figure 5). A Descent Stage which is responsible for inserting the LSAM, CEV and SM into lunar orbit and transferring the lander from orbit to the surface of the Moon. These two maneuvers require 60,000 lbm of propellant, which is more than 50 percent of the entire LSAM gross mass. The descent stage is powered by a LOX/LH2 propulsion system which is derived from the currently available RL-10 engine [ESAS, pp. 166]. The four descent engines generate 60,000 lbm of thrust with an Isp of 460s. The descent stage remains on the lunar surface at the completion of the missions. The ascent stage is primarily a pressurized living environment designed to house the crew during the seven day lunar surface mission. The ascent stage has a total pressurized volume of 1,100 cubic feet. This pressurized volume also contains a separating bulkhead to allow a section of the habitat to be depressurized to allow egress from the vehicle to the lunar surface. The ascent stage also returns the crew from the surface of the Moon to lunar orbit at the completion of the mission. This is accomplished with a single LOX/Methane engine capable of generating 10,000 lbm of thrust. The LOX/Methane engine was selected to provide commonality with future Mars

missions, since Methane can be processed from the Mars atmosphere. A number of alternative Ascent Stage propellant were considered during the ESAS and remain under consideration. This study will allow the ascent stage engine to vary among four possible alternatives. These alternatives include the baseline LOX/Methane engine, a storable propellant system like Apollo, and both a pressure and pump fed LOX/LH2 system. A more detailed description of each engine is discussed in Chapter 3. Once the crew has been returned to the CEV, the ascent stage is discarded. The LSAM is 100 percent expendable, and new vehicle is required for each mission.

The baseline lander is currently designed to perform the LOI maneuver, which requires 30,000 lbm of propellant. If the lander was not required to perform this maneuver (EDS is filled on orbit to do the LOI) than the gross mass, as calculated by the tools used for this study, would be decreased by 48,000 lbm. This is close to 50 percent of the current LSAM total gross mass. In addition to resulting in a smaller lander, this would reduce the LEO payload requirements of the CaLV, potentially resulting in a smaller launch vehicle. Another potential approach to removing the LOI maneuver from the lander would be to hold the gross mass of the vehicle constant and allow the payload capability to increase. Thus, the reduction in propellant mass could be replaced with additional payload capability.

2.1.4 CREW LAUNCH VEHICLE SUMMARY

The crew launch vehicle is designed to provide reliable transportation of humans and cargo from the Earth's surface to Low Earth Orbit. The ESAS results favor the use of Shuttle-derived launch vehicles for the goals of servicing the International Space Station

after the retirement of the STS and supporting the proposed lunar exploration program. The CLV is a Space Shuttle-derived launch vehicle. The CLV uses Shuttle heritage components such as the reusable solid rocket booster and the Space Shuttle Main Engine (SSME) to both reduce overall development cost and schedule as well as take advantage of the significant effort already spent on increasing the reliability of the Shuttle components. In the baseline architecture, the CLV is responsible for delivering the CEV to LEO.

The CLV is a 2-stage expendable launch vehicle designed to be the highest reliability launch vehicle ever built (Figure 4). The vehicle consists of a four segment solid rocket booster first stage, taking heritage from the SRBs used on the Space Shuttle. The 2nd stage is a LOX/LH2 propulsion system powered by one SSME. The SSME design will be modified to start at altitude. Both the SSME and SRBs have proven to be highly reliable launch systems. A key aspect of the CLV's crew safety is the additional of a launch abort tower place at the top of the vehicle. This escape system can be used separate the crew of the CLV in case of a catastrophic failure. The CLV is designed to carry a payload of approximately 59,900 lbm into a 30 X 100 nmi orbit injected at 60 nmi. This payload mass was chosen as a result of the ESAS study for the CEV design. This orbit will allow the CEV to rendezvous with the pre-launched EDS and LSAM. The resulting vehicle is 290 ft tall with a mass of 1.78 million pounds.

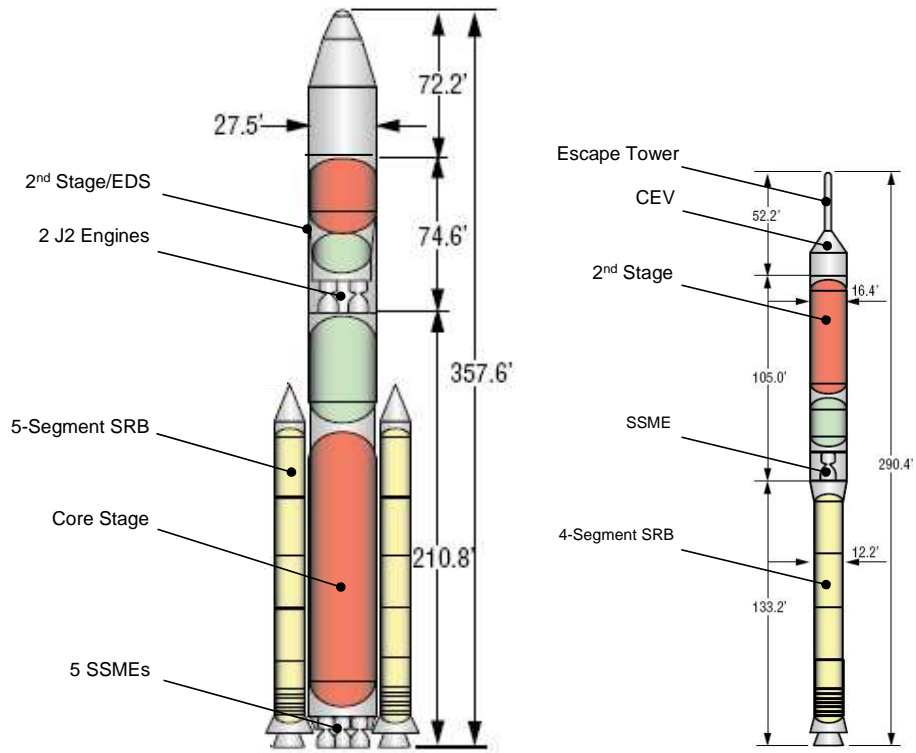


Figure 4: ESAS Baseline Launch Vehicles

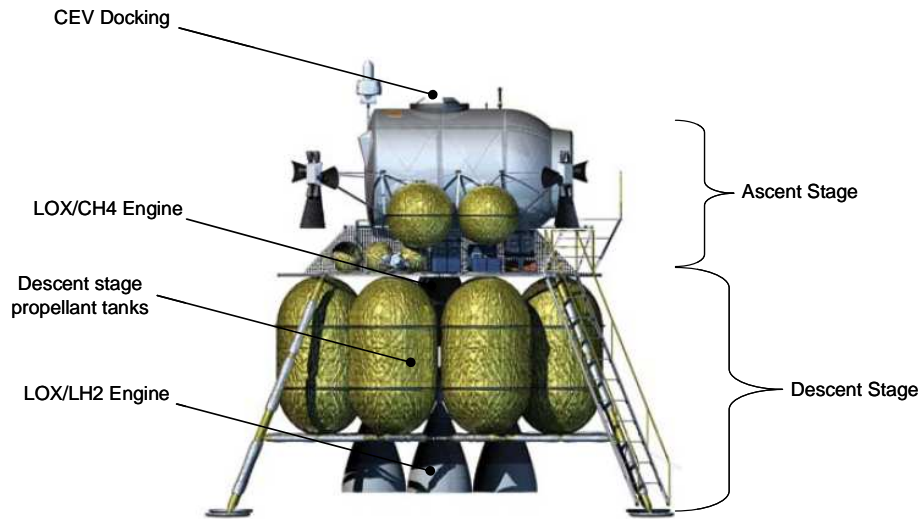


Figure 5: ESAS Baseline Lunar Surface Access Module

The work in this thesis will assume a constant CLV configuration and will make no design changes throughout the study. While the CLV has potential to take advantage of propellant refueling by offloading propellant from the service module or refueling the 2nd stage in LEO, this will not be considered in this work. This will be considered as potential future work.

2.1.5 CREW EXPLORATION VEHICLE (CEV) SUMMARY

The CEV consists of a Crew Module (CM) and Service Module (SM) which are both launched together aboard the CLV and remain attached until just prior to CM reentry (Figure 3). The CEV provides life support systems for the crew while transferring between the Earth and Moon and during LEO operations. This includes transportation to the International Space Station. The CEV is also responsible for reentry for both lunar and ISS missions. The Service Module (SM) is the propulsion system for the CM. This vehicle provides the Trans-Earth Injection (TEI) maneuver to return the CEV from lunar orbit and provides the capability to transfer the CEV from its insertion orbit to the ISS.

The CEV Crew Module (CM), shown in Figure 6, is a scaled up version of the 18 ft diameter Apollo capsule that is capable of transporting up to four crew members during lunar mission and up to six crew for missions to ISS. The CM provides from 425 to 525 cubic feet of habitable volume during lunar missions depending on the final configuration. The CM also utilizes a blunt-body capsule to provide a heritage design from previous human and robotic missions. The CM is designed to be completely reusable except for the ablative heat shield and landing systems that must be replaced after each mission. The CM has no main propulsion system and relies on the service module

for all major propulsive maneuvers. The SM was design to utilize a LOX/Methane propulsion system in order to obtain commonality with the Ascent Stage of the LSAM. Utilizing this system for initial ISS mission helps improve system reliability prior to beginning the lunar campaign. A solar array was selected as the primary power system to achieve better performance for long duration missions.

The configuration of the CM and SM are held constant throughout this study with a mass of 44,000 lbm. This mass is used when completing the TLI and LOI maneuvers. The SM is highly dependent on the amount of propellant it must carry and could potentially be refueled in LEO. Additional work, beyond the scope of this thesis, is needed to determine if potential value can be achieved by refueling the service module.

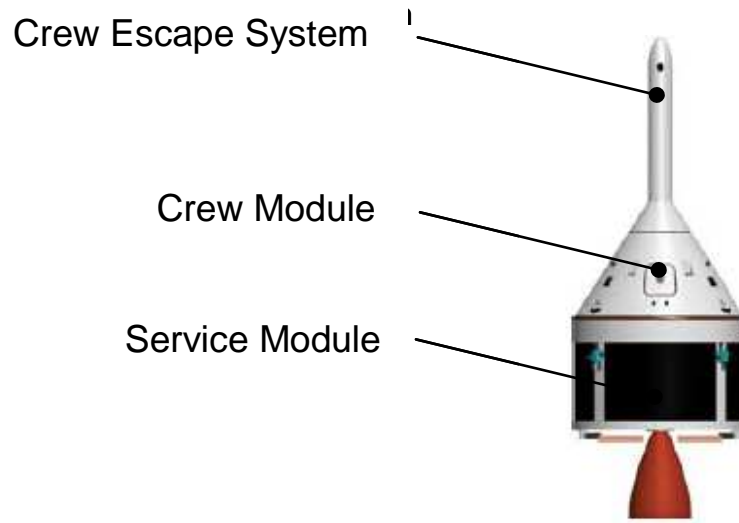


Figure 6: ESAS Baseline CEV

2.2 PREVIOUS PROPELLANT REFUELING DESIGN STUDIES

The concept of in-space propellant refueling has been studied since the 1950's, when the Air Force began investigating how its aircraft refueling techniques could be applied to in-space operations. The idea behind propellant refueling is that a vehicle can gain better overall performance if it does not need to carry all of its propellant from the start of the mission. Aircraft have been using this concept since the 1920's [10]. Long-range cargo aircraft such as the KC-135 are able to re-fuel short-range fighters. This greatly increases the range of the fighter aircraft, allowing them to perform a wider range of missions. This same concept can be applied to space exploration missions. In this case, the propellant required for in-space operations is delivered to LEO and stored in an orbiting propellant depot. The propellant can then be transferred to any of the architecture elements as needed. Providing this propellant on-orbit can reduce the payload requirement for the cargo delivery vehicle by as much as 75% for a lunar mission [11].

On-orbit propellant refueling has not yet been put into practice, but much research has been done on this subject. On-orbit propellant refueling research can be broken down into three general areas of focus. The first is the use of propellant depots in exploration missions, the second is utilizing propellant depots to provide increased life and performance for commercial satellites, and the third is the design and technological development of cryogenic in-space propellant storage and transfer. The following sections will summarize the literature that has been written on each of these areas, describe how it affects the work being done in this thesis, and how the work here will expand upon what has already been studied.

2.2.1 PROPELLANT REFUELING IN EXPLORATION MISSIONS

A thorough search of the literature was conducted to investigate how propellant refueling had been applied to previous exploration mission studies. These studies showed that much of the research conducted so far has focused on human missions to the Moon and Mars. There was also limited discussion on the possible use of propellant refueling for robotic science missions. The bulk of the previous research focuses on a more conceptual understanding of propellant refueling and the possible benefits and challenges associated with its development. Only a limited amount of work has been done to provide analytical results as to the benefits and costs propellant refueling would add to an exploration architecture. The following will outline the work done in utilizing propellant refueling in exploration missions.

The lunar orbital rendezvous concept of operations leading to the Apollo architecture, discussed in much of the literature, has similar core components as the ESAS architecture discussed above and of that shown in Figure 7. It requires a launch vehicles to deliver crew and cargo to LEO, vehicles to transfer the crew and cargo to low-lunar orbit, vehicles to perform lunar maneuvers, and Earth return vehicles. The main differences in these studies are which vehicles are needed to perform each leg of the mission and which architecture elements are re-fueled.

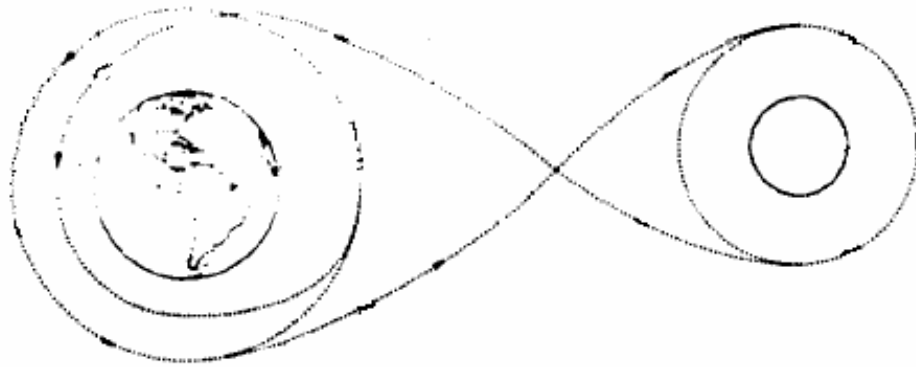


Figure 7: Typical Lunar Concept of Operations

2.2.2 APOLLO LUNAR ARCHITECTURE

The first notable study of propellant refueling was during the initial development of the Apollo lunar architecture. The original lunar architecture was a Direct approach that relied on the use of a very large NOVA [12] class launch vehicle. This vehicle would not require an Earth or lunar orbit rendezvous and would deliver all architecture elements directly to the lunar surface. A single direct launch vehicle was shown to be technically impossible within the time frame of the Apollo program [13]. The Earth Orbit Rendezvous (EOR) solution, Figure 8, was proposed to solve the problems with the initial Direct approach [14]. The EOR utilized a tanker refueling option in LEO to reduce the size of the launch vehicle. While never selected, this option was considered by many within NASA, including Wernher Von Braun, to be the best option because of EOR's potential for future exploration systems [14]. The EOR architecture required the launch of two Saturn V class launch vehicles. The first launch delivered a refueling tanker and the second delivered the crew and in-space transfer elements. The two vehicles would

rendezvous and dock in LEO, and the tanker element would transfer liquid oxygen to the in-space propulsion vehicles. The EOR would allow a smaller launch vehicle to be developed because the in-space propellant would be provided during a separate launch thus reducing the payload requirements on the vehicle. The remaining architecture would follow the direct lunar mission approach.

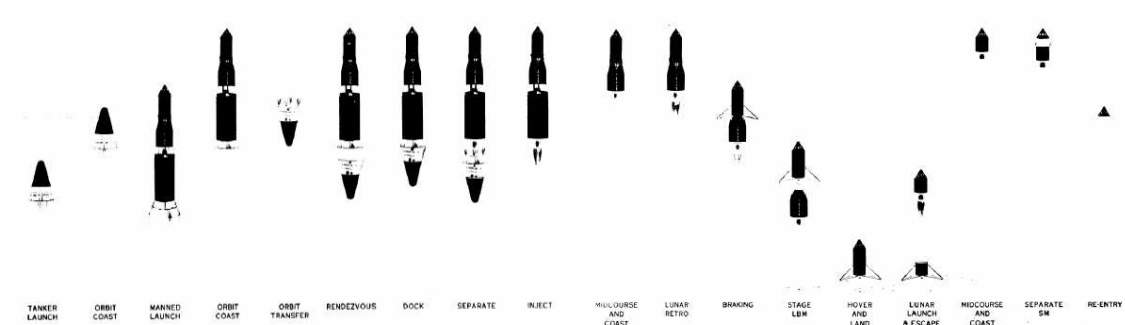


Figure 8: Apollo EOR Mission Mode [15]

The drawback of the EOR architecture is that it required the launch of two launch vehicles which increased the cost of the architecture and decreased mission reliability, because both launch vehicles had to be successful in order to complete the mission. The EOR approach would also rely on the use of propellant transfer which had no historical reference to draw upon. The EOR option was eventually not selected because the refueling technology could not be fully tested within the timeframe of the lunar program and it also required two launches per mission.

The final Apollo architecture utilized the Lunar Orbit Rendezvous. The primary reason LOR was selected over EOR was due to the shorter time frame needed to meet the goal of landing a man on the moon [13]. This architecture only required one reasonably sized launch vehicle because of the inherent in-space staging strategies. The initial

analysis showed that both the LOR and EOR modes were technically feasible and could meet the strategic needs of the nation, however the results showed that the LOR option offers a 10 – 15% lower cost and higher mission success probability because it relied on a single launch vehicle.

The Apollo EOR study showed that propellant refueling offers an improvement over systems where all elements are launched on a single vehicle. This study also demonstrated that launching the in-space propellant separately resulted in a more technically feasible architecture solution than a Direct approach because of the reduced payload requirements on the launch vehicle. This work will investigate how this concept can best be applied to the design of the cargo launch vehicle. The Apollo study also alluded to the fact that a low-cost propellant deliver method is required in order to reduce the cost of exploration systems.

Result: Propellant refueling can be utilized to reduce the payload requirement on the launch vehicle by eliminating the need to carry the in-space propellant. This could significantly affect the design of the NASA cargo launch vehicle.

Result: The primary draw back found during the Apollo lunar mode study was the additional launch cost of the tanker vehicle. Utilizing a low-cost existing or proposed commercial launch vehicle(s) could alleviate this concern.

2.2.3 REFUELING WITH CURRENT SPACE TRANSPORTATION SYSTEM

The study performed by Cady [11] utilizes the Space Transportation System (STS) and the derivative STS-C to deliver crew and cargo to LEO, the International Space Station as the refueling node, a re-usable Lunar Transfer Vehicle to transfer the architecture elements between Earth and lunar orbit and a re-usable Lunar Excursion Vehicle that provides transportation to and from the surface of the moon. This study primarily focuses on how the propellant transfer is handled at the refueling node and considered four initial options. In option one, the refueling tanks are directly transferred to the LTV at the ISS. In option two, the tanker docks with the ISS and provides direct propellant transfer to the LTV. In option three, an orbiting depot is developed instead of utilizing the ISS and the propellant tanks are transferred to the depot from the tanker. In the final concept, an orbiting depot is utilized and the tanker directly transfers propellant to the depots storage tanks. The results of the study provided no conclusions as to which method provided the best refueling option. The options which utilized the ISS resulted in lower cost solutions but provided an increase risk to the space station. The two solutions with the new depot offered a better performance because the depot was located at a lower orbital inclination, but had a larger development cost.

This study had a number of shortcomings and provided little insight into the potential benefits of propellant refueling. The most important shortcoming is that the study assumed an architecture that utilized propellant refueling and did not trade it against a baseline design that accomplished the same mission without the use of refueling. Therefore no conclusion could be made as to the potential benefits of adding it to the architecture. While the study did attempt to discuss the impact of various

propellant transfer strategies, it provided little detail to understand the benefits and cost of each option. Much of the study focused on developing which concepts to consider and how they should be evaluated. The study also failed to consider more than one potential refueling option. The lunar transfer vehicle was the only element of the architecture considered for refueling and details on the impact of this decision were not discussed.

The results from this study showed that both tank and direct fluid transfer offer both positive and negative impacts on the architecture with neither design choice showing any distinct advantage over the other. The location of the depot will likely correspond to the orbit already being utilized by the architecture to maximize the performance from the propellant delivery system. The author does point out that the results of this study are preliminary and additional work is required, including an investigation of a series of additional trades. To date, no additional work has been published.

2.2.4 REFUELING WITH REUSABLE LAUNCH VEHICLES

Koelle, in his paper “Lunar Space Transportation System Options,” [16] proposed three options where propellant refueling could benefit lunar exploration missions; these three concepts are outlined in Figure 9. A fourth option is also provided to represent an Apollo lunar orbit rendezvous type solution and serves as a baseline point of reference. In concepts 1 – 3 all architecture elements are re-usable. Option one utilizes a three stage heavy lift launch vehicle to perform a direct lunar mission, whereby the same vehicle is used from the Earths’ surface to lunar orbit. A re-usable lunar ferry is waiting in orbit to transfer the crew and cargo to and from the surface of the moon. The propellant for this

ferry is provided through fluid transfer from the 3rd stage of the launch vehicle. Option two utilizes three re-usable vehicles: a single stage to orbit launch vehicle (SSTO), a lunar transfer vehicle (LTV), and a lunar ferry. The SSTO provides transportation of crew, cargo and propellant to and from LEO. The LTV is re-fueled by the SSTO in LEO and provides transportation to and from lunar orbit. The LTV provides propellant to the lunar ferry which provides transportation of the crew and cargo to and from the lunar surface. The third option utilizes a single vehicle to transfer from Earth to the lunar surface and back with a stop in LEO to re-fuel at an orbiting depot. All three concepts could be designed to utilize propellant refueling in either lunar orbit or on the lunar surface. This propellant could potentially be developed directly from lunar resources. The author discusses the potential for payload improvement if a reliable and low-cost propellant delivery system was available on the Moon.

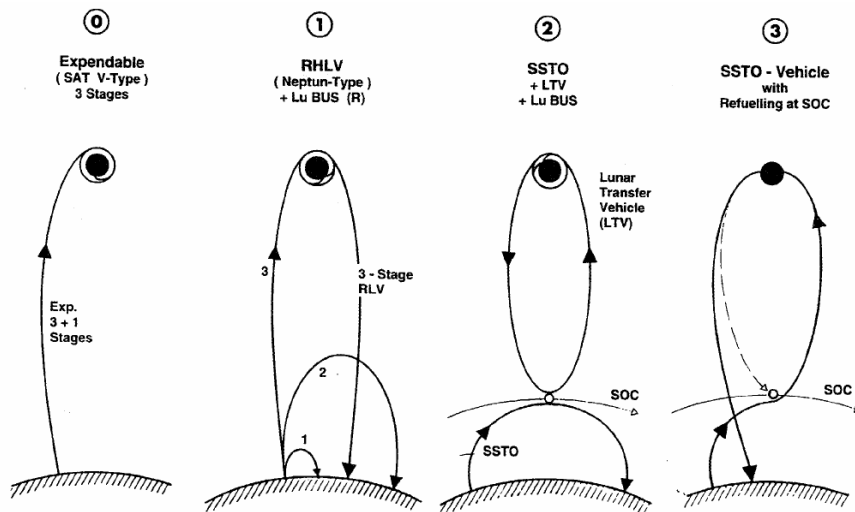


Figure 9: Lunar Transportation System Options [16]

In all three alternative concepts, a new re-usable launch vehicle is required. In the first option, a three stage re-usable launch vehicle is developed with the third stage being used as the in-space transfer stage. The second and third concepts require the development of a SSTO launch vehicle. The author also shows that the propellant required to transfer from the Earth's surface to LEO is similar to the propellant required to transfer from LEO to the moon. This would make a node located in LEO the most logical option. In this case, the same vehicle could be used for both ascent and lunar transfer and is seen in option three. Similar to the study by Cady, only re-usable elements are considered in this architecture, making it fundamentally different than the completely expendable baseline architecture currently being developed by NASA

The author provides all four of these concepts as possible lunar architectures to be considered for future development though little detail is provided as to the potential benefit of each. He states that a "best" solution can not be determined from the information provided and additional work is needed to truly investigate the viability of these concepts as lunar mission options. The author fails to make a comparison between the four architecture solutions and focuses most of the paper on concept three. The results of the author's analysis shows that a large amount of propellant is needed in order to perform the in-space maneuvers and requires a significant number of launches to provide all of the propellant to LEO. In some cases 32 launches are needed to provide sufficient propellant for the lunar mission. This leads the author to the conclusion that a dedicated tanker vehicle would be needed to provide sufficient propellant to the architecture and to achieve a launch price that makes this solution economically viable. The author also

discusses that this cost can be decreased if lunar resources are used to provide the propellant to the architecture. A detailed explanation of this conclusion was not provided.

Result: The Earth Departure Stage can be used to perform a greater portion of the in-space maneuvers. This would increase the payload mass that can be delivered to the lunar surface.

2.2.5 REFUELING IN DESTINATION ORBIT FOR RETURN MANEUVERS

The work done by Folta [17] considers the concept of propellant refueling by placing a depot in the destination orbit to provide the Earth return propellant. This study considers placing propellant depots in both lunar and Mars orbit. This approach significantly decreases the outbound payload requirements and the size of the in-space transfer vehicle. The cost to the architecture is the number of additional launches required to preposition the Earth return propellant. This refueling option is only a small part of the overall study presented by Folta. Most of the work presented in this paper focused on the idea of On-Orbit Staging, and how improved performance can be achieved through “basic staging” of the in-space transfer vehicle. The introduction of multiple new techniques makes it difficult to single out the potential benefits provided by propellant refueling. The author does provide a limited set of data that shows the potential payload improvement achieved through the addition of prepositions propellant. A summary of these are provided in Figure 10.

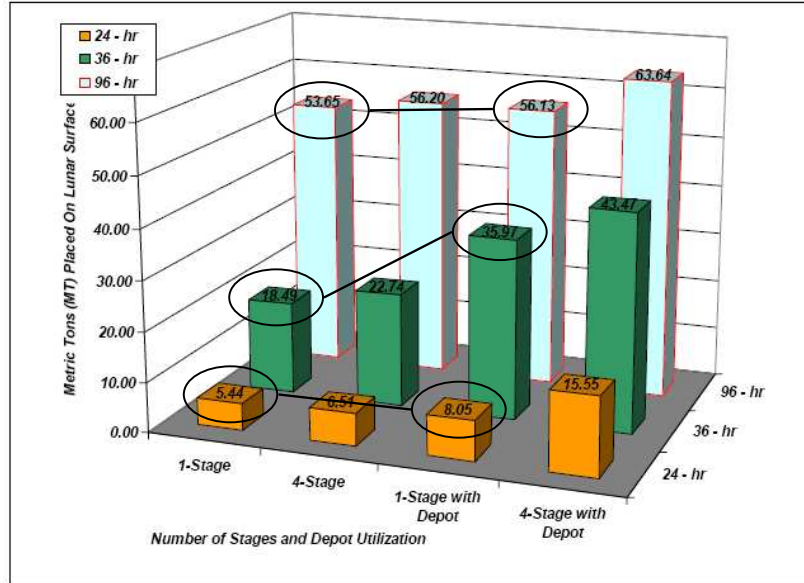


Figure 10: Lunar Surface Payload using OOS and Return Depots

In order to discuss the results shown in Figure 10 the reader should ignore the “4-stage” cases because these refer to the use of On Orbit Staging which does not apply to propellant refueling. The “1-stage” and “1-stage with Depot” results show the increase in lunar surface payload capability achieved when the architecture makes use of propositioned propellant in lunar orbit that is utilized for the return transfer maneuver. These results assume a 120 mt LEO payload capability and reusable transfer vehicle between Earth orbit and lunar orbit and a reusable lunar lander for transfer to and from the surface. These results show a potential improvement in the lunar surface payload of 95 percent depending on the return delta-V requirements can be achieved. A number of assumptions go into these results but they begin to provide insight into the potential payload improvement with this implementation of propellant refueling for return mission maneuvers.

There are two key concepts from this work. The first is that the introduction of a propellant depot in either Mars or Lunar orbit has the potential to increase surface payload capability. The second is that the amount of propellant needed for Earth return missions, in particular for Mars mission, can be substantial and the ability to decrease the propellant delivery price to \$1,000/kg can potentially save NASA's exploration program billions of dollars. As was also pointed out in the work done by Koelle, the need for low-cost propellant delivery is vital to the viability of propellant refueling.

Result: A depot in Lunar or Martian orbit that is capable of providing the Earth return propellants can increase the surface payload capability of the architecture.

Result: A low-cost propellant delivery method is required for the continuing development of propellant refueling. What price level constitutes a low cost solution?

2.2.6 REFUELING WITH NASA BASELINE ARCHITECTURE

A number of more recent studies have emerged since the announcement of the ESAS baseline architecture. These studies have focused on improving or in some way make use of the ESAS architecture elements. A number of concepts have been offer by Bienhoff as potential improvements to NASA exploration architecture. In his paper "Propellant Depots for Earth Orbit and Lunar Exploration" [18] Bienhoff investigates how the lunar surface payload capability can be improved if propellant refueling is available in LEO. Two potential concepts are proposed. The first is to re-fuel the portion

of the EDS propellant used during ascent which could improve the lunar surface payload capability by as much as 183% depending on the amount of propellant provided to the EDS. This would increase the capability of the EDS, but an additional means of providing an increase in payload to LEO would be needed. The second method would be to allow the EDS to perform both the TLI and LOI maneuvers. This would allow the lander to decrease the amount of propellant needed for its mission maneuvers. No longer requiring the LSAM to perform the LOI could potentially increase the surface payload capability from 18 mt to 51 mt, assuming the lander could be designed to house such an increase in payload capability. In both cases, the addition of propellant refueling in LEO can greatly increase the payload capability of the architecture. While this work discusses the performance benefits of propellant refueling, it does not investigate the additional costs or risks associated with implementing this capability into the current architecture. An additional investigation is needed to quantify these effects.

This study also discusses the cost advantages of incrementally building up the propellant depot utilizing the upper stages of commercial launch vehicle. The upper stages of both the Delta and Atlas class of launch vehicles utilize LOX/LH2 propellant and could be salvaged and utilized as the storage systems for the depot. A number of concepts are proposed and qualitatively compared based on the development/assembly cost, ease of integration and storage performance among a number of other criteria.

Result: Utilizing propellant refueling in LEO to increase the propellant on the EDS allows it to perform a wider variety of missions and increase the lunar surface payload capability of the baseline architecture.

2.2.7 NASA'S *REFUELING STUDIES*

The Marshall Space Flight Center (MSFC) has begun some initial work on In-space cryogenic propellant depots and how they could be applied to exploration applications. To date, little has been published on how they would apply a cryogenic depot to an exploration mission. A status report of their work was published in November 2006 [19]. This report outlines their work, which includes some initial propellant depot designs and explains how a LEO propellant depot could benefit commercial operators. This report suggests that a propellant depot could “offer significant advantages for NASA’s space exploration systems”. The details of these advantages are left up to future work; this work will include applying the propellant refueling concept to ESAS architecture. An outline of the future work to be completed as a part of this study is provided below. The first step in their future work aligns well with the work being done in this thesis, though little is known of the status of this work and the details being investigated.

1. Make in-space cryogenic propellant depots (ISCPD) part of the ESAS architecture
2. Encourage commercial development of ISCPD
3. Design cryogenic upper stage capable of propellant transfer with ISCPD
4. Conduct ground and flight experiments utilizing ISCPD components
5. Build and test prototype ISCPD module
6. Study lunar surface ISCPD

The NASA Langley Research Center has also conducted a recent study that involves the use of propellant refueling. The Orbital Aggregation and Space Infrastructure System (OASIS) [20] study was conducted over several years and involved the design of a permanent lunar architecture that could transfer crew and cargo from the ISS to the lunar surface. The architecture utilized re-usable in-space architecture elements in order to reduce the hardware that had to be launched to LEO for each mission. The chemical transfer stage and propellant module would provide transportation for crew and cargo between LEO and the first Earth-Moon Lagrange point (L1). A lunar transfer vehicle could be placed at L1 to provide transportation to and from the lunar surface. The baseline ESAS architecture requires that all architecture elements be delivered for each mission, which requires the development of a large heavy lift launch vehicle. Utilizing these re-usable stages would allow for a smaller launch vehicle design. In addition, a number of refueling flights would be needed to provide the needed in-space propellant which could be provided by a low-cost commercial operator. This study suggested that propellant would need to be delivered at a rate of less than \$1,000/kg. The feasibility of this price will be presented at the end of this chapter.

Result: Propellant refueling provides a path for developing re-usable in-space architecture elements. These re-usable elements would help reduce the launch vehicle payload requirements.

2.2.8 SUMMARY OF REFUELING DESIGN STUDIES

A summary of the different vehicles concepts that have been discussed in this chapter are provided in Table 2. While the general architecture for a lunar mission remains the same, each concept provided their own solution to accomplish each leg of the lunar mission. The most notable difference between these studies and the current lunar architecture is the use of re-usable launch elements instead of expendable vehicles. Re-usable architecture elements rely on the ability to be re-fueled in order to continue to provide their mission maneuvers. The work presented in this thesis will focus on the current lunar architecture elements and will not investigate the impact on re-usable architecture elements.

Table 2: Comparison of Vehicle Concepts Considered

Design	Previous Studies	Current Concepts
Launch Vehicle	Saturn V ^[13] , STS-C ^[11] , SSTO ^[16] , RHLV ^[16]	CaLV, CLV
In-Space Transfer	Upper Stage ^[13] LTV ^[11,16] , SSTO ^[16]	EDS
Lunar Lander	LuBUS ^[16] , SSTO ^[16] , LEV ^[11]	LSAM
Earth Return	SM ^[13] , LTV ^[11,16] , SSTO ^[16]	SM
Depot Location	LEO ^[13,16] , ISS ^[11,20] , LLO ^[18] , Mars ^[18]	--

A number of results have been presented in this chapter to summarize the important conclusions made during this literature review. Below are four hypotheses that will be examined during this thesis that have been developed from the results of the previous design studies.

- The concept of propellant refueling is technically feasible and does not result in a significant decrease in the architecture's mission success probability as discussed in the Apollo Mission Mode Analysis [13].
- Utilizing propellant re-fueling in LEO can increase the propellant on the EDS, allowing it to perform a wider variety of missions and increase the lunar surface payload capability of the baseline architecture. [13, 16, 18].
- A propellant depot in lunar or Martian orbit can improve the extensibility of NASA's exploration architecture by decreasing the amount of propellant that the architecture elements must deliver to LEO. [17, 18]
- A low cost propellant delivery price is needed to make re-fueling affordable to NASA's exploration program [13, 16, 17, 20].

A number of design concepts utilizing propellant refueling have been discussed in this chapter. In the previous section, a summary of the conclusions from these studies was presented. While these studies provided an initial look at propellant refueling, they failed

to provide a comprehensive analysis of the entire propellant refueling design space. This thesis will address the inadequacies of these previous studies and explain what must be addressed in order to obtain a complete understanding of how propellant refueling can impact future exploration missions.

The primary piece of information missing from the majority of the previous design work is a detailed quantitative analysis. The studies usually focus on describing the concept of interest and how it would utilize propellant refueling, while a detailed analysis of the overall performance is provided only as an afterthought or is left to future work making it difficult to understand the benefits that are achieved. Most of the previous work also only considers a single implementation of propellant refueling and does not provide a complete investigation of how various methods impact the design of the architecture. It is difficult to develop a complete understanding of propellant refueling because, depending on the study, each method is evaluated with various vehicles and design assumptions. A unified analysis would provide a clearer depiction of the effects of propellant refueling. A recurring theme throughout much of the previous work is that propellant refueling is required for future exploration missions, but no analysis is provided to verify this claim. In order to understand if exploration missions benefit from the introduction of propellant refueling, a reference architecture is required that does not utilize propellant refueling. In this study, the baseline ESAS lunar architecture is used as a point of comparison. By utilizing a set of FOMs, the impacts of propellant refueling can be measured. The primary analysis presented in these studies focuses on a single evaluation criterion. This is often the change in payload capability, but this metric does not consider the full impact of propellant refueling. The effects on life cycle cost,

reliability, and development risk, as well as payload capability, must also be evaluated to fully understand the total impact. The final shortcoming of these studies is that all but the work done by Beinhoff has focused on either out-dated concepts, such as the Space Shuttle, or on re-useable architecture elements. Neither scenario is a part of the next step in NASA's exploration program.

The work presented in this thesis will attempt to provide a more complete investigation as to the potential benefits and cost that would be associated with in-space refueling and examine how it would apply to NASA's current vision for space exploration. The results of this study will answer the following questions:

- What improvement in lunar surface payload can be achieved?
- Is there an improvement in the overall life cycle cost of the program?
- Can the mission success and overall reliability be improved?
- Does this capability provide an easier pathway to other exploration missions?
- Is low cost propellant delivery realistic at the quantities required for exploration?
- Is there a transportation architecture that can benefit from in-space refueling?

2.3 CURRENT PROPELLANT REFUELING TECHNOLOGY DEVELOPMENT

In addition to understanding how propellant refueling could benefit future exploration missions, it is also important to understand the feasibility of this new technology and the development risk associated with maturing it to the appropriate level. There are nine main areas of focus associated with the development of in-space cryogenic propellant refueling [21] as shown in Figure 11. The current research has focused on how

the fluid could be transferred in a zero-g environment and how propellant boiloff can be controlled through both active and passive systems.

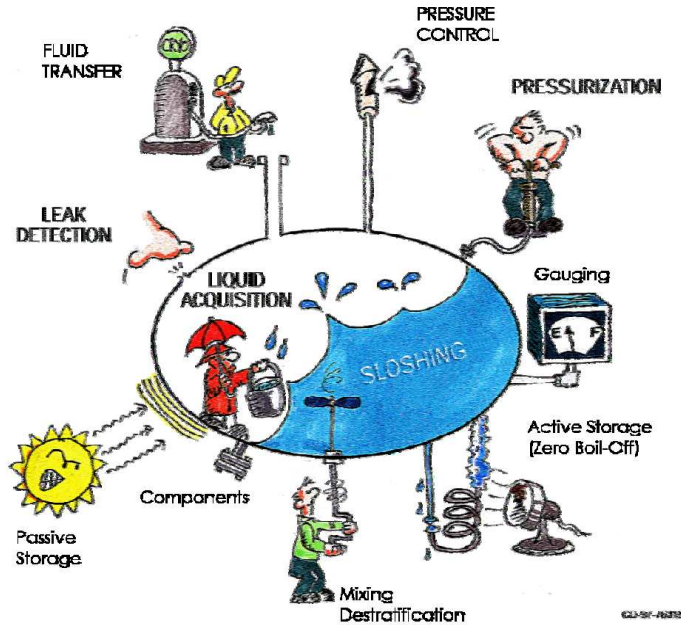


Figure 11: Cryogenic Fluid Management Key Concepts

The ability to develop these systems will be essential to the viability of propellant re-fuelling as a long-term solution to the growing needs of future exploration missions.

2.3.1 IN-SPACE PROPELLANT TRANSFER TECHNOLOGIES

There are several methods that provide the capability to transfer fluids in a zero-g environment. The ability to transfer propellant in such an environment is not a new technology and is routinely done in today's space operations. Propellant is transferred from tank to engine and, in some cases, from tank to tank. The ability to make and break the fluid transfer interface is what makes this so difficult because little has been

developed in this area [22]. It should be noted that, while little advancement has been made on the side of US space operations, the Russian Space Agency had began using this technology in the late 70s to re-fuel the Salyut Space Stations [22]. While this technology may not be directly applicable to current fluid transfer operation, it does provide a proof of concept that fluid transfer can be obtained in a zero-g environment for storable propellants. The most notable fluid transfer test performed to date by NASA is the Orbital Refueling System that was tested on STS 41-G [23]. This experiment made six successful transfers of 142kg of Hydrazine between two separate tanks. An extra-vehicular activity (EVA) was also performed to connect a fluid transfer line to a simulated satellite valve. There are significant differences between hydrazine and cryogenic fluids, but this was a significant initial achievement.

The simplest concept for cryogenic fluid transfer is the transferring of propellant through either linear or angular acceleration. In this case, the propellant is transferred from one tank to another through simple gravitational forces [24]. An example of a linear acceleration system is provided in Figure 12. Given a one foot diameter transfer line and a 10^{-4} acceleration environment, the fluid transfer of LH2 would occur at a rate of 8 lbm/sec [24]. The disadvantage with this type of transfer system is that a propulsion system is required that is capable of maintaining the gravitational field for several hours. This type of system may not be realistic for large propellant transfer. In that case, a pump or pressure system may provide a more effective means of fluid transfer.

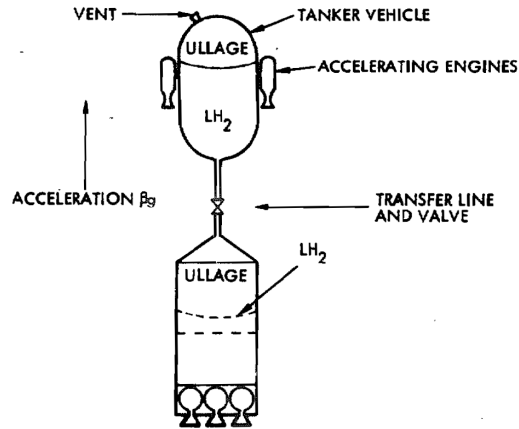


Figure 12: Linear Acceleration Fluid Transfer Technique [24]

Boeretz outlines several non-acceleration options that may be more applicable to large propellant transfer needs [24]. These options include the use of an inert or boiloff gas as the pressurant, a low net positive suction head transfer pump, and a gas generator pressurization option. The author points out that the selection of one of these methods greatly depends on the quantity of propellant to be transferred, the available transfer time, and the propellant fluid type. Additional research is required in each of these areas to more accurately determine the best option.

One of the most promising concepts for cryogenic propellant transfer is “no-vent fill”[23]. In this system the propellant is pressurized with its own vapor pressure and then liquid sub-cooling is used to return the remaining vapor back to a liquid at a small cost of propellant. In this case only minimal venting of propellant is required. Large-scale ground testing of a LH2 no-vent fill system has been conducted utilizing near flight ready hardware. These tests have shown that a 90 percent transfer of propellant can be achieved. To date, no in-space demonstration has been conducted.

2.3.2 LONG TERM PROPELLANT BOILOFF MITIGATION TECHNIQUES

Propellant boiloff mitigation can be achieved through the use of both active and passive systems. Passive techniques such as multi-layer insulation (MLI) and vapor-cooled shields have a more mature development than active systems, but they can not achieve zero boiloff levels. The current state of the art in passive insulation can limit propellant loss of liquid hydrogen (LH2) to approximately three percent per month [21], a level that would not be insufficient for long-term propellant storage. An active thermal management system uses cryo-coolers to keep the propellant below its vaporization temperature. A cryo-cooler is a refrigeration system design to maintain cryogenic temperature levels. In this case, near zero boiloff levels are achievable over long durations. An active system requires additional vehicle dry mass, but studies have shown that this additional mass can be offset by the propellant savings within as little as seven days [21]. Chato describes the technology readiness level of advanced passive thermal management methods to be around five and of active systems to be between three or four depending on the propellant selected. These TRL levels could be advanced to six, the minimal level NASA will consider, through a limited number of tests in a LEO environment.

The Marshall Space Flight Center (MSFC) has built a test bed that has been used for developing more efficient active and passive insulation systems. The initial work done using the test bed focused on a material similar to that used in the Shuttle External Tank (Isofoam SS-1171) [25] to protect during ground holds and ascent. The results of this study showed that a 41 percent heat leak reduction could be achieved with 25 fewer MLI layers than to that of the best previous MLI performance using variable density

MLI. Recent work utilizing the hydrogen test bed has focused on the development of active zero boiloff systems. The system was able to show that LH2 could be maintained at zero boiloff levels for the life of the cryo-coolers at a 25, 50 and 90% fill of the storage tank. The system has not been flight qualified nor has it been developed to a flight ready level. The test provided evidence that zero boiloff is obtainable. The issue now is developing a system that can reach these levels with minimal mass so that active thermal management systems provide a more attractive option than current passive systems.

Schuster has provided four conceptual-level designs for active propellant cooling. These systems use hydrogen boiloff that is passed through vapor-cooled shields to regulate the environmental temperature [26]. A schematic for each of these systems is provided in Figure 13. Concepts one through three have a minimal amount of boiloff that is stored for use in tanking, while the fourth re-liquefies all boiloff propellant reaching zero boiloff conditions. An additional pumping system is required for propellant transfer. Based on the assumptions of this study, the first concept is preferred from a development standpoint because it offers the lowest estimated development and production cost since a refrigeration system is not required. It does result in a 0.2% boiloff per month which would likely increase the price of propellant because more launches are required.

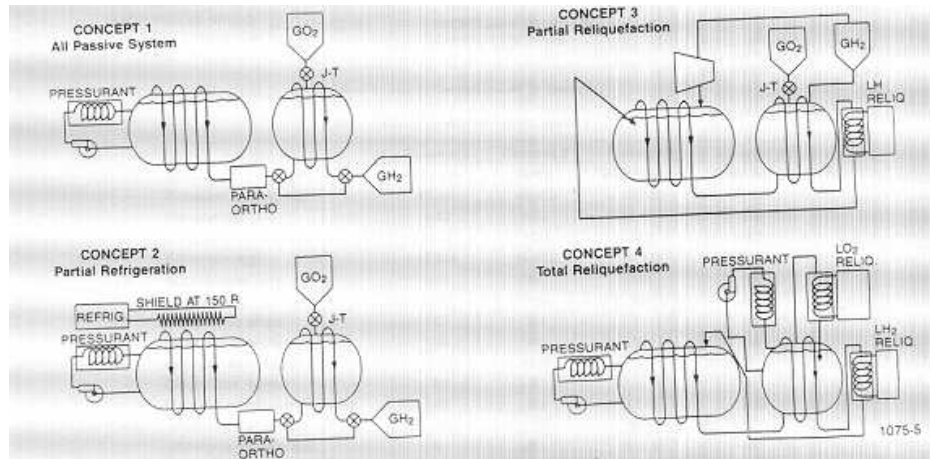


Figure 13: Boiloff Management Concept Schematics [26]

Platcha conducted a study in 2004 to test zero boiloff capabilities in a thermally relevant environment. The experiment used both MLI and cryo-coolers to control the internal pressure of the storage system to prevent the need of propellant venting. The use of both an active and passive system may provide a more optimal solution. The MLI is able to reduce the heat that reaches the cryogenic fluid thus reducing the heat that must be removed by the cryo-coolers. The test was performed under a vacuum at 230K with flight ready components where applicable; a detailed overview of this test can be obtained in reference [27].

A number of recent efforts have been presented to provide the current development state of propellant refueling technologies. These efforts have primarily focused on fluid transfer and long term propellant storage. The Orbital Express satellite demonstrated that automated docking and fluid transfer was possible in LEO. However, only storable propellants were tested by this system. Additional research and testing is required to verify that a system can be developed to provide cryogenic fluid transfer.

Considerable work has also been performed by Platcha and the Marshall Space Flight center to advance the development of zero-boiloff technologies. Both development projects have show that zero-boiloff of LH2 can be achieved. However, both test beds were performed on the ground, and future development is needed to develop a flight ready and flight weight system that could be used to verify the technology in LEO. These test demonstrations have shown that propellant refueling technologies are obtainable in the near future. While the development risk of these technologies is not zero, the current development effort has greatly decreased the risk.

2.4 COMMERCIAL LAUNCH INDUSTRY

One of the major requirements of propellant refueling is the ability to provide the large quantities of propellant to LEO that can then be utilized by the architecture elements. This propellant must not only be provided in possibly large quantities on a regular schedule, but it must also be delivered at a “low enough” cost that it remains a viable option for future exploration missions. This study will not focus on the cost of the propellant in LEO nor by whom it is provided, but rather assume a range of cost for deliver the propellant needed or each mission. The following section will outline the current launch vehicles in both the United States and international commercial launch markets. It will also outline the emerging industry of responsive space launch vehicles that promise to offer access to space at a much lower cost than is possible today.

2.4.1 DELTA FAMILY OF VEHICLES

The original Delta class launch vehicle was a derivative of the Air Force's ballistic missile Thor. In 1959, NASA contracted with Douglas Aircraft to build 12 Thor-Delta rockets that would be used to launch NASA's first series of scientific and exploration payloads [28]. Over the next 50 years, the Delta family of vehicles would be the main launch system used for all scientific and communication satellites. Boeing Integrated Defense currently operates two classes of Delta launch vehicles: the Delta II and Delta IV. The original Delta was made obsolete with the development of the Delta II, and the Delta III has been retired due to lack of demand in the commercial communication market. The Delta II began service in 1989 and has incurred only a single failure in its first 100 flights [28]. The Delta IV began flights in 2002 and has currently conducted six successful launches of the Delta IVM (medium payload). The Delta IVH (heavy payload) experienced a partial failure during its maiden flight that prevented it from reaching its desired orbit. A summary of the capability of these vehicles can be found in Table 3. The Delta IVH, which is in the final testing stages, offers to provide a much larger payload capability at a lower \$/lb.

Table 3: Delta Family Launch Vehicle Summary [29]

	Payload [lbm]	Launch Price [\$M]	Cost/Pound [\$ /lb]	Success Rate
Delta II -7320	6,300	40	6,300	108/110
Delta II -7925	10,900	52	4,700	108/110
Delta II -7920	11,300	50	4,400	108/110
Delta IVM	14,900	70	4,700	6/6
Delta IVM+	22,700	100	4,400	6/6
Delta IVH	45,200	140	3,100	0/1

2.4.2 ATLAS FAMILY OF VEHICLES

The Atlas launch vehicles can also trace their history back to the early development of Inter-Continental Baltic Missiles (ICBM). In 1953, the Atlas rocket program was given the Air Force's highest priority to accelerate its development efforts. In 1955, the program was given the highest national development priority due to reports on the status of the Russian ICBM program. Then in 1957, the first six Atlas D ICBMs were activated, operating out of Cooke Air Force Base. These ICBMs would later be converted into launch vehicles capable of delivering payload into Earth orbit. The Atlas D was first used as a delivery vehicle during the Mercury capsule program. The first commercial Atlas rocket was developed after the 1987 crash of the Space Shuttle. The program would develop four commercial launch vehicles with progressively increasing payload capability. Today, only the Atlas V is still in operation, though there are many derivatives of this vehicle with varying payload capabilities and cost as shown in Table 4. The Atlas V has conducted nine out of ten successful flights, including the launch of the Mars Reconnaissance Orbiter and the New Horizons Pluto Mission [30].

Table 4: Atlas V Launch Vehicle Summary [29]

	<i>Payload [lbm]</i>	<i>Launch Pric [\$M]</i>	<i>Cost/Pound [\$ /lb]</i>	<i>Success Rate</i>
Atlas V - 501	9,000	85	9,400	13/14 ^[31]
Atlas V – 531	15,200	100	6,600	13/14 ^[31]
Atlas V – 551	18,000	110	6,100	13/14 ^[31]

2.4.3 ORBITAL SCIENCES' FAMILY OF VEHICLES

Orbital Sciences' new class of launch vehicles are designed to offer a lower launch cost than current launch providers. These vehicles, however, offer a much smaller payload capability than many of the current launch vehicles, as can be seen in Table 5. These vehicles are able to achieve a lower launch cost through the use of similar stage components. They also utilize decommissioned Peacekeeper and Minuteman missile hardware to decrease the production cost. While these vehicles experience a higher \$/lb for payload delivery, they are able to offer a lower overall launch cost for the smaller satellite launch market.

Table 5: Orbital Sciences Launch Vehicle Summary [29]

	<i>Payload [lbm]</i>	<i>Launch Price [\$M]</i>	<i>Cost/Pound [\$ / lb]</i>	<i>Success Rate</i>
Pegasus	980	20	20,000	35/38
Taurus 2110	3,950	35	8,800	7/8
Minotaur	1,350	19	14,000	7/7

2.5 INTERNATIONAL COMMERCIAL LAUNCH INDUSTRY

In addition to the main US launch providers, there is a large list of international launch companies that can offer similar launch capabilities. In some cases, these vehicles can offer a lower launch cost, but in general these vehicles offer a similar launch cost to that of the United States launch providers. The following sections outline some of the major international launch providers.

2.5.1 ARIANE LAUNCH VEHICLES

The Ariane launch vehicles were originally designed by Arianespace, a commercial subsidiary of the French Space Agency Centre National d'Etudes Spatiales. Today the European Space Agency (ESA) works closely with Arianespace to coordinate all launches of the vehicles. The Ariane 1 was first launched in 1979; since then, there has been a total of five Ariane launch vehicles that have completed over 150 missions. Today only the Ariane 5 is still in operation. The Ariane 5 launches from Guiana Space Center, which has approximate latitude of zero degrees. This allows the Ariane 5 to optimize its geostationary transfer orbit payload as it does not have to waste energy to change inclination. The Ariane 5 has almost the same payload capability as the Delta IVH and can be offered at a slightly lower launch cost. While the Ariane 5 has experienced four failures during its life time, it has not experienced a failure in its last 20 launches. A summary of the Ariane 4 and 5 is provided in Table 6.

Table 6: Ariane Family Launch Vehicle Summary [29]

	<i>Payload [lbm]</i>	<i>Launch Price [\$M]</i>	<i>Cost/Pound [\$/lb]</i>	<i>Success Rate</i>
Ariane 4 - 40	4,600	60	13,000	97/100
Ariane 4 - 44P	7,600	80	10,500	97/100
Ariane 4 - 44L	10,800	100	9,300	97/100
Ariane 5	39,600	120	3,000	30/34

2.5.2 RUSSIAN LAUNCH VEHICLES

In the addition to the Soyuz rocket, the Russian Space Agency offers a series of crew and cargo launch vehicles that are used to launch non-human cargo into Earth orbit. The Soyuz's primary mission is that of humans, but in addition to human missions it has performed numerous cargo missions. Two of the most commonly used Russian rockets are the Proton and Kosmos 3. The Proton has flown over 300 times and is in the same category as the Delta IV H and Ariane 5, delivering in excess of 40,000 lbm to LEO. The Kosmos has a payload capability of around 3,000 lbm and has been providing cargo launches since the mid 1960's. Both of these vehicles have better than a 95% success rate and offer some of the lowest launch costs. A summary of these vehicles is provided in Table 7.

Table 7: Russian Launch Vehicle Summary [29]

	<i>Payload [lbm]</i>	<i>Launch Price [\$M]</i>	<i>Cost/Pound [\$ /lb]</i>	<i>Success Rate</i>
Proton D1	46,000	85	1,850	288/300
Kosmos 3M	3,300	12	3,600	420/440

2.5.3 ASIAN LAUNCH VEHICLES

There have been a number of launch vehicles developed by China, Japan, and Korea in the last 20 years. These include the Long March series developed by China, the H series by Japan, and the KSLV in South Korea. A sample of these vehicles is provided in Table 8. The payload capability of these vehicles is comparative to the other international countries discussed, though they have yet to develop a 40,000 lbm class

vehicle. Their launch price is somewhere between the Russian launch vehicles and the Ariane V.

Table 8: Asian Launch Vehicle Summary [29]

	<i>Payload [lbm]</i>	<i>Launch Price [\$M]</i>	<i>Cost/Pound [\$ /lb]</i>	<i>Success Rate</i>
Long March	8,500	40	4,700	20/24
H-11A 202	8,800	100	11,300	12/13
H-11A 222	20,900	140	6,700	n/a

2.5.4 US RESPONSIVE LAUNCH VEHICLES

In this work, the classification of a Responsive Space Launch Vehicle will include those which are being developed to significantly improve the cost of accessing space. An example of these companies includes SpaceX, Rocket Plane Kistler (RpK), and Air Launch. These companies have all been founded as new entrepreneurial enterprises that claim to be able to achieve a lower development and operational cost than either NASA or the larger commercial companies. They claim to be able to do this by streamlining the development and operational processes. This could result in launch costs that can be as much as 75% less than what is currently available with today's launch vehicles. The drawback with these companies is that they do not have any operational vehicles. SpaceX has conducted four test launches with the fourth achieving a successfully orbital insertion. SpaceX has completed its testing phase and will begin commercial operation in 2009 [32]. A summary of SpaceX's three main launch vehicles is provided in Table 9. Once these vehicles begin operation, their goal will be to prove to the industry that they can achieve the cost and reliability numbers that are promised.

Table 9: Responsive Space Launch Vehicles

	<i>Payload [lbm]</i>	<i>Launch Price [\$M]</i>	<i>Cost/Pound [\$ /lb]</i>	<i>Success Rate</i>
Falcon I	1,500 ^[33]	7	4,600	1/4*
Falcon 9	21,800 ^[34]	35	1,600	n/a
Falcon 9 H	62,600 ^[34]	90	1,500	n/a

* testing phase, final test scheduled for third quarter of 2008

2.5.5 NASA EXPLORATION ARCHITECTURE ELEMENTS

In addition to the numerous commercial launch companies that could provide propellant to NASA’s exploration architecture, the architecture itself could be used to provide propellant to LEO. The cargo launch vehicle has a payload capability of 100,000 lbm to LEO in addition to the 225,000 lbm of TLI propellant it also delivers to LEO. This equates to 325,000 lbm of potential propellant delivery capability which could be used for various propellant refueling activities. It is not clear what the propellant needs of the architecture will be or what the marginal cost of an additional launch would be, but the CaLV could potentially provide the lowest cost propellant delivery option with a possibility of achieving a marginal cost of lower than \$1,000/lb. Utilizing the CaLV would not help NASA promote the commercialization of space and would require the architecture to increase its flight rate every few years, but neither of these are potentially detrimental to this design option. A range of values is provided in Table 10 because the true costs of the CaLV are not publicly available. Case 1 represents an estimate of the marginal cost of a CaLV assuming an 80/20 split between the fixed and variable cost. Case 2 is an estimate of the Theoretical First Unit (TFU) costs, and Case 3 is the unit cost

after the 20th launch assuming a learning curve rate of 90%. A further investigation of the cost of the CaLV will be provided in this thesis.

Table 10: Cargo Launch Vehicle Delivery Capability

	<i>Payload [lbm]</i>	<i>Launch Cost [\$M]</i>	<i>Cost/Pound [\$lb]</i>
CaLV (1)	325,000	200*	600
CaLV (2)	325,000	700*	2,200
CaLV (3)	325,000	440*	1,350

* Estimated launch costs

2.5.6 RANGE OF \$/LB CONSIDERED FOR PROPELLANT REFUELING STUDY

The results of the previous sections showed that there are a number of potential launch providers available that offer a varying range of capability and price. These launch vehicle have demonstrated reliabilities that range from 0.83 – 1.0, but most launch providers can demonstrate a reliability greater than 0.95 (Figure 15). The results in Figure 14 and Figure 15 show a summary of the results of the previous sections. These figures provide a comparison of capabilities between the United States and the International launch Industry.

There are a number of factors that that must be considered when selecting a propellant refueling launch provider. When a single payload is launched, such as a satellite, the most important factors are to select the launch vehicle that has the capability to deliver the payload at the lowest possible price while achieving the minimally acceptable launch reliability. Because propellant is a more fluid medium, it can be delivered over a greater number of launches assuming a storage depot is available in

LEO. Therefore, the most important factor to consider is not the launch price or the payload capability but rather the cost per pound (\$/lb) to NASA. The weight of the propellant delivery system will reduce the amount of propellant that can be delivered to LEO. This can potentially increase the cost of delivering propellant.

The results in Figure 14 demonstrate how the \$/lb of payload delivery decreases as the capability of the launch vehicle increases. The same trend is seen for both US and international launch vehicles. The US launch vehicles generally offer a lower \$/lb for the small to medium class of launch vehicles while the international launch vehicles offer a lower \$/lb for vehicles with a payload capability of 40,000 – 50,000 lbm. In either case the difference between the two are small, except for two notable exceptions, which are marked with blue circles in the figure. These represent the Russian Kosmos and Chinese Long March launch vehicles. Both launch vehicle are able to achieve significantly lower \$/lb than the US launch vehicle of the same payload capability.

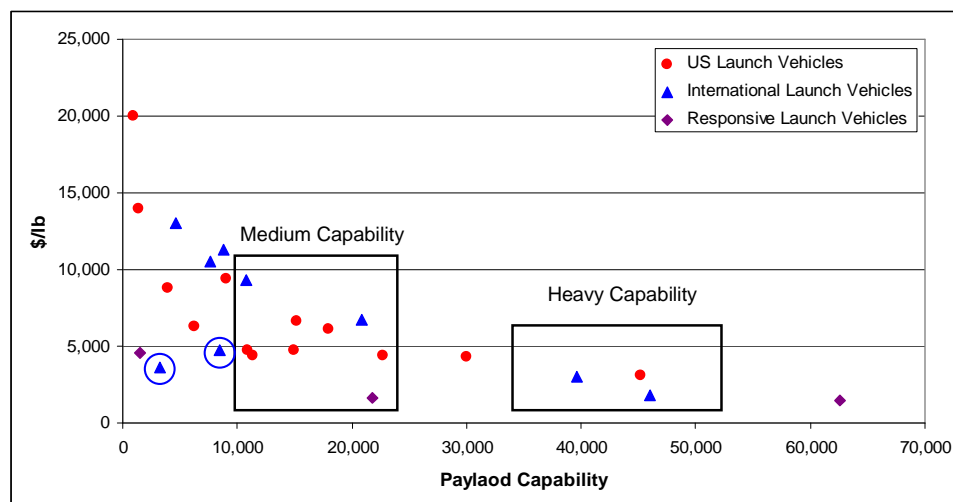


Figure 14: Summary of \$/lb as a Function of Payload Capability

While the international launch vehicles can, in some cases, provide a lower \$/lb than US launch vehicles, they have not demonstrated the same level of launch reliability. In all but two cases, the US launch vehicles provide the highest demonstrated launch reliabilities; these results can be seen in Figure 15. The Long March, which offers a low \$/lb, has a demonstrated reliability of 0.83. This is significantly lower than 0.98 – 1.0 reliability achieved by most US launch vehicles. While this vehicle can demonstrate a lower cost than its US counter part (Delta II), its lower reliability makes it a riskier launch provider. Most other international vehicles have a higher reliability than the Long March, but all are lower than the US vehicles. There is no reliability probabilities quoted for the responsive launch vehicle because these vehicles have not completed their development testing phase and have no commercial launch flights to reference. To date, Space X has attempted four test flights of the Falcon 1, and will begin operating commercially in 2009. These vehicles have potential to offer the lowest \$/lb, but there is additional risk in depending on their development.

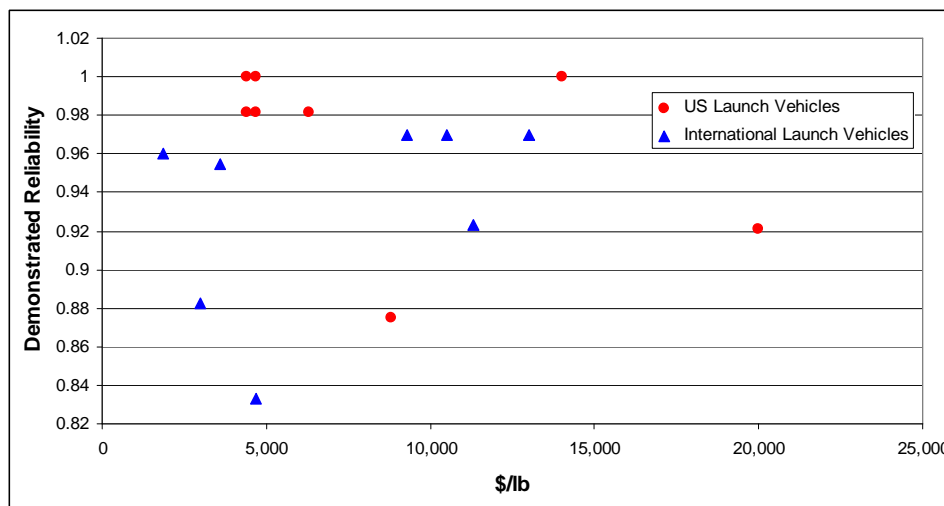


Figure 15: Summary of Demonstrated Reliability as a Function of \$/lb

Table 11: Summary of Potential Launch Vehicles

	<i>Payload [lbm]</i>	<i>Launch Price [\$M]</i>	<i>Cost/Pound [\$/lb]</i>	<i>Success Rate</i>
CaLV (1)	325,000	200	600	n/a
CaLV (3)	325,000	440	1,350	n/a
Falcon 9 H	62,600	90	1,500	n/a
Falcon 9	21,800	35	1,600	n/a
Proton D1	46,000	85	1,850	288/300
CaLV (2)	325,000	700	2,200	n/a
Ariane 5	39,600	120	3,000	30/34
Delta IVH	45,200	140	3,100	0/1
Kosmos 3M	3,300	12	3,600	420/440
Delta II -7920	11,300	50	4,400	108/110
Delta IVM+	22,700	100	4,400	6/6
Falcon I	1,500	7	4,600	n/a
Delta II -7925	10,900	52	4,700	108/110
Delta IVM	14,900	70	4,700	6/6
Long March 3	8,500	40	4,700	20/24
Atlas V - 551	18,000	110	6,100	13/14
Delta II -7320	6,300	40	6,300	108/110
Atlas V - 531	15,200	100	6,600	13/14
H-11A 222	20,900	140	6,700	n/a
Taurus 2110	3,950	35	8,800	7/8
Ariane 4 - 44L	10,800	100	9,300	97/100
Atlas V - 501	9,000	85	9,400	13/14
Ariane 4 - 44P	7,600	80	10,500	97/100
H-11A 202	8,800	100	11,300	12/13
Ariane 4 - 40	4,600	60	13,000	97/100
Minotaur	1,350	19	14,000	7/7
Pegasus	980	20	20,000	35/38

A number of studies, some discussed in this chapter, suggest that achieving a low-cost propellant delivery system is vital to the success of propellant refueling and future exploration architectures. These studies do not go into detail as to what the price of propellant would have to be in order to make propellant refueling a beneficial part of exploration systems. This work will define the price required to provide an architecture improvement to NASA's exploration architecture. This study will consider a range for the price of propellant from \$1,500 to \$6,000/lb. The \$1,500/lb represents the quoted potential of the Falcon class of launch vehicles. The \$6,000/lb represents the average launch price in today's market (Atlas, Delta) increased by 20 percent to account for uncertainty in launch price and final payload capability. This range will be used throughout the rest of this work to show the effect that propellant price has on the implementation of propellant refueling. It will also be noted again that the introduction of propellant refueling could provide the demand required to make reusable launch vehicles viable option for future transportation missions. This would ultimately drive down the cost of delivering payload to LEO to less than \$1,000/lb [35], which would allow propellant refueling to become and even more attractive solution.

CHAPTER 3

PROPELLANT REFUELING DESIGN SPACE

This chapter will discuss the design space investigated in this thesis. The design space is defined as the set of all design options considered for comparison. Included in this study are both refueling and non refueling design points. A Morphological Matrix [36] will be used to provide the inputs for this design space to the simulation environment where the FOMs can be evaluated. This design space exploration will provide an understanding of how the implementation of propellant refueling can affect the design NASA's baseline exploration architecture. A value proposition for propellant refueling can then be developed.

3.1 PROPELLANT REFUELING EVALUATION METHODOLOGY

The methodology employed in this thesis, to develop the value proposition for propellant refueling, can be broken down into three areas. A flow chart for this methodology is provided in Figure 16. Chapter 1 consisted of a discussion of the current exploration architecture and the major performance challenges that have emerged during its development. The introduction of propellant refueling was suggested as a means to mitigate these challenges. Chapter 2 provided a literature search on propellant refueling that summarized the work done to date and provided an initial set of propellant refueling concepts to investigate. These two chapters comprise the first section of this methodology and set the tone for why propellant refueling is being investigated in this thesis.

The development of the propellant refueling design space and the simulation environment used to evaluate the impacts of propellant refueling on the baseline architecture comprise the second phase of the methodology. These will be outlined in Chapters 3 and 4. Chapter 3 utilizes the information gathered in the first two chapters to select the set of design options and variables related to propellant refueling that provide the greatest benefit to the design of the architecture. The final set of nine variables is discussed in Section 3.2. A morphological matrix is generated from these variables to establish the allowable values for each of the design variables. For example, the LSAM ascent engine has four choices: Hypergols, LOX/CH₄, LOX/LH₂ (pressure) and LOX/LH₂ (pump). The entire morphological matrices for Scenarios One and Two are provided in Figure 17 and Figure 18. This matrix encompasses the entirety of the propellant refueling design space that will be explored, and results in over 15,000 possible design combinations between Scenarios One and Two. Chapter 4 discusses the simulation environment developed to evaluate the effects that propellant refueling has on the baseline architecture. The effect on the baseline architecture is measured by the impact on the architecture FOMs presented in Chapter 1.

The final part of this methodology is to use the results generated from the propellant refueling design space simulation to evaluate the potential value added to the exploration architecture. This will be presented in the form of Pareto frontiers (Chapters 5 and 6), an improvement in the cost per pound of payload to the lunar surface (Chapters 5 and 6) and the value proposition to NASA (Chapter 7).

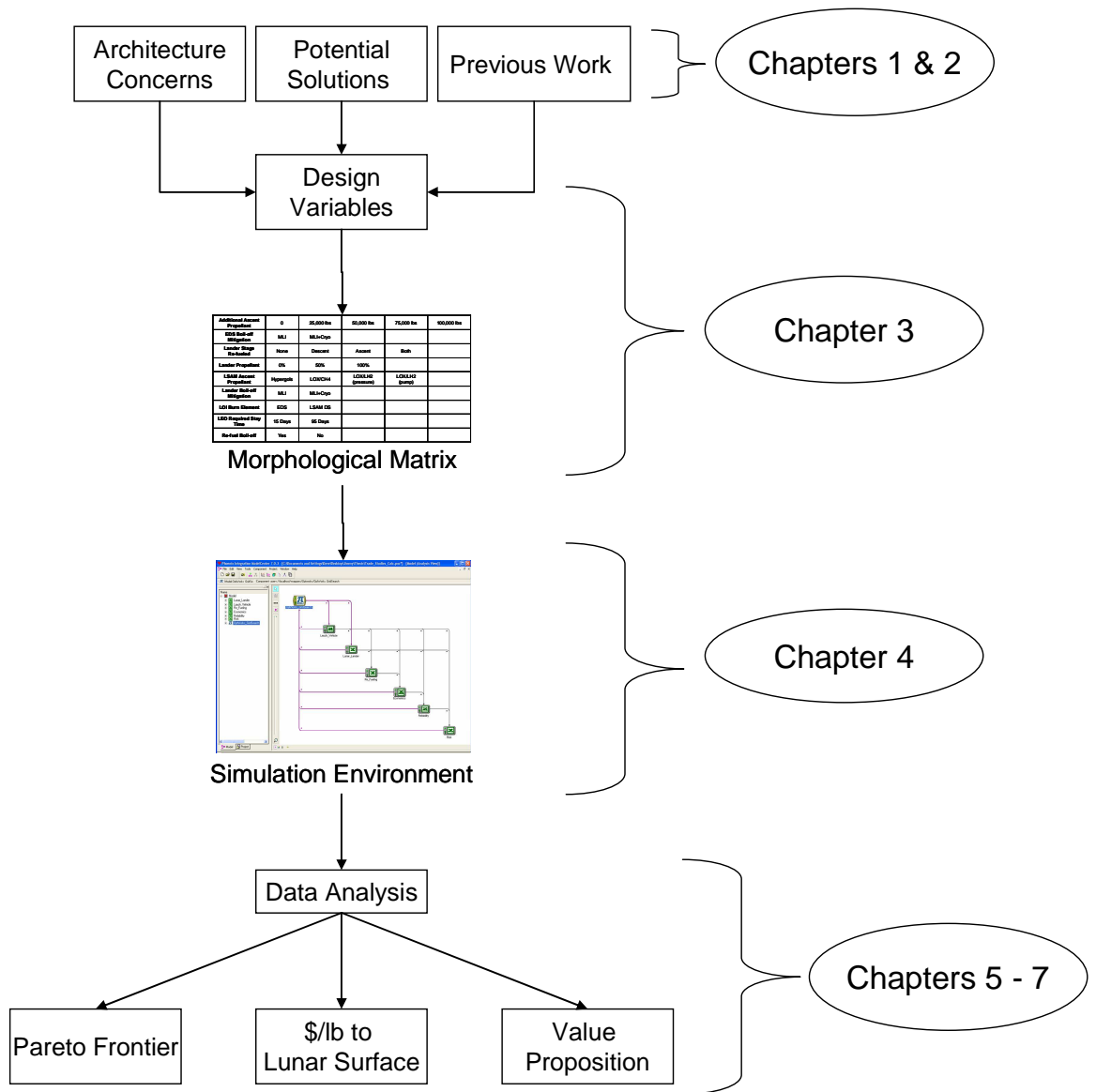


Figure 16: Propellant Refueling Evaluation Methodology

3.2 PROPELLANT REFUELING DESIGN SPACE

The propellant refueling design space represents the set of trades that will be investigated in this work. There are nine input variables for Scenario One and ten for Scenario Two that create a design space of 15,000 propellant refueling combinations. These design options were selected based on the results of the literature search provided in Chapter 2. These previous design studies provided an initial foundation for selection of the refueling option which will be evaluated throughout this dissertation. It is the goal of this work to establish which of these potential refueling strategies provides the greatest value to future exploration missions. The remaining design options were selected based on particular concerns that have emerged during the development of the baseline architecture (AS engine selection, mitigation method, and boil-off refueling). A set of inputs is created by selecting a value from each row of the morphological matrix. For example, the inputs in the second column represent the baseline configuration (Figure 17). There are a number of designs where no propellant refueling is utilized. This will be an important point of comparison in Chapters 5 and 6. These points of reference will show the improvements and drawbacks of introducing propellant refueling into the baseline architecture.

The morphological matrix is used to define the inputs to the simulation environment. In addition to the design variables provided in Figure 17 and Figure 18, a number of other design variables were initially considered. These include the in-space depot location, refueling the Service Module, and utilizing the CLV 2nd stage for the TLI maneuver. Refueling the SM and utilizing the CLV as the EDS were removed from this study because it is unlikely the development of the propellant refueling technologies

could be completed before these vehicles began operation. The benefits of a lunar stationed depot depend on the ability to provide propellant from the lunar surface. A feasibility study of in-situ resource utilization is beyond the scope of this thesis. These three choices were therefore eliminated from consideration. There is potential value in these options and they should be considered in future propellant refueling design studies. The following sections provide a description of each design variable and the range of inputs used in this work.

Additional Ascent Propellant	0	25,000 lbs	50,000 lbs	75,000 lbs	100,000 lbs
EDS Boil-off Mitigation	MLI	MLI+Cryo			
Lander Stage Re-fueled	None	Descent	Ascent	Both	
Lander Propellant	50%	100%			
LSAM Ascent Propellant	LOX/CH4	Hypergols	LOX/LH2 (pressure)	LOX/LH2 (pump)	
Lander Boil-off Mitigation	MLI	MLI+Cryo			
LOI Burn Element	EDS	LSAM DS			
LEO Required Stay Time	95 Days	15 Days			
Re-fuel Boil-off	No	Yes			

Figure 17: Trade Study Morphological Matrix, Scenario One

Offload TLI propellant (LOX)	0	25,000 lbs	50,000 lbs	75,000 lbs	
Offload TLI propellant (LH2)	0	5,000 lbs	10,000 lbs	15,000 lbs	
EDS Boil-off Mitigation	MLI	MLI+Cryo			
Lander Stage Re-fueled	None	Descent	Ascent	Both	
Lander Propellant	50%	100%			
LSAM Ascent Propellant	LOX/CH4	Hypergols	LOX/LH2 (pressure)	LOX/LH2 (pump)	
Lander Boil-off Mitigation	MLI	MLI+Cryo			
LOI Burn Element	EDS	LSAM DS			
LEO Required Stay Time	95 Days	15 Days			
Re-fuel Boil-off	No	Yes			

Figure 18: Trade Study Morphological Matrix, Scenario Two

3.2.1 ADDITIONAL ASCENT PROPELLANT

The first design option allows an increase in the amount of propellant burned during ascent on the Earth Departure Stage (EDS). In the baseline architecture the EDS is initially used as a second stage to deliver the LSAM to LEO. It is subsequently used to inject the LSAM, CEV and SM into a lunar approach trajectory or Trans Lunar Injection (TLI). A greater payload capability can be obtained if a fraction of the 225,000 lbm of TLI propellant is used during the second stage burn of the EDS to inject in to LEO. If this propellant is used during ascent, the EDS must be re-fueled in-orbit in order to have the propellant required for the TLI burn. The ability to burn additional propellant during ascent increases the mission payload that the launch vehicle can deliver to LEO and thus to the lunar surface. This work considers burning from 0 to 100,000 lbm of additional propellant from the EDS during ascent. A greater amount of propellant could be burned

during ascent, but the increase in payload capability is negligible, or in some cases reduced because the system thrust-to-mass decreases thus increasing the gravity losses. The total payload capability versus the additional propellant burned is discussed in Section 4.1.1.

3.2.2 *BOILOFF THERMAL MANAGEMENT SYSTEM*

The use of cryogenic propellants in the baseline architecture results in a loss of propellant due to boiloff when propellant temperatures go below the heat of vaporization. The baseline architecture utilizes a passive insulation system to reduce the amount of propellant lost to boiloff. Since the passive system cannot completely eliminate boiloff, the architecture must carry additional propellant to LEO in order to have sufficient propellant to complete the mission maneuvers once the crew is delivered to LEO.

The boiloff thermal management system is used to reduce or eliminate the propellant boiloff from the EDS and LSAM. Two thermal management strategies are considered in this study. The first is a passive system that utilizes MLI blankets. The MLI insulation reduces the heat flux from the external environment to the propellant and thus maintaining a lower propellant temperature. This is a relatively simple system that is currently used. MLI only limits the boiloff and cannot eliminate it completely. The second option is to implement a cryo-cooler with MLI. In this case the cryo-coolers actively remove heat from the tanks, keeping the propellant at a constant temperature. A small number of MLI blankets are used to reduce the heat that the cryo-coolers must remove from the system. It is assumed that the cryo-cooler system results in zero propellant boiloff [37]. The simulation has the option to put either thermal management

system on the EDS, ascent stage of the LSAM and the descent stage of the LSAM. Since each element carries different quantities of propellant and for different mission times, each may favor the selection of a different thermal management option. A mass comparison between MLI and the cryo-cooler system is provided in Chapter 5, which will discuss the tradeoff between adding a more complex cryo-cooler system versus utilizing a simple passive system and allowing a set amount of propellant to boiloff.

3.2.3 LSAM STAGE RE-FUELED

This design variable is used to trade the benefits of off-loading propellant from the LSAM prior to launch. In the baseline architecture, the Descent Stage contains 57,000 lbm of LOX/LH₂ and the Ascent Stage contains 9,100 lbm of LOX/CH₄. This design variable will help to determine if there is a benefit in removing this propellant prior to launch and refueling the LSAM once it reaches LEO. Because the LSAM propellant mass fraction is nearly 50%, the lunar surface payload can be increased by decreasing the initial propellant delivered to LEO; however, the LSAM inert mass must grow (engines, tanks, etc.) to deliver this extra payload to the lunar surface. In addition, the launch vehicle shroud must increase in size and mass to accommodate a larger LSAM. The increase in fairing mass was calculated by assuming a constant mass per surface area for the fairing design. The baseline fairing design was used as the point of reference and a value of 1.998 lb/ft² was determined. Utilizing this value along with the surface area provides a means of estimating the mass of the larger fairing design. A sample set of masses is provided in Table 12. The size of the lander as a function of payload mass will be discussed in Section 3.3.2.

Table 12: CaLV Fairing Mass Estimates

Fairing Diameter	Fairing Mass
27.5 ft	10,552 lbm
30 ft	11,670 lbm
33 ft	13,052 lbm

This study considers four options for refueling the LSAM: only the descent stage, only the ascent stage, both stages or neither stage. These combinations will allow a number of propellant quantities and propellant types to be considered. The more stages and propellant types that are involved in the transfer, the greater the cost and risk to the architecture, but the greater the possible benefit. The size, complexity and cost of the propellant depot is a function of the type of propellant, the number of propellants, and the quantity that is required by the architecture. A further discussion of the propellant depot will be presented in Section 4.3.3. If both LSAM stages were re-fueled from the baseline LSAM design, the propellant storage system would need to be designed to carry three propellant types with three transfer systems. However, if the ascent stage used a LOX/LH2 system instead of LOX/CH4, than only two storage systems would be needed. Section 3.2.5 will discuss which propulsion systems were investigated for use on the LSAM.

3.2.4 LANDER PROPELLANT QUANTITY RE-FUELED

The baseline architecture delivers both stages of the LSAM to LEO with full propellant loads. The previous section discussed the option of offloading the LSAM ascent and descent propellant and refueling it in LEO, but this variable only determines which stage and not the amount of propellant offloaded. This section will discuss the quantity of the LSAM propellant that is offloaded. The design variable has the option to refuel either 50 or 100 percent of either stage of the LSAM depending on which options are selected for refueling. The baseline utilizes no re-fueling on the LSAM. This case is established by the previous design variable when “None” is selected. Therefore a zero percent option is not required here and reduced the duplication of results. The greater the amount of propellant offloaded the greater the payload improvement but the larger the cost to the architecture. By selecting which stage and what percentage of the stage is refueled a large number of refueling combinations can be considered. This will help provide a complete picture of the cost of improving the payload capability of the architecture through propellant re-offloading.

3.2.5 LSAM ASCENT ENGINE

The LSAM ascent engine is the only propulsion system allowed to change during this study. The propulsion systems on the CaLV and descent stage of the LSAM were held constant. The propulsion systems on the CaLV and descents stage of the LSAM are high performance LOX/LH2 engines and are required to meet the mass goals of the architecture. The main draw back of these systems is their higher rate of propellant boiloff. The introduction of propellant refueling may eliminate this concern. There is no reason to trade this design variable because propellant refueling will only improve what

has already been selected as the best option. The ascent engine is allowed to vary because it is the one propulsion system still being analyzed for its potential effects on the architecture. Further performance, risk and cost analysis is being conducted before the final engine design is selected. Allowing this engine to vary will also provide additional insight into how propellant refueling can effect the selection of certain engine configurations.

There are currently four propulsion systems being considered for use on the ascent stage of the lander. A summary of these engine parameters is provided in Table 13. The first is the use of NTO/MMH (Hypergols). These engines have the lowest specific impulse of any of the engines considered and would require additional development work, but exhibit no significant propellant boiloff. The second engine considered is a LOX/CH₄ engine. This is the baseline design selected for the ESAS baseline architecture. This engine requires the most advanced development work because a LOX/CH₄ engine has never been flight tested. However, a recent test firing of a methane engine has been completed [38]. The LOX/CH₄ engine has a higher performance than Hypergols engine and a lower boiloff rate than a LOX/LH₂ system. This engine was originally selected because it was believed to have a greater extensibility to future Mars missions. The final two engines are LOX/LH₂ systems; both pressure and pump fed engines are considered. These two systems are categorized by their method of feeding propellant into the thrust chamber. The pressure fed system utilizes an increased tank pressure while the pump-fed system utilizes high energy pumps. The trade off between these two systems is the additional complexity and mass of the pump-fed system versus the increased tank mass of the pressure-fed system [39]. The summary in Table 13

illustrates the difference in T/m_e (lb/lbm) and tank pressure between these two systems. The LOX/LH2 propulsion systems offer the greatest performance, but also results in the greatest amount of propellant boiloff because hydrogen has the lowest heat of vaporization. The analysis in Chapters 5 and 6 will discuss how the payload capability and costs of each of these systems affects the overall architecture.

Table 13: Summary of Ascent Engine Assumptions

Propellant	Isp [s]	T/m_e	Thrust [lbm]	Tank Pressure [psi]	O/F
NTO/MMH	323	30.4	9,300	250	1.65
LOX/CH4	361	28	9,060	350	3
LOX/LH2 (pressure)	460	28	9,890	350	6
LOX/LH2 (pump)	463	38.8	8,970	50	6

3.2.6 LOI MANEUVER

The baseline ESAS architecture uses the Descent Stage of the LSAM to insert itself, the CEV, and Service Module into a circular low-lunar orbit. This three burn maneuver, called the lunar orbital insertion (LOI), provides global access to the lunar surface. This architecture design was selected to minimize the required payload mass capability of the EDS, for LEO and TLI insertions (Figure 3).

When a propellant depot is used, the TLI propellant can be offloaded (as much as 100,000 lbm) from launch to LEO insertion. This 100,000 lbm constraint was placed on the design to limit the total propellant cost to the architecture and the total size of the payload delivered to LEO. Chapters 5 and 6 will discuss how offloading this propellant

affects the design of the architecture and will show that the Pareto-efficient solutions always utilize less than 100,000 lbm of propellant. In LEO, the EDS can be re-fueled to perform both the TLI and LOI maneuvers without any changes (except re-fuel capability). Using the EDS to perform the LOI maneuver greatly reduces the size and mass of the LSAM that must be used to descend to the lunar surface. As will be shown later, the elimination of the TLI propellant from the EDS and incorporation of the LOI maneuver significantly increases the lunar surface payload capability of the architecture. In this study the LOI maneuver can be performed by either the Descent Stage, as on the baseline architecture, or by the EDS.

3.2.7 LEO REQUIRED STAY TIME

One of the issues with the baseline architecture is that there may be factors that delay the planned launch time of the second vehicle [40]. This can lead to substantial propellant boiloff or the need for large cryo-cooler systems on the EDS. If the time between the launch of the CaLV and CLV exceed the on-orbit design limits of the EDS, the mission will be canceled. Thus the EDS and LSAM will be lost because there is no planned refueling capability. In the current plan, the risk of losing a mission due to a launch delay is mitigated by placing a requirement on the architecture that the EDS and LSAM must carry enough additional propellant to cover the boiloff losses for the LEO loiter time. In this study both 15 and 95 day loiter times are considered. Because the boiloff losses are largely dependent on loiter, a 95 day loiter time requires approximately six times the propellant or nine percent of the TLI propellant over the 15 days. The propellant boiloff for the EDS and LSAM for both a 15 and 95 day loiter period are

provided in Table 14, these values are obtained from the boil-off model used in this thesis. .

Table 14: LSAM and EDS Propellant Boiloff Comparison

Loiter Time	LSAM			EDS
	LOX/LH2	LOX/CH4	Hypergols	LOX/LH2
15 Days	1,080 lbm	1,030 lbm	890 lbm	3,785 lbm
95 Days	6,360 lbm	6,060 lbm	5,370 lbm	23,900 lbm

The analysis done by Cirillo [40] shows that the baseline architecture can obtain a mission reliability of 75-80 percent with a 15 day loiter requirement verses a 95 percent mission reliability for the 95 day design. The length of the loiter period has a substantial effect on the design of the architecture. A longer loiter period increases the amount of propellant that must be delivered to LEO, but provides the highest mission success, while a shorter loiter period reduces the payload requirements at the expense of a lower mission success probability. The introduction of propellant refueling can remove the need to carry additional propellant to LEO while also improving the mission success probability. The loiter time would become infinite if there were multiple sources for filling the propellant depot as defined in the following section.

3.2.8 RE-FUEL BOILOFF

A strategy for preventing mission failures associated with excessive LEO loiter is to develop cryogenic cooling system technology that can reduce or totally eliminate

boiloff. Another strategy is to allow the boiloff to occur and re-fuel this propellant just prior to TLI. This second strategy eliminates the need to develop large cryo-cooler systems that are discarded every flight and still provide for an extended LEO stay time. The boiloff is less than ten percent of the propellant delivered to LEO, but would have the potential to save billions of dollars in case of a mission delay. The capability to re-fuel the boiloff would extend the LEO loiter period for any length of time assuming a sufficient supply of propellant to the depot. This would eliminate the need to design the architecture around a specific loiter period providing an increase in payload capability, a lower LCC and a greater mission reliability.

3.2.9 TLI PROPELLANT OFFLOADED FROM EDS, SCENARIO TWO ONLY

The final design variable is only used in Scenario Two and replaces the design variable in Scenario One used to increase the amount of propellant used during ascent (Section 3.2.1). This design variable allows the TLI propellant to be off-loaded from the EDS prior to launch resulting in a decrease in the payload delivered by the CaLV. Scenario Two allows the size of the launch vehicle to decrease as the LEO payload is decreased. As a result, offloading the TLI propellant will decrease the size and development and production cost of the CaLV.

A range of 0 to 80,000 lbm of LOX and 0 to 20,000 lbm of LH2 can be offloaded from the EDS. An example of how this affects the size of the CaLV is provided in Table 15. The amount of propellant was limited to these ranges to keep the gross mass of the CaLV within 20% of the baseline design. Increasing the amount of propellant offloaded beyond these ranges would begin to require configuration changes, because of the overall

decrease in size of the CaLV. Since the baseline configuration was held constant in this thesis, values outside of these ranges were not considered. This also provided a maximum offloading of 100,000 lbm which was the maximum amount of propellant refueling considered in Scenario One.

Table 15: Change in CaLV Dimensions as TLI Propellant is Offloaded

	Gross Mass [lbm]	Length [ft]	Diameter [ft]
Baseline	6,390,000	358	13.75
80,000 lbm (LOX)	5,150,000	315	11.89
20,000 lbm (LH2)	5,689,000	329	12.61
80,000/20,000 (LOX/LH2)	4,920,000	301	11.22

Offloading LOX allows a greater total mass to be removed from the EDS, but offloading the LH2 provides a greater improvement on a per pound basis. An example of this is provided in Table 16. The primary cause is the lower density of LH2 as compared to the density of LOX. Offloading equal quantities of each propellant will provide a greater reduction in the in the size of the LH2 tanks, further reducing the size of the vehicle. The EDS holds a maximum of 35,000 lbm of LH2 propellant, thus in order to increase the offloaded mass beyond this quantity, LOX must be offloaded as well. The results in Chapter 5 and 6 will discuss the trade off between the cost of propellant in LEO and the cost saving of decreasing the size of the CaLV.

Table 16: Offloading LOX versus LH2

	Gross Mass [lbm]	Length [ft]	Diameter [ft]
20,000 lbm (LOX)	5,802,000	338	12.99
20,000 lbm (LH2)	5,689,000	329	12.61

This concludes the discussion on the design variables that are considered in this study. These variables are input into the simulation environment in order to measure their effects on the ESAS baseline architecture. This simulations environment will be discussed in great detail in Chapter 4.

CHAPTER 4

PROPELLANT REFUELING ANALYSIS AND SIMULATION ENVIRONMENT

This chapter will focus on the development of the propellant refueling simulation environment used to evaluate the affects of propellant refueling on the baseline architecture. This simulation environment provides an automated process for evaluating the design inputs discussed in Chapter 3. This environment models the effects that the input variables have on the architecture elements and then evaluates the resulting change to the Figures of Merit. The results of this simulation environment can then be used to begin developing an understanding of the total value of introducing propellant refueling in to NASA exploration architecture. The results from this simulation will be presented in Chapters 5, 6 and 7.

4.1 MODELING AND SIMULATION ENVIRONMENT

The lunar architecture propellant refueling simulation environment was developed using the ModelCenter [41] integration framework developed by Phoenix Integration. ModelCenter is a commercially available software that provides an architecture for passing information between different analysis models. In this case, the models have been developed using Microsoft's Excel[®]. The ability to automatically pass information between the different models greatly reduces the time required to run each simulation. After an initial setup, any number of simulations can be run without any human

interaction. An illustration of the flow of information within this environment is provided in Figure 19, and the variables that are passed between each module are provided in Table 17. There are six analysis models and one simulation controller. The six analysis models include the cargo launch vehicle, the lunar surface access module, an in-space propellant storage system, economic analysis, reliability analysis and a technology development risk assessment. These integrated modules (Figure 19) provide the analysis needed to investigate the trade options presented in the morphological matrix.

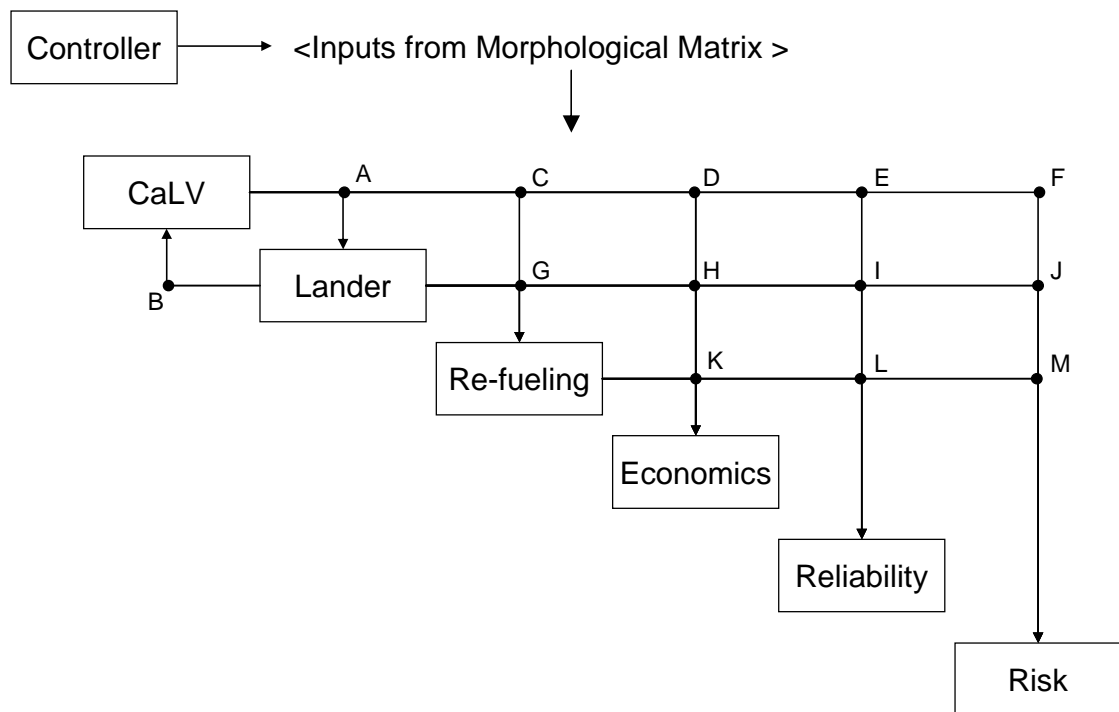


Figure 19. Lunar Architecture Simulation Environment

Table 17: Summary of Variables Passed Between Analyses

A	CaLV payload capability (only active for Scenario One)
B	Lander gross mass (only active for Scenario Two)
C	Propellant mass re-fueled on CaLV
D	Subsystem masses, mitigation method, # of engines
E	# of tanks, # of engines, propulsion system type, tank material
F	Mitigation method
G	Propellant mass re-fueled on lander
H	Sub system masses, mitigation method, # of engines
I	# of tanks, # of engines, propulsion system type, tank material
J	Engine type, mitigation method
K	Subsystem masses, mitigation method, dimensions
L	Number of propellant transfers
M	Refueling used (Y/N)

The simulation runs from the top left to bottom right and passes information between the models signified by a solid line and a black dot. The controller in the top left is the link between the design choices and the simulation. This controller translates the design trades, developed from the morphological matrix, into a set of inputs for the various analyses. An example set of inputs is provided in Table 18. These inputs represent the baseline design and include no propellant refueling options.

Table 18: Case 1 from the Morphological Matrix

Additional Ascent Propellant	0
EDS Boiloff Mitigation	MLI
Lander Stage Re-fueled	None
Percentage of Lander Propellant	0%
LSAM Ascent Propellant	LOX/CH4
Lander Boiloff Mitigation	MLI
LOI Burn Element	EDS
LEO Required Stay Time	95 Days
Re-fuel Boiloff	No

The diagram in Figure 19 shows the flow of information from the CaLV into the LSAM, but this can be flipped depending on the scenario being investigated. In Scenario One the payload capability of the CaLV is determined, and this value is passed to the LSAM, which calculates its lunar surface payload capability based on the maximum allowable lander gross mass. In Scenario Two the lunar surface payload capability is kept constant; therefore the lander is sized first, and the total mass is passed to the CaLV to determine the launch vehicle size required to deliver this payload capability to LEO. Once the design of these vehicles is complete, the amount of propellant refueling required is passed to the refueling analysis to size the propellant storage system. Once the first three analyses are complete, the design of the architecture is set and the remaining models are used to evaluate the remaining FOMs. The economic model takes inputs of the vehicle mass from the CaLV, LSAM, and in-space depot and determines the life cycle cost of the campaign. The reliability model requires input of the vehicle characteristics and number of times propellant is transferred and generates a loss of mission probability

estimate for the architecture. The final risk analysis provides a relative risk assessment of the design choices made on the CaLV, LSAM and the in-space depot. The following sections provide a more detail description of the analysis completed within each of these modules.

4.1.1 LAUNCH VEHICLE (CALV) MODEL

The cargo launch vehicle model is developed to size the system to meet mission and payload requirements and predict the inert and gross mass of the system. A typical launch vehicle model is comprised of configuration, aerodynamics, propulsion, trajectory and weights and sizing disciplines [42]. The Design Structure Matrix (DSM) for a standard launch vehicle model is provided in Figure 20. The “configuration” analysis provides design details such as the number of stages, basic shape, and launch configuration. These design choices are held constant during this study so the configuration analysis is removed. This DSM provides the breakdown of the model analyses and where information passes between them. The variables passed between each analysis are provided in Table 19. This process requires iteration to converge to a design point. Iteration is required when information is passing in both directions between two analyses. For example, an iteration loop is required between the Trajectory and the Weights and Sizing analyses.

Because a computationally intensive Monte Carlo simulation is performed, a fast simulation is needed. Therefore, the trajectory, propulsion and aerodynamics model are replaced with a meta-model in the form of a single equation. For this present simulation, the CaLV shape and thrust were held constant; thus the only variable affecting the CaLV

performance, measured by the mass ratio ($M_{\text{initial}}/M_{\text{final}}$), is the mass that the CaLV must deliver to the EDS staging point. In Scenario Two the total thrust is allowed to change in the form of a reduction in the number of engines, but in Scenario One this remains fixed. The following section will discuss the process used and the assumptions made in developing this meta-model.

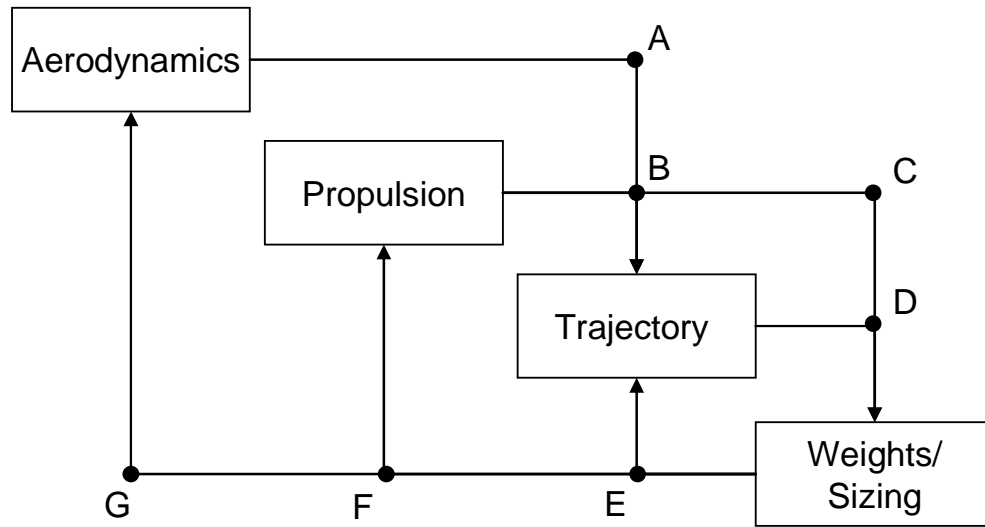


Figure 20. General Launch Vehicle Design Structure Matrix

Table 19: Summary of the Variables Passed between Analyses

A	Lift and drag coefficients, function of Mach and Angle of Attack
B	Thrust, Isp, Exit Area
C	O/F, T, Engine T/m, Isp
D	MR_{required}
E	M_{initial} , M_{inert}
F	T/m_{initial} , m_{initial}
G	Vehicle Dimensions (length, diameter)

In order to develop the meta-model representing the aerodynamic, propulsion, and trajectory disciplines, a number of converged vehicle designs must be obtained with the original design tools. The original design tools used in this analysis include the Aerodynamic Preliminary Analysis System (APAS) [43] and the Program to Optimize Simulated Trajectories (POST) [44]. The values for the propulsion systems remain constant at the baseline values because these engines do not change in this study. These values can be found in Table 21. The Weights and Sizing discipline utilizes historical Mass Estimating Relationships (MERs) within an Excel[®] spreadsheet [45]. The MERs are not replaced with the meta-model, but are needed to converge each vehicle design point.

The trajectory simulation requires aerodynamic, propulsion, and initial mass data. The APAS model provides the aerodynamics data in the form of lift and drag coefficients as a function of Mach and angle of attack. Two sets of coefficients are developed: one with the solid rocket boosters attached and one without them attached. These tables of coefficients are then used along with the reference area, which is the cross-sectional area for each configuration, to calculate the actual lift and drag. The reference areas are provided in Table 20. It is assumed that these coefficients remain constant to the baseline configuration because drag losses are small, accounting for only one percent of the total performance. This assumption has little effect on the design of the launch vehicle, but allows the aerodynamics model to be removed from the analysis while its effect can still be incorporated into the meta-model.

Table 20: CaLV Reference Areas

With SRBs attached	825 ft ²
Without SRBs attached	593 ft ²

The propulsion data parameters (Thrust, Isp, Ae) are held constant at the baseline values. An estimate for the initial mass and stage inert mass is passed into the POST model from the Weights and Sizing model. Given this information, the trajectory can be optimized to minimize the mass required to deliver a specified payload into a 30 x 160 nmi transfer orbit. The procedure used to close the vehicle design is provided in Figure 21. A closed design is defined as a solution where the performance (trajectory and mass) analysis is converged to within a given tolerance. This requires an iterative solution between the trajectory and the Weights and Sizing models.

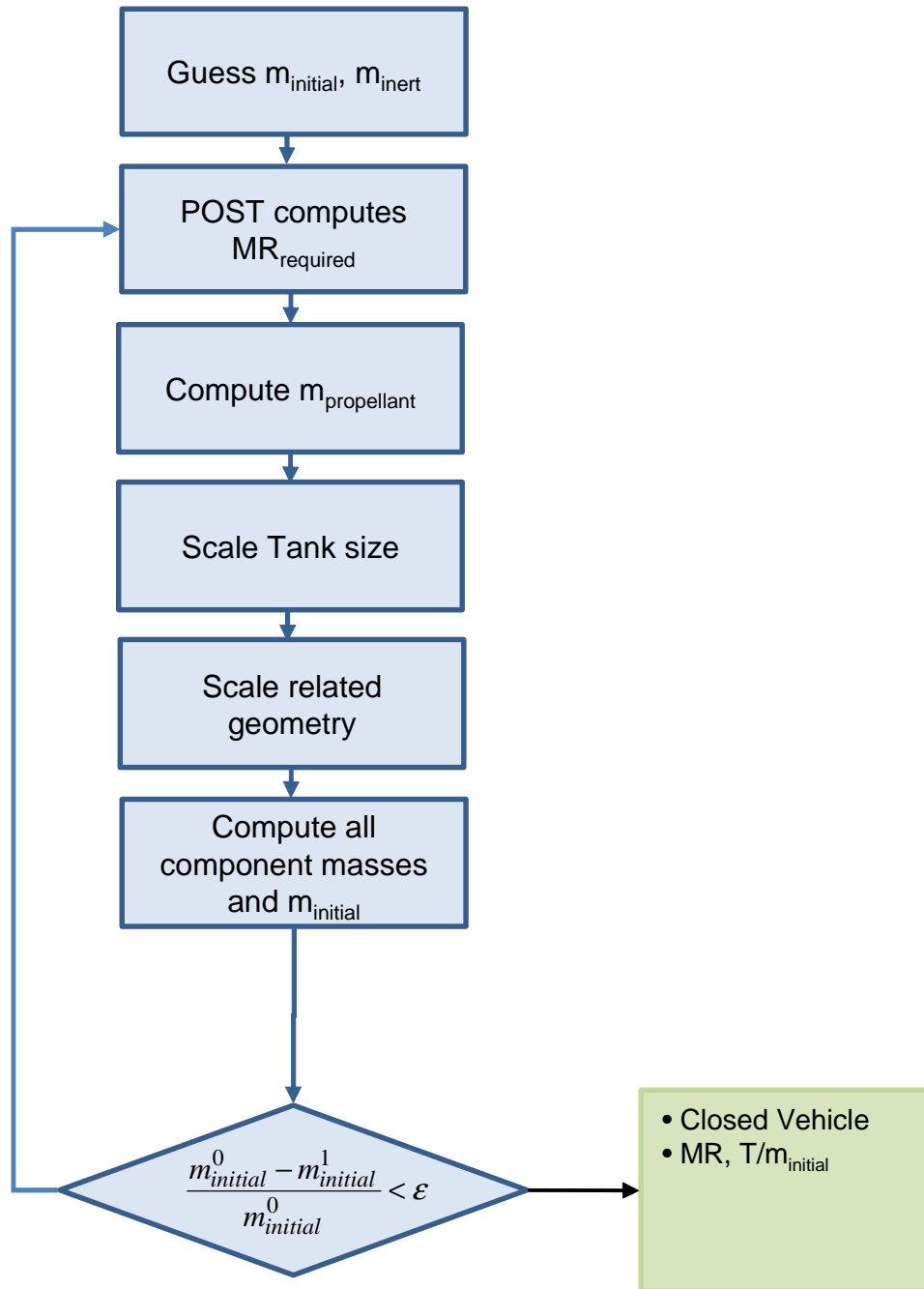


Figure 21. Procedural Flow Chart for the Trajectory Meta-Model

An initial set of mass estimates (m_{initial} , m_{inert}) is passed into the POST model; these values initiate the iteration loop. The trajectory analysis is then performed to determine the required mass ratio. Next, this value is passed to the Weights and Sizing model, in which the vehicle is scaled to match the required mass ratio. The required mass of propellant is calculated from the required mass ratio and ideal rocket equation. This is provided in Equation 1.

$$M_{\text{propellant}} = \frac{(MR_{\text{Required}} - 1)M_{\text{Initial}}}{MR_{\text{Required}}} \quad (1)$$

Once the propellant mass is known, the tanks are scaled to hold the required propellant and the remaining subsystem inert masses are calculated. Based on the subsystems and propellant masses, the initial mass is determined. If this mass is the same as the initial guess, then the vehicle is closed. If it is not the same as the initial guess, then the new initial mass and inert mass are passed back to the POST model and another iteration begins. Once the vehicle design is closed, the MR_{required} and the T/m_{initial} are recorded. This process is repeated for a range of payloads in order to change the T/m_{initial} . The response surface equation (RSE) for MR_{required} versus T/m_{initial} can then be developed using a least squares regression. These curves are provided in Figure 23 and Figure 24 for the 1st and 2nd stages, respectively. These meta-models can now be used to replace the aerodynamic, propulsion and trajectory disciplines, as shown in the final DSM provided in Figure 22.

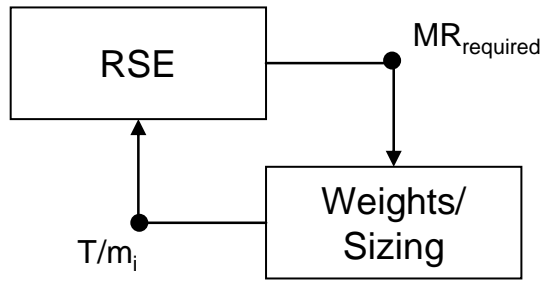


Figure 22. Final CaLV Design Structure Matrix

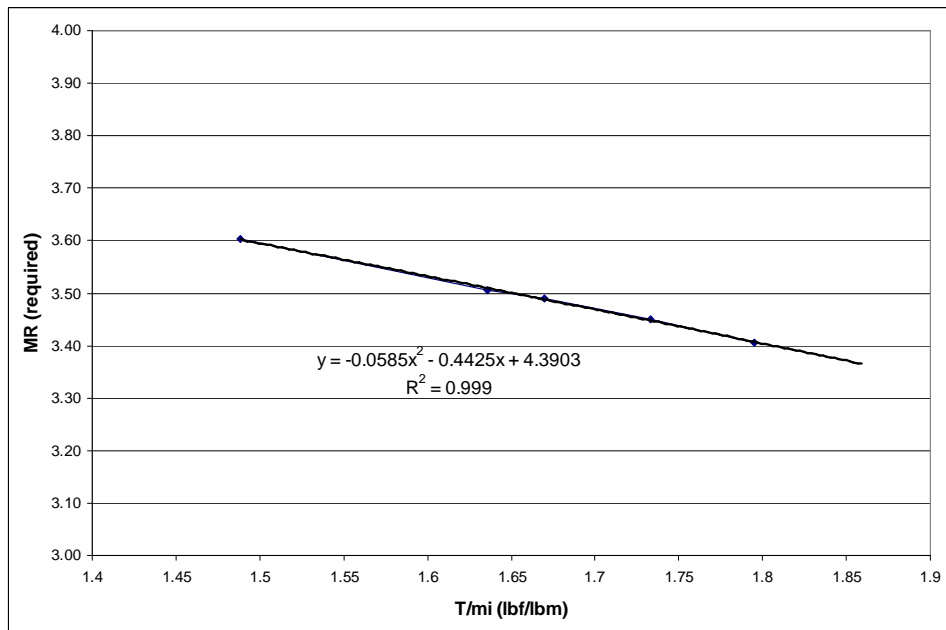


Figure 23. Trajectory Meta-Model for CaLV 1st Stage

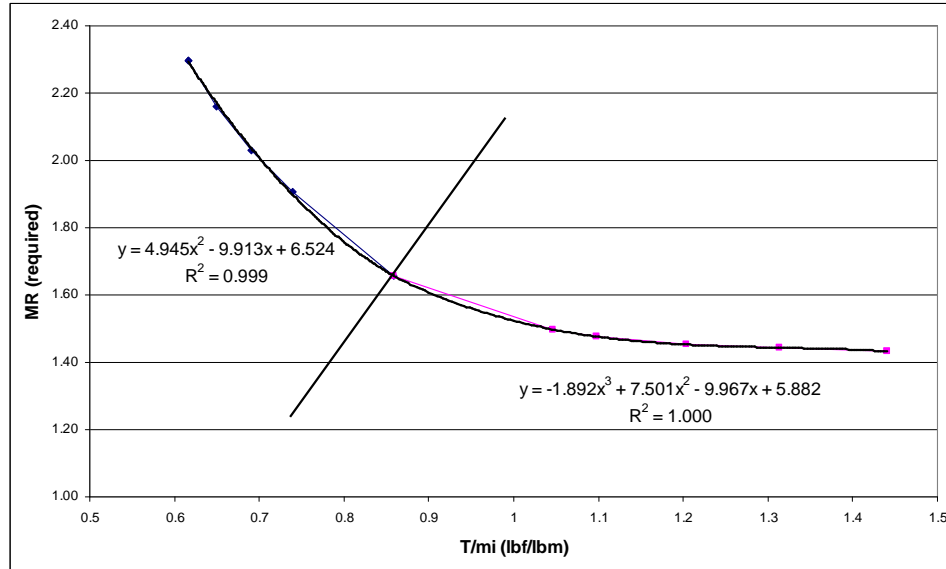


Figure 24. Trajectory Meta-Model for the EDS

This model can now be used to evaluate the impacts of the simulation inputs on the CaLV. There are two design scenarios that affect the design of the CaLV. In Scenario One the introduction of propellant refueling is used to increase the lunar surface payload capability, and in Scenario Two propellant refueling is used to decrease the size of the CaLV while maintaining the same lunar mission capability.

Under the assumptions in Scenario One, the configuration of the CaLV is not affected by the introduction of propellant refueling. This is because any reduction in the mass of the in-space propellant delivered to LEO results in a corresponding increase in payload capability. This keeps the initial mass of the CaLV constant. There is a special case where the initial mass is affected by propellant refueling. When additional EDS propellant is burned during ascent, the total payload delivered to LEO (LSAM + TLI propellant) also increases, therefore increasing the initial mass of the vehicle. Because the

stage thrust is held constant as the initial mass increases, the T/m_i decreases. This leads to an increase in the required mass ratio.

In order to model the simulation in which additional EDS propellant is burned, a second meta-model was created using the tools previously discussed. The POST optimization was modified to maximize the payload capability for a given amount of propellant rather than minimizing the propellant required to deliver a specific payload. The amount of propellant used by the 1st stage was set to the baseline value of 2,201,119 lbm. The amount of propellant used on the EDS was then varied and the total payload capability for each design point was determined. The final converged design points are provided in Figure 25. The total payload capability increases until an additional 150,000 lbm of propellant is burned. As additional propellant is used, the total payload begins to decrease. This is due to the first stage being held constant, and the staging condition for the EDS being reduced. As additional propellant is used, the initial mass of the CaLV increases, which decreases the T/m_i of the 1st stage. These additional gravity losses reduce the staging condition between the 1st and 2nd stages, both velocity and altitude. Therefore the 2nd stage must perform a larger portion of the total required mass ratio. Eventually the performance benefit of increasing the upper stage ascent propellant is less than the additional mass ratio that the 2nd stage must provide to achieve orbit. A velocity plot of this trajectory is provided in Figure 26. Data for the baseline design and Scenario Two are also included to illustrate the differences in the three trajectories. The reduction in EDS staging conditions and the increase in performance required by the upper stage is clearly seen in these results.

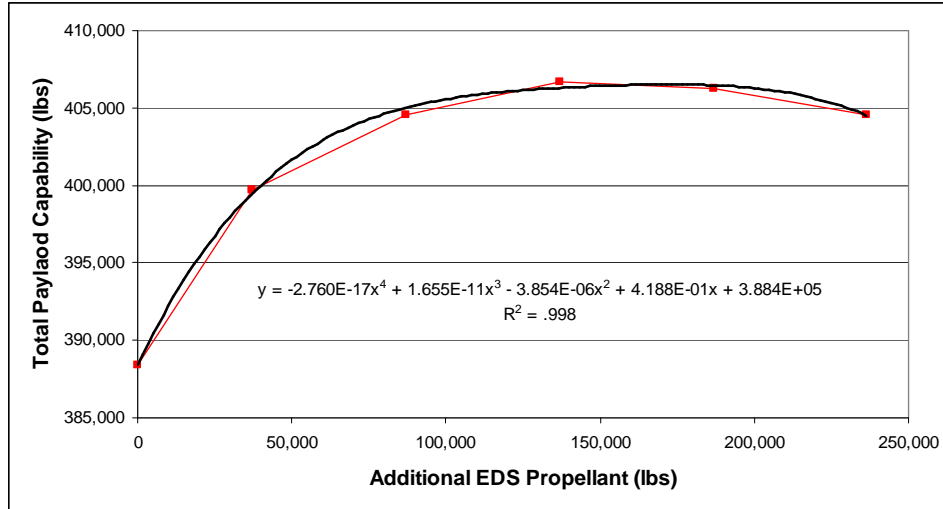


Figure 25. Additional EDS Propellant Meta-Model

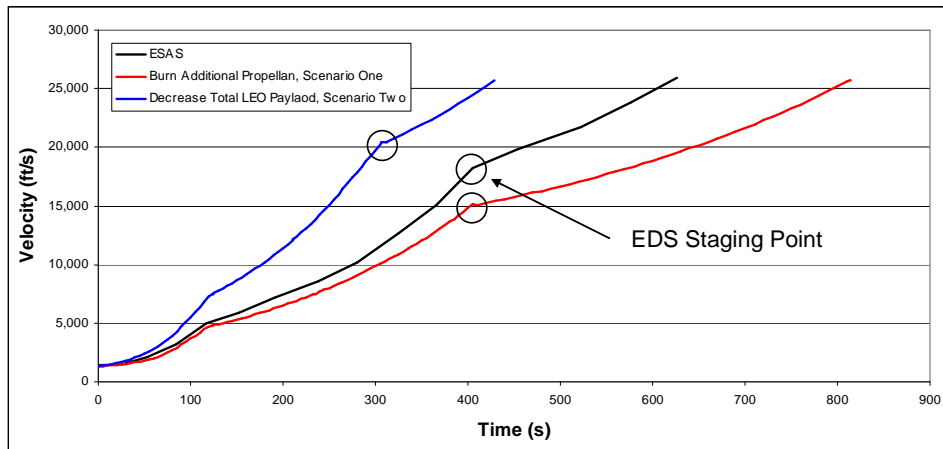


Figure 26. Trajectory Comparison for Scenarios One and Two

In Scenario Two, as the total LEO payload is decreased, the total propellant required to achieve the desired mass ratio also decreases. The reduction in propellant mass leads to smaller tanks which lead to an overall smaller CaLV. This results in a decrease in the initial and inert mass of the vehicle. The smaller inert mass leads directly to a decrease in the development and production cost of the vehicle. This will further be discussed in section 4.3.4. The decrease in initial mass allows the number of engines to also decrease in order to keep the T/m_{initial} as close to the baseline design as possible, but never below. Achieving the exact T/m_{initial} cannot always be achieved because the engine thrust is held constant. The total thrust can only be reduced by discrete quantities. This results in a range of T/m_{initial} on the 1st stage of 1.5 – 1.8 and a range of 0.86 – 1.44 on the 2nd stage.

A mass comparison of the CaLV created in this model and the baseline design is provided in Table 21. A further discussion of the comparison of the baseline CaLV and the model developed here is provided at the end of this chapter. An example mass breakdown for Scenario Two is provided in Table 22 to illustrate the decrease in vehicle size that is achieved by reducing the TLI propellant delivered to LEO by 100,000 lbm.

Table 21: Cargo Launch Vehicle Mass Comparison

	1 st Stage		EDS		Boosters	
	ESAS	Model	ESAS	Model	ESAS	Model
Burnout Mass (lb)	215,258	215,474	50,360	50,835	221,234	221,234
Usable Propellant (lb)	2,215,385	2,201,119	488,370	493,029	2,869,812	2,869,812
Gross Mass (lb)	6,393,922	6,388,185	--	--	--	--
LSAM Mass (lb)	101,441	101,441				
Total Vac. Thrust (lb)	2,347,245	2,347,245	549,000	549,000	7,680,246	7,680,246
Vac. Specific Impulse (s)	452	452	451	451	265	265
Diameter (ft)	27.5	27.5	27.5	27.5	176	176
Length (ft)	210	210	76.4	74	12	12

Table 22: Cargo Launch Vehicle Mass Comparison, Scenario 2

	1 st Stage		EDS		Boosters	
	ESAS	Model	ESAS	Model	ESAS	Model
Burnout Mass (lbm)	112,632	215,474	32,940	50,835	221,234	221,234
Usable Propellant (lb)	1,157,255	2,201,119	218,181	493,029	2,869,812	2,869,812
Gross Mass (lb)	4,949,949	6,388,185	--	--	--	--
LSAM Mass (lb)	101,441	101,441	--	--	--	--
Total Vac. Thrust (lb)	938,898	2,347,245	549,000	549,000	7,680,246	7,680,246
Vac. Specific Impulse (s)	452	452	451	451	265	265
Diameter (ft)	22.6	27.5	27.5	27.5	12	12
Length (ft)	171	210	60	74	176	176

4.1.2 LUNAR LANDER (LSAM) MODEL

The lunar lander model is similar to the CaLV sizing logic with the exception of a change to vacuum space flight. It is built using parametric relationships that allow changes in the propulsion system, required mission maneuvers, and payload capability to be simulated. The LSAM model consists of Propulsion, Trajectory, and Weights and Sizing disciplines. The aerodynamics analysis is not required for in-space and lunar maneuvers. The design structure matrix and flow of information for the LSAM model is illustrated in Figure 27 and Table 23. An additional iteration loop is required in order to keep the T/W constant and allow a constant set of delta-Vs to be used for the trajectory model. The baseline ESAS configuration is again used, but the size of the vehicle is allowed to adjust depending on the inputs to the model.

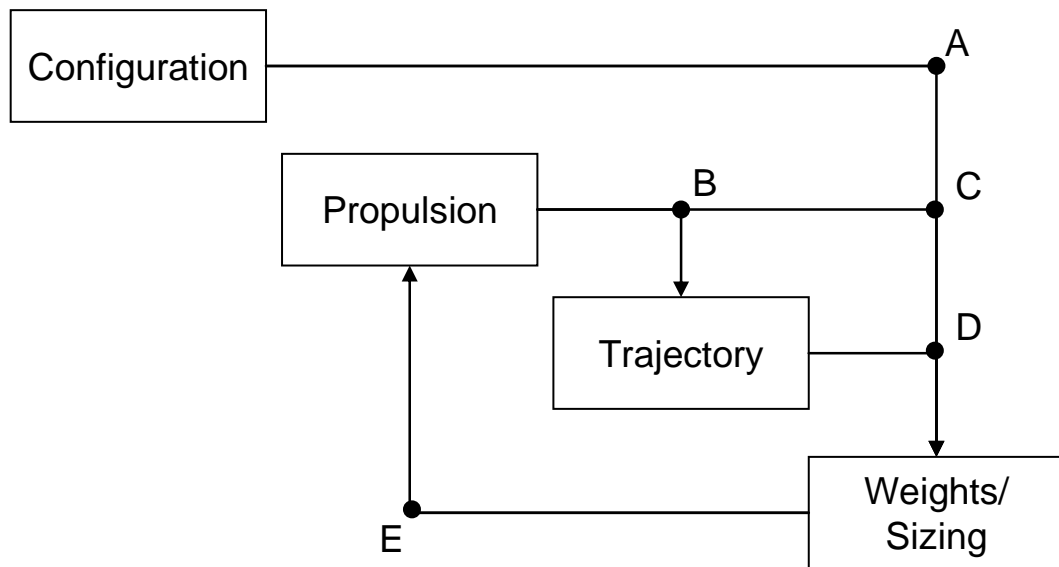


Figure 27. LSAM Design Structure Matrix

Table 23: LSAM Propellant Boiloff Comparison

A	Baseline configuration used
B	Isp
C	T, T/W_{engine} , O/F, # of engines
D	Descent and ascent propellant
E	Component masses

The propulsion model is responsible for providing the thrust, specific impulse, oxidizer to fuel ratio (O/F), and T/m_{engine} of descent and ascent engines to the trajectory and iteration loop. This model keeps the T/m of each stage constant by adjusting the thrust and number of engines used by each propulsion system. This analysis assumes that the engines can be designed to minimize the effect that a change in thrust has on specific impulse. The design of the RL-10 has shown that a relatively constant specific impulse can be achieved over a wide range of thrust [46]. This assumption affects the total lander mass or payload capability by less than five percent. A more detailed engine model is needed to completely capture the effect that different engine and engine sizes have on the LSAM design, but this was not a focus of this work. In the baseline configuration, the descent stage utilizes four RL-10 derivative engines to generate 60,000 lbf of thrust with a vacuum Isp of 460s. The baseline ascent propulsion system uses a LOX/CH₄ engine, but due to ongoing trade studies, three other possible ascent engines are considered. A summary of these engines is provided in Table 24, where the thrust values represent the initial engine data used. The T/W of the descent and ascent stages is maintained at 0.6 and 0.45 respectively.

Table 24. Summary of Ascent Engine Assumptions

Propellant	Isp [s]	T/W _e	Thrust [lb]	O/F
NTO/MMH	323	30.4	9,300	1.65
LOX/CH ₄	361	28	9,060	3
LOX/LH ₂ (pressure)	460	28	9,890	6
LOX/LH ₂ (pump)	463	38.8	8,970	6

The trajectory model requires the Isp from the propulsion model and the stage inert masses from the sizing model to calculate the amount of propellant required to perform each of the mission maneuvers. The descent stage requires two calculations, one for the LOI maneuver and the second for the lunar descent maneuver, while the ascent stage requires just the ascent maneuver calculation. The mass of propellant required is calculated from Equation 1. The delta-V used for each maneuver is provided in Table 25. The propellant mass is then passed to the weights and sizing model and will be used in sizing the required propellant storage tanks.

Table 25. Lunar Lander Delta-V Table [ESAS, pg. 165]

Delta-V Maneuver	Delta-V [ft/s]
Ascent Delta-V	6,122
LOI Delta-V	3,608
Descent Delta-V	6,233
AS RCS Delta-V	144
DS RCS Delta-V	55

A flow chart is provided in Figure 28 to outline the process used to close the LSAM design. An initial mass for the LSAM is provided to the model; this is generally taken from the previous design point. From the initial mass and delta-V table, an initial estimate for the propellant mass is calculated. The propellant mass is then used to size the vehicle tanks using an empirical sizing routine that factors in total propellant volume, strength of the tank material and internal tank pressure [47]. The engines are then sized to maintain their require stage T/m. The remaining subsystems are sized based on historical mass estimating relationships. The MERs for the LSAM are provided in Appendix B as a reference. A new initial mass can then be calculated and compared against the initial guess. If the two values are not equal the new initial mass is returned to the propellant sizing step and the entire process is repeated. Once the two values are with the required tolerance the vehicle is considered closed for that design point. A summary of the baseline LSAM masses are provided in Table 26.

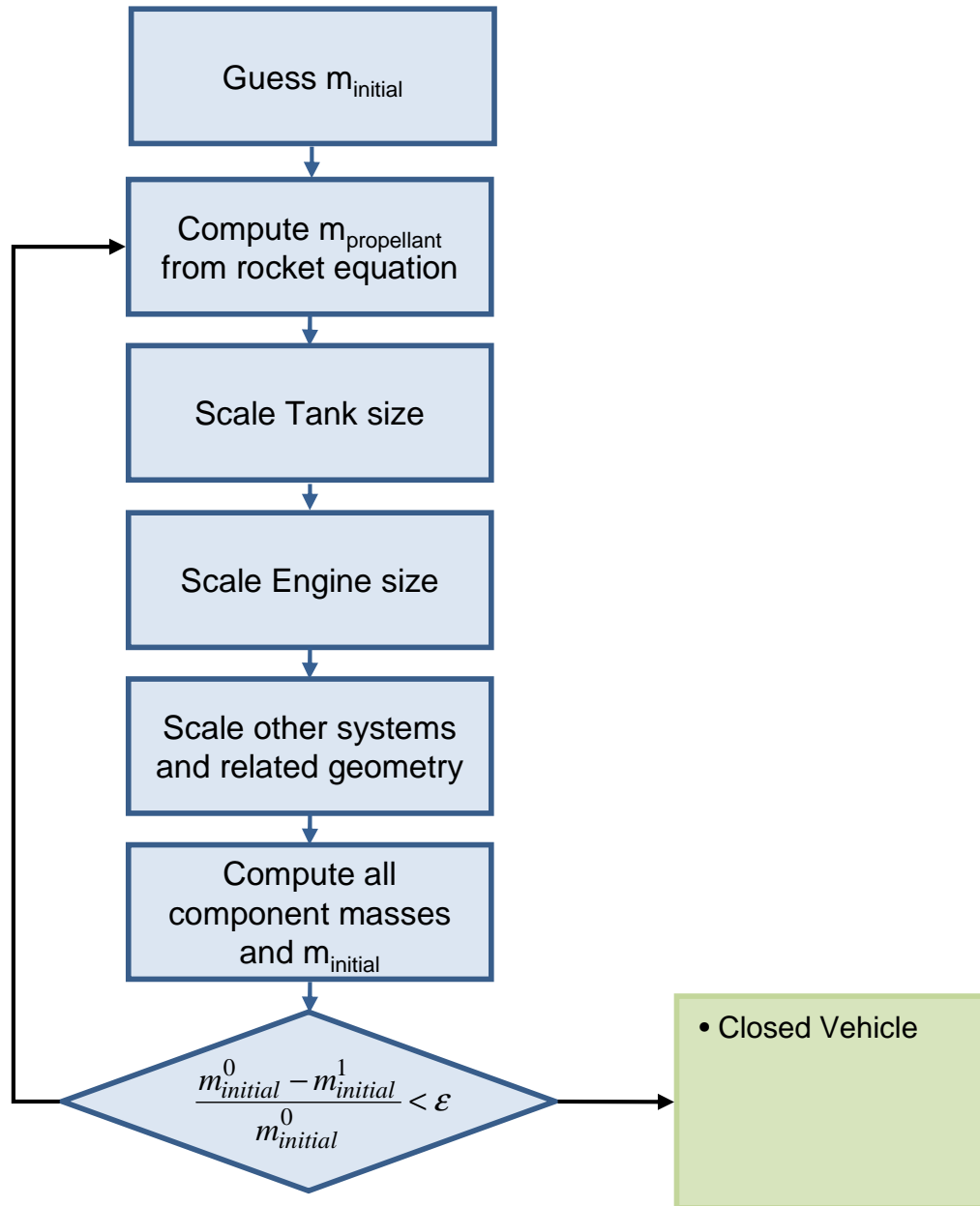


Figure 28: LSAM Mass Sizing Flow Chart

Table 26: Lunar Surface Access Module Mass Comparison

	Descent Stage		Ascent Stage	
	ESAS (lb)	Model (lb)	ESAS (lb)	Model (lb)
Dry Mass	13,500	12,770	11,300	11,060
Total Propellant	55,400	56,100	10,400	9,800
Lunar Surface Payload	5,057	5,039	--	--
Gross Mass	101,411	101,007	--	--

4.1.3 PROPELLANT REFUELING MODEL

The results of this thesis will assume that all propellant refueling is done via a propellant depot located in LEO. This depot is designed to receive regular propellant refueling deliveries from either NASA exploration launch vehicles or a commercial launch provider, depending on who can offer the lowest price. The propellant is then transferred from the delivery vehicle to storage depot. The depot is able to store the propellant until required by NASA for an exploration mission. Tank transfer offers an alternative to propellant transfer, but this was not considered (see Scher [48] for an analysis of the pros and cons of each method.) The following section provides a description of the propellant depot model utilized in this work.

The model of the propellant storage systems is designed to determine the mass and size of the system needed to accommodate the propellant needs for the NASA lunar exploration program. The amount of propellant required is dependent on which propellant refueling concept is being considered. The model inputs are the required mass and propellant type needed for the exploration mission. The model then calculates the mass of

the propellant tanks, cryo-cooler, power system (solar and fuel cells), supporting structure, shielding, and maneuvering system. A mass allocation of 1,000 lbm is used for the docking and transfer system and 100 lbm for the avionics system [49]. To be conservative, the required amount of propellant is always assumed to be twice that needed of a single mission. This allows the depot to store enough propellant for two missions in case a delay occurs that prevents a sufficient amount of propellant from being delivered to the depot. This helps to mitigate the risk of the architecture being delayed due to a malfunction with the refueling system.

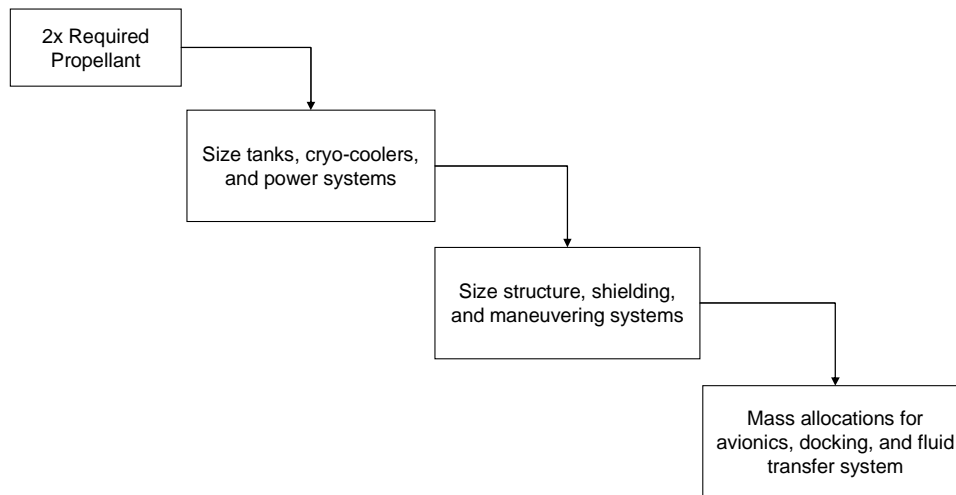


Figure 29. Mass Sizing for LEO Propellant Depot

The tanks are sized using the same empirical sizing routine performed in the CaLV and LSAM models. This requires input of the total required propellant, propellant type, and oxidizer to fuel ratio if more than one propellant is used. Up to three separate propellant storage tanks can be modeled. The results in the following chapters will show that, in most cases, two propellants are preferred. An overall length and diameter

constraint is also placed on the size of the tanks to allow it to fit inside the current cargo launch vehicle payload fairing. It is also possible that, if the propellant requirements are small enough, the depot could be deployed on an existing EELV, which would offer a lower cost than the CaLV. A comparison between the Delta IVH and the CALV fairings is provided in Figure 30. The EELVs offer sufficient payload capability to deliver the depot, but the EELV fairing diameter is 40 percent less than that of the CaLV, limiting the total volume of the depot. The depot dimensions provided in Table 27 show that a LOX/LH2 depot designed to hold 50,000 lbm of propellant would violate the Delta IVH payload volume constraints.

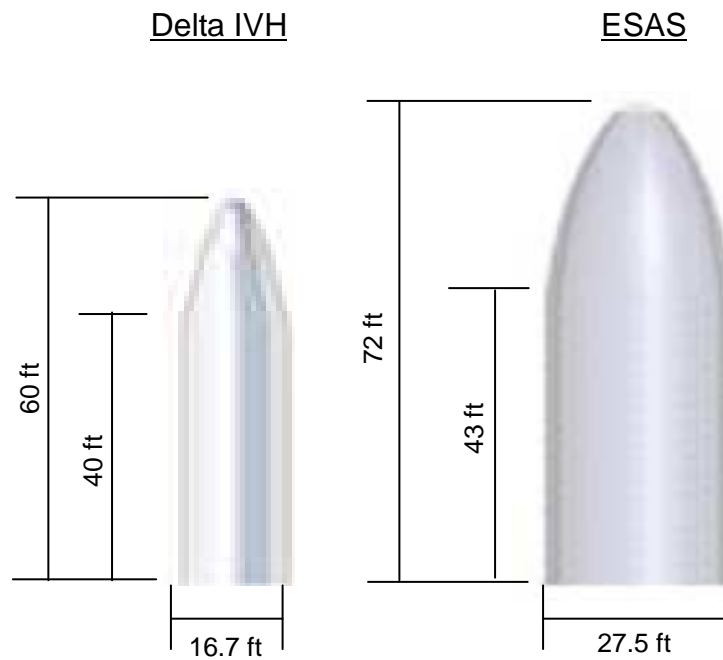


Figure 30. Depot Delivery Fairing Comparison

Once the sizes of the tanks are established, the propellant thermal management system can then be sized. This model assumes that an active cryo-cooler plus passive MLI system is used to eliminate all propellant boiloff aboard the depot. MLI alone was not considered because it results in a more expensive system since the continuous loss of propellant would result in an increase in propellant cost to NASA, leading to an overall increase in the life cycle cost. This is the same cryo-cooler that could potentially be used on the CaLV and LSAM vehicles. The remaining systems are sized with historical mass estimating relationships: supporting structure, power, shielding and RCS. A more detailed look at the development of each subsystem can be found in reference [49], including a mass break down and an example depot design. The notional depot configuration is provided in Figure 31, including the main subsystems included in this model. Any number of depot configurations could be considered without significantly affecting the results presented in this thesis. The model was developed to provide an estimate of the overall dimensions and provide mass estimations to the cost module. A number of additional configurations are outlined by Chandler [50]. A summary of the depot dry mass and overall dimensions for three propellant combinations is provided in Table 27. At these propellant quantities, the tanks are spherical in shape, but they become cylindrical as the propellant quantities increase and the diameter constraint is reached.

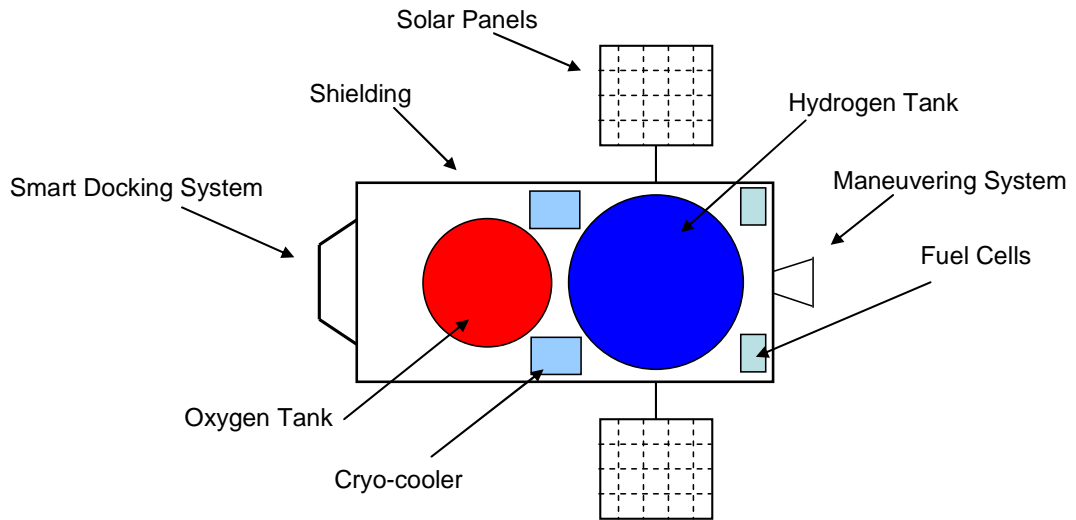


Figure 31. Notional Propellant Refueling Depot

Table 27. Summary of Depot Sizes for Various Propellant Mass

	Dry Mass [lb]	Diameter [ft]	Length [ft]
50,000 lbm LOX/LH2	14,000	17.0	40.65
42,850 lbm LOX	5,950	17.0	17.0
7,150 lbm LH2	11,500	23.16	23.16
100,000 lbm LOX/LH2	24,000	21.4	51.2

4.1.4 LIFE CYCLE COST MODEL

The NASA Systems Engineering Handbook defines the system life cycle in terms of phases that includes Phase A (Concept and Technology Development), Phase B (Preliminary Design), Phase C (Final Design and Fabrication), Phase D (System Assembly, Integration, & Test), Phase E (Operations) and Phase F(Closeout). Typically, Phase A and Phase B are preliminary analyses and designs of the system to determine feasibility and initial requirements and are conducted by multiple contractors leading up to the selection of the prime contractor for the final design, development, production, and operations of the system. Phase A and Phase B costs are approximately 10 percent of the total program costs as demonstrated by programs such as the Hubble Space Telescope, the Space Shuttle (costs up to the first flight), Voyager, and Pioneer/Venus. Because these initial Phase A and B costs are fairly constant for NASA programs, these costs were not included with the present analysis to compare system architectures.

The Phase C, D, and E Life Cycle Cost of an architecture accounts for the other 90 percent that include all costs associated with the campaign from final design to completion of the program. Included in these costs are all design, development, production, operation and disposal costs [51]. These costs are broken down into three categories System Acquisition Cost, Operations and Support Costs, and Disposal Costs, as illustrated in Figure 32 [52].

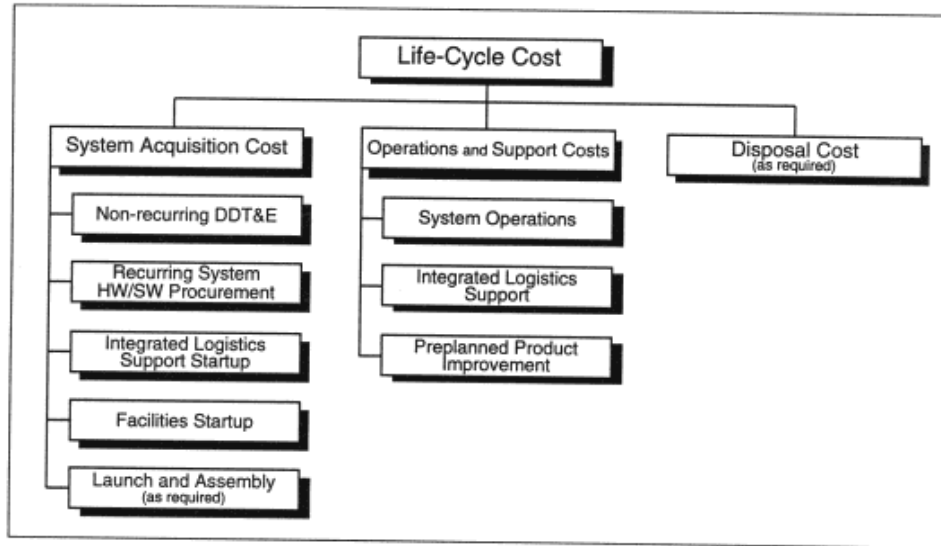


Figure 32: Breakdown of Life Cycle Cost

The System Acquisition Costs are calculated using the NASA Air Force Cost Model (NAFCOM) [53]. A summary of the NAFCOM costs breakdown of the System Acquisition Cost are shown in Table 30.

Table 28. Summary of System Acquisition Costs

Non-recurring DDT&E	
Engineering Drawings	NAFCOM CERs
Computer Aided Design (CAD)	NAFCOM CERs
Configuration Control	NAFCOM CERs
Specifications and Requirements	NAFCOM CERs
Production of Test Article	NAFCOM CERs
Redesign after Testing	NAFCOM CERs
Integrated Logistics and Support	
System Test Operations	NAFCOM Wraps
Ground Support Equipment	NAFCOM Wraps
Systems Engineering and Integration	NAFCOM Wraps
Program Management	NAFCOM Wraps
Recurring System Procurement	
Theoretical First Unit	NAFCOM CERs
Facilities Startup	
Launch Infrastructure	Not included
Launch and Assembly	
Integration, Assembly and Checkout	NAFCOM Wraps

The Non-recurring Design, Development, Test, and Evaluation (DDT&E) cost element of the System Acquisition Costs includes the “labor, materials, Special Test Equipment and tooling, and other direct and allowable indirect expenses incurred by the prime contractor including all subcontracts to the prime required to determine compliance with all design requirements documentation and to perform the subsequent analysis, design, development, and redesign of test and development hardware” [53].

The Integrated Logistics and Support costs include the “labor, materials, Special Test Equipment and tooling, and other direct and allowable indirect expenses incurred by the prime contractor including all subcontracts to the prime required to determine compliance with all design requirements documentation and to perform the subsequent

analysis, design, development, and redesign of test and development hardware”[54]. The System Test Operations element includes “development testing and the test effort and test materials required for qualification and physical integration of all test and qualification units. Also included is the design and fabrication of test fixtures.” The Ground Support Equipment includes “the labor and materials required to design, develop, manufacture, procure, assemble, test, checkout, and deliver the equipment necessary for system level final assembly and checkout. Specifically, the equipment utilized for integrated and/or electrical checkout, handling and protection, transportation, and calibration, and items such as component conversion kits, work stands, equipment racks, trailers, staging cryogenic equipment, and many other miscellaneous types of equipment are included.” The Systems Engineering and Integration element encompasses: “(1) the system engineering effort to transform an operational need into a description of system requirements and/or a preferred system configuration; (2) the logistics engineering effort to define, optimize, and integrate logistics support considerations to ensure the development and production of a supportable and cost effective system; and (3) the planning, monitoring, measuring, evaluating, and directing of the overall technical program.” The Program Management (PM) function consists of the “effort and material required for the fundamental management direction and decision-making to ensure that a product is developed, produced, and delivered.”[54]

The Recurring System Hardware/Software (HW/SW) Procurement cost is discussed at the end of this section because it is highly coupled to the yearly operational costs.

The Facilities Startup costs are not included in the present analysis because it is assumed that the facilities at Cape Kennedy will be sufficient for the architecture.

The Launch and Assembly cost contains “all labor and material required to physically integrate (assemble) the various subsystems into a total system. Final assembly, including attachment, and the design and manufacture of installation hardware, final factory acceptance operations, packaging/crating, and shipment are included.”[54]

As shown in Table 28 the NAFCOM model utilizes cost estimating relationships (CERs) and percentages of estimated cost, i.e. wraps, to estimate the System Acquisition Costs. A logarithmic regression of the historical data is developed for each vehicle subsystem to define a Cost Estimating Relationship (CER) between the dry mass and the cost of the system. The standard regression equation used for this analysis is provided in Equation 2. The a and b values are obtained from the regression of the historical data. The Complexity Factor (CF) is a translation of this curve to represent differences between the current system and the historical systems used for the regression. Most historical systems were built with aluminum, but today’s systems utilize many different materials including titanium and composites. These materials weigh less, but should cost more, hence the CF accounts for this difference. Other cost complexity factors are used in NAFCOM, such as program management skill, funding stability, etc., but were assumed to be the same for all the system comparisons and were not changed in this analysis.

$$Cost = aW^b \times CF \quad (2)$$

To obtain the wrap costs in Table 29, the NAFCOM multiplies the CER based costs from Table 12 by simple historical based percentages. The CER and wrap costs are

then summed for each vehicle subsystem. An additional 20 percent cost margin is used to obtain the final System Acquisition Cost. All architecture vehicles and Propellant Depot are costed using this method.

Table 29. Summary and Description of NAFCOM Wraps

System Wrap	Description
Integration, Assembly, & Checkout	All labor and material required to physically integrate the various subsystems into a total system.
System Test Operations	Development testing, test effort and materials required for qualification and integration.
Ground Support Equipment	All labor and materials required to design, develop, manufacture, procure, assemble, test, checkout, and deliver the equipment necessary for system level final assembly and checkout.
System Engineering & Integration	Specific functions include those for control and direction of engineering activities, cost/performance trade-offs, engineering change support and planning studies, technology utilization, and the engineering required for safety, reliability, and quality control and assurance
Program Management	The effort and material required for the Fundamental management direction and decision-making to ensure that a product is developed, produced, and delivered

A summary of the predicted system acquisition costs (DDT&E) developed in this model are provided in Table 30. These values are for the baseline architecture vehicle models. The production costs include the cost from the NAFCOM CERs, the additional system-level costs, and a 20 percent cost margin. The life cycle analysis assumes that the production cost is the total cost required to produce the architecture elements needed of each mission. Since all flight elements are expendable, except the CEV, there is no additional overhaul done at the end of each mission, so the only costs are the hardware and its assembly. The depot cost is included to provide an example of the typical cost of the propellant depot. This example is for a depot that is capable of holding 50,000 lbm of

LOX/LH2 at an O/F ratio of 5.5. The results for the DDT&E and production are fed into the economics model, which calculates the life cycle cost at each design point. The CERs used in these calculations are provided in Appendix D.

Table 30. Baseline Architecture Cost Summary

[FY07]	DDT&E (\$M)	Production (\$M)
CaLV	6,041	643
LSAM	5,582	730
CLV	3,778	633
CEV/SM	4,200	500
Depot (50,000 lbm, LOX/LH2)	940	190

The second element of the Life-Cycle Cost is the Operational and Support costs (Figure 1) that include the System Operations, Integrated Logistics Support, and Pre-Planned Product Improvement elements. In the present analysis, the System Operations is broken down into the ground and flight operations because of the way that NAFCOM computes cost.

Because the operation of the architecture is spread over 15 years and because of the embedded NAFCOM costs, the Recurring System HW/SW Procurement costs are considered as operational costs. These procurement costs are modeled in NAFCOM as a Theoretical First Unit (TFU) cost. These TFU costs are those incurred by “the prime contractor and all subcontracts to the prime include the labor, materials, and other direct charges and allowable indirect charges required to produce the flight article”.[13] Specifically the TFU cost include the following:[13]

- Fabrication and Processing
- Subassembly and Final Assembly
- Rework and Modification
- Experimental Production
- Installation of Parts and Equipment Including GFE
- Quality Control Inspection
- Repair, Rework, Modification, and Replacement of Initial Tooling and STE
- Sustaining Engineering
- Production Control
- Materials Handling
- Manufacturing Engineering
- Subcontractor/Supplier Liaison
- Source Inspection

Thus the NAFCOM computed TFU includes the Operations and Support cost elements (Figure 1) of Integrated Logistics Support (e.g. materials handling, subcontractor/supplier liaison, etc.) and Pre-Planned Product Improvement (e.g. sustaining engineering).

The remaining Operations and Support Cost is the System Operation cost that is broken down into ground and flight operations. As shown in the breakdown of the TFU costs, the fabrication and final assembly costs are included. Not included in the costs are the payload integration and launch pad operations. However, these costs are considered negligible as compared to the unit costs of the flight systems expended after every flight as an architecture comparison discriminator.

Two methods were considered to determine the cost of the expended flight units. The first method assumes that the cost of each expended system is the TFU with a learning curve applied [53]. The learning curve is a manufacturing term that expresses the

amount of knowledge carried over from one unit to the next as a decrease in production cost [54]. The learning curve model used in this analysis assumes that the production cost is decreased by certain percent every time the number of units produced doubles. This learning curve is then applied to the TFU to determine the cost of the N^{th} unit produced. The yearly cost for this method is calculated using Equation 3. The N^{th} is carried over from one year to the next.

$$Yearly\ Cost = TFU \sum_i^n N_i^{\frac{\ln(2)}{\ln(LC)}} \quad (3)$$

The second method is a more detailed analysis which breaks the yearly cost into a fixed and variable portion. This more detailed analysis may be required to discriminate between certain design options. The fixed portion is all costs that are independent of the vehicle flight rate and thus remain constant for any flight rate. Even at a flight rate of zero the fixed portion remains. The variable portion is the costs that are dependent on the vehicle flight rate, and increases as number of missions completed each year increases. At a flight rate of zero, the variable portion is also zero. The yearly cost is calculated using Equation 4, the N^{th} unit is carried over from one year to the next. The total cost is derived from the estimate of the TFU.

$$Yearly\ Cost = Fixed\ \% (Total\ Cost) + Variable\ \% (Total\ Cost) \sum_i^n N_i^{\frac{\ln(2)}{\ln(LC)}} \quad (4)$$

Both Methods One and Two utilize the TFU for calculating the annual cost of the lunar campaign. In the case of Method One all cost are assumed to be variable and the total cost depends completely on the yearly flight rate. In the case of Method Two the variable cost is decreased and a fix portion is added to account for those cost that are independent of flight rate. When the flight rate remains constant either method may be used to provide a relative comparison for the LCC between two design options. The results presented in Chapters 5 and 6 will utilize Method One and in Chapter 7, where the flight rate varies, Method Two will be used to compare the use of refueling to the baseline architecture.

The final Operations and Support Costs are the Flight Operations or Mission Control of the system. Because all of the different architectures studied include the same launch and orbital vehicles, it was assumed that the Flight Operations for these systems were constant and were not a discriminator for Life Cycle Cost comparisons. However, the architecture with the Propellant Depot would require additional Flight Operations. Since there are no historical data for the operational cost of a propellant depot, the operational cost of the Hubble Observatory was used as an analogy. The Hubble data processing facility and workforce that analyze the observational data were not included. Thus, the flight operational cost of the propellant depot is estimated to be \$100M per year which assumes to address system health monitoring, station keeping, and mission planning for the refueling events.

In order to determine the total Life-Cycle costs of the system architecture, a yearly economics model was developed to spread the DDT&E costs over Phase C and D and the Operations cost over Phase E (Figure 2). Phase F (Closeout) or Disposal was not

considered in this present analysis because it is not a discriminator for architecture comparisons.

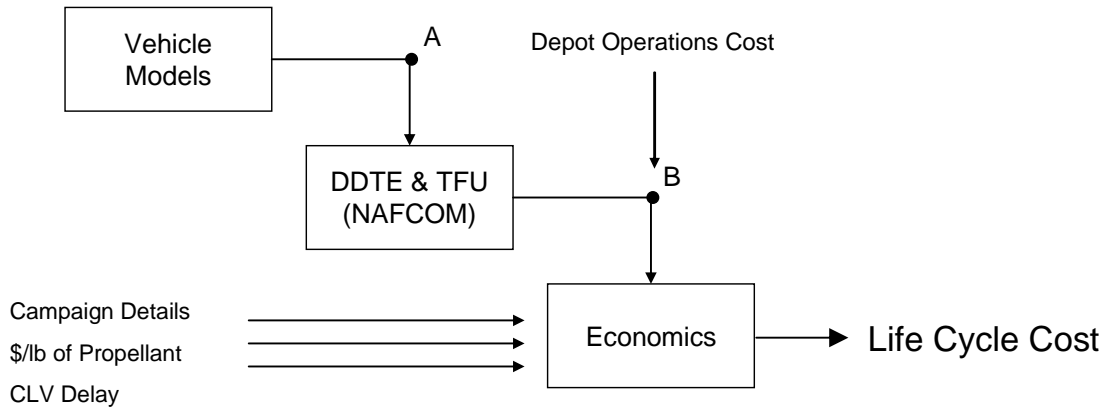


Figure 33. Life Cycle Cost Analysis Flow of Information

The life cycle cost estimate used in this thesis spreads the DDTE out over a number of years at the beginning of the program for each architecture element. The CLV, CEV, and in-space depot developments are spread out over five years while the CaLV and LSAM are spread out over six years based on the complexity of these systems. This DDTE is spread as a Beta function over the specified number of years [52]. The development of the CEV and CLV begins in 2007 and the CaLV, LSAM, and in-space depot begin in 2011. The life cycle analysis will assume a campaign that begins with the CEV and CLV operating two flights per year for the five years immediately following their development program. The development of the CaLV, LSAM and in-space depot is completed during these five years. Once all of the development work is completed the architecture begins operation of a 15 year lunar campaign with an assumed flight rate of two missions per year. The LCC results presented in Chapters 5 and 6 will utilize Method

One with an initial assumption of no learning throughout the campaign. As discussed previously various learning rates and the fixed versus variable cost analysis will be investigated in Chapter 7 to understand their effect on the implementation of propellant refueling. The discounted yearly cash flow [53] analysis is provided in Figure 34. The initial peaks and valleys represent the development period of the different architecture elements. These development periods could be designed to overlap to eliminate the drop off in LCC, but this has no impact on measuring the impact of propellant refueling on the architecture. A discount rate of three percent is applied when developing the discounted life cycle cost. The results presented throughout this thesis are provided in 2007 dollars (FY 2007 \$M).

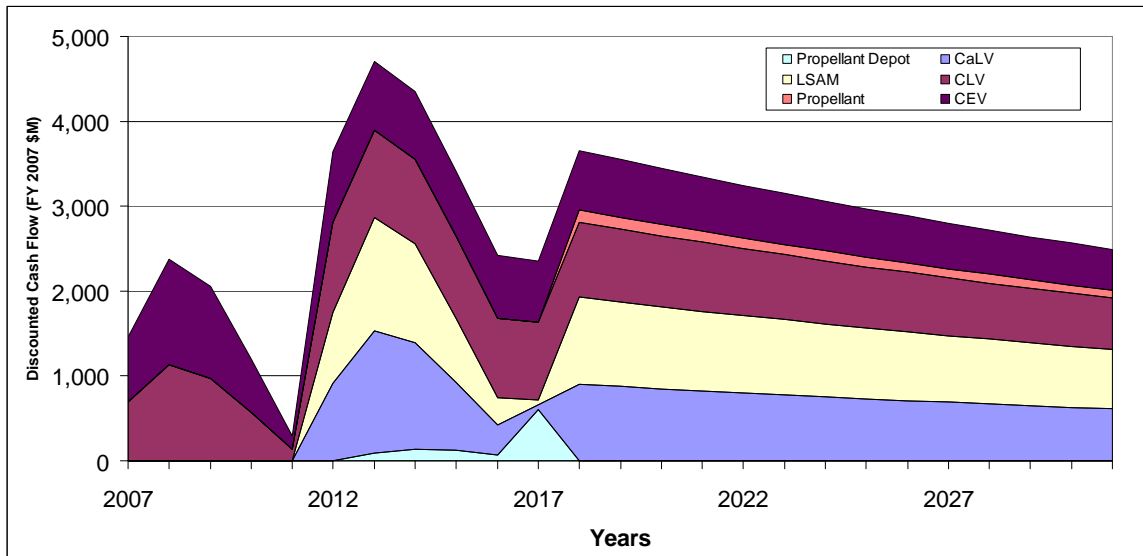


Figure 34. Life Cycle Cost Spreading for Baseline Architecture

The two development periods between 2007 – 2011 and 2011 – 2016 followed by the 15 year lunar campaign starting in 2018 are shown in Figure 34. The spike in cost in 2017 accounts for the deployment of the in-space depot. The calculation assumes that only one depot is required throughout the program. Later in the thesis, the depot costs are varied to determine overall LCC impacts. This life cycle cost analysis and lunar campaign will be used for all design points in Chapters 5 and 6.

4.1.5 RELIABILITY MODEL

The reliability model is designed to determine the system-level reliability for the entire lunar architecture. The overall system reliability is dependent on the reliability of the individual elements and events within the architecture. The model uses a Fault Tree Analysis, a technique used during the Apollo program [55], where the reliability of the entire architecture is built up from individual events. In this case, the reliability hierarchy is broken down into three levels: the overall architecture, the six phases of operation (Ascent, LEO Operations, Propellant Refueling, Lunar Transfer, LLO Operations, and the Lunar Mission), and the individual underlying events. This structure is outlined in Figure 35. The metric of interest is the loss of mission probability. This is the reliability most affected by the addition of propellant refueling. The loss of crew reliability is not affected because all refueling can occur before the crew is delivered to LEO. The mission phases that occur after lunar ascent are not considered, as they are not affected by the addition of propellant refueling.

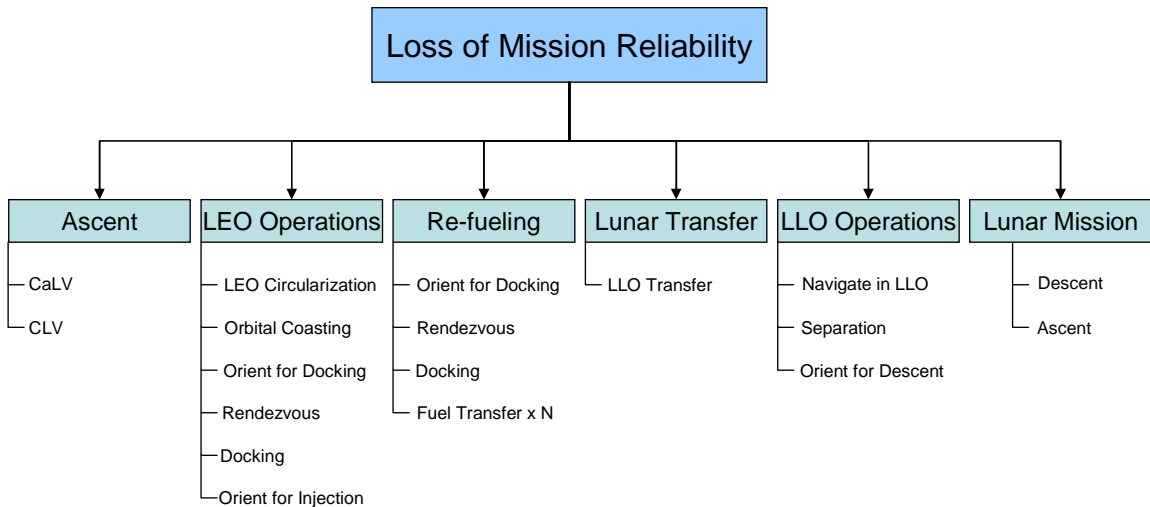


Figure 35. Reliability Model Fault Tree Analysis Structure

The reliability for the overall architecture is calculated using the Fault Tree Analysis technique, which builds up the overall system reliability from the reliability of the mission events. In this case, the event reliability numbers are taken from historical programs, such as the Apollo [55] and Space Shuttle programs [56]. The individual event reliabilities are provided in Appendix C. The in-space reliability values were taken from the reliability estimations made during the initial Apollo mode comparison. A secondary calculation is also made to provide an estimate of how these reliabilities have improved since the beginning of the Apollo program. This calculation assumes that a ten-fold improvement in each system has been achieved. The reliability calculations for the CaLV and LSAM were developed using a dynamically allocating fault tree calculator that is able to determine the reliability of each vehicle based on a number of system parameters, such as the engine type and required mission maneuvers[57]. The reliability of the launch vehicles was not greatly affected by this study because their basic configurations are not changed, and the major design changes, such as burn time, do not have a large impact on

the vehicle reliability. The lunar lander design space contained a number of different engine and propellant combinations, all of which have a substantial impact on the overall reliability of the lander. The dynamically allocating fault tree predictor was able to update and re-calculate the reliability for both the CaLV and LSAM without having to create a new model for each design point.

The addition of propellant refueling adds an additional point of failure to the architecture, and as a result, the overall reliability is decreased. The Apollo-based reliability estimate for the entire propellant refueling operations is 0.9676, resulting in less than four failures in 100 refueling trips. This is a higher reliability than the Apollo program predicted for the LEO operations (0.916) and lunar transfer (0.762) phases. This reliability is further reduced as the number of propellant refuelings is increased, as all refueling must occur in order for the mission to continue. This model accounts for the total number of refueling events utilized by the architecture.

The loss of mission calculation made in this model provides a relative reliability comparison for each of the propellant refueling trades considered. While the addition of the refueling event decreases the reliability of the architecture, the addition of the capability can improve the reliability of other areas of the architecture. It was discussed in Chapters 1 and 2 that the addition of propellant refueling can de-couple the success of each mission from the successful on time launch of both launch vehicles. This trade in reliability allocation will be considered further in Chapter 7.

4.1.6 TECHNOLOGY RISK MODEL

The risk module provides an estimation of the technological development risk associated with maturing the technologies that are currently not at TRL 9. A list of the technologies that factor into the risk calculation are provided in Table 31 along with the TRL number assumed for each. All other technologies are assumed to not influence this study and are not considered in this calculation. The risk associated with developing each technology is assumed to be an exponentially increasing function of TRL [58]. The lower the TRL, the greater the risk encountered to fully mature the technology. This is due to the uncertainty in the cost and schedule required to mature the technology and the final performance level obtained. The total risk score for each design is a summation of the individual risk score for each technology; therefore, the more technologies that must be matured, and with lower starting TRL level, the greater the risk to the architecture. It is difficult to accurately determine the development risk of any technology because so many unknown factors exist. This model utilizes a simple exponential function to equate the development risk to the starting TRL; this is provided as Equation 5. The exponent is a scaling factor that set the risk score of a technology at TRL nine to ten and a technology at TRL one to zero. This is an arbitrary scale used to provide a relative comparison between the design points that require additional technology development before they can be utilized by the architecture.

$$Risk = e^{(TRL-1)^{0.29973}} - 1 \quad (5)$$

Table 31. Summary of Development Risk Assessment

Technology	TRL	Risk Score
Ascent Engine		
Storable	7	5.04
LOX/CH4	5	2.32
LOX/LH2 (pressure)	8	7.15
LOX/LH2 (pump)	8	7.15
Propellant Thermal Management		
MLI	8	7.15
Cryo-cooler + MLI	4	1.46
Refueling	4	1.46

4.2 VALIDATION OF BASELINE MODELS

The final section of Chapter 4 discusses the validation process that was conducted to confirm the results for each of the vehicle models. The goal of the models was to match the payload capability and mass of the vehicles developed during the ESAS study. The payload capability is one of the key measures for each vehicle and the dry mass leads directly to the overall cost of the vehicle. These vehicles were designed and calibrated to match the ESAS results so that these models could provide a direct comparison when the propellant re-supply elements are added to the architecture. The vehicle mass, propellant requirements, and payload delivered were all within a few percent of the ESAS results. These results are provided in the following sections. A detailed discussion as to the development of these results can be found in reference [59].

4.2.1 CARGO LAUNCH VEHICLE

The cargo launch vehicle (CaLV) is designed to deliver large non-human cargo elements to LEO for lunar exploration missions. This includes in excess of 320,000 lbm of payload comprised of the LSAM and TLI propellant. A detailed description of the cargo launch vehicle is provided in Chapter 2. A mass comparison of the ESAS results for the cargo launch vehicle and the one developed during this study were provided in Table 21. These results showed that the dry mass of the two vehicle differed by less than one percent. This was achieved because the MERs used for the sub-system mass were calibrated to match the results outlined in the ESAS report [pg. 428]. This allowed the basis of the launch vehicle models to be to the same so that the trajectory and cost analysis would provide a better comparison.

The ESAS report [pg. 433] provided a set of trajectory plots for the ascent phase of the CaLV which provide another means of comparison between the two models, Figure 36 and Figure 37. These results are taken directly from the output of the POST optimized trajectory. The main difference between the two trajectories is that the optimized path of the model pulls up out of the densest part of the atmosphere later than the ESAS CaLV exposing it to a higher thermal load. This additional load last for approximately 10 seconds. The dynamic pressure peak remains the same at around 550 psf. The other aspects of the trajectory, (altitude, velocity, and acceleration) match up well with the published ESAS results. A comparison of the trajectory profiles are provided in Figure 36 and Figure 37. The fact that the final trajectories are nearly identical suggests that this model will predict the behavior of the CaLV well.

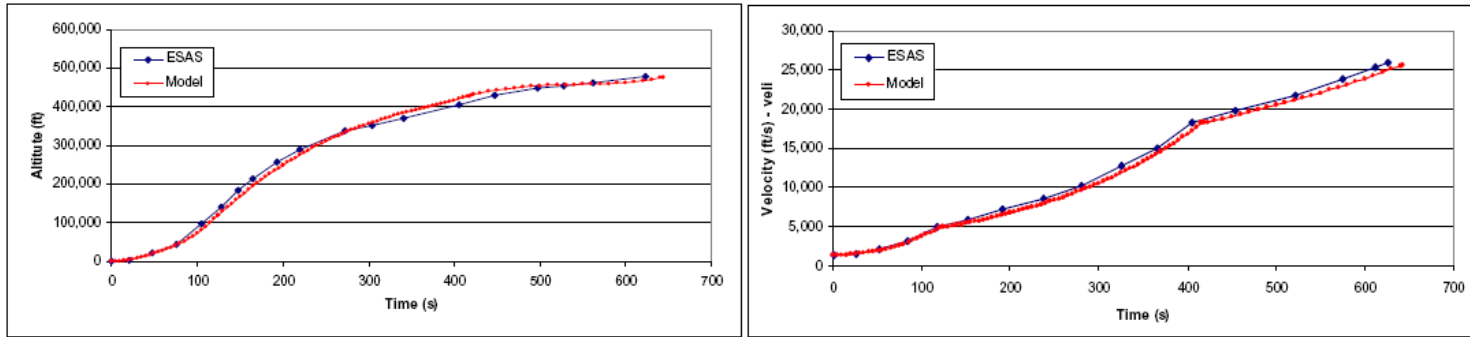


Figure 36: CaLV Altitude and Velocity Profile Comparison

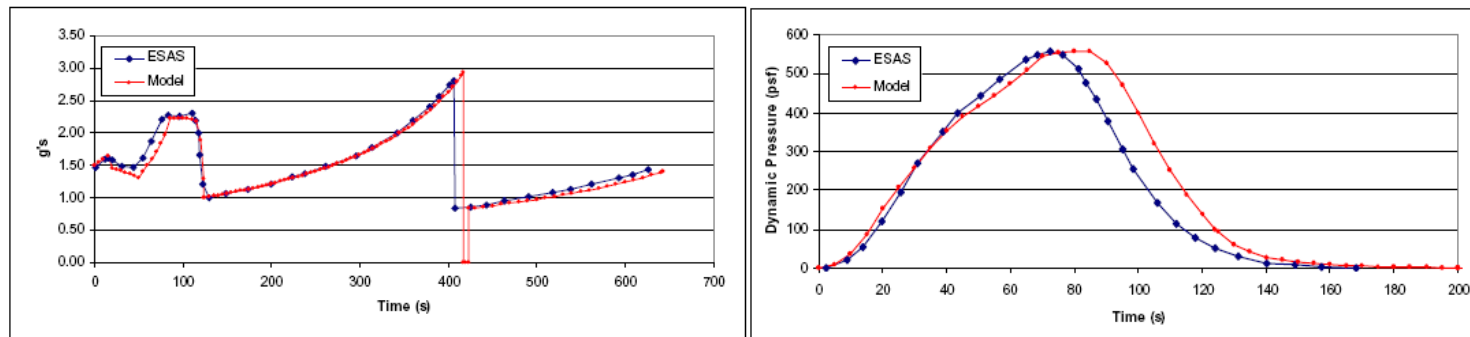


Figure 37: CaLV Acceleration and Dynamic Pressure Profile Comparison

A summary of the key trajectory results are provided in Table 32. The main differences seen here is the timing of the vehicle separations. The stage separation events of the model are around eight to sixteen second off from the ESAS trajectory data. This is primarily due to an increase in the burn time of the solid rocket boosters. The overall propellant requirements and mass ratio were shown to provide an accurate estimate of the ESAS results.

Table 32. Summary of Trajectory Analysis

	ESAS	Model
Mass Ratio	4.84	4.83
Max Dynamic pressure (psf)	523	558
SRB Separation (s)	117	125
1 st Stage Separation (s)	405	418
2 nd Stage MECO (s)	627	643
Max g's	2.8	2.94
Final Velocity (ft/s)	25,900	25,700

4.2.2 LUNAR SURFACE ACCESS MODULE

The Lunar Surface Access Module (LSAM) provides both access to the lunar surface and a habitat for humans during exploration missions. Once in Low Lunar Orbit (LLO), the crew transfers to the LSAM for descent to the surface. The crew utilizes the LSAM as a base of operations while on the surface. At the end of the mission the LSAM separates and a smaller ascent stage is used to return the crew to the CEV in LLO (Figure 5). Chapter 2 provides further details on the LSAM design and function.

The LSAM model again provides a close match to the results presented in the ESAS reports, as shown in Table 26. The largest difference between the two models is seen in the dry mass of the descent stage. While there is a 5.5% error between the model and the ESAS results, this is only a mass difference of 350 lbm. This is primarily due to differences in the structural mass of the vehicle. It is difficult to model the subsystems mass of the lunar lander because there is little historical mass information to base the analysis. The remaining vehicle parameters, specifically the lunar surface payload capability and total lander mass, match up well with the published results for the ESAS lunar lander.

The results from these validation cases provide enough evidence to conclude that the development of these models resulted in an accurate representation of the baseline ESAS architecture elements for reference comparison. A cost and reliability validation was not possible, as the ESAS results were not made public. The models and tools discussed in this chapter are used to evaluate the propellant re-refueling design space. These simulation results will be discussed in Chapter 5 – 7.

CHAPTER 5

A PARETO FRONTIER FOR LUNAR SURFACE PAYLOAD CAPABILITY AND LIFE CYCLE COST: SCENARIO ONE

The term *non-dominated solution* refers to the locus of points within a design space where no additional improvements in the responses can be made without violating constraints. These points define the design space boundary and represent the best achievable solutions. This boundary is referred to as the Pareto frontier. Any solution not along the frontier is considered dominated and can be improved by moving to a solution on the frontier. A point along this frontier can then be selected based upon the preferences of the decision maker to one response or another. This helps the decision maker understand how his or her preferences and the uncertainty of these preferences affect the final architecture selection.

This chapter will discuss the Pareto frontier for the lunar surface payload versus life cycle cost metrics and categorize the non-dominated design points which bound this design space. The results will demonstrate that, in general, in order to increase the lunar surface payload capability, the life cycle cost of the architecture must increase. There are, however, a number of design points that can improve the lunar surface payload capability while also achieving a lower life cycle cost than the baseline. As will be shown, all points along the frontier include the use of propellant refueling. The ESAS baseline design point, described in Chapter 2, is not on the Pareto frontier, suggesting that an

improvement in the architecture can be achieved through the addition of propellant refueling. These two FOMs were selected to provide a screening for the best refueling strategies. The other FOM were not selected because for a given refueling options there is little difference in the risk, extensibility and reliability of the architecture. Therefore, these do not act as good discriminators for the screening process. The impact on these three FOM will be further examined in Chapter 7.

5.1 THE IDENTIFICATIONS OF NON DOMINATED SOLUTIONS

The procedure described in this section is intended to define a Pareto frontier using the propellant refueling trade space simulation discussed in Chapter 3. This chapter will focus on the results for Scenario One; the design philosophy for this Scenario is to utilize propellant refueling to improve both the lunar surface and LEO payload capability of the architecture. Given any two Figures of Merit, such as life cycle cost and lunar surface payload, the steps in Figure 39 can be used to develop the set of non-dominated solutions. The trade space morphological matrix is shown in Figure 38. Where the nine propellant design variables used in this study are listed in the first column, and the remaining columns represent the design choices for each input variable.

5.1.1 DEVELOPING THE PARETO FRONTIER

A logic flow diagram of the steps used to generate the Pareto frontier is provided in Figure 39. The first step in developing the Pareto frontier is to eliminate any extraneous design points that do not make practical sense. These cases were only

included to simplify the automation of generating the entire trade space. For example, all cases that include both cryo-coolers and Hypergols on the LSAM ascent stage are removed since no propellant boiloff will occur in these cases.

Design Variable	Design Options				
Additional Ascent Propellant	0	25,000 lbs	50,000 lbs	75,000 lbs	100,000 lbs
EDS Boil-off Mitigation	MLI	MLI+Cryo			
Lander Stage Re-fueled	None	Descent	Ascent	Both	
Lander Propellant	50%	100%			
LSAM Ascent Propellant	LOX/CH4	Hypergols	LOX/LH2 (pressure)	LOX/LH2 (pump)	
Lander Boil-off Mitigation	MLI	MLI+Cryo			
LOI Burn Element	EDS	LSAM DS			
LEO Required Stay Time	95 Days	15 Days			
Re-fuel Boil-off	No	Yes			

Figure 38: Trade Study Morphological Matrix

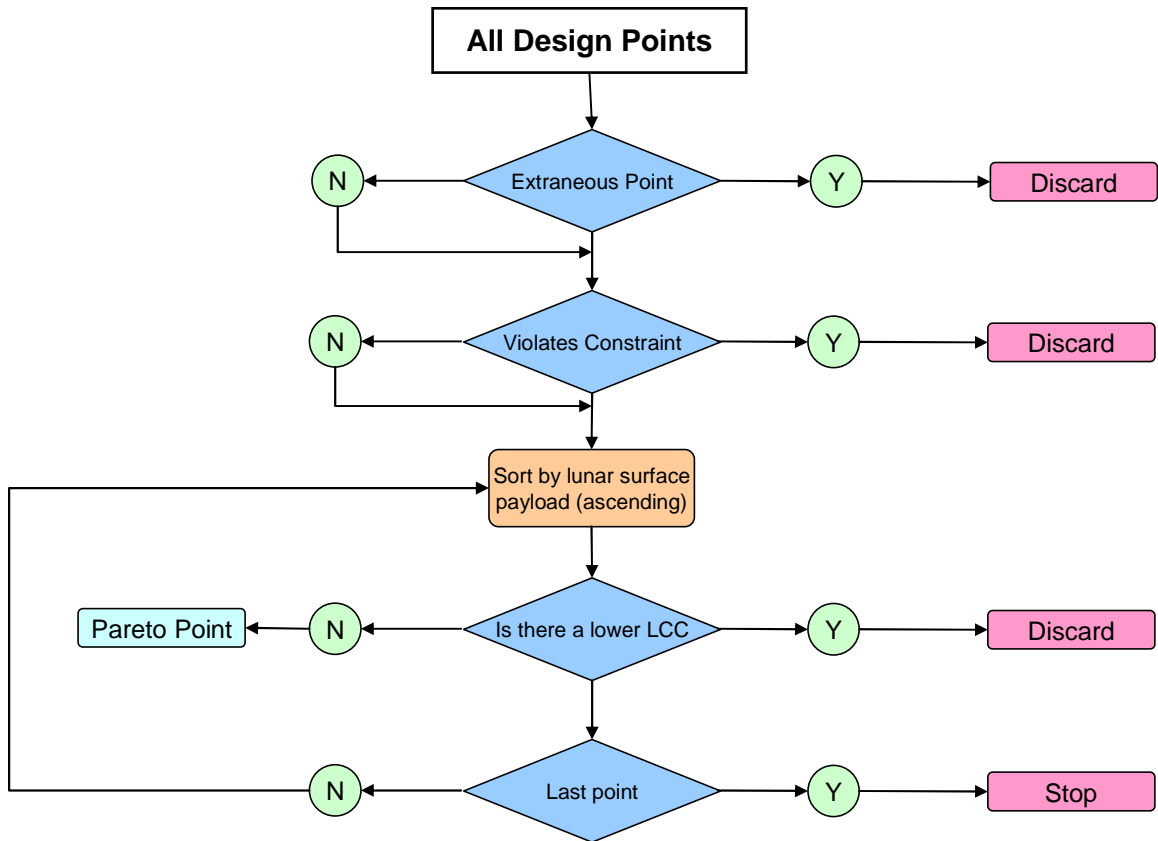


Figure 39: Pareto Frontier Creation Flow Chart

The next step is to place a limit on the payload capability of the architecture, where the addition of propellant refueling can increase payload capabilities that increase the size of the LSAM beyond the limits imposed by the fairing of the CaLV. The black design points in Figure 40 represent the designs that were removed from consideration due to this fairing constraint. The red points represent an 8.5m diameter constraint, and the blue points represent a 9.5m diameter constraint. The results discussed in this chapter will assume an 8.5m diameter constraint as it used in the baseline configuration. In all cases, a 10m maximum height constraint is also applied to the payload section of the lander (Figure 41). As will be discussed later in this chapter, the points that offer the

lowest cost per pound of payload to the lunar surface are well below this height constraint.

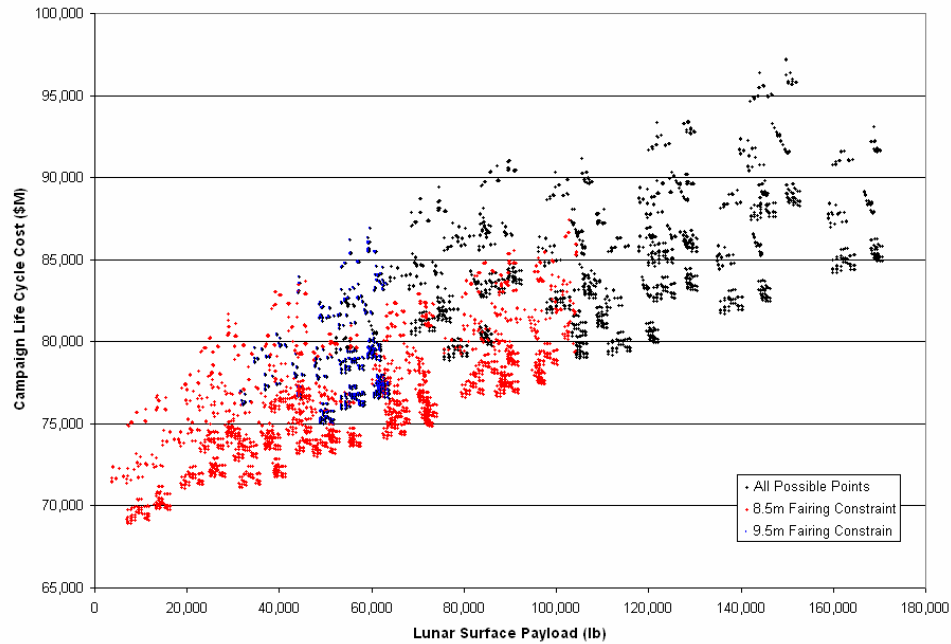


Figure 40: All Design Point with Fairing Constraint Applied

Constraining the fairing diameter to 8.5m and a height of 10m restricts the payload to 100,000 lbm as is shown in Figure 41. This assumes the same packing density for the baseline LSAM design. The fairing diameter constraint has no effect on the design points that fall on the Pareto frontier. As shown in Figure 40, the design points that would be added if the fairing constraint was increased to 9.5m lie within the Pareto frontier. Therefore, this constraint is not active for the points along the frontier. The active constraint along the frontier is the maximum allowable payload height. Placing this constraint at 9m would remove all points with a payload capability greater than 90,000 lbm, and increasing this constraint to 12m would increase the maximum payload

capability to 125,000 lbm assuming the packing density of the payload remains the same as the current LSAM configuration. A larger payload would raise the landing CG, which may require a more sophisticated landing control system. This effect is not considered in this analysis.

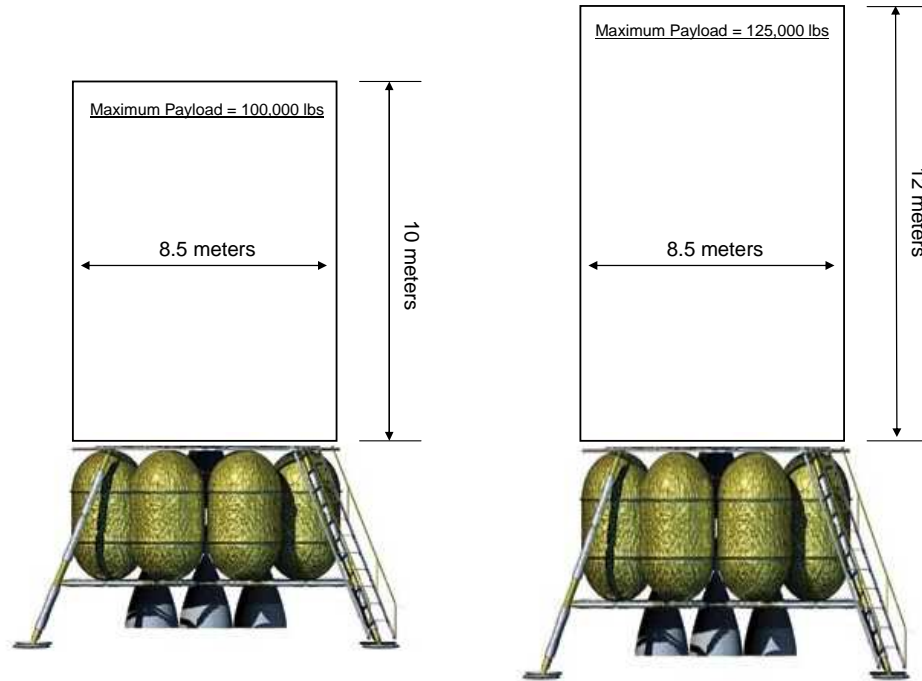


Figure 41: LSAM Volume Constraint Dimensions

Once the infeasible trade set and geometry constrained data has been eliminated, the non-dominated solutions in the design space can be determined (Figure 39). The remaining designs are sorted in ascending order by lunar surface payload capability. The design with the lowest payload is selected, and a search is performed for designs with a lower life cycle cost. If such a design is found, the current one is discarded, as it is not Pareto optimal. This process is repeated for the design with the next higher lunar surface payload capability and is continued until all design points have been examined. The

design points that remain represent the Pareto frontier. In this case, the Pareto frontier is comprised of 27 design points, which have the lowest LCC that can be achieved for a given payload capability. The Pareto frontier generated from this analysis is shown in Figure 42. These are broken down into two sets. The pink points, near the baseline, represent the design points where no propellant refueling was considered, and the blue points represent where propellant refueling was utilized.

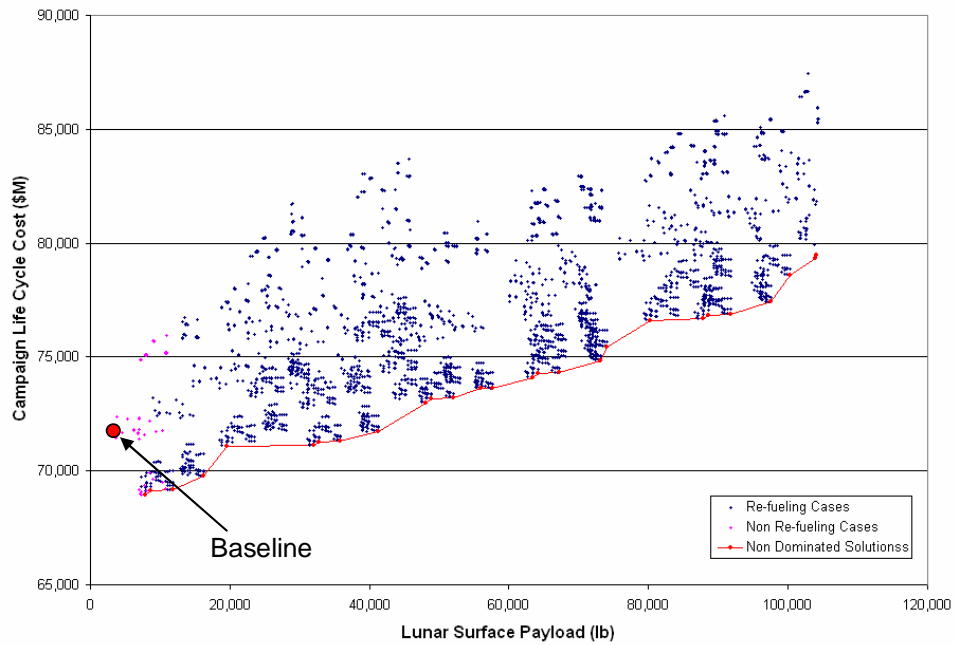


Figure 42: Path for Establishing the Set of Non-Dominated Solutions, Scenario One

5.2 BASELINE IMPROVEMENTS FOR NON PROPELLANT REFUELING OPTIONS

Figure 43 shows ten circled design points that do not require propellant refueling have a better solution than the baseline design. These points are summarized in Table 33. These solutions either have a lower LCC and provide the same payload capability, or

they have a higher payload capability without increasing the LCC of the baseline architecture. There are a number of solutions that show an improvement in both the LCC and the payload capability of the architecture. Examining the region around the baseline design point reveals ten designs (circled data points) that offer a greater payload capability without increasing the LCC of the architecture and do not require propellant refueling.

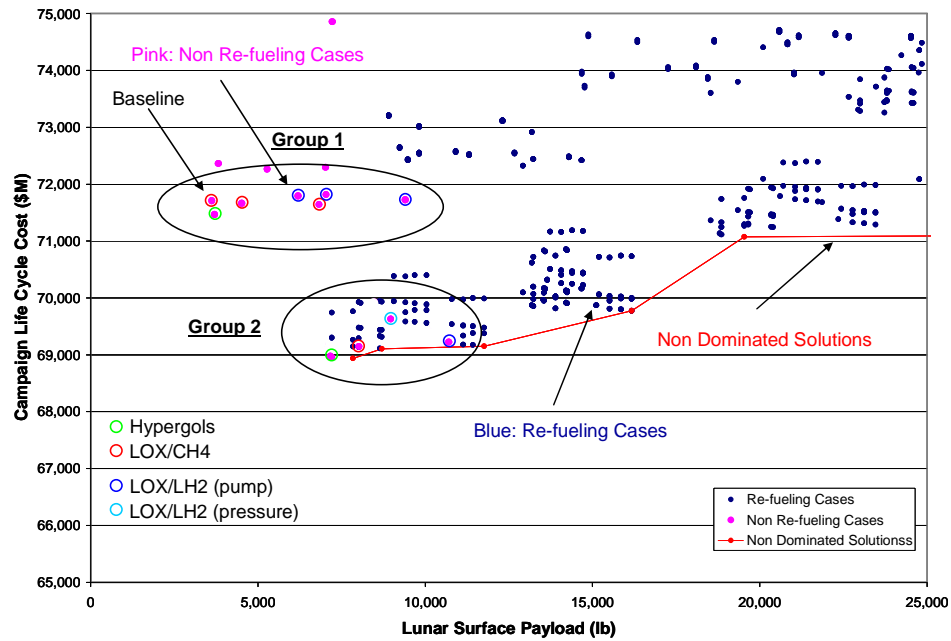


Figure 43: Improvements in Baseline Architecture

Table 33: Improvements in Baseline Design without Propellant of Refueling

Case #	Ascent Stage Propellant	Ascent Stage Thermal	Descent Stage Thermal	EDS Thermal	LEO Stay	LCC (\$M)	Payload (lbm)
1	(B) LOX/CH4	MLI	MLI	MLI	95	71,710	3,619
2	Hypergols	MLI	MLI	MLI	95	71,467	3,704
3	LOX/CH4	Cryo-cooler	MLI	MLI	95	71,664	4,518
4	LOX/LH2 (pump)	MLI	MLI	MLI	95	71,793	6,198
5	LOX/CH4	MLI	Cryo-cooler	MLI	95	71,642	6,827
6	LOX/LH2 (pump)	Cryo-cooler	MLI	MLI	95	71,818	7,038
7	Hypergols	MLI	Cryo-cooler	Cryo-cooler	15	68,957	7,211
8	LOX/CH4	Cryo-cooler	Cryo-cooler	Cryo-cooler	15	69,147	8,018
9	LOX/LH2 (press)	Cryo-cooler	Cryo-cooler	Cryo-cooler	15	69,630	8,970
10	LOX/LH2 (pump)	MLI	Cryo-cooler	MLI	95	71,725	9,406
11	LOX/LH2 (pump)	Cryo-cooler	Cryo-cooler	Cryo-cooler	15	69,225	10,709

There are two distinct groups of designs: those that can increase the baseline payload capability for the same life cycle cost (Group 1) and those that can both increase the payload capability and decrease the life cycle cost of the baseline architecture (Group 2). The only differences between the two groups is the propellant boiloff thermal management system utilized by the EDS and the required LEO loiter time. In Group 1, the EDS and LSAM utilize a passive MLI thermal management system to minimize the boiloff propellant during a 95-day loiter period. The points in Group 2 utilize an active cryo-cooler plus MLI system to eliminate all propellant boiloff and are designed for a shorter 15-day loiter period.

The benefit of utilizing a cryo-cooler to eliminate propellant boiloff is due to an increase in the lunar surface payload and a decrease in the LCC as shown in Figure 43. The payload increases because the cryo-cooler system has a lower total mass than the MLI only system plus the propellant lost to boiloff, as is shown in Figure 44. Eliminating the need to carry additional propellant directly leads to an increase in architecture

payload. Examining Case #4 and Case #11 in Table 33 shows that a 5,200 lb increase in payload is achieved when transitioning from an all MLI system to a cryo-cooler plus MLI system. A more detailed model of the thermal managements system is needed to determine if refueling the LEO boiloff is a better solution than utilizing a cryo-coolers to eliminate this loss of propellant.

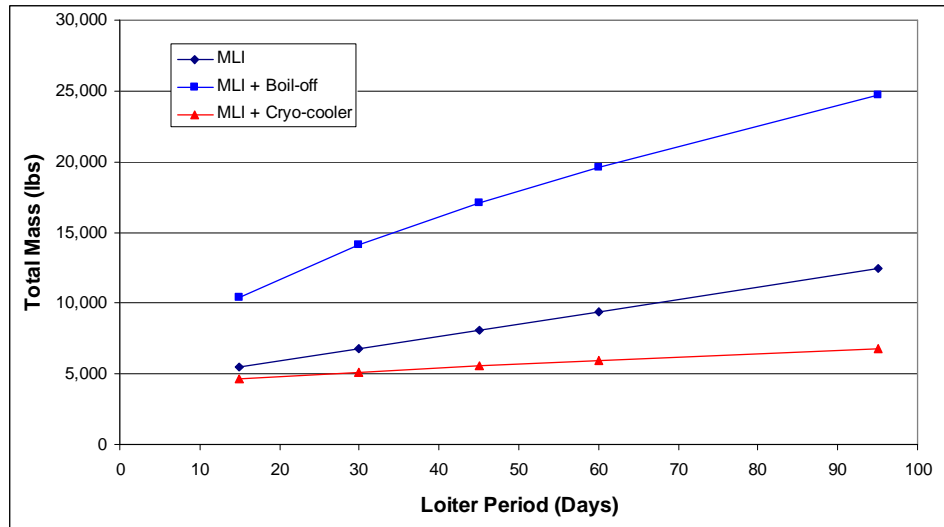


Figure 44: Total Mass of the Potential Thermal Management Systems

The LCC is also less for the points in Group 2 than in Group 1 because the elimination of propellant boiloff allows the CLV to be delayed without resulting in a loss of the LSAM and EDS. In the design points where only MLI is used, once the designed loiter period is exceeded, the EDS and LSAM no longer have sufficient propellant to complete the remaining mission maneuvers. These elements must then be replaced before the mission can be completed. The probability that this will occur is dependent on the designed LEO loiter period. This change in probability is illustrated in Figure 45 along with the increase in LCC to account for the replacement missions. The shorter the design

loiter period, the higher the probability that a mission will be lost and the greater the cost to the architecture. The benefit of a short loiter is that less propellant must be carried to LEO resulting in a greater payload. A decrease in LCC of \$2.5B can be achieved by switching from an MLI system (case #4) to a cryo-cooler system (Case #11) on all architecture elements. These results and all of the results that follow in this chapter and in Chapter 6 assume that once the designed loiter period is exceeded than the mission is lost and must be replaced. In actuality this may not always be the case, because the architecture is designed to perform the worse case mission during the worse Earth-Moon alignment. Since these conditions are rarely both active the architecture may be able to remain in LEO for a longer period of time. This work will require that that architecture always be ready to perform the worse case mission, but this may be an optimistic assumption and should be considered when evaluating the results of this study.

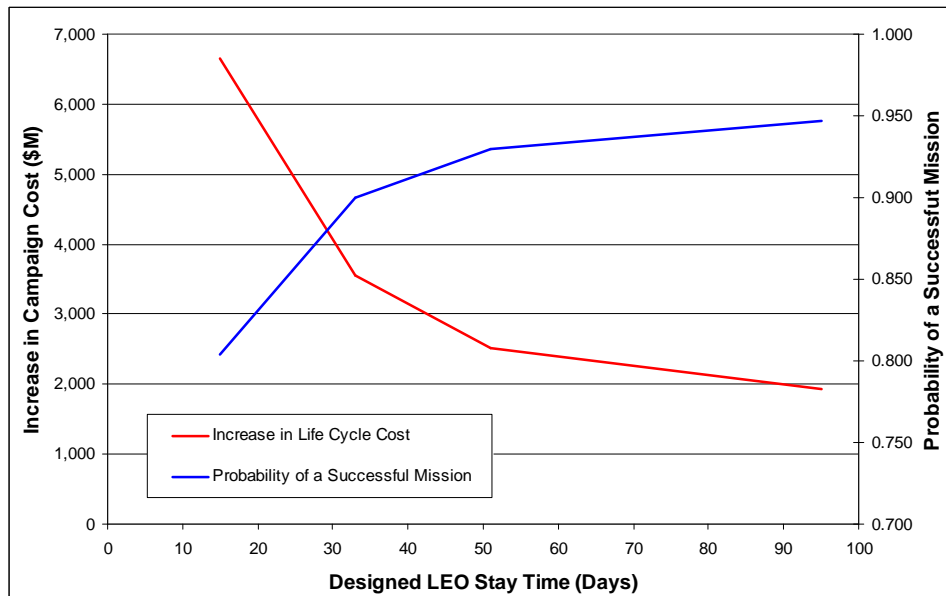


Figure 45: Loss of Mission effect on LCC

There is a secondary trend relating to the engine selection on the LSAM ascent stage that can be observed within each of these groups as shown by the circles and the data points in Figure 43. In both groups, the LCC varies only slightly while the payload capability can vary by as much as 200%. The Hypergol engine (green points) has the lowest payload capability while the pump-fed LOX/LH2 engine (dark blue circles) has the highest. This is due to the increase in performance of each engine (Isp and T/W_E , Figure 40), which directly affects the payload of the vehicle. The engine performance values along with the corresponding payload are provided in Figure 46. This figure shows that, as the Isp and T/W_E increase, the lunar payload also increases. The LOX/LH2 pump-fed engine offers the greater payload because it has the highest Isp (460) and T/W_E (38). A greater Isp and T/W_E reduce the amount of propellant required to complete the mission maneuver, and since the total mass of the LSAM is held constant, a reduction in the required propellant results in an increase in payload. A more detailed cost analysis is needed than provided here in order to account for all of the differences between the various engine options. An engine with a greater performance has a higher engine cost, but lower inert mass which results in a lower vehicle cost. A more detailed cost analysis would help provide a better discriminator for the AS selection, but this is not a primary result of this work. The work in this chapter shows that the engine selection is not greatly effected by the addition of propellant refueling and that the engine selection has a smaller overall effect in the architecture than the introduction of propellant refueling.

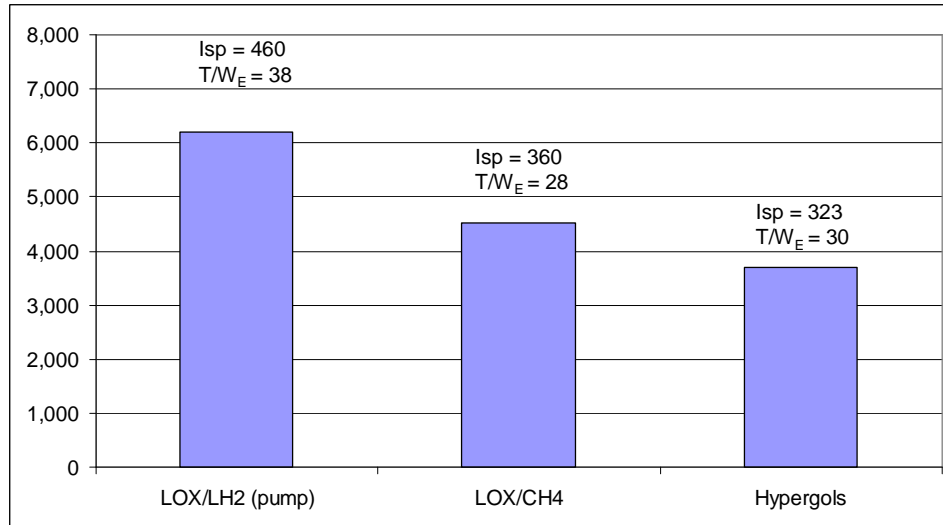


Figure 46: Engine Performance Values and Payload Capability

As an example, a configuration that utilizes a passive thermal control system on all architecture elements with a LOX/LH2 ascent engine (Case #4) can provide 2,500 lbm more payload capability than utilizing a Hypergol engine (Case #2). The LOX/LH2 engine increases the cost of the LSAM Ascent Stage because of its greater complexity [Humble]. The complexity factors used for estimating the DDT&E and TFU for the ascent engine are provided in Table 34 [60]. The Hypergol engine is the simplest design considered and results in the lowest development and production cost. The LOX/LH2 pump-fed engine option is the most complex, and therefore results in the highest cost to the architecture. The LCC is increased by \$325M when a LOX/LH2 pump-fed engine (Case #4) is used instead of a Hypergol engine (Case #2). The cost of the ascent engine is a small component of the overall LCC of the architecture. Thus it has less of an impact than an increase in the payload capability.

Table 34: LSAM Ascent Stage Engine Complexity Factors

Engine Type	DDT&E CF	TFU CF
LOX/LH2 (pump)	3	2.28
LOX/LH2 (pressure)	2.2	1.88
LOX/CH4	2.6	1.97
Hypergol	1.0	1.0

The results of this study demonstrate that an improvement in the lunar surface payload can be achieved by utilizing a higher performing engine on the LSAM ascent stage and by utilizing cryo-coolers on each of the architecture elements. The change in Ascent Stage engine has a small effect on the LLC, while the switch to cryo-coolers shows a larger decrease because it is able to improve the LOM of the architecture. It is also evident that the elimination of propellant boiloff concerns with an advanced technology can greatly affect both the payload capability and the cost of the exploration architecture. This is why non-refueling designs show the best payload and cost when their propellant storage systems utilize an active boiloff thermal control system. In the case when hydrogen is used on the ascent stage it is assumed that zero-boiloff is achieved. In the case of a long term outpost mission this zero-boiloff level may be difficult to achieve. A further study of this is needed in order to fully address the limitation of propellant boil-off when the hydrogen engine is selected for the ascents stage. The Hydrogen engine may also results in a lower reliability because of the increase in engine complexity.

5.3 DESIGN TRENDS IN NON-DOMINATED SOLUTIONS

The previous section discussed how the baseline design could be improved without the implementation of propellant refueling technologies. While the previous section discussed a number of designs that can improve upon the baseline design, none of these designs fall on the Pareto frontier. This section will describe the Pareto-optimal designs and discuss how they differ from the non refueling cases and the baseline design. The solutions that lie on the Pareto frontier (red line) can be organized into five groups as shown in Figure 47. The Pareto frontier is comprised of design points that all utilize propellant refueling. The blue points in this figure represent the designs that utilize propellant refueling, while the pink points represent those that do not. The points on the Pareto frontier offer an increase in lunar surface payload capability, but generally result in a greater life cycle cost. The following section will discuss the points along the frontier and characterize how the introduction of propellant refueling affects the payload capability and the life cycle cost of the architecture.

The LCC results presented in this chapter and again in Chapter 6 will utilize the analysis outlined in Section 4.1.4. The components of the LCC include the development cost of the architecture elements, including the cost of developing a propellant depot for the refueling cases. The acquisition cost for the architecture element are also included, plus the cost of building and launching the propellant depot to LEO. The final component of the LCC is used for the refueling cases which must purchase propellant before completing each mission. This propellant is purchased at a set price and will be represented by a \$/lb.

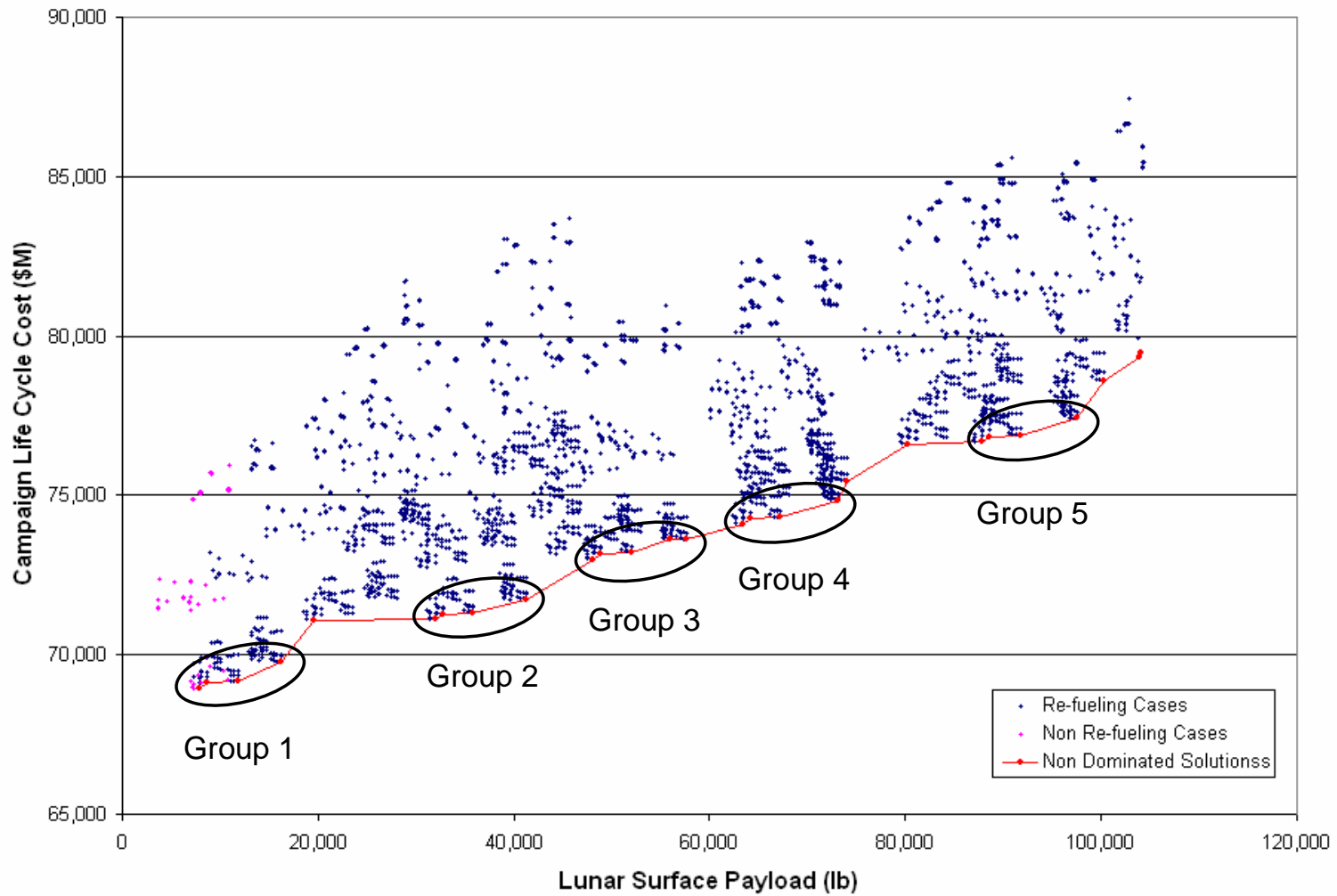


Figure 47: Propellant Refueling Pareto Frontier Groups

The initial results will utilize a price of \$2,000/lb and then sensitivity analysis will be conducted to see how the results change as the price of propellant is increased.

Before determining the best strategy for moving the baseline architecture onto the Pareto frontier, it is important to understand the makeup of the design points that fall along this frontier. There are five design variables that remain constant at every point along the frontier. These variables are the Descent Stage, Ascent Stage and EDS boiloff thermal control systems, the ability to re-fuel the LEO propellant boiloff, and requiring a 15 day LEO loiter. The ability to re-fuel the propellant lost to boiloff is the primary driver for the LEO loiter period and the thermal control system selected for the EDS and LSAM. The baseline architecture requires the EDS and LSAM to carry additional propellant to LEO to account for the propellant boiloff lost during the loiter period. Because the boiloff propellant can be re-fueled with a depot in LEO, the additional propellant required for boiloff with the baseline architecture can be replaced with payload (5,000 lbm or 140 %). This design choice allows the EDS and LSAM to be re-fueled prior to the trans-lunar injection maneuver and eliminates the need to carry additional propellant to LEO. As a result, the cargo launch vehicle can deliver a larger lunar surface payload capability. A second benefit of refueling the boiloff is that the CLV can experience a delay without resulting in a loss of mission and pre-deployed hardware (EDS and LSAM) because the boiloff propellant can be re-fueled at any time. As a result, a designated loiter period is not required. This drives the section of the 15 day LEO loiter which is the shortest period considered. Theoretically this should be driven to zero but this was not considered during the design space exploration. A lower life cycle cost is therefore achieved because these elements do not have to be re-launched as in the

baseline architecture which required 1 – 2 missions to be replaced during the lunar campaign based in a reliability of 0.947 (Figure 58).

Since the propellant boiloff is re-fueled and no longer an architecture concern, MLI becomes the best solution for the thermal management system on the EDS and LSAM. The results in Figure 48 illustrate that the use of a cryo-cooler plus MLI results in a lower total mass than MLI plus the mass of propellant lost to boiloff. However, if the propellant lost to boiloff is replaced then the total mass of the two systems is similar, especially for the 15 day loiter period. The cost of utilizing MLI is less than the development of a cryo-cooler system, and since the two system offer a similar total mass, the use of MLI becomes the best architecture design choice when the boiloff propellant is re-fueled. Since propellant boiloff is not a concern, cryo-coolers do not provide a benefit to the architecture. A passive system is still needed in order to reduce the total amount of boiloff and the amount of propellant that must be delivered.

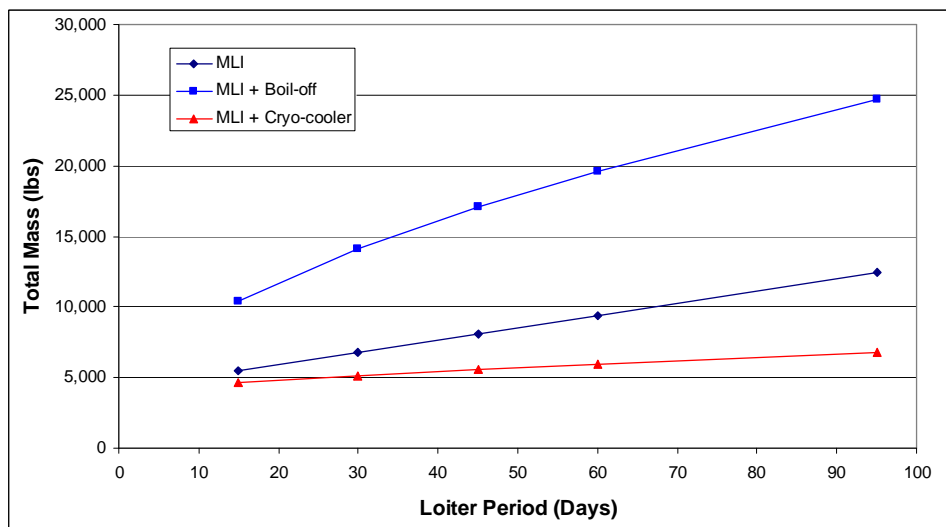


Figure 48: Total Thermal Management System Mass

Table 35: Scenario One, Non-Dominated Solution Description, Points 1 - 14

Case #	Group #	Ascent Propellant	Lander Refueling	LEO Stay Time	Re-fuel LEO Boiloff	LOI Maneuver	Additional Burn (lbm)	DS % Re-fueled	LCC (\$M)	Payload (lbm)	\$/lb
1	1	Hypergols	None	15	Yes	DS	0	n/a	68,939	7,840	293,107
2	1	LOX/CH4	None	15	Yes	DS	0	n/a	69,109	8,701	264,745
3	1	LOX/LH2 (pump)	None	15	Yes	DS	0	n/a	69,154	11,765	195,933
4	1	LOX/LH2 (pump)	Ascent Stage	15	Yes	DS	0	100	69,774	16,169	143,840
5	--	Hypergols	None	15	Yes	DS	25,000	n/a	71,076	19,539	121,257
6	2	Hypergols	None	15	Yes	EDS	0	n/a	71,110	31,942	74,207
7	2	LOX/CH4	None	15	Yes	EDS	0	n/a	71,280	32,803	72,432
8	2	LOX/LH2 (pump)	None	15	Yes	EDS	0	n/a	71,322	35,867	66,285
9	2	LOX/LH2 (pump)	Ascent Stage	15	Yes	EDS	0	100	71,742	41,213	58,026
10	3	Hypergols	None	15	Yes	EDS	25,000	n/a	72,999	48,045	50,647
11	3	LOX/CH4	None	15	Yes	EDS	25,000	n/a	73,169	48,906	49,871
12	3	LOX/LH2 (pump)	None	15	Yes	EDS	25,000	n/a	73,212	51,969	46,958
13	3	Hypergols	Ascent Stage	15	Yes	EDS	25,000	50	73,615	55,924	43,878
14	3	LOX/LH2 (pump)	Ascent Stage	15	Yes	EDS	25,000	100	73,620	57,599	42,605

Table 36: Scenario One, Non-Dominated Solution Description, Points 15- 27

Case #	Group #	Ascent Propellant	Lander Refueling	LEO Stay Time	Re-fuel LEO Boiloff	LOI Maneuver	Additional Burn (lbm)	DS % Re-fueled	LCC (\$M)	Payload (lbm)	\$/lb
15	4	Hypergols	Descent Stage	15	Yes	EDS	0	100	63,339	74,104	38,999
16	4	LOX/CH4	Descent Stage	15	Yes	EDS	0	100	64,200	74,275	38,564
17	4	LOX/LH2 (pump)	Descent Stage	15	Yes	EDS	0	100	67,263	74,317	36,829
18	4	LOX/LH2 (pump)	Both	15	Yes	EDS	0	100	73,116	74,854	34,126
19	--	LOX/LH2 (pump)	Ascent Stage	15	Yes	EDS	50,000	100	73,989	75,438	33,986
20	--	Hypergols	None	15	Yes	EDS	75,000	100	80,265	76,611	31,816
21	5	Hypergols	Descent Stage	15	Yes	EDS	25,000	100	87,794	76,668	29,109
22	5	LOX/CH4	Descent Stage	15	Yes	EDS	25,000	100	88,655	76,838	28,890
23	5	LOX/LH2 (pump)	Descent Stage	15	Yes	EDS	25,000	100	91,719	76,880	27,941
24	5	LOX/CH4	Both	15	Yes	EDS	25,000	100	97,544	77,414	26,454
25	--	LOX/LH2 (pump)	None	15	Yes	EDS	100,000	100	100,231	78,613	26,144
26	--	Hypergols	Ascent Stage	95	No	EDS	100,000	100	103,927	79,343	25,448
27	--	LOX/CH4	Ascent Stage	95	No	EDS	100,000	100	104,055	79,462	25,455

There are five remaining design variables which do not remain constant along the Pareto frontier: the Ascent Stage engine, which element performs the LOI maneuver, how much additional propellant is burned during ascent, which LSAM stage is re-fueled and how much propellant is re-fueled. These design variables can be grouped into five categories that make up the design points along the frontier. The five groups are shown in Figure 47, and the details of each are depicted in Table 35 and Table 36. The thermal management design variables are removed from these tables because they remain constant along the frontier.

The four groups can be distinguished by their implementation of propellant refueling and their values for the remaining design variables. For example, the only change between Group One and Group Two is that the LOI maneuver is performed by the descent stage in Group One and by the EDS in Group Two; the remaining design variables are the same. The makeup of the five groups along the frontier can be differentiated by the vehicle that performs the LOI maneuver, the amount of additional propellant burned during ascent, and the lander stages that are re-fueled. The Ascent Stage engine selection does not affect the makeup of the groups along the frontier, but rather forms a repeating pattern within each group. The following section will describe how the remaining design variables define the points along the Pareto frontier.

The choices of ascent engine and LSAM refueling scenario create a repeating pattern within each of the five groups. This pattern can be seen by examining how the ascent stage engine selection and LSAM refueling strategy change for Cases 10 – 14. The ascent stage engine follows the following pattern while moving from low to high payload capability within each group: Hypergols, LOX/CH₄, LOX/LH₂ (pump), *Hypergols*,

LOX/LH2 (pump). This pattern is illustrated in Figure 49. The second Hypergol case is italicized because it only occurs in some of the groups while the other four points are always present. As an example of this trend, consider the points in Groups Three (Cases 10 – 14). The first three points include no lander refueling while the final two points re-fuel the ascent stage. This example is illustrated in Figure 49, where the ascent engine selection and LSAM refueling strategy are noted.

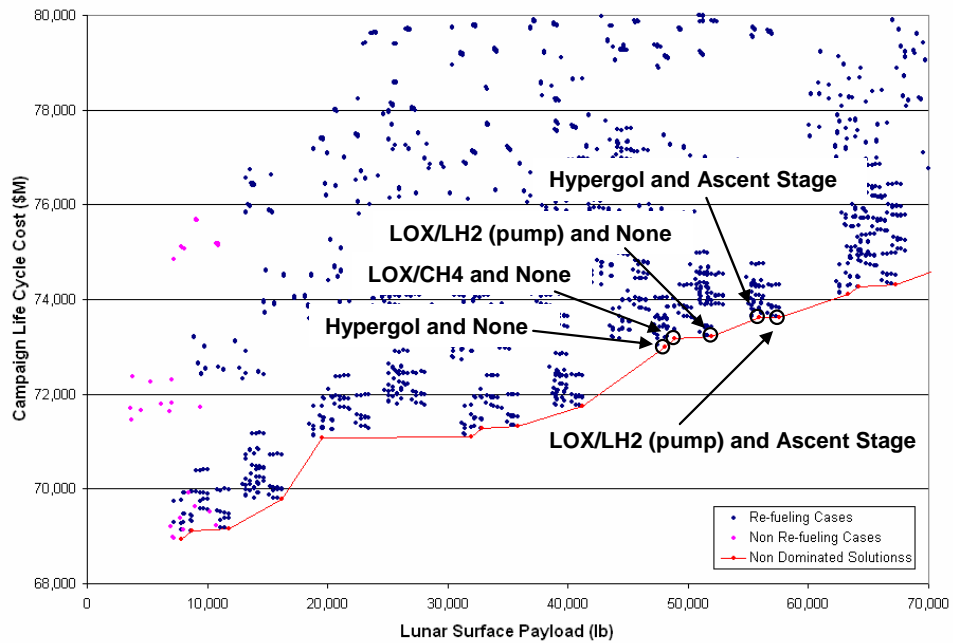


Figure 49: Ascent Engine and Lander Refueling Pattern

This pattern is a result of the engine performance factors (I_{sp} and T/W_E) and the amount of propellant offloaded from the LSAM. The five cases in Group Three can be used to outline this pattern. Cases 10 – 12 utilize no propellant off-loading from the LSAM while Cases 13 and 14 off-load all of the propellant from the ascent stage. As a result Cases 10 – 12 have a lower payload capability and LCC than Cases 13 and 14. This is because, when propellant is offloaded from the LSAM, it is replaced with additional

payload (constant gross mass); the more propellant offloaded from the LSAM the greater the payload. This increase in payload results in an increase in LCC because additional propellant must be purchased as more propellant is offloaded. As an example, Case #13 provides an increase of 7,819 lbm of payload over case #10 and an increase in LCC of \$616M. The only difference between these two design points is the amount of propellant offloaded from the LSAM.

This pattern also shows how the selection of the ascent stage engine affects the lunar surface payload and the LCC of the architecture. Figure 50 illustrates the change in payload for Cases 1 – 3 as the ascent engine changes. The LOX/LH₂ engine (Case #3) has the highest Isp and T/W_E which results in the greater payload. The LOX/CH₄ (Case #2) and Hypergol (Case #1) have a comparable payload because they have similar performance factors with Case 1 providing a lower Isp and a slightly higher T/W_E. The performance factors affect the mass of propellant required to complete the mission maneuvers, a greater T/W_E and Isp results in less propellant. The total mass of the LSAM is held constant during this scenario, thus a decrease in required propellant leads to an increase in the payload that can be delivered to the lunar surface. This resulting change in payload is seen in all five groups along the Pareto frontier. The relative close vicinity of these points suggests that the engine type, and how the lander is re-fueled, have less of an impact on the life cycle cost of the architecture than the other design variables. The other design variables contribute to larger jumps in both the LCC and payload capability.

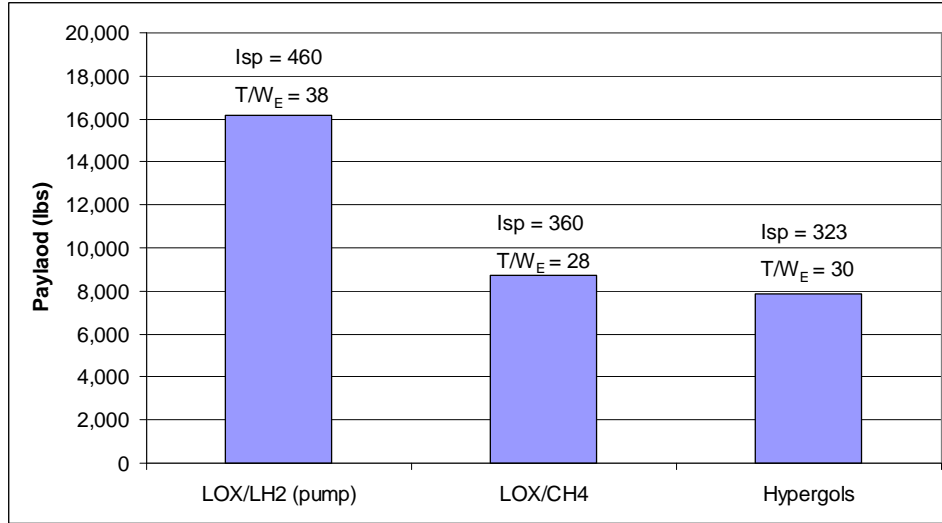


Figure 50: Change in Payload for Difference Engine Performance Parameters

The distribution of the five groups, shown in Figure 47, can be explained by the final two design variables: the stage that performs the LOI maneuver and the additional propellant burned during ascent. These two design variables have the largest impact on the payload capability and require the most propellant refueling. The refueling of the LSAM also provides a significant increase in the lunar surface payload when the Descent Stage is re-fueled in addition to the Ascent Stage.

As mentioned earlier, the only difference between Group One (Case #s 1 – 4) and Group Two (Case #s 6 – 9) is that, in Group One, the descent stage performs the LOI maneuver, while the EDS performs this maneuver in Group Two. Figure 51 illustrates how the LSAM payload can be increased when the LOI maneuver is performed by the EDS instead of the descent stage. The improvement between the baseline and Case #7 is noted in this figure. This change to the architecture increases the payload capability to the lunar surface of the baseline architecture by more than a factor of eight (3,619 lbm to 32,803 lbm) while only increasing the total LCC by 3.5%. An additional example that

occurs between two points along the Pareto frontier is the increase in payload and LCC between Case #2 and Case #7. The only change between these two design points is that the EDS is utilized for the LOI maneuver in Case #7. This results in a 24,100 lb increase in payload (277%) and a \$2.2B increase in LCC (3.1%). This payload improvement is possible because removing the LOI maneuver from the LSAM's manifest decreases the propellant requirement by 40% (22,000 lbm). There are two potential possibilities for the impact of this trade on the design of the architecture. The first is that the overall size of the LSAM can be reduced; a result that will be investigated more in Chapter 6. The second option is that the LSAM can maintain the baseline gross mass and increase the payload capability of the vehicle by replacing the LOI propellant with additional payload. Both of these options can be seen in Figure 51. Since the gross mass of the LSAM is shifted down when it is not required to perform the LOI maneuver, it is able to achieve a greater payload while maintaining the original gross mass. In the ESAS study the EDS was not used for the LOI because the CaLV did not have the payload capability to deliver the propellant required for the EDS to complete both the TLI and LOI maneuvers. In this case, the LOI propellant is delivered to LEO separately and therefore does not increase the payload requirement on the CaLV.

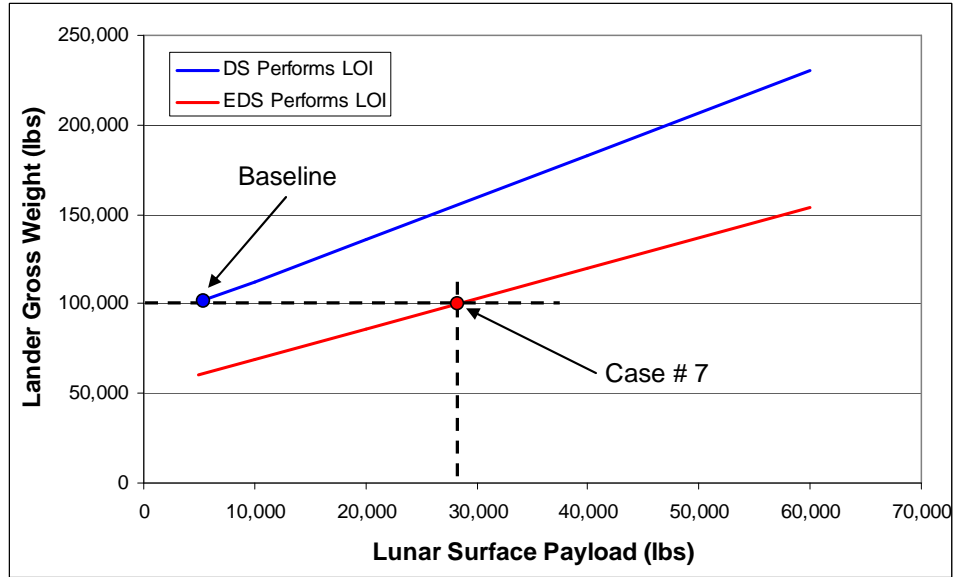


Figure 51: LSAM Gross Mass as a Function of Lunar Surface Payload

The change in design inputs from Group Two (Case #s 6 – 9) to Group Three (Case #s 10 – 14) increases the amount of propellant burned on the second stage of the CaLV during ascent. The LOI maneuver is completed by the EDS as in Group Two. As the second stage is also the EDS, there is a large amount of propellant left in the stage when the baseline vehicle reaches LEO. This propellant is then used for the trans-lunar injection maneuver. Increasing the propellant burned during the ascent phase of launch increases the payload that can be delivered to LEO, but the EDS would have insufficient propellant to complete the remaining mission maneuvers. The EDS then becomes dependent on the propellant depot to provide the propellant required to complete the lunar mission. Increasing the amount of propellant burned during ascent does not drastically improve the total payload capability to LEO, but rather increases the mission payload by replacing the unburned propellant delivered to LEO with mission payload. The total payload is the unburned EDS propellant plus the LEO mission payload. This

trade of TLI propellant for mission payload is shown in Figure 52. The four columns represent the amount of additional propellant burned during ascent. The total payload improvement is approximately 25,000 lbm when all of the EDS propellant is used, but the mission payload is increased by 250,000 lbm. The improvement in mission payload is more dramatic and directly leads to an overall improvement in lunar surface payload capability.

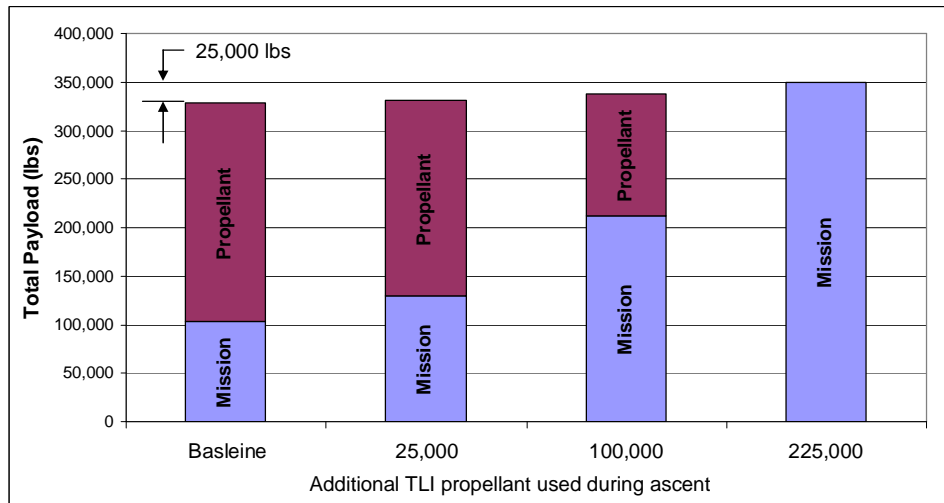


Figure 52: Change in Payload Capability as the Ascent Propellant is Increased

The design space investigation included an increase in the amount of propellant burned on the upper stage of the CaLV between 0 and 100,000 lbm. The designs in Group Three utilize a 25,000 lb increase in the upper stage burn, which leads to a corresponding increase in lunar surface payload capability of 16,100 lbm between Case #7 and Case #11. This increase in payload is in addition to the improvement already provided by utilizing the EDS for the LOI maneuver and refueling the propellant lost to boiloff.

The remaining two groups (Groups Four and Five) utilize a similar refueling strategy to that employed in Group Three. The payload is increased by decreasing the amount of propellant that is delivered to LEO. In Group Three this was accomplished by increasing the EDS propellant that is used during ascent, and in Groups Four and Five this is done by further increasing the propellant used during ascent and by offloading additional propellant from the LSAM. Since burning additional propellant does not significantly increase the total payload, offloading propellant accomplished almost the same result.

The design points in Group Four (Case #s 15 – 18) are more closely related to Group Two than they are to Group Three. In this group, the EDS performs the LOI maneuver as in Groups Two and Three. The EDS upper stage burn is unchanged from the baseline design and propellant refueling is used to remove the LSAM propellant prior to launch. The distinguishing characteristic in Group Four is that the Descent Stage propellant is now offloaded for all points, whereas only the ascent propellant had been offloaded previously. All other design variables remain the same between Groups Two and Four. The increase in propellant refueling increases the mission payload capability, but it also results in a greater life cycle cost because of the cost of providing propellant to LEO. Examining Case #7 and Case #16 shows that the payload can be increased by 31,400 lbm (95%) when the descent stage propellant is offloaded. This also results in an increase in LCC of \$2.99B (4.2%). The descent maneuver requires approximately 57,000 lbm of propellant which can be offloaded prior to launch. With the LSAM propellant removed, prior to launch, the CaLV is able to launch more mission payload to LEO because additional payload capability can replace the off-loaded propellant. The increase

is not one-to-one, however, because any increase in payload also increases the descent propellant needed.

The final group (Case #s 21 – 24) is a combination of Groups Three and Four. This group utilizes propellant refueling to offload the Descent Stage propellant and increases the amount of propellant that is burned on the EDS during ascent. This is in addition to refueling the propellant lost to boiloff and utilizing the EDS for the LOI maneuver. Including these two implementations of propellant refueling increases the lunar surface payload capability to 88,000 lbm (Case #22), but increases the discounted life cycle cost of the architecture by \$5B (7.2%).

The overall trend in the points along the frontier shows that as more propellant refueling is added to the architecture, a greater payload can be delivered to the lunar surface. This increase in refueling results in an increase in the life cycle cost of the architecture. This trend would likely continue along the Pareto frontier, but it is ultimately constrained by the physical limitations of the launch vehicle as discussed earlier. A summary of the major driving design changes between each of the five groups is provided in Table 37.

Table 37: Description of the Changes between the Five Groups

Initial Group	End Group	Major Driving Design Change	Average LCC	Average Payload
--	Group 1	Change from Baseline	\$69.2 B	11,100 lbm
Group 1	Group 2	LOI maneuver changed from DS to EDS	\$71.3 B	35,300 lbm
Group 2	Group 3	Burn an additional 25,000 lbm	\$73.3 B	52,500 lbm
Group 2	Group 4	Increase lander refueling	\$74.4 B	67,000 lbm
Group 4	Group 5	Burn an additional 25,000 lbm	\$76.9 B	91,400 lbm

In summary, the points along the Pareto frontier show that an improvement in the baseline architecture can be achieved. The previous section discussed how an improvement to the baseline architecture could be accomplished without introducing propellant refueling. This section showed how further improvements could be made with various implementations of propellant refueling. There are three methods for improving the baseline architecture. The first is to eliminate the dependence of the architecture on the rate of propellant boiloff. This solution increases the payload capability and reduces the life cycle cost, and is the only strategy that can improve both Figures of Merit. The second is to allow the EDS to provide both the TLI and LOI maneuvers. This trade provides a large increase in payload capability while only slightly increasing the LCC. The additional cost of propellant is balanced by a reduction in the cost of the LSAM. The final method is to reduce the amount of propellant that the architecture must deliver to LEO, either by burning additional fuel during ascent, or by offloading the propellant before launch. In either case, the payload capability is increased as propellant is traded for additional mission payload.

The amount of propellant refueling that should be adopted depends on the demand for lunar surface payload capability and the increase in LCC that NASA can absorb

within its current budget. If an increase is not possible, then there are propellant refueling scenarios that exist that would not violate the current budget profile while still achieving an improvement over the baseline architecture (Group One). Additional scenarios will be investigated in Chapter 7 to show that an increase in the lunar surface payload can also lead to a lower campaign cost. This occurs by altering how payload is delivered to the lunar surface for the lunar campaign. The following section will expand upon the results in this section and discuss the efficiency of the different propellant refueling methods at delivering propellant to the lunar surface as compared to the baseline architecture.

5.4 COST PER POUND OF DELIVERING PAYLOAD TO THE LUNAR SURFACE

The previous section discussed the points along the Pareto frontier, but did not detail which points along the frontier would provide the most benefit to the exploration architecture. By definition, the points along the frontier are Pareto efficient and cannot be distinguished without input from the decision maker. This frontier says nothing about which design should be selected only that it should be one of these points if these were the only decision criteria. Additional information is needed about the preferences of the decision maker in order to select the final design.

In addition to considering the Pareto frontier, another way to look at the results is to compare the cost of delivering payload to the lunar surface. In this section, the cost of delivering a pound of payload (\$/lb) to the lunar surface will be calculated. This includes all development, operational, and refueling costs associated with the lunar architecture. A large amount of resources are required to develop the infrastructure and hardware needed to deliver the initial payload to the lunar surface. Once this has been established,

additional payload can be delivered at a much lower cost. This work has investigated how various propellant refueling techniques can be applied to the baseline architecture to improve the payload capability. This cost per pound of payload delivered to the lunar surface for the points along the Pareto frontier is shown in Figure 53. Because each point along the frontier increases the payload capability of the baseline architecture, the \$/lb for these points will be less than that of the baseline. The degree of improvement in this metric will depend on the cost of each propellant refueling case relative to the improvement it provides the architecture.

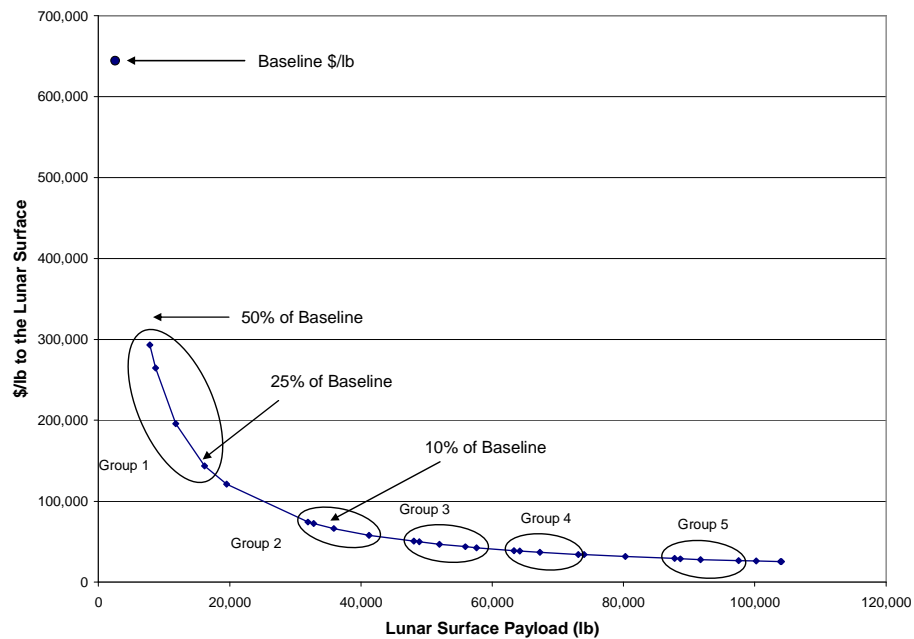


Figure 53: Effect of Propellant Refueling on Payload Capability, LCC and \$/lb

The ESAS baseline architecture has a lunar surface payload estimated delivery cost of approximately \$660,000/lb using the methodology in this dissertation. This result is high because the architecture is designed to deliver a relatively small payload to the

lunar surface, but requires an expensive infrastructure. When the entire LSAM mass is considered payload, this value decreases to \$35,000/lb. The results in Figure 53 do not include the mass of the LSAM, only the payload carried to the surface. This can be considered all payload (no crew) or an Ascent Stage and an assumed payload for crewed missions.

It is evident in these results that the use of propellant refueling can drastically reduce the \$/lb of delivering payload to the lunar surface. The \$/lb can be reduced to almost one twentieth of the baseline value when all aspects of propellant refueling are applied to the architecture. However, this results in a large increase in the life cycle cost of the architecture. It is still possible to reduce the baseline \$/lb by 90 percent without increasing the LCC of the architecture. This is accomplished by implementing Case #9 from Table 35. This design point includes both the utilization of refueling to eliminate propellant boiloff and the switch of the LOI maneuver from the LSAM to the EDS. The combination of these improvements greatly enhances the efficiency of delivering payload to the lunar surface.

The \$/lb curve presented in Figure 53 can be broken into two regions of interest. These regions include an initial area where a large improvement in the \$/lb is experienced and a region where there is little to no improvement. The separation of these regions is noted in Figure 54. The first region has the steepest decrease in \$/lb and represents the points where the life cycle cost of the baseline architecture is not increased by the additional of propellant refueling. Since these designs improve both the LCC and the lunar surface payload the \$/lb experiences the greatest decrease from the baseline.

The remaining designs build upon the refueling cases in Region One and thus do not experience as large a drop in \$/lb. As additional propellant refueling is added there is a diminishing return on the improvement in the \$/lb of payload to the lunar surface. This diminishing return is evident by the decrease in the slope of the curve as more propellant refueling is added to the architecture. While these designs continue to provide greater payload capability, they also required a greater LCC. The two competing FOMs result in a smaller improvement in the \$/lb. This region contains the design points that increase the payload capability by decreasing the amount of propellant that the architecture is required to deliver to orbit and replacing it with additional mission payload. The results in Figure 54 show the separation of these two regions. The improvement in \$/lb in the second region is significantly less than in the first.

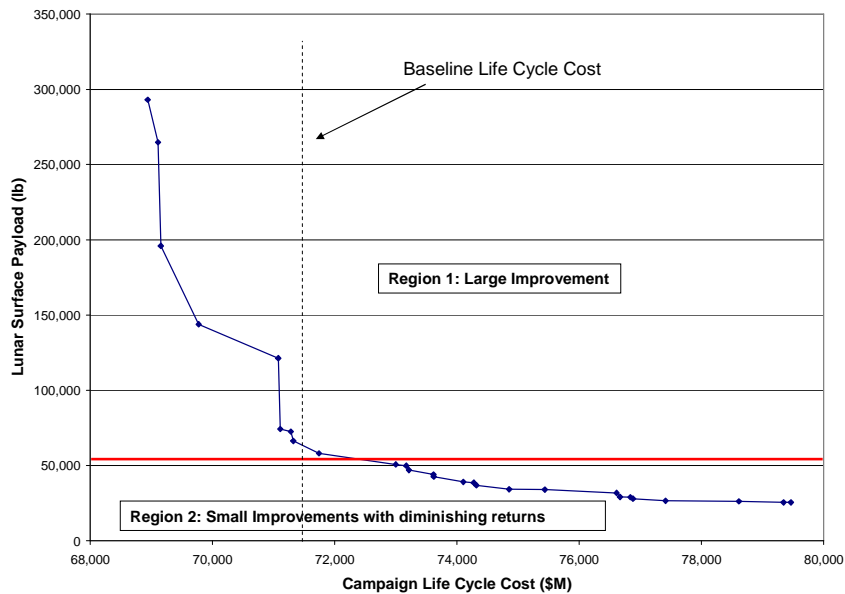


Figure 54: Regions of Different Rate of Change in the \$/lb

The results discussed in the previous section outlined the improvement in the cost of delivering payload to the lunar surface. In the previous example the “payload” was equal to the mission payload and did not include ascent stage of the LSAM. It is also important to understand what the \$/lb of delivering the “total payload” delivered to the lunar surface. The “total payload in this case refers to the mass that is delivered to the lunar surface by the descents stage of the LSAM and includes the ascents stage or an additional cargo element. This is a useful calculation when comparing the refueling ass to a cargo only mission. In this example the improvement in the \$/lb of payload delivered to the lunar surface is not as large because the improvement in payload between the baseline and the refueling cases is not as large as when the ascent stage is not included. Since the improvement in \$/lb is not as large it may be possible to achieve the same improvement as the seen in the refueling cases by increasing the number of cargo mission conducted during the lunar campaign. A more detailed comparison of these two cases will be investigated in Chapter 7. The marginal cost of launching an additional cargo mission will be compared against the cost of refueling the architecture elements.

The results for the \$/lb for the “total payload” are provided in Figure 55. In these results the baseline \$/lb is \$92,000/lb, where as, it was \$600,000/lb when the ascent stage was not included in the calculation. It is still possible to decrease the \$/lb by 50 percent without increasing the LCC beyond that of the baseline. This is achieved because of the savings offered by eliminating the dependence of the architecture on the propellant lost to boiloff. It was noted previously that this assumptions may over predict the actual results and would effect these results.

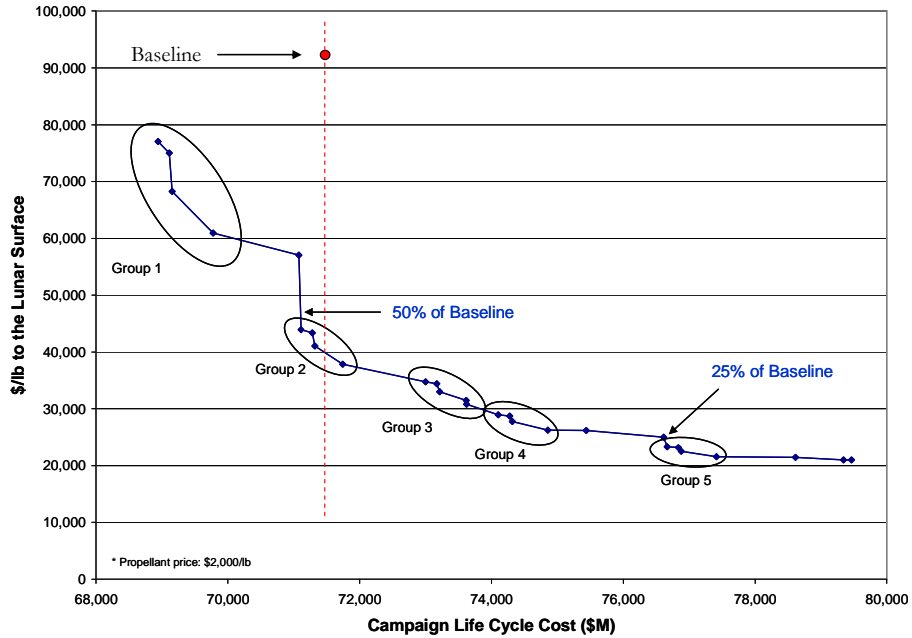


Figure 55: Effect of Propellant Refueling on Total Payload Capability

It is useful to examine the \$/lb as a relative change from the baseline architecture. This way, only the cost and benefits of refueling are considered and the comparative cost of delivering the baseline payload is removed from the calculation. This is known as the marginal cost per pound. The marginal cost per pound is calculated using the results of Equation 6. As a result of this formulation, when plotted, the results are separated into positive and negative values depending on the impact to the exploration life cycle cost.

$$M \text{ arginal } \$/\text{lb} = \frac{Cost - Cost_{Baseline}}{Payload - Payload_{Baseline}} \quad (6)$$

The results of this calculation for the designs along the Pareto frontier are provided in Figure 56. These results are plotted against the lunar surface payload

capability instead of the LCC to provide the maximum payload capability that can be achieved without surpassing the LCC of the baseline architecture. The first two groups still show a decrease in the LCC, which is indicated by the negative values for the marginal \$/lb. The designs in Groups Three through Five show that the additional cost to increase the lunar surface payload capability beyond 40,000 lbm is less than \$5,000/lb, significantly less than the cost of delivering the original payload. This result is expected because the additional cost of adding propellant refueling to the architecture is small compared to the cost of the initial infrastructure.

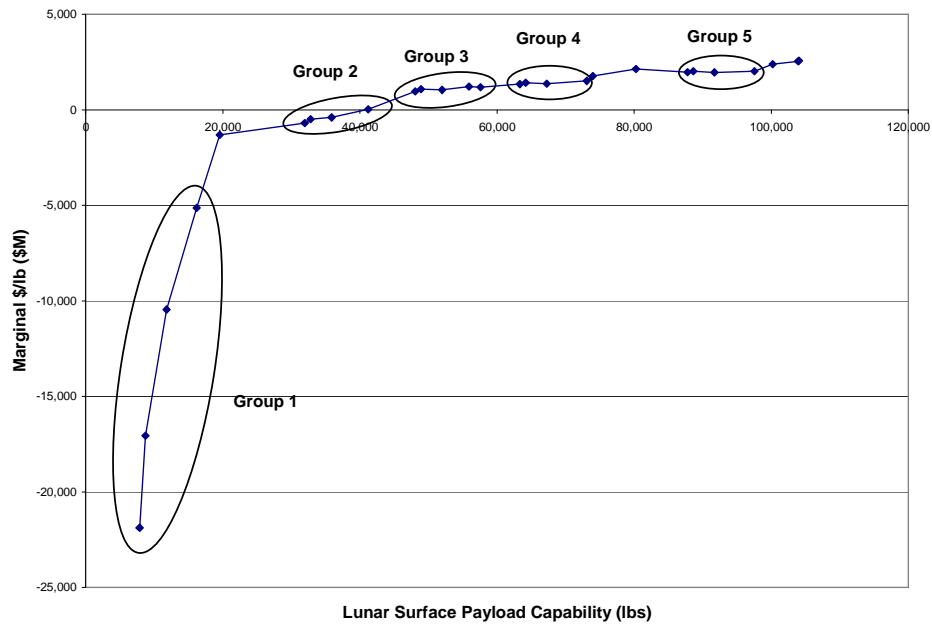


Figure 56: Marginal Cost of Increasing the Lunar Surface Payload

These results do not indicate which design is best, but rather provide additional information about the points along the Pareto frontier. The discussion in the previous section established that the architecture should operate at one of the points along the frontier in order to maximize the improvement in the baseline architecture. Since the

other FOM do not significantly vary along the frontier this should enable the best refueling strategies to be identified. It may be that considering the remaining FOM could result in different strategies. An additional study would help validate or invalidate this assumption. The Pareto frontier provides the decision maker with the capability to trade the life cycle cost and payload capability of the architecture. These results illustrate how propellant refueling methods can be used to deliver a greater payload to the lunar surface, and the cost associated with it. These tools help the decision maker evaluate the use of propellant refueling and select the propellant refueling methods that should be adopted by the project management.

5.5 ASSUMPTIONS AFFECTING THE DESIGN POINTS ALONG THE FRONTIER

The Pareto frontier discussed in the previous section is built around specific assumptions about the nature of the architecture and the ability to provide propellant to the various architecture elements. These assumptions include the cost of delivering propellant to the architecture, the maximum payload volume that can be carried by the CaLV and LSAM, the efficiency and cost of the thermal management systems, the effects of the two launch solution, and a number of other assumptions that, if changed, could affect the look of the frontier. The following section will discuss a number of these assumptions and how variations in these assumptions affect the points along this frontier. The results here will show that the points discussed previously are robust and continue to hold true even as the underlining assumptions change.

5.5.1 THE EFFECT OF AN UNCERTAIN PROPELLANT PRICE ON THE PARETO FRONTIER

The propellant delivery price is a difficult parameter to estimate and has a significant impact on the LCC of the architecture. It will be important to the decision maker to understand how the Pareto frontier changes as the price of propellant changes. A propellant price of \$2,000/lb was assumed for the results already presented in this chapter, but as was discussed in Chapter 2 this is at the lower bound of the potential cost of propellant in LEO. The Pareto frontier for a propellant delivery cost of \$3,000/lb and \$4,000/lb is provided in Figure 57. These two frontiers show a similar pattern to the Pareto frontier discussed previously in this Chapter.

There are only a few designs that differ between the three frontiers. The differences are circles in Figure 57 and summarized in Table 38. There is only one point that appears on the original frontier that does not appear on the higher propellant cost curves (Case #D1). This case, from the original Group Three, is the additional Hypergol ascent engine point that does not appear in the ascent engine pattern of the other groups. Section 5.3 discussed the ascent engine pattern and noted that this point was not present in the other groups along the frontier. Hypergolic propellants do not lose propellant to boiloff, so as the price of propellant increases, these designs become relatively lower cost solutions because they require less propellant to be provided to LEO. In Groups A and B two new design points emerge that were not on the frontier at a propellant price of \$2,000/lb. A third design point also emerges in Group C that only appears on the frontier at a propellant price of \$4,000/lb. These points (A2, A3, B2, B3 and C3) form a new group between original Group One and Two. This new group is similar to the original Group One, but includes an additional 25,000 lbm of propellant burned on the EDS

during ascent. These points exist in the higher propellant price cases because these designs utilize less propellant than the points in the original Group Two. At a propellant price of \$2,000/lb, this new group is dominated by the original Group Two because of its lower payload capability. As the price of propellant increases, the points in the original Group Two show a larger increase in LCC than the new group because the amount of refueling required, and eventually these new points are no longer dominated solutions. The remaining points along the frontiers are the same across all propellant delivery costs, suggesting that they are robust against a change in the price of propellant.

The points in Group 1 have been shown to offer a lower LCC than the baseline architecture, but as the price of propellant increases this savings is reduced. At a propellant price of \$8,600/lb there are no refueling solutions that offer a lower LCC than the baseline design. However, propellant refueling still offers potential value because of its ability to increase the lunar surface payload.

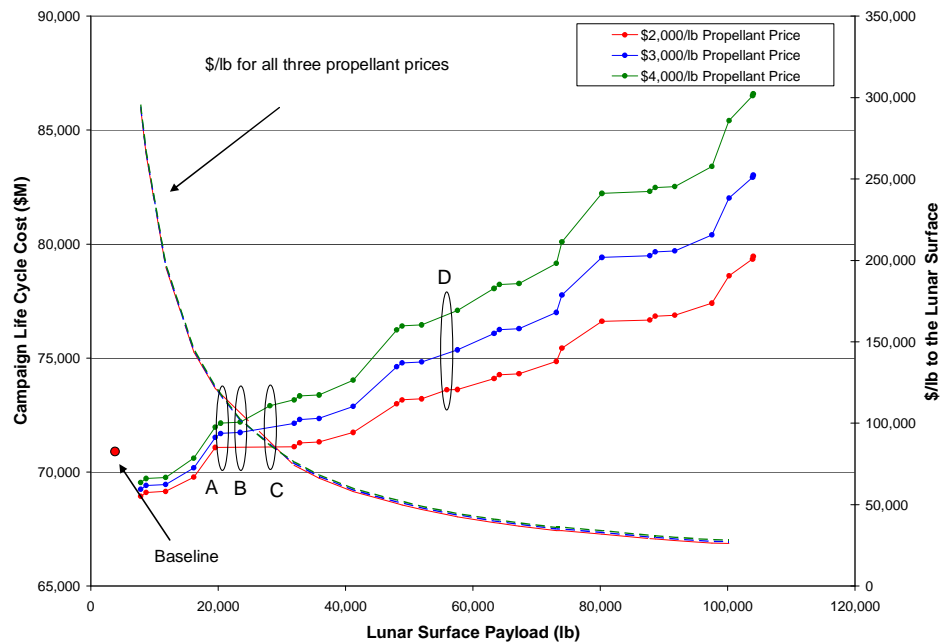


Figure 57: Changes to the Pareto Frontier with Increases in Propellant Cost

Table 38: Summary of Pareto Frontier Changes as Propellant Price Increases

Case #	Ascent Propellant	Lander Refueling	LEO Stay Time	Re-fuel LEO Boiloff	LOI Maneuver	Additional Burn (lbm)	DS % Re-fueled	LCC (\$M)	Payload (lbm)	\$/lb
A1 (\$2,000/lb)	--	--	--	--	--	--	--	--	--	--
A2 (\$3,000/lb)	LOX/CH4	None	15	Yes	DS	25,000	100	71,695	20,400	117,151
A3 (\$4,000/lb)	LOX/CH4	None	15	Yes	DS	25,000	100	72,144	20,400	117,884
B1 (\$2,000/lb)	--	--	--	--	--	--	--	--	--	--
B2 (\$3,000/lb)	LOX/LH2 (pump)	None	15	Yes	DS	25,000	100	71,739	23,464	101,917
B3 (\$4,000/lb)	LOX/LH2 (pump)	None	15	Yes	DS	25,000	100	72,189	23,463	102,556
C1 (\$2,000/lb)	--	--	--	--	--	--	--	--	--	--
C2 (\$3,000/lb)	--	--	--	--	--	--	--	--	--	--
C3 (\$4,000/lb)	LOX/CH4	Ascent Stage	15	Yes	DS	25,000	100	72,910	28,113	86,448
D1 (\$2,000/lb)	LOX/CH4	None	15	Yes	EDS	25,000	100	73,615	55,924	43,878
D2 (\$3,000/lb)	--	--	--	--	--	--	--	--	--	--
D3 (\$4,000/lb)	--	--	--	--	--	--	--	--	--	--

5.5.2 THE EFFECT OF LAUNCH UNCERTAINTY ON THE PARETO FRONTIER

Another important sensitivity to investigate is the separation time between the launch of the CaLV and CLV. The separation time is different from the designed loiter period discussed previously in this chapter. The separation time represents the expected time between the launch of the cargo and crew, while the design loiter period represents the additional margin built into the architecture to account for a delay in the launch of the crew. The results presented in this chapter assume that the separation time is seven days, but it can be shown that decreasing this separation time could greatly increase the probability of launching the CLV within the designed loiter period. Increasing this probability reduces the potential number of missions that are lost during the lunar campaign, which decreases the LCC of the architecture, as shown in Figure 58.

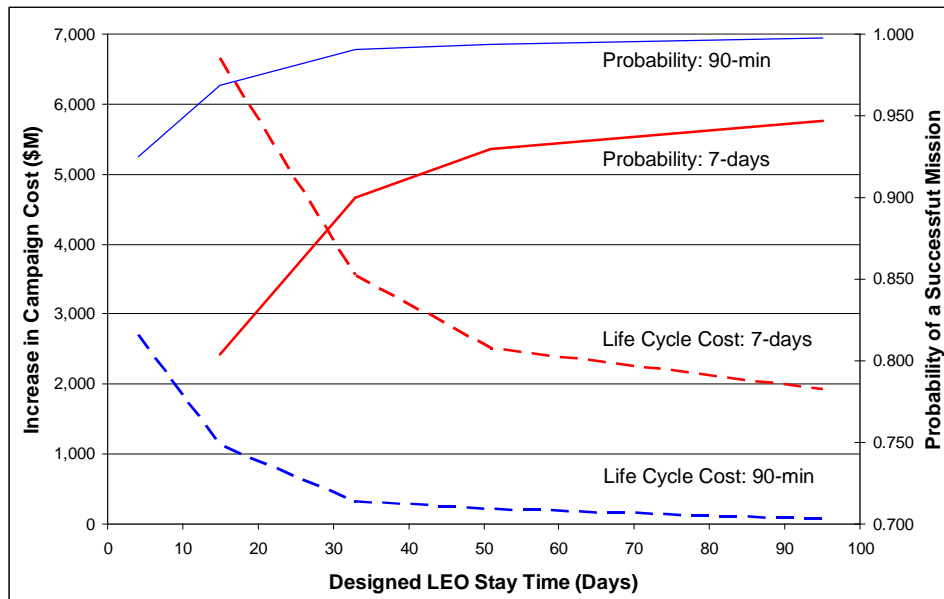


Figure 58: Effect of a Lower Launch Separation on Mission Success

Propellant refueling eliminates the dependence of the architecture on the launch timing of the CaLV and CLV by replacing the lost propellant once all of the architecture elements have been delivered to LEO. This allowed the EDS and LSAM to remain in LEO for longer periods without decreasing the payload capability of the architecture. Another potential means of reducing the impact that a one and a half launch solution has on the architecture is to launch both vehicles as close together as possible. This will increase the likelihood that the second launch vehicle, the CLV in this case, will be launched within the original window. This is because there is less uncertainty in the launch countdown within a 90-min period than over a 7-day period, because outside factors such as weather are more predictable. With a higher probability of launching the CLV, the architecture can be designed for a shorter loiter period without greatly decreasing the reliability of each mission. A shorter separation time will decrease the impact that propellant refueling has on the architecture. NASA has also considered switching the order of launching the Ares I and Ares V. In this scenario the crew would be launched before the cargo. Since the Service Module relies on storable propellant it does not experience the same level of propellant boiloff than is experienced on the EDS and LSAM. The crew can then remain in LEO until the EDS and LSAM are delivered without the potential of losing a mission. The draw back of this scenario is that the crew must wait in LEO until the Ares V is launched; increasing the risk they are exposed to during the mission. This could also lead to a situation where the crew are forced to return to Earth without completing a mission if the Ares V is delayed beyond a specified time.

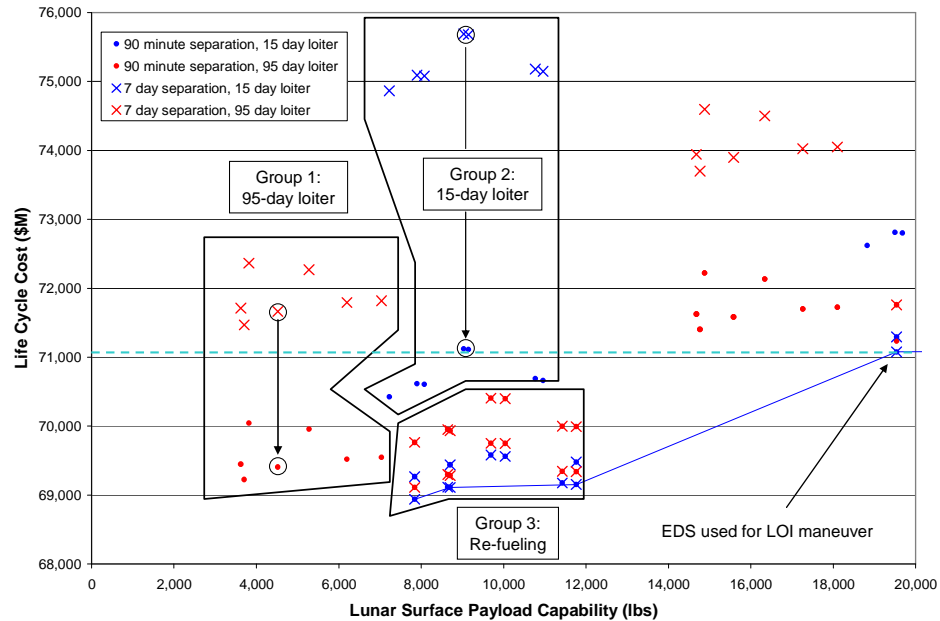


Figure 59: Sensitivity to Assumptions in LEO Boiloff Refueling

The results of this sensitivity study are provided in Figure 59. The Pareto frontier is again provided assuming of propellant refueling price of \$2,000/lb. Three groups have been noted in this chart to illustrate how the designed loiter period, and launch separation time impact the architecture and how these solutions compare to the refueling case where the propellant is replaced in LEO. The designs in Groups One and Two do not re-fuel the propellant lost to boiloff as in the baseline design. The designs in Group One are for a 95-day loiter period and the designs in Group Two are for a 15-day loiter. These points show the same results presented previously in this Chapter. The shorter the loiter period the greater the payload capability (less boiloff), but the higher the life cycle cost because of the degradation in the mission success probability (Figure 58). The new information shown in Figure 59 is that when the launch separation time is reduced from 7-days to 90-min the LCC of the architecture is reduced. These results do not include any additional

cost to account for the operational cost of two launch count downs occurring in close proximity. The shorter separation time reduces the number of missions that would be lost over the life of the lunar campaign which leads to a reduction in LCC. This trend is seen in both Groups One and Two. A larger decrease in LCC is seen for the shorter loiter period as it has the higher probability of losing a mission so the reduction in separation time has a greater impact on the launch success. This change in LCC between these two groups for the different launch separation times and design loiter periods is provided in Table 39.

Table 39: Change in LCC with a Change in Launch Separation

	P(7-days)	LCC(7-days)	P(90-min)	LCC(90-min)
Group 1	0.947	\$72B	0.998	\$69.5B
Group 2	0.804	\$75B	0.969	\$71B

The reduction in separation time improves the design points, but it does not bring them onto the Pareto frontier. The designs in Group Three utilize refueling to replace the propellant lost to boiloff. In this case, decreasing the separation time has little impact on these designs. Since the architecture elements are able to remain in LEO for any period of time, reducing the launch separation time only slightly increases the amount of propellant that must be delivered to LEO, and has no impact on the payload capability. The designs in Group Three also include the points along the Pareto frontier (Cases 1 – 4, Table 35). The frontier does not include the non-refueling cases, even when the launch separation is assumed to be as low as 90 minutes. The designs with the shorter separation time are

moved closer to the frontier than those with the original seven day assumption, but still result in a greater LCC and a smaller payload capability. However, decreasing the launch separation time lowers the LCC below that of the refueling cases that utilized the EDS for the LOI maneuver (Cases 6 – 9, Table 35). The LCC for these cases are noted in Figure 59. It is clearly shown that the LCC for the designs in Groups One and Two are moved below this line when the launch separation is shortened from 7-days to 90-min. The 90-min separation cases are still dominated by the frontier, but they are no longer dominated by the refueling cases that utilize the EDS for the LOI maneuver because these points offer a lower LCC. The decision maker must now consider the impact to the LCC when considering the EDS for the LOI maneuver. The launch separation time does have a significant effect on the LCC of the architecture, but the ability to replace the propellant lost to boiloff while in LEO is still shown to offer a better architecture solution at a propellant price of \$2,000/lb.

5.6 SUMMARY OF NON-DOMINATED SOLUTIONS

In summary, the results illustrate that the baseline architecture can be improved in terms of payload capability and LCC with the addition of propellant refueling. It was also shown that there are design alternatives that can improve the baseline design, without the use of propellant refueling, by altering the engines used on the LSAM ascent stage. A Pareto frontier was identified to define the set of Pareto-optimal solutions that bound the design space. These solutions show that there are design variables that are consistent among all points along the frontier. In fact, the difference between each group is primarily due to a single design variable that increases the amount of propellant refueling

in the architecture. The robustness of these designs has also been discussed in comparison to the cost of delivering propellant to the architecture. It was shown that the frontier was not significantly altered despite a propellant price increase from \$2,000/lb to \$4,000/lb. The final conclusion from this section is that the utilization of propellant refueling can greatly improve the capability of the architecture without a large increase in the LCC, and is robust against changes in the propellant delivery cost. There are, however, only a limited number of cases that can achieve a lower LCC with the addition of propellant refueling. Chapter 6 will discuss how propellant refueling can be used to specifically reduce the LCC of the exploration program.

CHAPTER 6

A PARETO FRONTIER FOR LEO PAYLOAD CAPABILITY AND LIFE CYCLE COST: SCENARIO TWO

The Pareto frontier discussed in Chapter 5 was for Scenario One, which used propellant refueling to increase the payload capability of the architecture. This generally required an increase in life cycle cost because of the additional propellant costs. The goal of Scenario Two is to reduce the life cycle cost of the architecture while maintaining the same lunar surface payload capability. The introduction of propellant refueling reduces the size of the architecture elements because only the dry mass of the in-space stages need to be delivered to LEO instead of the total gross mass that includes propellant. The pros and cons of Scenario Two will be discussed in this chapter. This chapter will also include a discussion of the LEO payload capability versus life cycle cost Pareto frontier. These results will be similar to those presented in Chapter 5 and will identify the design points that provide the most benefit to the architecture. A comparison will be made between the results for Scenarios One and Two, to understand the overall effect that propellant refueling can have on the exploration architecture.

The results presented in Chapter 5 showed how propellant refueling could be used to increase the payload capability of the lunar exploration architecture. It is possible; however, that increasing the payload capability does not provide additional value to NASA. The development of Scenario Two attempts to address this point by utilizing

propellant refueling to lower the life cycle cost of the architecture while maintaining the same lunar surface payload capability. This is achieved by reducing the size and mass of the architecture elements as the performance requirements of the vehicles are reduced through the introduction of propellant refueling. The methods for architecture elements sizing discussed in Chapter 4 were utilized in the analysis presented in this chapter.

6.1 DEVELOPMENT OF A PARETO FRONTIER FOR SCENARIO TWO

Scenario Two's design space is similar to that of Scenario One, though one design variable is changed. Rather than increasing the amount of EDS propellant used during ascent to increase the payload capability, some TLI propellant is offloaded to reduce the LEO payload requirement on the CaLV. The morphological matrix for Scenario Two is provided in Figure 60. In Scenario Two, the lunar surface payload capability could not be used as one of the metrics for the design comparison, as this quantity remained constant among all design points. Therefore the total LEO payload capability is used. The total LEO payload is a summation of the mission payload (LSAM) and the in-space propellant (TLI) delivered aboard the EDS. This metric was selected because it represents one of the major drawbacks of this design philosophy: An architecture which is less extensible to future missions. As more propellant refueling is utilized, the CaLV becomes smaller, which decreases total payload capability that the launch vehicle can deliver to LEO. The use of propellant refueling can reduce both the mission payload (smaller LSAM) and the in-space propellant (offloading TLI) while maintaining the same lunar mission capability.

Design Variable	Design Options			
Offload TLI propellant (LOX)	0	25,000 lbs	50,000 lbs	80,000 lbs
Offload TLI propellant (LH2)	0	5,000 lbs	10,000 lbs	20,000 lbs
EDS Boil-off Mitigation	MLI	MLI+Cryo		
Lander Stage Re-fueled	None	Descent	Ascent	Both
Lander Propellant	50%	100%		
LSAM Ascent Propellant	LOX/CH4	Hypergols	LOX/LH2 (pressure)	LOX/LH2 (pump)
Lander Boil-off Mitigation	MLI	MLI+Cryo		
LOI Burn Element	EDS	LSAM DS		
LEO Required Stay Time	95 Days	15 Days		
Re-fuel Boil-off	No	Yes		

Figure 60: Design Space Morphological Matrix, Scenario Two

The method for determining the points along the Pareto frontier developed in Chapter 5 (Section 5.1) was again applied to the designs in Scenario Two. This method determines which points within the design space are Pareto optimal. The Pareto frontier and the dominated solutions are provided in Figure 61. Section 5.2 will discuss the designs along this frontier, and Section 5.3 will discuss how this frontier changes as the price of propellant changes.

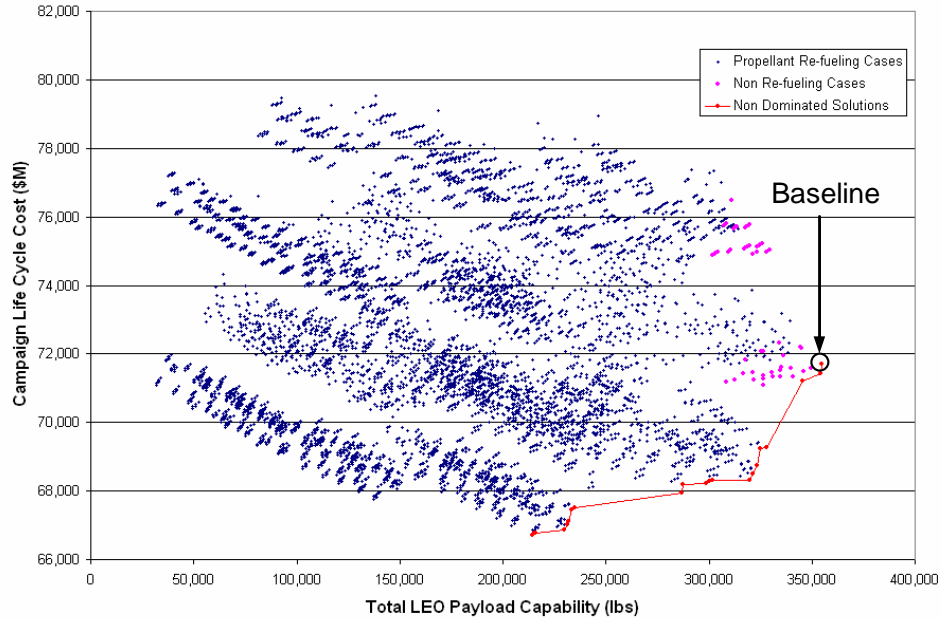


Figure 61: Pareto Frontier and Design Points for Scenario Two

There are two general trends that can be seen in the results of the trade space exploration shown in Figure 61. The first is that the introduction of propellant refueling can provide a lower cost solution than the current baseline design. A reduction of seven percent in the total life cycle cost can be achieved. The second trend is that, as discussed earlier, the introduction of propellant refueling decreases the LEO payload required to meet the lunar mission requirements and thus the size, mass, and cost of the architecture elements as shown in Figure 61. The following sections will discuss the points that dominate the design space (Pareto frontier) and provide a breakdown of the design variables throughout this design space.

6.2 DESIGN TRENDS IN THE NON DOMINATED SOLUTIONS

The points along the Pareto frontier can be broken down into three distinct groups that share a number of commonalities among their designs. These three groups are noted for the Pareto frontier shown in Figure 62, which depicts the same frontier that is shown in Figure 61, but with the dominated solutions removed. A summary of the design points along the frontier are also provided in Tables 41 and 42. There are three design variables that do not appear along the frontier: off-loading hydrogen from the CaLV, off-loading oxygen from the CaLV, and off-loading propellant from the LSAM, and these inputs are set to the baseline value of zero. These design variables lead to a decrease in the payload capability delivered to LEO by the CaLV and results in a decrease in the LCC of the architecture. Utilizing these methods to offload propellant from the EDS and LSAM does provide a lower cost solution than the baseline, but these points do not appear on the frontier because there are other propellant refueling techniques that offer a lower LCC. This will be explained further in Section 6.4. Therefore, while offloading the in-space propellant can improve the baseline architecture, this technique is dominated by other propellant refueling strategies. The designs along this frontier assume a propellant price of \$2,000/lb. It will be discussed in Section 5.3 that, at a propellant price of \$1,500/lb, that a limited number of solutions appear along the frontier that offload in-space propellant. The remaining design variables vary along the frontier and are discussed in the following sections.

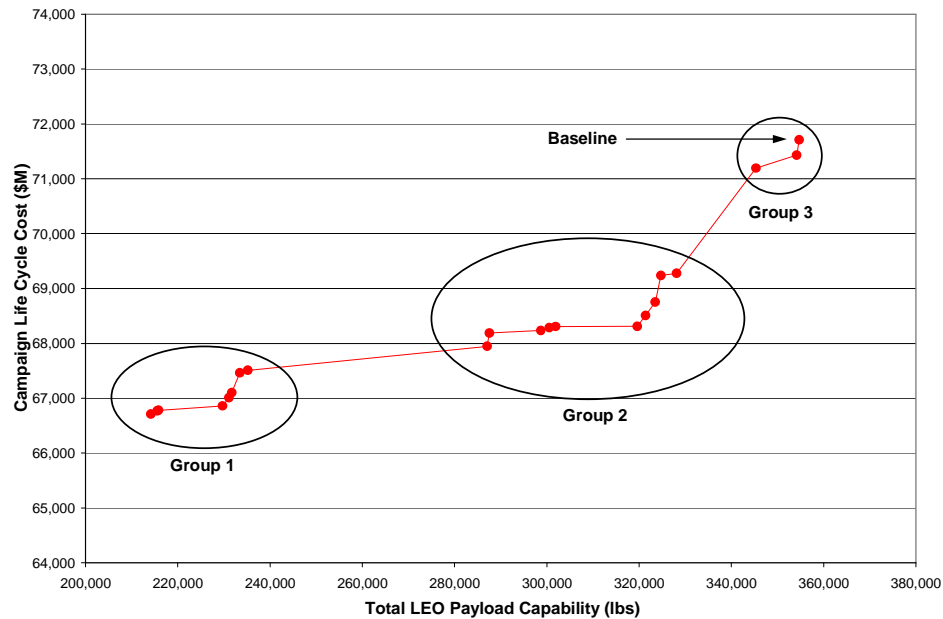


Figure 62: Scenario Two Pareto frontier Groups

6.2.1 DESIGN POINTS IN GROUP THREE

The designs in Groups One (Case #s 14 – 21) and Group Two (Case #s 1 – 10) utilize propellant refueling in some respect while the designs in Group Three (Case #s 11 – 13) do not. The appearance of non refueling design points on the frontier is different than was seen in Scenario One, where all non refueling cases were dominated by propellant refueling designs. The three points in Group Three offer the greatest payload capability because the CaLV remains at or near its original size, and its payload capability is not reduced through the use of propellant refueling. These three designs must also account for propellant lost due to boiloff and therefore have a chance of losing a mission when a significant delay occurs between launching the crew and cargo, thus resulting in an architecture design with a higher life cycle cost than those that utilize propellant refueling. The baseline design also appears along this frontier, offering the

highest LEO payload capability, but also the highest LCC. The designs in Group Three differ only by the LSAM ascent engine and the thermal management system employed on the Descent Stage as shown in Table 41. All other design options remain the same as the baseline design. These differences have little impact on the payload capability and LCC of the baseline design, improving the LCC by less than one percent and decreasing the payload capability by less than four percent.

6.2.2 DESIGN POINTS IN GROUP TWO

The remaining points along the frontier utilize propellant refueling and are referred to as Group One and Group Two in Figure 62. These two groups include two significant implementations of propellant refueling. In Group Two, the only use of propellant refueling is the ability to replace any propellant lost to boiloff while the EDS and LSAM loiter in LEO, except that the AS is refueling in cases 1 and 2. This reduces the amount of propellant that must be carried to LEO by the CaLV, resulting in a smaller launch vehicle. Refueling the propellant lost to boiloff also reduces the probability that a mission will be lost because the EDS and LSAM can remain in LEO for an extended period of time before the crew are launched, preventing the loss of hardware (EDS and LSAM) and the need to re-launch it (CaLV). A more detailed description of the architecture benefits of eliminating propellant boiloff was presented in Chapter 5.

In general the design points in Group Two only utilize propellant refueling to replace the propellant lost to boiloff, with the exception of Case 1 and 2 (Table 41). These two cases also include offloading a small amount of propellant from the LSAM in addition to refueling the propellant boiloff in order to further reduce the payload the

architecture must deliver to LEO. These two points are inferior to the rest of the points within Group Two because they experience a large decrease in capability for only a slight decrease in LCC. Table 40 illustrates the reduction in LCC and LEO payload capability when the Ascent Stage of the LSAM is re-fueled. A 0.5 percent reduction in LCC is achieved while the payload capability is reduced by 19 percent. This demonstrates that offloading the in-space propellant provides little benefit to the architecture because the LCC savings is small as compared to the reduction in payload.

Table 40: Relative Improvement in Groups 2 Design Points

	Payload % from Baseline	LCC % from Baseline
Case #1	5.2%	19%
Case #6	4.7%	9.9%

The initial introduction of propellant refueling to replace the propellant boiloff offers benefit to the architecture as it is capable of reducing the LCC by 4.7 percent with only a 10 percent reduction in the payload that can be delivered to LEO. It is up to the decision maker to determine if the tradeoff of payload for LCC is an overall benefit to the architecture.

Table 41: Summary of Pareto Frontier, Groups Two and Three

Case #	AS Propellant	AS Thermal	DS Thermal	Lander Refueling	EDS Thermal	Re-fuel LEO Boiloff	LEO Stay Time	LOI Maneuver	Additional Burn (lbm)	DS % Re-fueled	LCC (\$M)	Payload (lbm)
1	LOX/LH2	MLI	MLI	Ascent Stage	Cryo-cooler	Yes	15	DS	0	0	67,946	287,077
2	LOX/LH2	MLI	MLI	Ascent Stage	MLI	Yes	15	DS	0	0	68,191	287,557
3	LOX/LH2	MLI	MLI	None	Cryo-cooler	Yes	15	DS	0	0	68,235	298,688
4	LOX/LH2	Cryo-cooler	MLI	None	Cryo-cooler	Yes	15	DS	0	0	68,285	300,510
5	LOX/LH2	MLI	Cryo-cooler	None	Cryo-cooler	Yes	15	DS	0	0	68,309	301,927
6	Hypergol	MLI	MLI	None	Cryo-cooler	Yes	15	DS	0	0	68,309	319,636
7	Hypergol	MLI	MLI	None	Cryo-cooler	Yes	95	DS	0	0	68,509	321,396
8	Hypergol	MLI	MLI	None	MLI	Yes	95	DS	0	0	69,239	324,740
9	Hypergol	MLI	Cryo-cooler	None	MLI	Yes	15	DS	0	0	68,756	323,528
10	Hypergol	MLI	Cryo-cooler	None	MLI	Yes	95	DS	0	0	69,276	328,136
11	Hypergol	MLI	Cryo-cooler	None	MLI	No	95	DS	0	0	71,195	345,337
12	Hypergol	MLI	MLI	None	MLI	No	95	DS	0	0	71,433	354,188
13	LOX/CH4	MLI	MLI	None	MLI	No	95	DS	0	0	71,710	354,684

The thermal management system for the EDS is typically an active system, while the LSAM is typically passive on both stages. Cases 1 and 3 provide an example of this result. This difference is due to the total amount of boiloff that occurs between the two vehicles. The EDS experiences a larger total boiloff than the LSAM because of the larger volume of propellant that it carries. The addition of a cryo-cooler reduces the amount of propellant that must be delivered to LEO to provide sufficient propellant to re-fuel the architecture elements. The trade off for utilizing a cryo-cooler depends on the cost of the system verses the cost of providing propellant to LEO. Chapter 7 will further address this issue and discuss which of these options is preferred depending on their relative costs. The use of passive systems is always favored on the LSAM because the total boiloff is small. The primary improvement to Group Two is the introduction of propellant refueling to replace the propellant lost to EDS boiloff, allowing the architecture to remain in LEO for an extended period of time.

6.2.3 DESIGN POINTS IN GROUP ONE

The designs in Group One introduce the refueling strategy to allow the EDS to perform the LOI maneuver rather than the Descent Stage of the LSAM. The design points in Group One are summarized in Table 42. In this case the LSAM LOI propellant is removed (30,000 lbm), which allows the size and mass of the LSAM to be reduced. Section 5.3 provided a summary of how the size of the LSAM is affected by removing the LOI maneuver from its mission requirements. The reduced LSAM mass decreases the payload requirement on the CaLV, which leads to a smaller launch vehicle design. Group One offers the lowest cost solution because the smaller LSAM results in a lower cost

solution for both the LSAM and the CaLV. Case #14 from Group One provides a 2.2 percent reduction in the LCC as compared to Case #3 from Group Two. The only design change between these two cases is which stage performs the LOI maneuver. This is a small reduction in LCC compared to the 28 percent reduction in LEO payload that is a result of removing the LOI propellant from the design of the LSAM and providing it to the EDS once delivered to LEO. The design points in Group One follow the same trends seen in Group Two with respect to the thermal management system and LEO loiter period. The design points favor the use of a cryo-cooler on the EDS and MLI and the LSAM and, because the propellant boiloff is re-fueled, the designs also favor the use of a 15-day loiter period.

No other uses of propellant refueling are active along the frontier; this indicates that allowing the EDS to perform the LOI maneuver offers the lowest cost solution to the architecture because it has the largest impact on the most architecture elements. The disadvantage of this solution is that the lower LCC comes at the expense of a significantly lower LEO payload capability. A seven percent decrease in LCC is obtained between case # 11 (baseline) and case # 14 at the cost of a forty percent decrease in LEO payload capability. While this does not impact the current plans for the lunar campaign it will make it more difficult to expand the architecture to other missions, especially if large payloads are required.

The Pareto frontier is primarily defined by the two propellant refueling strategies presented in Groups One and Two. The remaining design variables either do not change from their baseline values or have a small effect on the LCC and the LEO payload capability. This result was also seen in Scenario One, where the introduction of

propellant refueling provided the largest impact on the architecture, and the remaining design variables (ascent stage engine and the thermal management system) resulted in small changes around the main refueling strategies. This Pareto frontier illustrates that the selection of a propellant refueling strategy has a much higher impact on the architecture figures of merit than the other design variables being traded including: the selection of the LSAM ascent engine, the boiloff thermal management system, or the length of the LEO loiter.

Table 42: Summary of Pareto Frontier, Group One

Case #	AS Propellant	AS Thermal	DS Thermal	Lander Refueling	EDS Thermal	Re-fuel LEO Boiloff	LEO Stay Time	LOI Maneuver	Additional Burn (lbm)	DS % fueled	Re-	LCC (\$M)	Payload (lbm)
14	LOX/LH2	MLI	MLI	None	Cryo-cooler	Yes	15	EDS	0	0		66,710	214,171
15	LOX/LH2	Cryo-cooler	MLI	None	Cryo-cooler	Yes	15	EDS	0	0		66,769	215,522
16	LOX/LH2	MLI	Cryo-cooler	None	Cryo-cooler	Yes	15	EDS	0	0		66,780	215,808
17	Hypergol	MLI	MLI	None	Cryo-cooler	Yes	15	EDS	0	0		66,861	229,702
18	Hypergol	MLI	MLI	None	Cryo-cooler	Yes	95	EDS	0	0		67,012	231,108
19	Hypergol	MLI	MLI	None	MLI	Yes	95	EDS	0	0		67,461	233,450
20	Hypergol	MLI	Cryo-cooler	None	MLI	Yes	15	EDS	0	0		67,105	231,715
21	Hypergol	MLI	Cryo-cooler	None	MLI	Yes	95	EDS	0	0		67,508	235,188

6.3 EFFECT OF PROPELLANT PRICE ON THE PARETO FRONTIER

One of the largest uncertainties when introducing propellant refueling into the lunar exploration architecture is the cost of providing propellant to LEO. In the results of Section 6.2, a propellant price of \$2,000/lb was assumed. As the price of propellant increases, the designs which rely heavily on propellant refueling become increasingly less attractive because of their increase in LCC. At a propellant price greater than \$3,000/lb, the designs in Group One become dominated by Group Two because they now have a higher LCC with the already lower payload capability. The designs in Group Two utilize less propellant and are therefore not as affected by an increase in price as are the design in Group One. This section will discuss how the points along the Pareto frontier change as the assumed price of propellant changes. A number of Pareto frontiers are provided in Figure 63 with varying assumed propellant prices. This figure includes the Pareto frontier discussed in the previous section along with two additional curves that assume a price of \$3,000/lb and \$1,500/lb. These illustrate how the frontier changes as a function of propellant price.

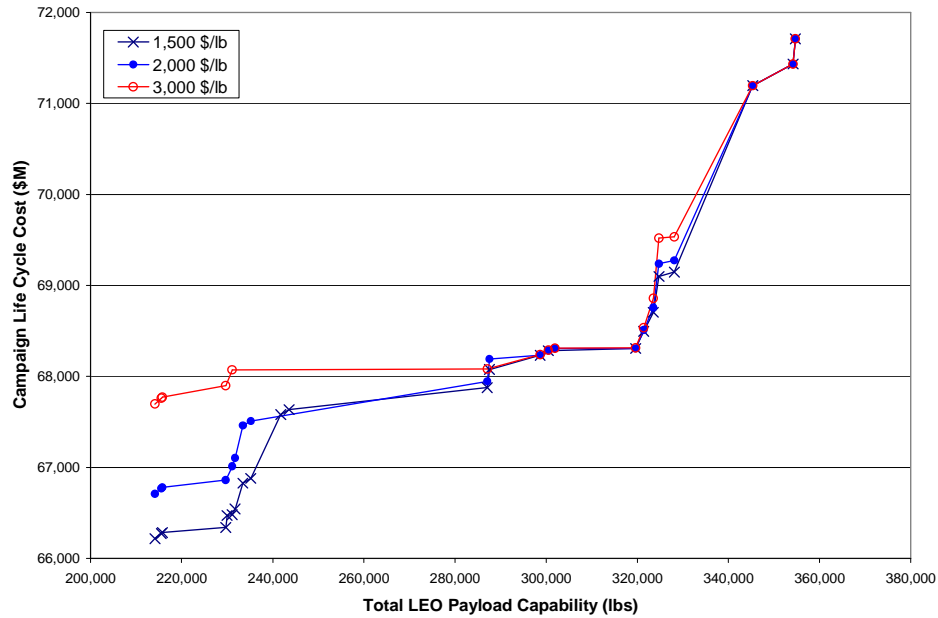


Figure 63: The Effect of a Change in Propellant Price on the Pareto frontier

The design points in Group One (Case #s 14 - 21) have the largest dependency on the price of propellant because they require propellant refueling of any of the design points considered in Scenario Two. Therefore, this group has the largest fluctuations as the price of propellant changes. There are two trends to consider when evaluating the effect of a change in propellant price. The first is how one group changes relative to the rest of the Pareto frontier, and second is how the points within each group change relative to each other.

When the price of propellant decreases from \$2,000/lb to \$1,500/lb as shown in Figure 63, the design points in Group One shift down relative to the rest of the designs along the frontier. This is because a larger amount of propellant is required for the designs in Group One as compared to the rest of the frontier. As the price of propellant decreases, the general shape of the frontier remains intact with Group One, becoming a relatively more attractive solution. When the price of propellant increases, the frontier

begins to take on a different shape. Figure 64 shows how the shape of the frontier changes as the price of propellant increases. At a propellant price of \$3,000/lb, the LCC for the points in Group One are only slightly less than the design in Group Two, while offering a significantly lower LEO payload. As the price of propellant increases from \$3,000/lb to \$4,000/lb, the design points in Group One completely disappear from the frontier. This is because the LCC of Group One becomes greater than Group Two, and since Group One offers a lower LEO payload, they become completely dominated by Group Two. At a propellant price of \$4,000/lb, the value of utilizing the EDS for the LOI maneuver is eliminated as it is no longer capable of offering a lower cost solution.

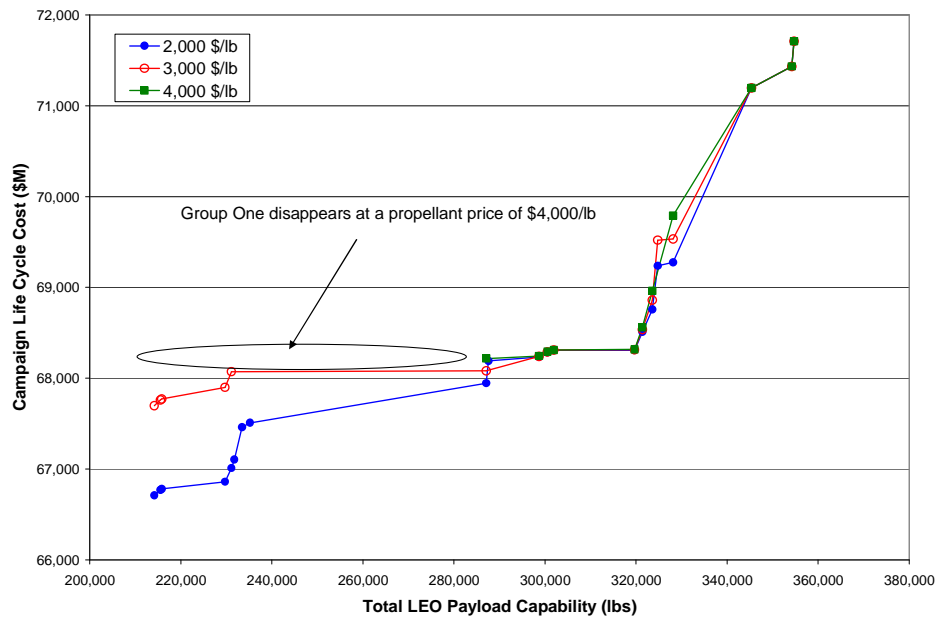


Figure 64: Propellant Price for the Elimination of Group One from the Frontier

Examining the points in Group One closer, as shown in Figure 65, it is evident that there are changes to the points that appear within this group as the propellant price increases or decreases. As the price of propellant decreases from the initially assumed \$2,000/lb, there are three additional points that appear on the new frontier. These are noted by the red circles in Figure 65. Point B introduces a new design that does not utilize a cryo-cooler on the EDS, but instead uses a passive MLI system. This case still implements propellant refueling to replace the propellant lost to boiloff so that the EDS and LSAM can remain in LEO as long as needed. With the EDS now utilizing MLI, instead of a cryo-cooler, a greater amount of propellant is required; however, at the lower propellant price, MLI becomes a better solution than adding the cryo-cooler to the design of the EDS.

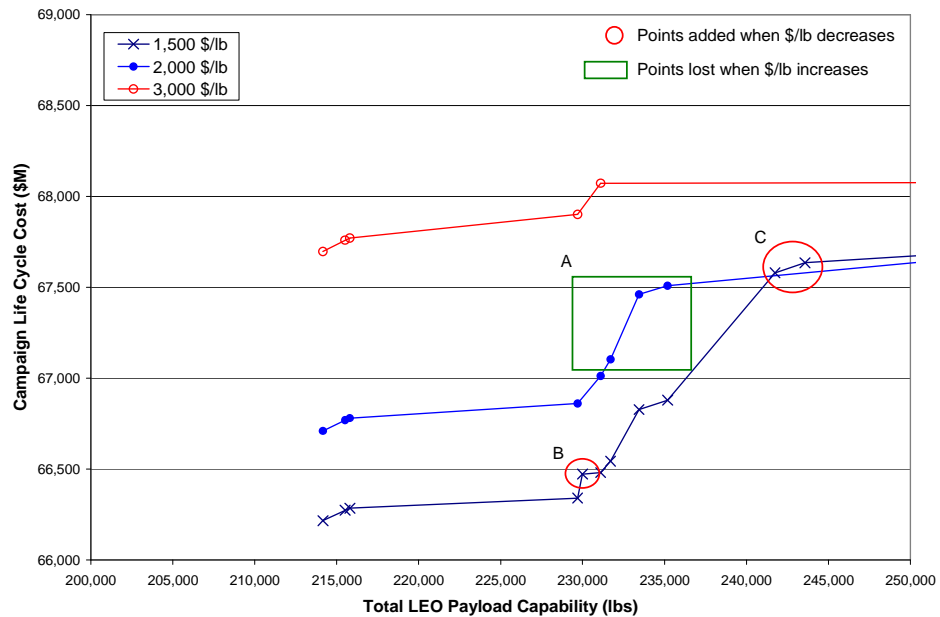


Figure 65: The Effect on Group One of a Change in Propellant Price

The points in Group C offer a new propellant refueling strategy that is not seen at a propellant price greater than \$1,500/lb. These two points offload some TLI propellant from the EDS. This reduces the payload requirements on the launch vehicle greatly reducing its size and cost. This design point is not seen on the frontier at a propellant price of \$2,000/lb or greater because the cost of propellant is more than the savings generated from the smaller architecture elements. In these two cases, 50,000 lbm of LOX is removed from the launch vehicle and provided after the EDS is delivered to LEO; this is equal to 15 percent of the total LEO payload. While this new design doesn't offer as low a cost solution as utilizing the EDS for the LOI, it does provide an in-between point that trades the cost and benefits between Groups One and Two. A lower LCC is achieved than in Group Two with sacrificing as much LEO payload as in Group One.

As the price of propellant increases, the number of designs in Group One decrease. The designs that require a greater amount of propellant begin to disappear first, and this trend continues until all points are gone at a propellant price of \$4,000/lb, as discussed previously in this section. The first three points that disappear are those that utilize a passive thermal management system on the EDS, noted as Group A in Figure 65. These three MLI cases require a greater amount of propellant refueling and thus become dominated as the price of propellant increases. This change shows that a cryo-cooler is the best option for the EDS thermal management system at a propellant price of \$2,000/lb. If a price of \$1,500/lb can be achieved, then the cost of providing propellant becomes less than placing a cryo-cooler on the EDS, and a passive thermal management system becomes the superior architecture choice.

The design points in Group Two (Case # 1 – 10, Table 41) are not greatly affected by a change in propellant price, and in most cases, no notable change is seen. These points utilize propellant refueling to replace the propellant lost to boiloff. The boiloff for the LSAM can range from 500 to 5,000 lbm depending on the LEO stay time and the ascent engine selection. In the cases where the EDS utilizes a cryo-cooler, this is the total amount of propellant that must be delivered to the architecture, resulting in a very small change in LCC as the price of propellant changes. When the EDS does not utilize a cryo-cooler, the quantity of propellant required can increase by more than 400 percent as the EDS is a much larger propellant storage system than the LSAM. In these cases, there is a larger dependency on the price of the propellant. Both of these cases are noted in Figure 66; the relative change can be seen for the various propellant prices.

The initial two points, noted as Group A (Cases # 1 and 2), also have a larger amount of refueling, because in these two designs, the Ascent Stage of the LSAM is empty during launch to LEO, after which it is re-fueled. This equates to an additional 10,000 lbm of additional propellant that must be provided to the architecture. Case #1 disappears from the frontier at a propellant price of \$3,000/lb, while Case #2 remains. This is because Case #2 utilizes a passive thermal management system on the EDS and requires a greater amount of propellant during refueling than Case #1 which utilizes a cryo-cooler on the EDS. In general all designs in Group Two have a smaller dependence on the price of propellant than those in Group One because they use less propellant refueling. These results also illustrate that, even at a high propellant price, the introduction of propellant refueling would provide for a lower cost solution than the current baseline design. This is because the cost of the propellant is a small portion of the

total LCC (less than 1%) and, even with a significant increase in the price of the propellant, the LCC is only slightly increased.

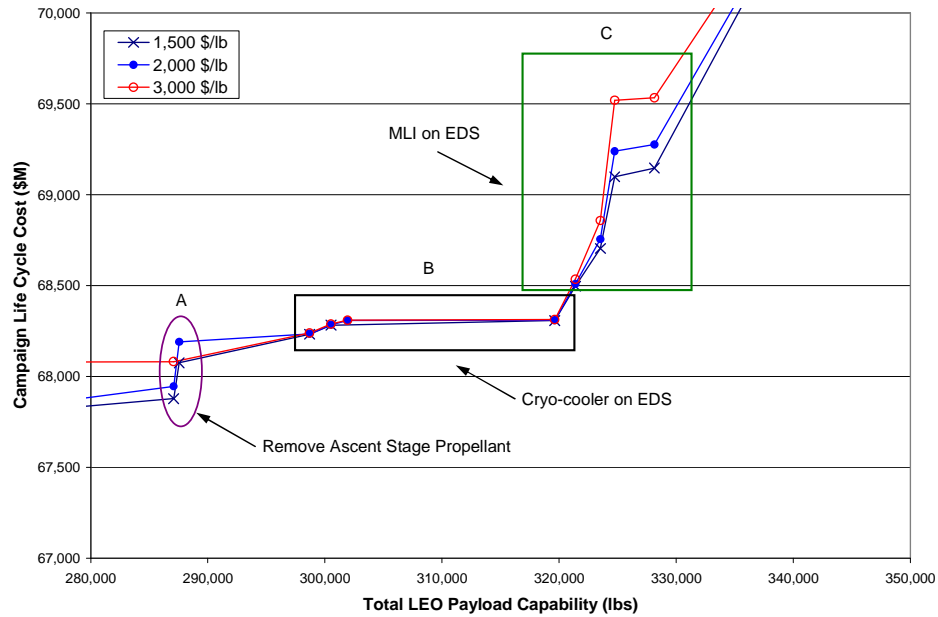


Figure 66: The Effect on Group Two of a Change in Propellant Price

6.4 EXPLORATION OF THE DESIGN SPACE WITHIN THE FRONTIER

In addition to understanding the designs that fall on the Pareto frontier, it is important to understand the designs that fall just off this frontier. With the uncertainty that is associated with developing the propellant refueling technology, it is important to understand how much variation can be handled along the frontier before the non refueling cases begin to dominate. The results of Figures 67, 68, and 69 will demonstrate how the design space, within the frontier breaks down for a number of the design variables: which stage performs the LOI maneuver, whether propellant refueling is used for propellant

boiloff, and whether propellant should be removed from the design of the EDS. The greater the distance between the frontier and the non refueling design points, the less concern there is about the uncertainty in developing this capability. If the non refueling cases are right along the border of the frontier, propellant refueling becomes a considerably more risky venture, as any variation from the baseline assumptions degrades the value of this choice.

Figure 67 illustrates which design points utilize the EDS and which use the LSAM for the LOI maneuver. The Pareto frontier was split into two refueling groups: the first utilized the EDS and provided the greatest decrease in LCC, and the second group continued to use the Descent Stage and provided less of a decrease in LCC, but also a better LEO payload capability than Group One. The design space in the vicinity of each of these groups shows the same results as seen in the frontier. In fact there is a distinct trend that shows the use of the EDS in the lower half of the design space and Decent Stage in the upper half. There is a middle set of data that shows a lot of overlap between the two choices, but this is due to the influence of other design variables that are not considered here. The distinct split shows that utilizing the EDS for the LOI maneuver instead of the LSAM forces the decision maker to trade improvements in one FOM (LCC) for a reduction in the other (LEO payload). This is not the case for utilizing propellant refueling to replace the LEO boiloff, as this option is always active along the frontier where propellant refueling is considered.

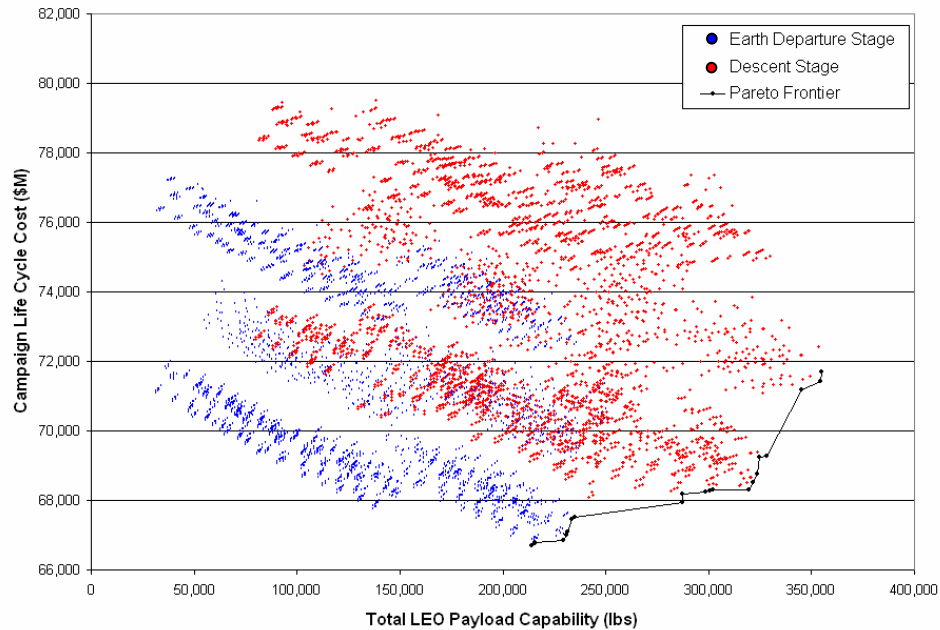


Figure 67: Lunar Orbit Injection Maneuver Breakdown

The results in Figure 68 depict the use of propellant refueling to replace any propellant lost due to propellant boiloff, whether on the EDS or LSAM. The results here show a similar split as seen in Figure 67, but the design space is split horizontally instead of vertically. This horizontal split shows that the introduction of propellant refueling in this manner is a benefit to the architecture in spite of the selection of the remaining design variables. There is also a large gap between the frontier and those points that do not utilize this option for propellant refueling, except near the baseline where no propellant refueling is considered. This would allow a significant increase in the cost of propellant refueling to be absorbed before this strategy would become a higher cost solution. These are both promising traits that help lower the risk of implementing this capability into the lunar exploration architecture.

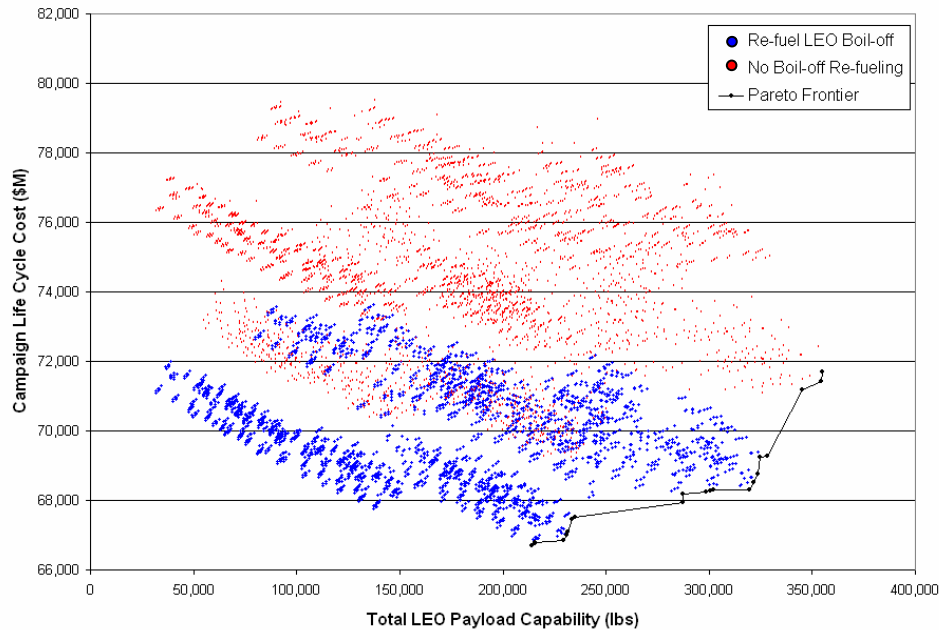


Figure 68: LEO Propellant Boiloff Refueling Breakdown

The final figure, Figure 69, depicts the impact of removing the TLI propellant from the design of the EDS and providing it in LEO. The blue points in this figure represent all design in which some quantity of propellant was removed from the design of the EDS. This includes just one of the propellants (LOX or LH2) or both and in the various quantities outlined in the Morphological Matrix. In general, the trend in these results shows that the cost of removing this propellant has little effect on the overall design of the architecture, assuming a propellant price of \$2,000/lb. At this price, the cost of propellant is slightly more than the savings achieved by reducing the size of the CaLV. The reason this option is not active on the frontier is that it offers the same cost, but results in a lower the payload capability. There is, however, less of a separation between the frontier and these design points; it was shown in Section 6.3 that lowering the price of propellant to \$1,500/lb would bring some of these points onto the frontier. A similar

result is also seen if larger cost savings could be achieved by reducing the size of the launch vehicle. This becomes a possibility if a new technology development programs are required to help mitigate unexpected mass growth on the CaLV or LSAM.

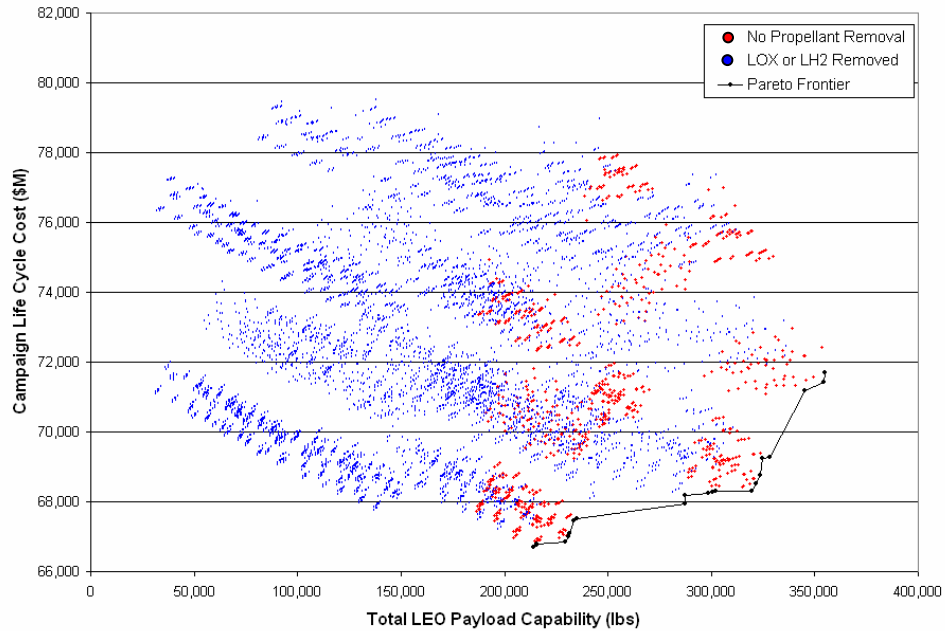


Figure 69: Breakdown of EDS Propellant Removal

The results of Figures 67 - 69 help to show the robustness of propellant refueling strategies against changes in the assumptions of the analysis. If small changes in assumptions can negate the benefits of introducing this capability into the architecture, the risks of implementation become too great. The results in Figure 67 and Figure 68 provided limited evidence that the introduction of propellant refueling to mitigate propellant boiloff and to allow the EDS to perform the LOI maneuver is relatively insensitive to changes in propellant refueling assumptions.

6.5 COST PER POUND OF DELIVERING PAYLOAD TO LEO

An important metric discussed in Chapter 5 was the cost of delivering a pound of payload to the lunar surface as shown in Figure 53. This was useful when discussing Scenario One because the introduction of propellant refueling changes both the payload capability and the LCC. This cost per pound metric was then used to track the relative change in both values. In Scenario Two, the lunar surface payload remains constant, so this metric would track the change in the LCC only, which was discussed along with the Pareto frontier presented previously in this chapter. It may, however, be useful to look at how the cost of delivering payload to LEO changes with the introduction of various propellant refueling strategies. This metric is calculated by dividing the LCC by the total payload delivered to LEO during the lunar campaign. This metric is plotted in Figure 70 as a function of the LCC and propellant price.

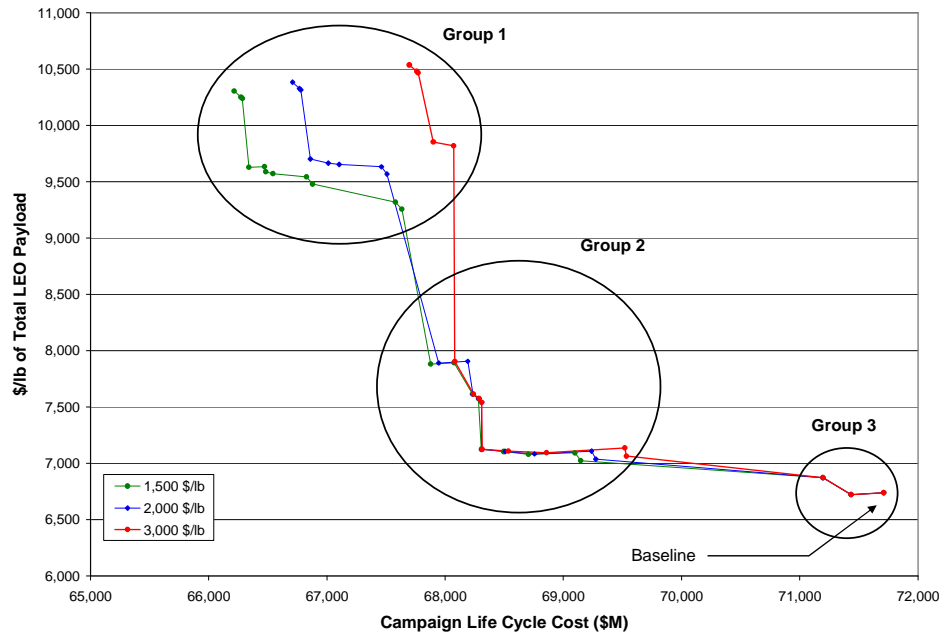


Figure 70: Effect of Propellant Refueling on Payload Capability, LCC and \$/lb

This metric, “cost per pound of payload to LEO,” illustrates that the introduction of propellant refueling increases the cost of delivering payload to LEO. This is because the LEO payload capability is reduced by up to 40 percent, while the LCC is at most reduced by seven percent. Since the LCC is decreased by a smaller amount, the cost per pound to LEO increases. The cost per pound for Group One increases by nearly \$4,000/lb from the baseline value. The difference between the baseline and Group Two is smaller because there is a smaller decrease in payload capability while achieving nearly the same improvement in LCC as Group One. The difference in cost per pound between the baseline and Group Two is \$500/lb, an order of magnitude smaller increase than seen for Group One.

The focus of Scenario Two is to decrease the cost of the lunar campaign without reducing the lunar surface payload capability of each mission. The introduction of propellant refueling accomplished this goal because it is able to lower the LCC while holding the lunar surface payload capability constant. As shown in Chapter 5, the cost per pound to the lunar surface could be greatly reduced through the introduction of propellant refueling, which greatly increases the payload capability for a small additional cost to the architecture. In Scenario Two, the cost per pound to the lunar surface is reduced, but because the payload capability was held constant, the effect is smaller than experienced in Scenario One. A summary of the cost per pound to the lunar surface for both Scenarios One and Two is provided in Table 43. The designs in Scenario Two provide at most a seven percent reduction where as the designs in Scenario One can provide between a 50 and 92 percent reduction in this metric. This is primarily because of the significant increase in payload capability achieved for the designs in Scenario One.

Table 43: Description of Changes between Groups

	\$/lb to the Lunar Surface
Baseline	660,000
Group 1 (Scenario Two)	620,000
Group 2 (Scenario Two)	635,000
Scenario One	50,000 – 300,000

6.6 SUMMARY OF SCENARIO TWO RESULTS

The introduction of Scenario Two was used to develop an alternative to Scenario One where the LCC was decreased by reducing the size of the architecture elements. The results provided in this chapter showed that this could be accomplished and the best refueling strategies for this scenario were identified. These strategies included refueling the propellant lost to boiloff and utilizing the EDS for the LOI maneuver. These are the same solutions identified for Scenario One. The impact of these solutions on the architecture is a maximum reduction in LCC of seven percent. This is a greater reduction in LCC than is achieved in Scenario One, but the reduction in the cost per pound of lunar surface payload is much less (7 percent vs. 90 percent). The main drawback of Scenario Two is that any reduction in LCC results in a corresponding reduction in the LEO payload capability. This decrease in LEO payload capability reduces the ability of the architecture to be extensible to missions beyond the Moon. The total LEO payload capability is reduced by as much as 40 percent, whereas in Scenario One it remained constant. This reduction in extensibility may make Scenario Two a less attractive option because the total decrease in LCC is small and can also be accomplished with Scenario One without reducing the ability to perform exploration missions to Mars and beyond.

CHAPTER 7

VALUE PROPOSITION FOR PROPELLANT REFUELING

Chapter 7 describes the value proposition of propellant refueling to NASA's exploration program. A *value proposition* is defined as: "A business or marketing statement that summarizes why a consumer should buy a product or use a service. This statement should convince a potential consumer that one particular product or service will add more value or better solve a problem than other similar offerings" [61]. In this problem, the service is the addition of propellant refueling to NASA's exploration architecture, and the value is the ability to provide improvement to each of the architecture's figures of merits. The value proposition will be described in order to provide evidence that the implementation of this service will provide greater value to NASA than the current baseline.

7.1 NASA'S PROPELLANT REFUELING VALUE PROPOSITION

In order to develop NASA's value proposition, the concept of what is value to NASA must be clearly defined. During the Exploration Systems Architecture Study five Figures of Merit (FOMs) were established to provide a set of metrics to evaluate the various concepts that were considered during this study; these were outlined in Chapter 1. These criteria establish the value added to the exploration architecture. An improvement in one or more of these criteria without degrading another would provide a more valuable design in the eyes of the decision maker. Therefore, the value of a design change, such as

including propellant refueling, is measured by how well it improves each of these FOMs. The five FOMs are: safety and mission success, affordability, performance, extensibility, and programmatic risk; the first two FOMs were considered the most important. In this study, the third metric, performance, is considered a constraint in the system sizing, thus all design changes meet the performance requirements. The implementation of propellant refueling can have a positive impact on each of these criteria depending on the selected configuration. The following sections will discuss how the introduction of propellant refueling affects each of these criteria. The value proposition will then be presented to establish which implementation of propellant refueling provides the best alternative to the baseline design and if this selection is affected by the weighting of the selection criteria.

7.1.1 IMPROVEMENT IN ARCHITECTURE CAPABILITY

The ability of propellant refueling to provide value to the exploration architecture stems from its ability to increase the payload capability per unit of LCC of the architecture, to increase mission and design flexibility, and to improve the mission success probability. These improvements provide design freedom to the architecture, allowing it to achieve a greater performance without significantly altering the design of the baseline vehicles. This section will discuss how the improved payload capability affects the architecture life cycle cost, the operational and development risk, and the overall extensibility of the program to future missions.

The screening process presented in chapter 5 showed that there are three refueling strategies that can effectively increase the payload capability of the architecture: reducing the performance requirements on the LSAM by allowing the EDS to perform the LOI

maneuver, providing the ability to re-fuel the propellant lost to boiloff while the EDS and LSAM are in LEO, and increasing the LEO payload by burning additional propellant on the second stage during ascent. The design points along the Pareto frontier were combinations of these three primary refueling strategies. In order to understand the potential benefits that each of these strategies offer they will be investigated independently throughout this chapter. These options are not the same as those on the Pareto front discussed in Chapter 5 because they do not combine multiple strategies. They are all identical to the baseline concept, except that they introduce a single refueling strategy.

The lunar surface payload capability for these three options is provided in Table 44. The “w/ Crew” case has a smaller payload because it must also deliver the crew and the Ascent Stage to the lunar surface. The “w/o Crew” case is a purely cargo mission. The cargo version of the LSAM replaces the Ascent Stage and crew with additional payload and a cargo delivery platform. Replacing the Ascent Stage of the LSAM with the cargo carrier increases the payload capability by 23,000 lbs [62]. The following section will provide a more detailed discussion of how these three cases can improve the lunar surface payload capability than was presented in Chapter 5 and 6.

Table 44: Lunar Surface Payload Capability

	w/ Crew	w/o Crew
Baseline	3,619 lbm	26,800 lbm
EDS Performs LOI	28,800 lbm	51,900 lbm
Re-fuel LEO Boiloff	8,600 lbm	31,800 lbm
Burn Additional 25,000 lbm	14,700 lbm	37,800 lbm

Utilize the EDS for the LOI Maneuver

The most significant increase in payload capability comes from the case where the LOI maneuver is performed by the EDS instead of the lunar lander. The baseline lander design includes approximately 32,500 lbm of propellant just for the LOI maneuver. If the LSAM LOI propellant is removed, then the payload capability of the lander can increase assuming the total LEO payload capability remains the same. The payload capability does not improve on a one to one scale because both the descent propellant and support structure must increase. A six fold increase in payload is possible with the crewed version of the lander and the payload of the cargo only lander can be nearly doubled.

Utilizing the EDS for more than the TLI maneuver provides the ability to deliver greater payloads to the lunar surface if additional propellant is available in LEO because the EDS is less than 50 percent full in LEO. The results shown in Figure 71 provide the lunar surface payload capability as a function of the amount of propellant that is transferred to the EDS in LEO. This additional propellant is used to increase the delta-V capability of the TLI maneuver or allow the EDS to perform the LOI as well. The initial point along the blue line represents the capability of the baseline design where no refueling occurs. The red curve represents the situation where the EDS is used for the LOI maneuver. Case #7 is noted; at this point the total gross mass of the LSAM is the same as the baseline configuration. The points along this curve with a greater lunar surface payload than Case #7 require the CaLV to deliver a greater LEO payload than in the baseline design. The points below Case #7 are able to achieve a greater lunar surface payload than the baseline while decreasing the total payload that the CaLV has to deliver to LEO. These points represent a hybrid solution between Scenarios One and Two. These

curves show the increase in payload capability that is possible by adding propellant refueling to the baseline. The EDS-LOI red curve can provide both a greater maximum increase in payload capability and a greater improvement in the payload capability per pound of propellant re-fueled. The EDS-LOI blue curve has a lower slope because the size of the lander must grow at a faster rate to account for the increase in LOI propellant needed for greater payload designs.

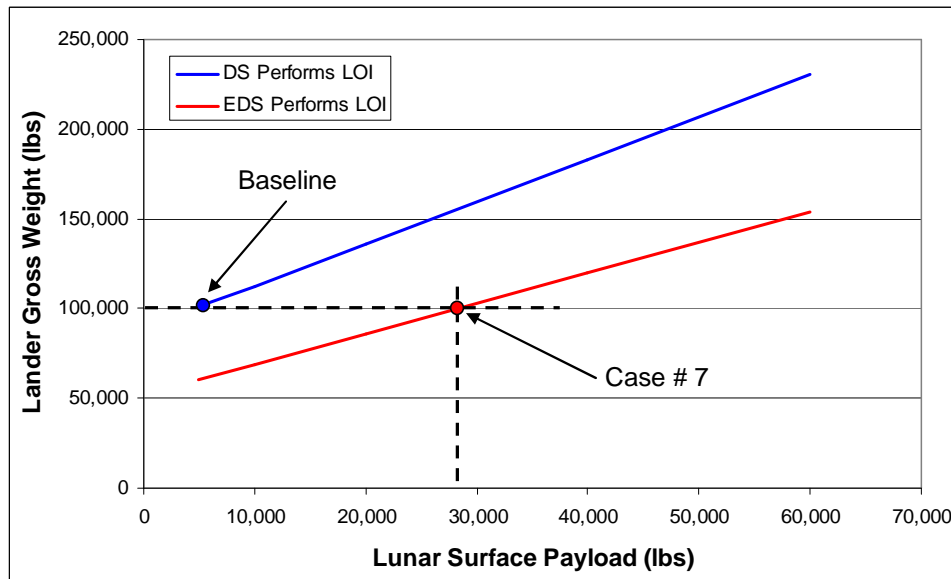


Figure 71: Lunar Surface Payload Capability as a function of EDS Propellant

The results in Figure 71 show the theoretical increase in payload capability but do not consider the practicality of placing the payload in the current vehicle fairing configuration. The larger the payload requirement, the larger the vehicle needed to complete the mission. The results in Figure 72 show how the maximum diameter of the lander increases as the payload requirement increases. The red line again represents the case where the EDS performs the LOI maneuver. The dotted lined represents the current

maximum allowable lander diameter based on the current fairing configuration. In order to handle an increase in payload capability either the payload fairing must be redesigned or the size of the baseline lander must be reduced so that the vehicle does not violate the fairing constraint when additional payload is added. In the latter case, eliminating the LOI maneuver from the lander can reduce the vehicle size by 37% enabling the vehicle to handle up to 60,000 lbm of payload before violating the fairing constraint.

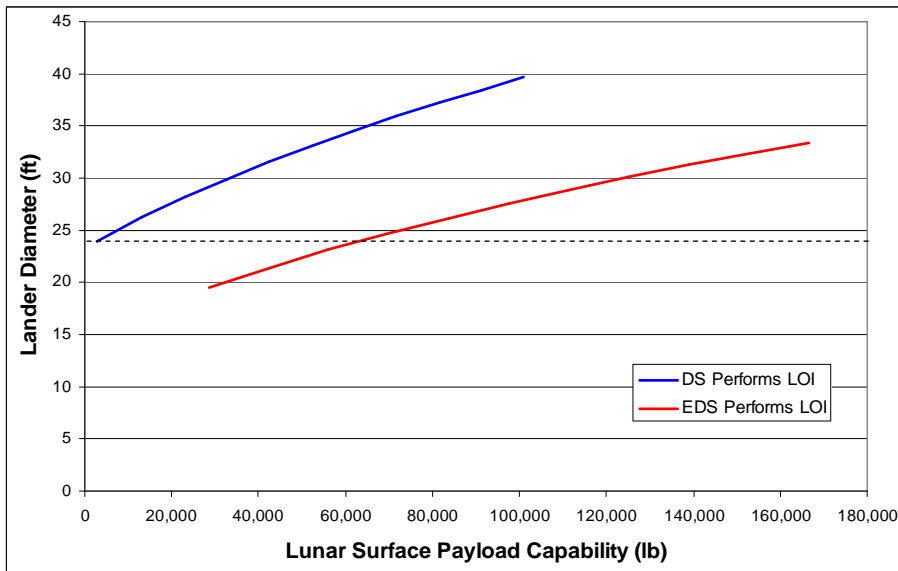


Figure 72: Lander Size Comparison as a function of Payload Capability

Refueling the LEO Boiloff on the EDS and LSAM

The payload capability of the architecture can also be improved by eliminating the need to carry additional propellant to account for boiloff that occurs while the EDS and lander are in LEO. The addition of MLI can reduce the amount of boiloff that occurs, but without the addition of a zero boil-off cryo-cooler system, there will always be some

boiloff that must be accounted for with additional propellant that must be carried to LEO. A range of anywhere from four to ninety five days has been considered for NASA's baseline architecture. There are two main factors that influence the selection of this stay time. The first is that, the longer the designed stay time, the more propellant that must be stored on the vehicles, and thus a lower payload capability or a greater vehicle size. The change in payload capability as function of the designed stay time can be seen in Figure 73. This chart was developed by linking the propellant boiloff model discussed in Chapter 3 with the CaLV model and varying the number of days the EDS was required to remain in LEO. As the number of days increased, a greater quantity of propellant was required to maintain the minimal propellant levels needed to complete the required mission. The launch vehicle is physically constrained; therefore, any increase in propellant directly decreased the payload capability of the vehicle. The decrease in payload capability is greater than the additional propellant required due to the additional hardware needed to store the propellant aboard the vehicle. A 15 day stay time was used at the zero point of reference. These results show that there is a 15,000 lb difference in payload capability or design margin between the 4 and 95 day cases.

The second factor is that, in the design of a multi-launch architecture, the mission is dependent on the successful launch of both vehicles. If the delay in launching the second vehicle is longer than the designed stay time, then the vehicles (EDS and LSAM) no longer have the propellant capability to complete the mission. As discussed in Chapter 5 and 6 depending on the difficulty of the mission the EDS and LSAM may have the ability to remain in LEO for longer than the designed period. The results presented here assume that once the designed limit is exceeded the mission is lost. The probability of

losing a mission and the associated cost to the architecture are provided in Figure 74. The details behind the creation of this chart are provided in Chapter 4. The chart shows the trends for the two separate launch separations times considered. The separation is the time between launching the cargo launch vehicle and the crew launch vehicle. The shorter the time between these two launches the less likely there will be an outside influence that affects the timing of the launch. As an example, it would be much easier to predict the weather patterns within a 90 minute window than over a 7 day window. The concern with launching both vehicles within a relatively short time period is that the operational complexity of coordinating the countdown of two independent launches is higher than a single launch. There is however a significant increase in the mission success if both vehicles can be launched within this small window. These two competing factors make it difficult to select an optimal stay time, either the architecture has a low payload capability and high success rate or it has a low success rate and a high payload capability. The introduction of propellant refueling introduces the possibility of a high payload capability without compromising the success of each mission. Propellant refueling eliminates the need to carry additional propellant to LEO to account for possible propellant boiloff. Any propellant that is lost while the vehicles are in LEO is refueled once all mission related hardware has been delivered to LEO. This eliminates the chance that a mission will be lost due to a delay in launching the second launch vehicle. A comparison of this improvement in reliability due to propellant refueling is offered in Section 7.1.4.

The lunar surface payload capability for the 7 day separation and 95 day LEO stay time can be increased by approximately 12,000 lbm when propellant refueling is

implemented to provide the boiloff propellant. While this is less of an increase than can be obtained from reconfiguring the LOI maneuver, it comes at a much lower cost to the architecture. Depending on the price of propellant, this solution may provide a lower cost solution than the baseline design while achieving a greater payload capability. This was shown in Chapter 5.

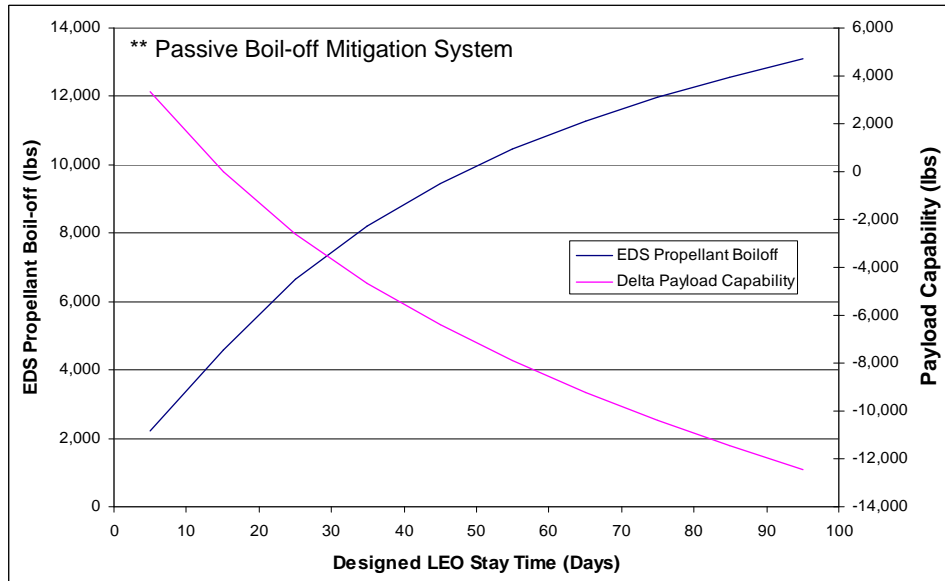


Figure 73: Change in Payload Capability as a function of Boiloff

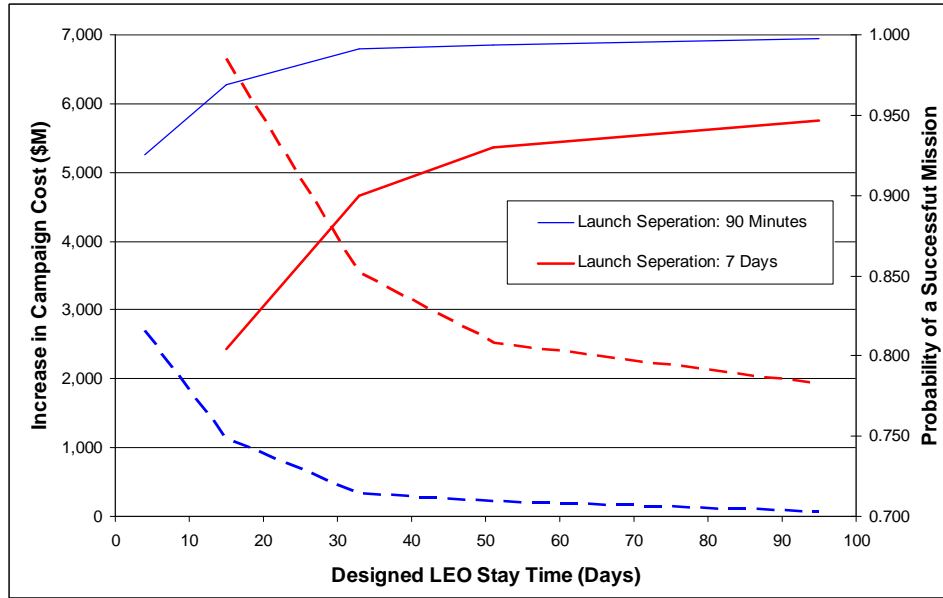


Figure 74: Effects of LEO Stay Time on Overall Campaign Cost and Mission Success

Decrease In-space Propellant Delivered to LEO

The final method that can be utilized for improving the payload capability of the architecture is to increase the amount of propellant that is used during ascent. Since the upper stage of the cargo launch vehicle is also the EDS, there is additional propellant available that, in the baseline architecture, is reserved for the TLI maneuver. The utilization of this propellant during the ascent phase allows the launch vehicle to insert a larger payload into LEO. In this trade study the launch vehicle configuration remained fixed and the only change made to the design was the quantity of propellant used during ascent. The total propellant at liftoff remained the same as in the baseline design. The results provided in Figure 75 show the relationship between the propellant burned and the payload capability of the vehicle. The increase in total payload capability is dependent on

how much additional propellant is used, but an increase of approximately 10 percent can be obtained if all of the EDS propellant is used.

The total LEO payload capability is defined by two main terms. The first is the mission payload that includes the lunar lander and its corresponding payload. In the baseline design the mission payload is approximately 101,000 lbm. The second term is the propellant payload that includes the in-space propellant aboard the EDS once it reaches LEO. This was approximately 225,000 lbm in the baseline configuration. As the ascent propellant utilized increases, the mission payload increases, and the propellant payload decreases. This trend can be seen in Figure 75; note that the total EDS LEO payload increase is small, whereas the in-space mission payload increases dramatically. There are two reasons why there is only a small increase in the total payload. The first is that the gross lift off mass of the vehicle increases by 175,000 lbm to account for the additional mission payload while still carrying the same propellant load. This significantly decreases the capability of the core stage, reducing its separation velocity by nearly 4,000 ft/s, assuming there is no change in the design of the first stage. The second factor is that the T/W of the upper stage is decreased from 0.84 to 0.61 requiring a longer burn time to reach the same final conditions. Both are a T/W and gravity loss problem. Section 4.1.1 further discussed why the total payload is improved only slightly when the total propellant burned is increased. Additional engines could be used to improve the performance providing a greater capability per pound of propellant burned, but would increase the design dry mass, and cost of the vehicle.

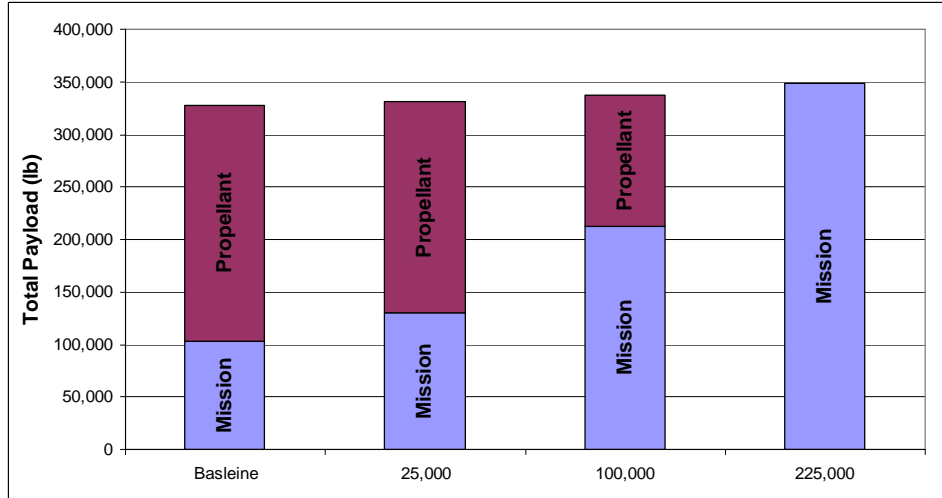


Figure 75. Change in Payload Capability and the Ascent Propellant is increased

The ability of the launch vehicle to deliver a greater payload to LEO leads directly to a greater lunar surface capability. However, as the LEO payload mass increases, so does the required TLI propellant. In the final case shown above, where the EDS is delivered to LEO empty, the required TLI propellant is increased from 225,000 lbm to 473,000 lbm, more than doubling the baseline propellant. The lunar surface payload capability and the required TLI propellant are provided in Table 45. The 100,000 lb case requires that 205,000 lbm of propellant be delivered to LEO for propellant refueling in order to meet the new propellant requirements for the greater payload capability.

Table 45: Lunar Surface Payload Capability for an Increase in the Ascent Burn

	w/ Crew	w/o Crew	TLI Propellant
Baseline	3,619 lbm	26,800 lbm	225,000 lbm
Burn Additional 25,000 lbm	14,700 lbm	37,800 lbm	245,900 lbm
Burn Additional 100,000 lbm	47,900 lbm	71,100 lbm	331,200 lbm

The main concern with increasing the payload capability of the CaLV/EDS is that the lander would quickly violate the fairing constraint for any increase in payload capability without a reduction in lander requirements (see Figure 72). The 25,000lb additional propellant case will be used to evaluate this method as it is the closest to the current fairing constraint. In order to consider greater payload capabilities this method would have to be coupled with other changes to the lunar architecture that reduce the requirements on the lander. There is however potential use for this method outside of a lunar mission as it provides the greatest LEO payload capability.

7.1.2 REDUCTION IN ARCHITECTURE CAMPAIGN COSTS

The additional of propellant refueling offers two direct methods for reducing the life cycle cost of exploration missions. The first is through an increase in payload capability where the architecture has the capability of reducing the required number of years needed to complete the lunar campaign. The second is by designing the launch vehicle to only be responsible for delivering the mission payload to the LEO while providing the in-space propellant once the architecture elements are delivered to LEO. Removing the in-space propellant can reduce the payload requirement on the launch vehicle by more than 70 percent, thus greatly reducing the size of the vehicle needed to complete the mission. Smaller vehicles results in lower development and production costs. As the results in Chapter 6 discussed reducing the size of the architecture elements results in an overall poor architecture solution, therefore only the refueling strategies develop in Chapter 5 will be considered.

The NASA reference lunar campaign [63] will be used to provide a more detailed estimate of cost for the lunar exploration missions than was used for the architecture screening in Chapters 5 and 6. In order to remain within the proposed budget this campaign has been changed from that proposed during ESAS, which was designed to conduct two missions per year. The lunar campaign includes two phases: the first phase is the deployment of the lunar outpost which has an approximate total mass of 135,000 lbm, and the second phase is the completion of 10 years of extended stay missions at the lunar outpost, consisting of one 180 day human mission per year. The 135,000 lbs is an estimate based on the number of required cargo missions, assuming the maximum payload is delivered during each mission. The delivery of the outpost in the baseline architecture is deployed over nine missions with five being exclusively cargo missions and four crew and cargo missions. The details for the outpost deployment and extended stay phases of the campaign are provided in Figure 76. The deployment of the outpost is limited by the number of missions that can be conducted in a given year and the payload capability of each mission. The extended stay missions consist of two separate missions; the first is the launch of the Pressurized Logistics Module (PLM) containing mission consumables which must be deployed to the outpost prior to the arrival of the crew, and the second is the delivery of the crew to the lunar outpost to begin their 180 day stay. These two missions rotate with one complete 180 day stay being completed each year. The LSAM baseline payload of 3,600 lbm is used as the reference cargo delivery capability for the combined crew and cargo lander; the cargo only lander has a reference payload capability of 26,800 lbm. This cargo payload was determined by replacing the ascent stage with a cargo platform and assuming the remaining mass difference to be

additional payload capability [63]. Figure 76 outlines the details of the campaign including how the outpost is delivered to the lunar surface, when the outpost is completed, and the number of days the crew is on the lunar surface. The number of surface days increases as the outpost is assembled and eventually leads to a 180 day stay at the completion of the outpost.

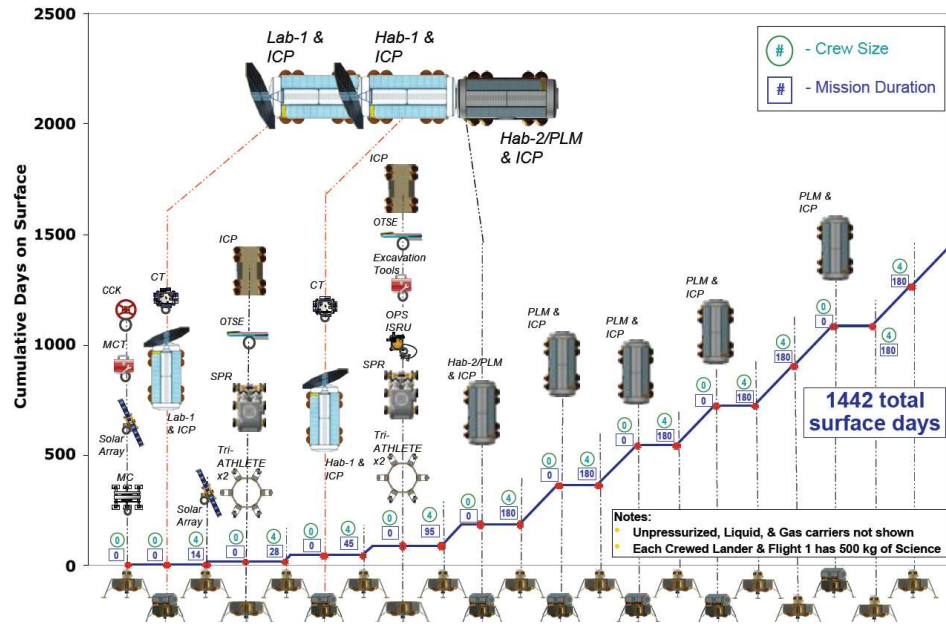


Figure 76: Baseline lunar Campaign Mission Summary [64]

The lunar exploration extended stay missions may extend beyond a 10 year time-frame but these costs will not be considered in the propellant refueling value assessment. In addition, any International Space Station and robotic precursor mission will also not be included as these costs will not be affected by the implementation of refueling. Using the NASA cost model (NAFCOM), the baseline Design Development Test and Evaluation (DDT&E) and Theoretical First Unit (TFU) costs for each of these vehicles is provided in Table 46.

Table 46: Cost Values for Baseline Exploration Architecture

	CEV	CLV	LSAM Cargo	LSAM Crew	CaLV
DDTE	4,200	3,778	--	5,582	6,041
TFU	500	633	547	730	643

Increasing the payload capability can affect both phases of the lunar campaign. During the outpost deployment phase, the increase in payload allows a greater amount of cargo to be delivered during each mission. This decrease the total number of mission required to deploy the permanent outpost hardware. During the extended stay phase of the campaign the greater payload capability can be used to pre-deploy the resources needed for each mission. Therefore each cargo mission can deploy enough payload to provide for two crewed missions. In the baseline campaign the cargo missions only have the capability to provide enough payload for a single crew mission. Decreasing the number of mission required to achieve the goals of the campaign allows it to be completed in a fewer number of years. Since the campaign is completed sooner the fixed cost required to operate the campaign can be transferred to other programs reducing the total cost of the lunar campaign. These recourses can then be transferred to other exploration missions.

In order to maintain a fair comparison between the refueling case and the baseline architecture three constraints must be maintained. The first is that the total payload delivered to the lunar surface during the lunar campaign must remain constant between the baseline and the various refueling cases. This constraint is primarily used to verify that the total mass of the lunar outpost has been deployed, since the refueling case has a

larger payload capability it can accomplish this task in a shorter period of time than the baseline. The time required to deploy the mass of the outpost is provided in Figure 77. In this example it is clear that the refueling architecture can deploy the outpost in less time than the baseline. In fact it is able to reduce the total length from 4.5 years to two years.

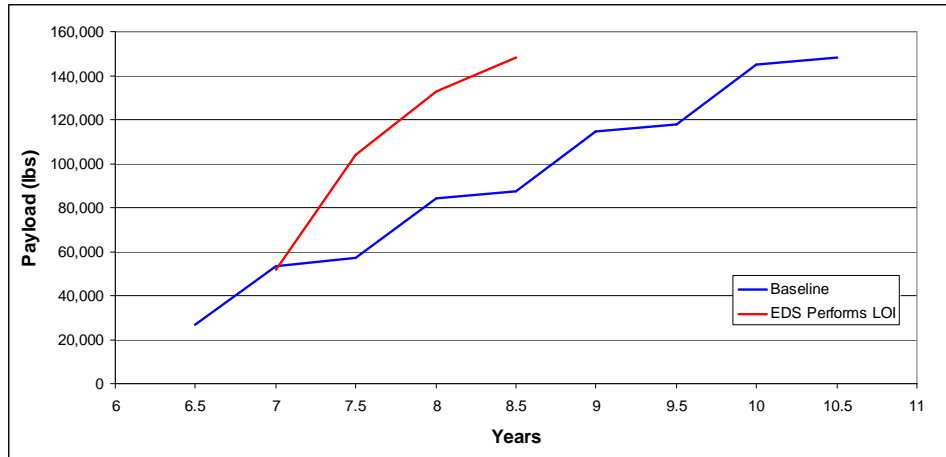


Figure 77: Improvement in the Lunar Surface Payload Capability

The second constraint is that the same amount of science must be conducted during the lunar campaign. A useful metric to evaluate this is to use the total days spent on the lunar surface. The baseline campaign discussed in Figure 76 resulted in 2,000 days on the lunar surface and therefore all architecture comparison will maintain this total surface stay. The number of surface days achieved versus the length of the campaign is provided in Figure 78. In both cases the total number of days on the lunar surface is 2,000. The refueling case is able to achieve this requirement in a shorter period of time than the baseline as it is able to reduce the number of required missions.

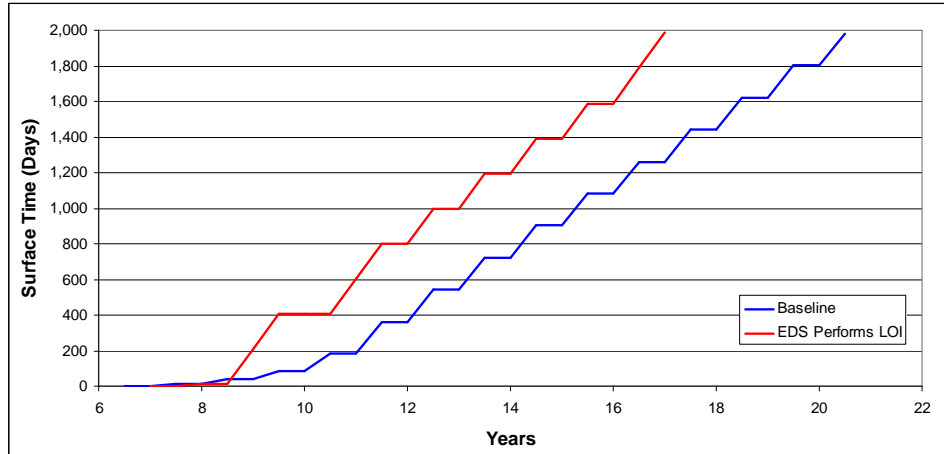


Figure 78: Improvement in the Lunar Surface Payload Capability

The final constraint is that the annual budget must remain within the budget of the baseline campaign. This is illustrated in Figure 79 at a propellant delivery price of \$2,000/lb. Since the refueling case has a higher development cost and a higher cost per mission than the baseline campaign, the operation must be altered in order to remain within the total yearly budget of the baseline. The refueling campaign will be altered in order to minimize the total length while remaining within these three constraints.

The three options for increasing the payload capability that were discussed in the previous section will be considered here to help characterize how the cost of the campaign can be reduced through an increase in the lunar surface payload capability. The results in Table 44 provide the payload capability for each of these cases. The effect of increasing the payload capability has two direct effects on the campaign. The first is a decrease in the number of missions needed to deploy the lunar outpost because a greater amount of payload can be delivered during each mission. The second is, with a greater payload capability available during the extended stay missions, there is potential to increase the science performed during each mission, increase the lunar surface stay time,

or to combine the crew and cargo missions reducing the number of missions needed for the extended phase.

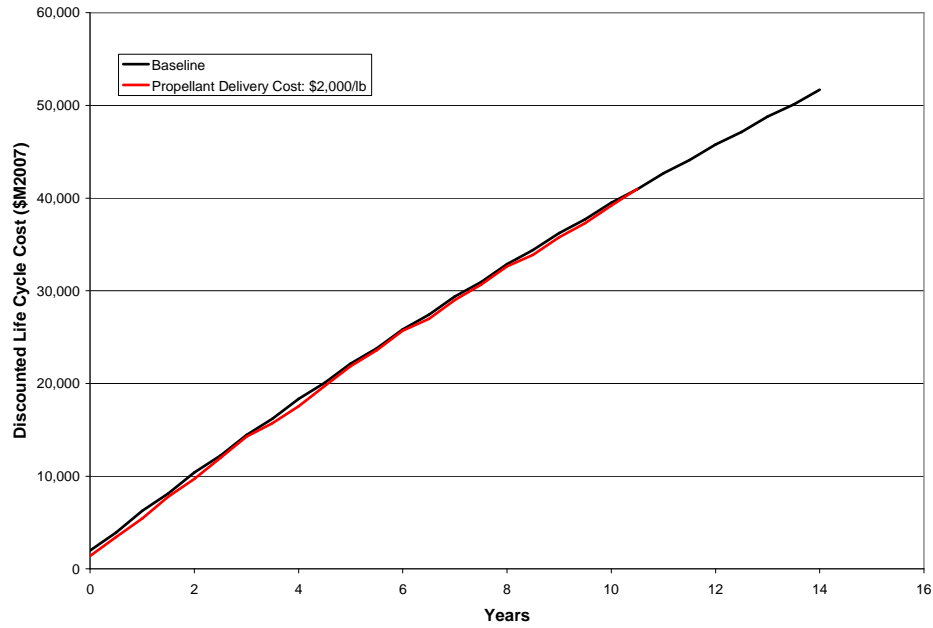


Figure 79: Budget Matching for the Propellant Refueling Option

The results presented in this section will detail how the introduction of propellant refueling affects the design of the baseline lunar campaign. The refueling case where the EDS performs the LOI maneuver will be used for the initial comparison. The campaign will be altered to remain within the yearly budget of the baseline campaign while still obtaining the mission requirements discussed previously. These results are presented in Figure 80 and Figure 81. These two figures describe how the three phases of the campaign (development, outpost deployment, and extended stay) are affected by the introduction of propellant refueling. It is important to understand if the length of the campaign can be shortened through the introduction of propellant refueling. The architecture is able to save \$5.2B for every year that is cutoff from the end of the. This accounts for the yearly

cost of operating the baseline architecture which can be transfer to other missions once the objectives for the lunar campaign are achieved.

The results in Figure 80 show the number of years required to complete the lunar campaign for a fixed to variable ratio of 80/20. These results also include three propellant delivery prices (\$2,000/lb, \$4,000/lb, \$6,000/lb). These results show that it is possible to shorten the length of the lunar campaign by as much as 2.5 years, including a six month delay in the start of the campaign to account for the increase in development cost. Even at the highest propellant delivery price the campaign can still be shortened by six months. This reduction in the length of the campaign results in a savings between \$2.6B and \$13B to account for the yearly cost of operating the baseline campaign that is no longer required.

In order to account for the higher cost of operating the refueling architecture a number of breaks are placed into the campaign. During these breaks no lunar missions are conducted, but the architecture must pay the fixed cost associated with the program. These breaks can clearly be seen in Figure 80. In the case of a propellant delivery price of \$2,000/lb there are three required breaks during the campaign. At a propellant delivery price of \$6,000/lb the number of requires breaks increases to nine in order to stay within the budget of the baseline program. At this price the length of the campaign is almost as long as the baseline, even though the number of mission required is less. The number of breaks is dependent on the cost of propellant and the fixed cost of operating the exploration architecture.

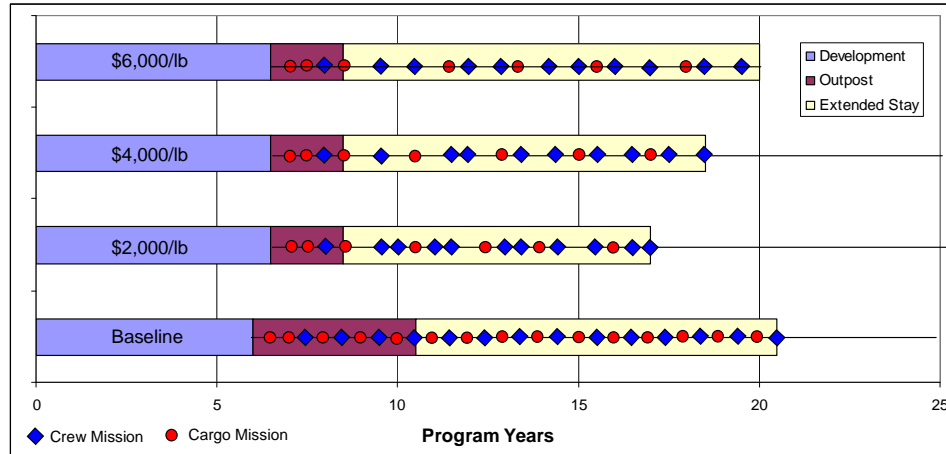


Figure 80: Decrease in Length of Lunar Campaign, F/V: 80/20

The results in Figure 81 are similar to those illustrated in Figure 80 except that they assume a ratio of fixed to variable cost of 60:40 instead of 80:20. This new ratio results in a lower fixed cost than the previous case and a further reduction in the length of the lunar campaign when refueling is added. This additional reduction in the length of the campaign is due to the smaller penalty the refueling architecture must pay when no missions are being conducted. As the assumption for the percentage of fixed costs decreases, these breaks have a smaller impact on the LCC of the campaign. This decreases the number of breaks required to remain within the yearly budget of the baseline architecture. At a propellant price of \$2,000/lb the length of the campaign is further reduced by six months and at a propellant price of \$6,000/lb the length of the campaign is further reduced by 1.5 years. At the higher propellant delivery costs a greater number of breaks in the campaign are required, as shown in Figure 80; therefore a lower fixed cost will have a greater impact on the designs that have the highest cost of propellant. The fixed to variable assumption has a dramatic impact on the design of the

campaign, but in both cases discussed the length of the campaign can be reduced and a significant reduction in the LCC of the architecture can be achieved.

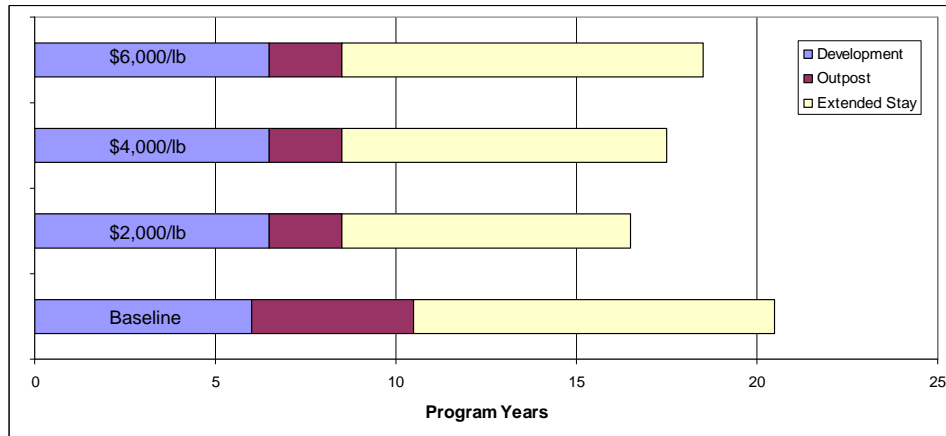


Figure 81: Decrease in Length of Lunar Campaign, F/V: 60/40

These two figures show how the introduction of propellant refueling, which increases the payload that is delivered to the lunar surface during each mission, can effect the different phases of the lunar campaign. Even though the refueling cases cost more per mission to operate they are able to reduce the overall LCC of the architecture by reducing the total length of the campaign. This reduces the total fixed cost that must be paid to operate the lunar missions. The greater the cost of providing propellant to the architecture the smaller the impact that propellant refueling has on the operation of the lunar campaign because more breaks in the operation of the campaign are required to remain within the baseline budget. The ratio of fixed to variable costs are an important parameters to understand as a lower fixed cost tends to favor the refueling cases more than the baseline design as they are more dependent on the fixed cost than the non-refueling architectures. The overall results of these two figures are that the length of the

lunar campaign can be reduced through the introduction of propellant refueling which results in a decrease in the LCC of \$2.5B and \$15.6B depending on the cost of propellant and the final ratio of fixed to variable costs.

7.1.3 REDUCTION IN ARCHITECTURE DEVELOPMENT AND OPERATIONAL RISK

There are two areas of risk that are important to the exploration program. The first and maybe the most important factor concerning the architecture design is the risk associated with loss of crew (LOC) or loss of mission (LOM). The loss of mission is a probability that an event will occur that will keep the mission from being completed, however the crew are able to return safely. The Apollo 13 mission would be an example of a loss of mission, but not a loss of crew. The loss of crew probability is the chance a failure will result in the loss of human life. The second area of risk is that associated with the development of the architecture that includes the development of new technologies and the risk of advancing a vehicle from the conceptual phase to a production design. Value would be achieved if propellant refueling can reduce the risk in developing such a complex and robust architecture.

The introduction of propellant refueling can greatly impact the reliability and mission success of the architecture. It however has little or no impact on the safety of the crew. The transfer of propellants always occurs in LEO. If a mission critical failure occurs, then the crew can simply return to Earth utilizing the CEV (unless a catastrophic failure occurs). The effect on the crew can also be minimized by performing the fuel transfer at a safe distance. The results in Table 47 provide the Apollo estimate for LEO propellant refueling. However, with propellant refueling, the payload can be dramatically

increased, which can be traded in the design for an increase in the redundancy of critical systems, provide engine out capability, and/or provide greater safety margins. These changes would result in a lower LOC and LOM for the architecture. These redundancy trades are beyond the scope of this dissertation, but will be included as possible future work.

Table 47: Apollo Propellant Refueling Reliability [65]

Event	Reliability	10x Apollo
Orient for docking maneuver	0.9925	0.99925
Rendezvous Maneuver w/ depot	0.9749	0.99749
Docking with depot	0.9795	0.99795
Fuel transfer and separation	0.9835	0.99835
Total	0.9676	0.99676

The main improvement in the LOM provided by propellant refueling is the ability to decouple the mission success from the propellant boiloff that occurs in LEO. In the baseline architecture, the EDS is required to handle a specific amount of propellant boiloff to account for the time between its deployment and the launch of the crew. Once this boiloff time is exceeded, the mission can no longer be completed as the architecture has insufficient mission propellants, which result in a loss of mission. The launch separation time between the CaLV and CLV has also been traded by NASA to help mitigate this risk. The closer the two vehicles can be launched, the less likely an outside or unexpected event can influence the launch of the second vehicle. In many cases, it is easier to predict the weather over a 90 minute period than over a 7-day period. The

problem with launching two vehicles so close together is that two separate count downs must be running at the same time increasing the launch operational costs.

The introduction of propellant refueling eliminates the dependency of the architecture on the boiloff rates and allows the EDS and lander to remain in LEO for an extended period of time. This could also be accomplished by utilizing cryo-coolers, but would required them to be placed on all architecture elements in order to eliminate all boil-off concerns. Refueling accomplished this without adding the additional mass to any of the elements. Refueling increases the separation time permitted between the two launch vehicles, resulting in a more simplified operational timeline to be developed. The probabilities of a successful launch of both vehicles within the required timeframe are provided in Figure 82. It is evident that, the longer the stay time built into the mission, the more likely the mission will be completed successfully. There is a considerable drop off in reliability as the required stay time decreases, dropping to close to a 1:5 chance for a 15 day stay time with a 7 day launch separation. This probability can be greatly increased by shortening the stay time to 90 minutes, as was discussed in Chapter 5. The probability curves tend toward a maximum rate of success that is highly dependent on the separation time between the two launches. In the case of a 7-day launch separation, the maximum obtainable probability is approximately 95:100, while the chance of losing a mission is almost eliminated when a launch separation of 90 minutes is used (998:1000). The theoretical best solution is to achieve a 100 percent mission success rate while designing for the minimal LEO stay time and allowing for an adequate separation between launch of crew and cargo. This solution can not be achieved with the current architecture, as an improvement in one area directly leads to degradation in another. The addition of

propellant refueling decouples these design factors, allowing the best case for each to be achieved simultaneously. The concern with the addition of propellant refueling is that it adds an additional point of failure during the refueling phase, however this can be easily offset with the subsystem redundancies as discussed above.

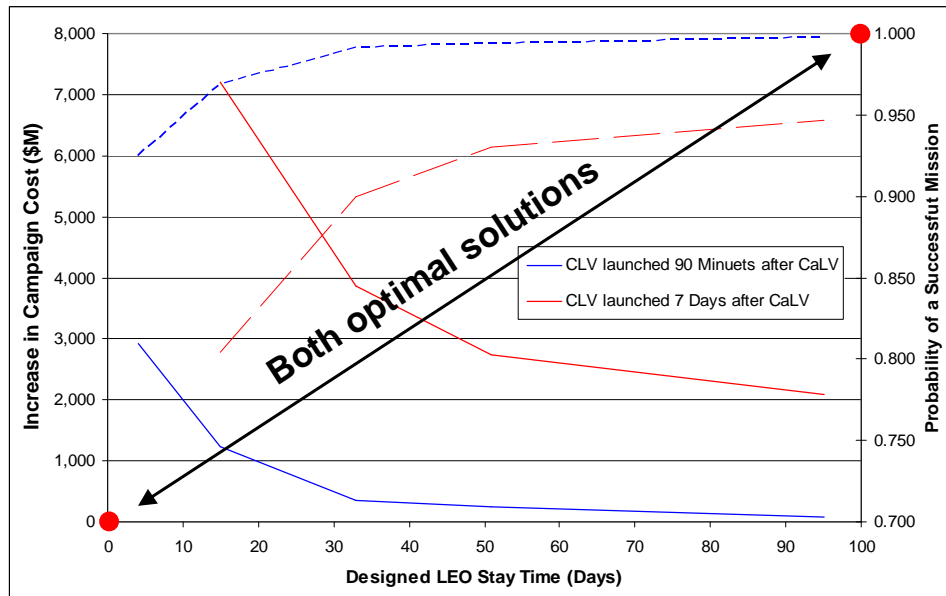


Figure 82: Risk and Cost of a 2-Launch Solution

This additional point of failure may reduce the overall reliability of the architecture; however a more reliable solution can be achieved as long as the reliability of the refueling event is greater than the chance of losing a mission due to LEO propellant boiloff. The Apollo program estimated the reliability of the LEO refueling event at 0.9676 [65]. The refueling event was broken down into the four phases shown in Table 47. It is likely that the reliability of these systems has been improved in the past 50 years

due to an increase in experience with LEO operations and therefore the Apollo reliability numbers likely represent a highly conservative estimate.

The Apollo reliability has been plotted in Figure 83 to show how it compares against the probabilities of losing a mission due to a launch delay. The bold red lines represent the calculated reliability of propellant refueling. The blue and green curves show the probability of losing a mission due to a launch delay as a function of the designed LEO stay time. These are the same curves discussed in the previous section. In this figure, it is evident that the addition of propellant refueling always provides a more reliable architecture for the 7 day launch separation case no matter the designed LEO stay time, up to 100 days. The improvement in reliability increases as the stay time decreases due to a decreasing window of opportunity for the EDS. In the case of a 90 minute separation, the 10x Apollo propellant refueling prediction provides a more reliable solution for stay times under 30 days. For stay times greater than 30 days the two reliabilities are almost indistinguishable. Using the original Apollo reliability estimate, propellant refueling only provides a more reliable solution for stay times less than 15 days. These results show that, unless the architecture is designed with a high LEO stay time or a short launch separation time, the introduction of propellant refueling provides an improvement to the architecture LOM. These two solutions have severe negative effects of the design of the architecture, increasing the cost of the launch and lowering the capability of the launch vehicles. The introduction of propellant refueling allows the reliability goals to be met without compromising on the capability of the architecture or increasing the complexity of the launch countdown.

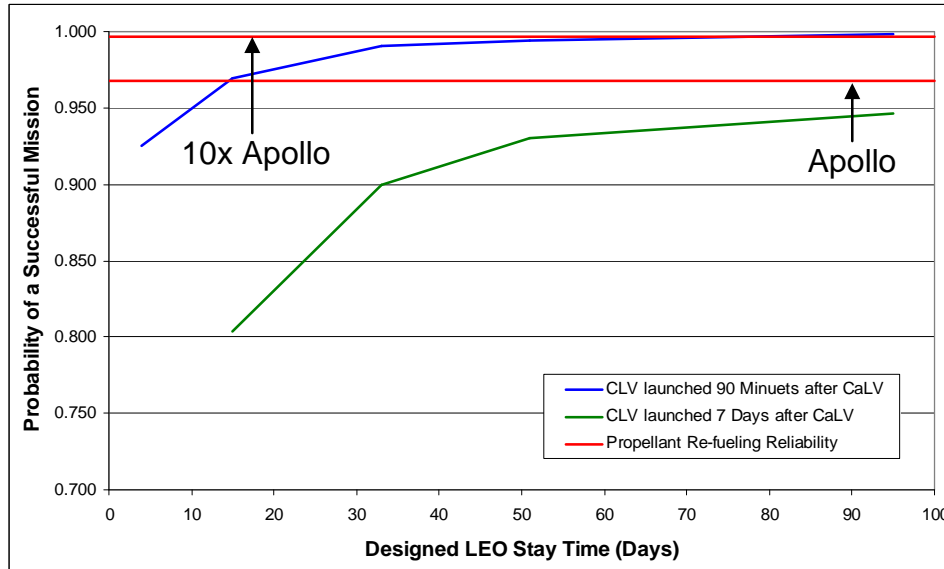


Figure 83: Improvement in LOM vs. Risk of Refueling Maneuver

The second area of risk that must be taken into an account when designing a new and complex system is the risk of advancing a concept from conception to production. There are a number of factors that could lead to the demise of the project, including: under performing systems, mass growth, failure to mature required technologies, and exceeding budgetary constraints. These and a number of other factors can push the design into an infeasible region, forcing a reduction in mission requirements or a redesign of the system with advanced technologies. Redesign can lead to considerable program delays and cost increases that further hamper the development of the program. A common factor affecting the design of a program between conception and production is the increase in mass that occurs throughout the life of the development process, unacceptable reductions in system level performance, and inadequate maturation of technologies. These all have an impact on the progression of the total system mass. Mass growth is a part of all new vehicle designs and must be accounted for during the initial design phase

of the program [66]. The concern is that most programs include 18 to 20 percent of mass margin reserves [67] while most aerospace programs experience closer to 30 percent in mass growth and can be as high as 50 percent for systems that have limited historical background (heritage). Wilhite's paper discussed in Chapter 1 provides the background for these results and also looks at how mass growth on one area affects the rest of the architecture. This section will investigate what the cost of mass growth is on the development of the architecture and how this can be mitigated through the use of propellant off-loading and refueling. A discussion will also be provided as to the benefit of utilizing propellant refueling to help close the architecture if the CEV and/or lunar lander exceed the maximum capability of the launch vehicles

This study looked at increasing the mass growth on the lunar lander and the cargo launch vehicle to determine how this would affect the overall size of each systems and what the corresponding increase in development and production cost would be. These results are provided in Figure 84. The additional dry mass percentage is on top of the 17 percent margin assumed during the ESAS study. These results show a significant increase in cost as the additional growth increases the mass and overall size of each vehicle. Based on the reference lunar campaign, a 10 to 20 percent additional growth on both vehicles would increase the total campaign costs by \$3.0 to \$6.3B.

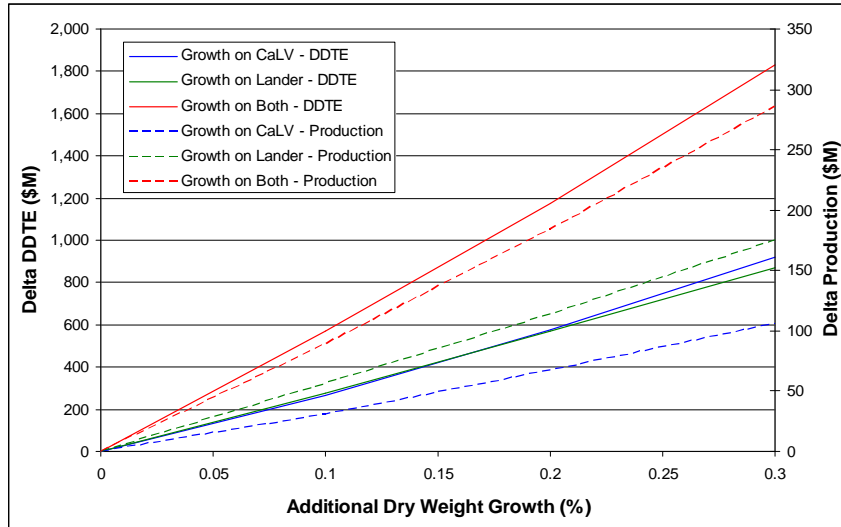


Figure 84: The Effect of Vehicle Growth on Development Costs

These costs assume that the vehicle is able to grow to accommodate the increase in dry mass, but in some situations the vehicle is physically constrained and can not grow as needed. In this case the vehicle would have to find an alternative and likely more expensive route to gaining the additional performance such as the addition of advanced technologies like composite structures or a higher specific impulse propulsion system. The cargo launch vehicle is a perfect example of this type of constrained problem. The size of the launch vehicle is currently being constrained by the entry way to the Vehicle Assembly Building (VAB). While it is possible to still increase the width of the launch vehicle, the height has reached the limit that the VAB can handle. Any additional growth would have to be grown horizontally, but eventually this limit will be exceeded as well. The physical growth of the launch vehicle as a function of an increase in the dry mass of the system is provided in Figure 85. The two curves represent the increase in vehicle size needed in order to achieve the same mission requirements under the given mass growth. The two curves are independent and assume that the growth only occurs in one dimension

while the other remains fixed. These results show that a 30% increase in dry mass can lead to a 5ft increase in the diameter and a 75ft increase in the height of the launch vehicle. These are undesirable results, the height due to the limitations of the VAB and the diameter due to manufacturing and VAB limitations.

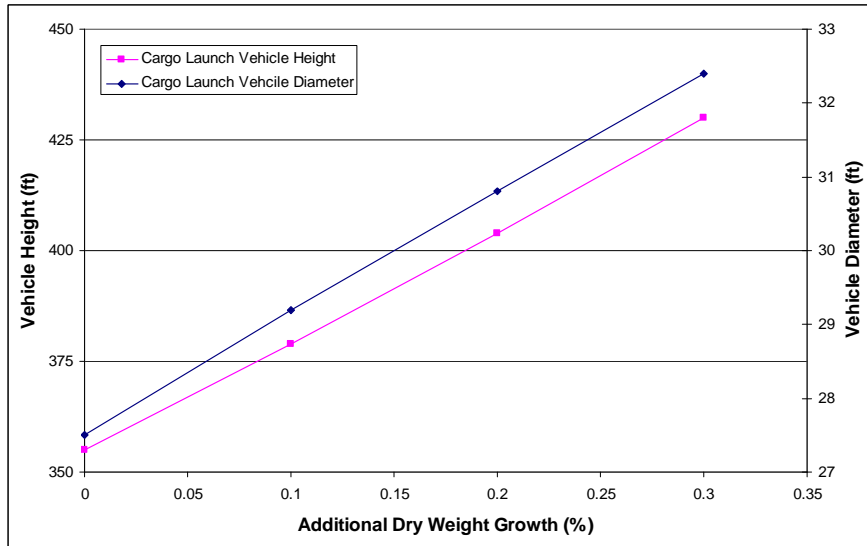


Figure 85: Increase in Cargo Launch Vehicle Dimensions as a Function of Growth

If the vehicle is unable to grow to meet the increase in system mass, then the payload capability has to decrease in order for the vehicle to reach the desired orbit. In this case a 30 percent increase in the system mass would result in a 26,000 lb decrease in the payload capability of the cargo launch vehicle. This would represent a more than 25 percent decrease in the mission payload of the CaLV. The addition of propellant refueling allows the mission payload to remain the same while the total payload capability is reduced.

This mass growth can be offset by reducing the amount of in-space propellant that must be delivered to LEO for delivering the payload to the lunar surface. In the

current configuration, approximately 75 percent of the payload that is delivered to LEO via the cargo launch vehicle is propellant. If this propellant is delivered separately, the payload requirements on the architecture can be reduced, allowing it to handle additional mass growth without increasing the size of the different vehicles. The architecture can then mitigate any mass growth by simply reducing the propellant requirements and purchasing the needed propellant from a low cost commercial operator once reaching LEO. Depending on what is meant by “low cost” determines if this solution provides a lower cost solution than redesigning the vehicle to be capable of handling the additional mass growth. In some cases a redesign may not be possible, and propellant refueling may offer the simplest or only means of handling the system mass growth. The results in Figure 86 show how the cost of refueling the architecture compares to the case where the vehicle size is increased to handle the additional mass growth. The curves represent the total savings to the lunar campaign at the given propellant price. At a propellant price of \$1,500/lb or less the cost of offloading propellant is less than the cost of growing the architecture elements. In this case it makes more sense to remove the in-space propellant, therefore reducing the requirements on the vehicle, rather than paying the additional cost associated with vehicle growth. This is a propellant price that is on the lower end of what may be achievable in the next 20 years and would be a risky decision to develop a vehicle dependent on achieving this propellant price. At a propellant price greater than \$1,500/lb, the delta campaign cost is negative indicating that the propellant refueling costs are more than the cost of increasing the size of the vehicle to handle the additional growth. While this option provides a benefit to the architecture by maintaining the initial payload capability even when the architecture experiences significant mass growth the cost are

likely to be too large to for this to be the primary reason refueling is introduced. It however is a secondary benefit that further improves the value of adding propellant refueling to the architecture. It can be added for a small additional cost as the development and operation of the propellant depot is already an aspect of the exploration architecture.

There is a problem if there is mass growth with the LSAM, as propellant refueling cannot eliminate this growth through offloading. It can help by reducing the number of maneuvers the LSAM must perform as noted previously. The real value of implementing refueling into the exploration architecture is that it allows the payload requirements to be decreased while still achieving the mission goals of the architecture. The same lunar surface payload capability can be achieved without increasing the size of the launch vehicle even though the system may undergo a mass growth of 30 percent.

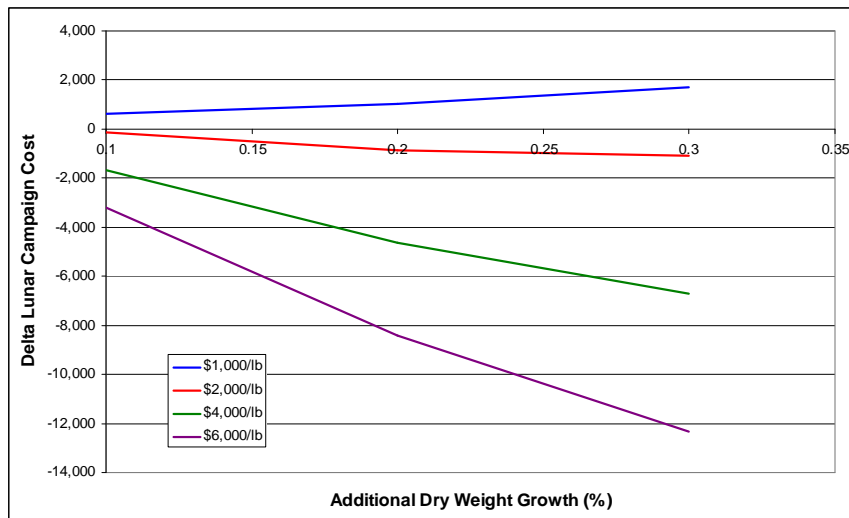


Figure 86: Cost Comparison of Propellant Offloading vs. Increase in Vehicle Size

Another example of how propellant off-loading can add value to the design of the architecture is the effect on the design of the CLV and CEV. In the baseline design, the CLV is designed to deliver the CEV and SM to LEO. Assuming mass growth on the SM, CEV and upper stage of the CLV either from requirements changes, design changes or underestimated mass during the initial design study, the CLV design may have to deliver a greater payload. In most cases, the CLV would grow in size to handle the additional requirements, but the use of a shuttle derived solid rocket booster on the first stage prevents this from happening. This system has very little design freedom and is all but fixed to its current design configuration. This makes it very difficult for the CLV to handle any increase in payload requirements. With the introduction of propellant refueling, the methane and oxygen propellant on the SM can be removed from the launch configuration and provided to the architecture once the SM and CEV reach LEO. In this case, the additional margin needed to counter the mass growth is achieved by reducing the total amount of propellant that must be delivered to LEO. The cost to the architecture would be approximately \$10 – \$20M for every 5,000 lb of propellant that was removed from the SM at a propellant price of \$2,000/lb - \$4,000/lb. This additional capability can be used to counter the mass growth or to add additional capability top the system, such as an improved reliability on the CEV.

Utilizing propellant refueling in this manner allows the launch vehicle designer to build in insurance that can be drawn upon in situation where the mass growth becomes too large or the performance targets can not be achieved. This insurance provides a level of risk reduction that can help to secure the future of the exploration program. The development of a new architecture, no matter how related it is to current or past designs,

always comes with substantial risk. This risk is both from new launch operations and from the development of new design concepts. This section has shown that the addition of propellant refueling can help mitigate these risks. Since risk mitigation is one of NASA's main concerns when conducting exploration missions, this capability provides a high degree of value to the entire program.

7.1.4 IMPROVEMENT IN ARCHITECTURE EXTENSIBILITY

The extensibility is measured by how easily an architecture can be converted from one mission to the next and much it can benefit other missions. In a perfect situation the architecture would be able to accomplish a various range of missions with a minimal increase in investment costs. In most cases this is not a practical solution, as the architecture would be over designed for it primary mission, increasing the initial development costs. Within a fixed budget, it is difficult to expend additional resources to achieve long term goals at the expense of the short term future of the program. While extensibility is an important factor in designing a long term exploration program it often gets overlooked and future missions are adapted to utilize the resources available. This section will discuss a possible means of increasing the extensibility of the architecture through the use of propellant refueling.

One possibility of building extensibility into the architecture is to develop variable components that are easily expanded as the program expands and are able to increase the capability of the architecture by simply expanding its operations. An example of this would be to use propellant refueling to provide additional propellant to the EDS once it is delivered to LEO. This would increase the performance capability of

this stage allowing it to perform a wider variety of missions. During the lunar campaign this depot could be used for any of the concepts discussed previously. The EDS and the upper stage of the CLV are enormous propulsive stages that can deliver significant payload to destinations beyond the Moon. The curves provided in Figure 87 show the payload capability of these vehicles for a range of delta-V. The requirements for a lunar, Mars and Jupiter mission have been labeled. A fully fueled EDS can provide more than 300,000 lbm of payload through Mars TMI. This could provide a significant portion of the Mars outpost in a single launch. This would also eliminate the need to development of a NTP system currently being considered for the extensibility of the baseline architecture.

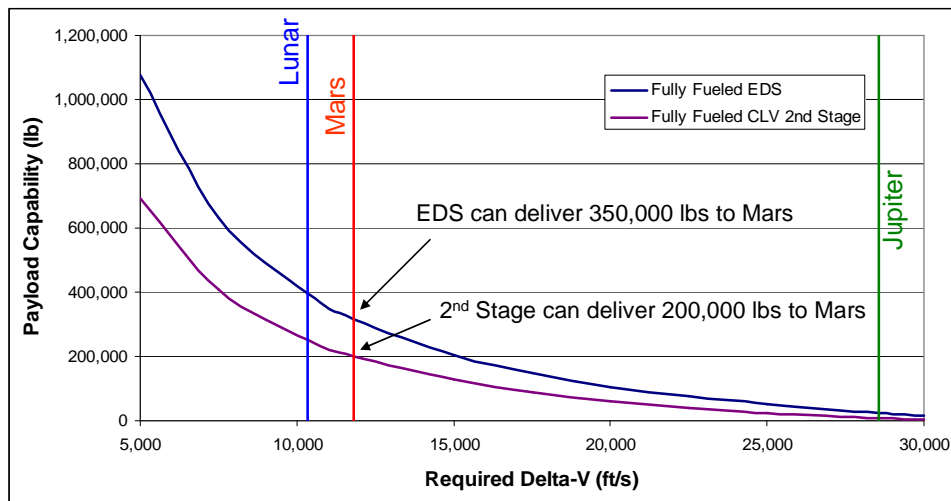


Figure 87: Max Payload Capability of ESAS Propulsive Stages

While the EDS can provide a significantly greater payload capability when fully re-fueled it slightly less efficient than the upper stage of the CLV, due to its large size, for smaller scale missions. This can be seen in Figure 88. For the same available propellant, the Upper Stage of the CLV can deliver slightly more payload capability than the

baseline EDS. The issue with the CLV Upper Stage is that it is delivered to LEO without any remaining propellant and thus requires refueling to obtain the same propellant level as the EDS, which is delivered partially full. The upper stage of the CLV is design to discarded over the ocean, this would require a change in trajectory and reduction in payload in order to design the upper stage to reach LEO. All of the EDS propellant can be used during ascent to increase the LEO payload capability. In this case the EDS would require a greater amount of propellant to deliver the same payload as the CLV Upper Stage because it has a higher inert mass. In general, the EDS is likely to be the better choice from a logistics standpoint because it is already attached to the payload assembly. The key point to take away from these two charts is the incredible payload capability that can be generated with these stages by simply providing additional propellant to LEO. The addition of propellant refueling allows these stages to be extensible to almost any conceivable exploration mission.

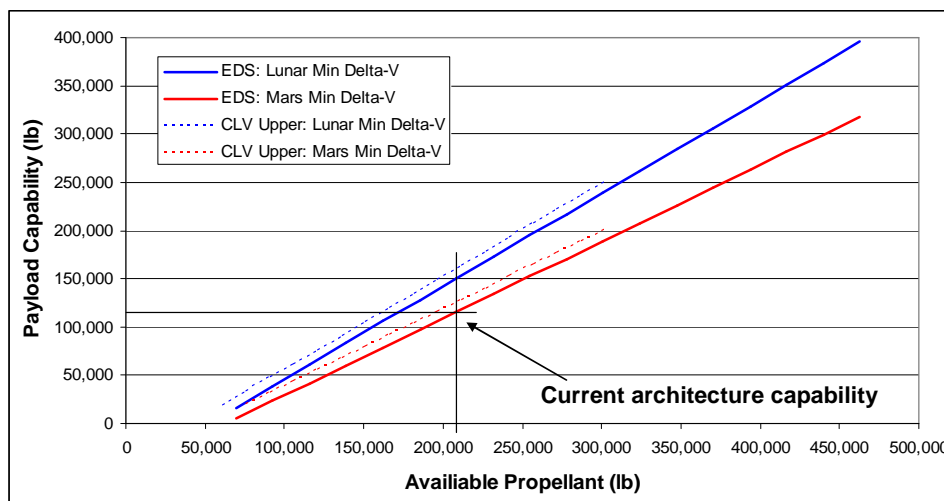


Figure 88: Payload Capability as a Function of Available Propellant

The ESAS report provided an initial concept for utilizing the exploration hardware to accomplish a Mars missions, based on Mars design reference mission 3.0 [68]. The major change to the architecture, besides an increase in the required number of launches, was the development of a nuclear thermal propulsion stage (NTP) that would be used as the in-space transfer stage. The concept of operations included the launch of six cargo launch vehicles and one crew launch vehicle. The six cargo launches are used to deliver the Mars outpost and crew living modules along with three NTP stages to LEO. The addition of the NTP stage is what allows the architecture to be extended from a lunar to a Mars mission. The extensibility of the architecture is then driven by the cost and risk associated with the development of this new propulsion system. A number of estimates have been performed to predict the development and production cost needed to produce a flight ready system. These predictions are based off of the Nuclear Engine for Rocket Vehicle Application (NERVA) program which estimated the total development cost to be on the order of \$4 to \$5B with the engine development and construction cost alone being \$2.5B [69]. The TFU was assumed to be 20 percent of the development cost (\$500M) [70] not including the lunch required to deliver the stage to LEO. This is a substantial cost to the program and requires dependency on a technology that has met heavy resistance throughout its history, severely limiting the advancement of the technology. This additional cost and risk can be avoided by utilizing the EDS instead of developing a new in-space propulsion stage that provides no additional capability to the architecture. Introducing this capability into the Mars architecture reduces the number of cargo launches from six to three and the number of NTP stages from three to zero. The reduction in the number of cargo launched is because the three NTP stages are no longer

delivered to LEO. This alone would be a savings of \$2.6B/mission, but a propellant cost must be paid that decrease this savings to around \$2.7B/mission. A breakdown of the cost used in determining these estimates is provided in Table 48. In this example the architecture elements used of the lunar campaign are used to transfer the crew and cargo to Mars (EDS) and provide the return transportation for the crew (Upper Stage of the CLV). Utilizing these stages allows the Mars architecture to be operated without relying on the development of a new advanced propulsion system. If the EDS and CLV Upper Stage can be used as the in-space propulsion stages then almost no additional costs are needed to extend the current lunar architecture to a Mars architecture. The exception to this would be the Martian lander and outpost, but these additions would be needed no matter the initial architecture selected. All other costs should be similar between the two architectures concepts and so are not included.

Table 48: Comparative Cost for Mars Mission

	Baseline	Refueling
Cargo Launch Vehicles	6 x \$379M	3 x \$379M
Crew Launch Vehicle	1 x \$500M	1 x \$500M
NTP DDT&E Costs	\$5,000M	--
NTP Stage Costs	3 x \$500M	--
Propellant	0	400,000 lb x \$2,000/lb
Total	\$4.2B/mission	\$2.4B/mission

There are a number of assumptions in the calculation presented in Table 48 that effect the difference in cost between the two mission scenarios. The most important are

the number of launches needed to deliver the Mars mission hardware to LEO and the cost of propellant to re-fuel the EDS and CLV Upper Stage. The trends presented in Figure 89 show how these two parameters affect the cost savings of switching to a Mars architecture that utilizes propellant refueling. There are two notable trends to consider in this chart. The first is that, as the number of required cargo missions increase, the greater the saving of switching to a propellant refueling architecture. This is because for each additional cargo mission required an additional NTP stage must be built and delivered to LEO. The second trend is the savings between the two scenarios is a function of the propellant delivery price. It is shown that even for a propellant delivery price of \$3,000/lb there is still a large cost savings when refueling is used. This is because the development of an advanced NTP system is removed from the Mars architecture. The savings for the refueling architecture becomes increasingly more significant as the price of propellant delivery drops because this architecture requires that a significant amount of propellant be delivered to LEO.

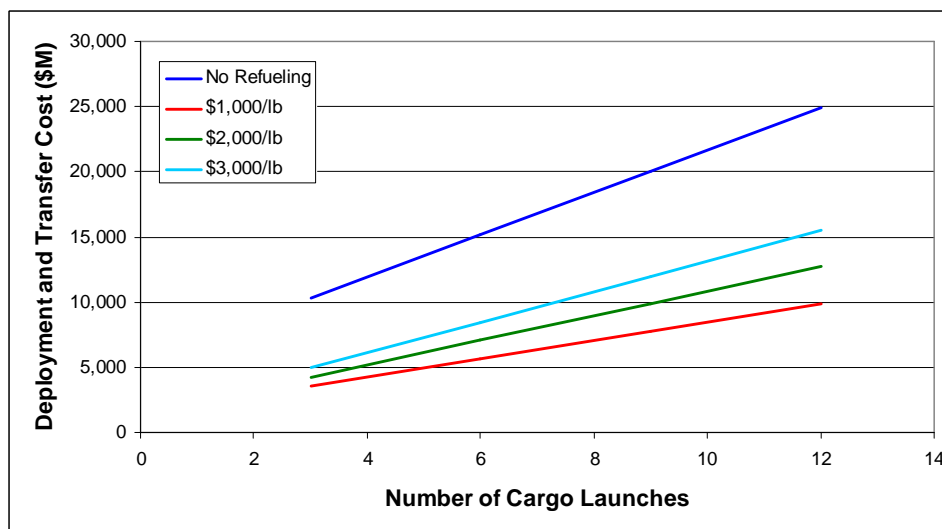


Figure 89: Increase in Mars Mission Payload Requirements [71]

These results assume that CLV Upper Stage can be used for the return maneuver. This allows the NTP stage to be completely removed from the design of the Mars missions. In order to utilize this stage the propellant required for the return journey must be stored on the stage for as long as 2-years, depending on the design of the mission. This would either require additional propellant be placed on the Upper Stage or the use of zero-boiloff cryo-coolers. Based on the information discussed in Chapter 5 and 6, the use of cryo-coolers would likely provide the lowest cost solution. This is a study not provided in this research and requires additional study. Even if this can not be achieved an NTP stage is still required there is a savings to the architecture as shown in Table 48 as the number of cargo launches is decreased. The ability to eliminate the NTP stage completely would further reduce the development cost by \$5B.

7.2 ESTIMATING THE VALUE AS THE TOTAL EFFECT ON LIFE CYCLE COST

The results presented previously in this chapter discussed the impacts of propellant refueling on each of the FOMs. Because each of these metrics utilize a different scoring system (payload, cost, reliability, risk, and extensibility), it is difficult to interpret the total value added to the architecture. An evaluation standard is needed in order to develop a consistent measure of how an improvement in each of the FOMs affects the total value of propellant refueling. This section will discuss how the life cycle cost can be used to represent the impact that propellant refueling has on each of the FOMs. This metric was selected because any impact on the FOMs can be represented by a corresponding impact on the life cycle cost of the architecture. The major drawback of propellant refueling is the additional cost to the architecture, which directly leads to an

increase in the LCC. Utilizing this metric allows both the benefits and costs of propellant refueling to be represented utilizing a single decision making criterion.

The impacts of propellant refueling have been characterized in this chapter by four main effects on the NASA exploration architecture. These include: improvements to the LEO and lunar surface payload capability, the ability to mitigate system mass growth and design changes, improving the architecture reliability by decoupling propellant boiloff from the probability of a mission success and extensibility to future exploration missions. The first three will be evaluated by their effect on the life cycle cost of the lunar campaign that was outlined at the beginning of this chapter, while the extensibility to future exploration will use the cost reduction for a single human Mars mission. The following sections will outline the total value of propellant refueling as it applies to each of these figures or merit.

7.2.1 LIFE CYCLE COST VALUE FOR MASS MITIGATION

Decreasing the amount of propellant that must be delivered to LEO by the architecture provides value to NASA by reducing the uncertainties during development. These uncertainties affect the performance of the architecture and generally lead to an increase in the mass and size of the design. It was discussed previously how the introduction of propellant refueling can help mitigate this mass growth by decreasing the amount of propellant the architecture must deliver to LEO. Using propellant refueling to minimize the mass growth effects provides value because it allows unforeseen challenges to be addressed without requiring substantial changes to the baseline design. As such, it can be considered as a design insurance policy and helps reduce both development cost and risk of the exploration program. The total value of introducing propellant refueling to

mitigate the mass growth experience by the architecture is the ability to prevent: an increase in development and production costs, an increase in the number of technologies required to achieve the new performance requirements, the ability to prevent the architecture design from becoming infeasible, and preventing a reduction in architecture objectives. These are typical design concerns in any new engineering problem, but are particularly difficult to overcome in large aerospace projects due to the increase in cost and size that can result from substantial design changes.

It is difficult to quantify the total value that this propellant refueling strategy can provide NASA. The increase in cost of the architecture elements can be determined as a function of mass growth and additional technology cost can be estimated, but quantifying the effects of development and schedule risk is not within the scope of this thesis. For the purpose of providing an estimate of the value that can be achieved when mass growth is mitigated with propellant refueling the following equation is provided (Equation 7). This does not include the value of preventing an infeasible design or maintaining the architecture objectives, both of which provide significant benefit to the program.

$$V_{\text{Mass Mitigation}} = \Delta Cost_{\text{Development}} + \Delta Cost_{\text{Production}} + Cost_{\text{Technologies}} - Cost_{\text{Propellant}} \quad (7)$$

The increase in development cost includes the additional work required to design larger architecture elements plus any additional re-design that must be performed to take into account a large vehicle design. The production costs include the increase in cost to manufacture and assemble the vehicle, and the technology costs include the development cost required to introduce a new technology into the design and achieve the required

performance levels. NAFCOM is used to calculate the change in DDT&E and TFU and a percentage increase in DDT&E is used to estimate the cost of re-design and new technology programs. Since these costs are not known, a range of 0 – 30 [72] percent was used to estimate this increase in development costs. The savings of preventing system mass growth for the CaLV and LSAM is provided in Figure 90. The initial blue bar represents the effect that an increase in DDT&E and TFU have on the cost of the lunar architecture, and the remaining bars represent the increase in development cost to account for new technologies and re-design work. The greater the mass growth and the more re-design work that is required, the greater the potential benefit of this refueling strategy.

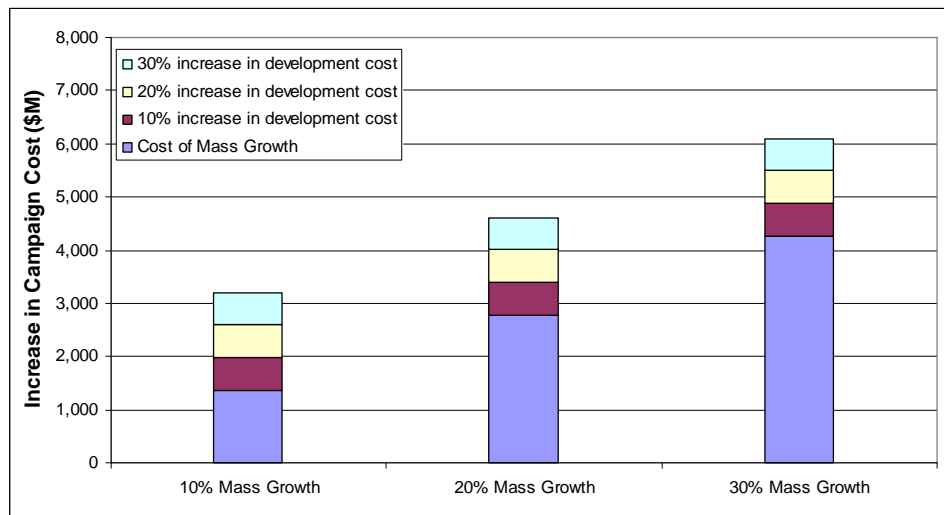


Figure 90: The Savings for Mitigating the Effects of Mass Growth

These results, however, do not include the additional cost of providing the offloaded propellant to the architecture. The additional costs of providing propellant to the architecture in LEO are provided in Figure 91. The difference between the two bars

represents the value of this refueling strategy. The required propellant delivery price is calculated by determining the mass of propellant that is required to maintain the same initial system mass for a given mass growth percent. In these results a propellant deliver price of less than \$2,000/lb is required in order to achieve a positive value for mitigating the mass growth.

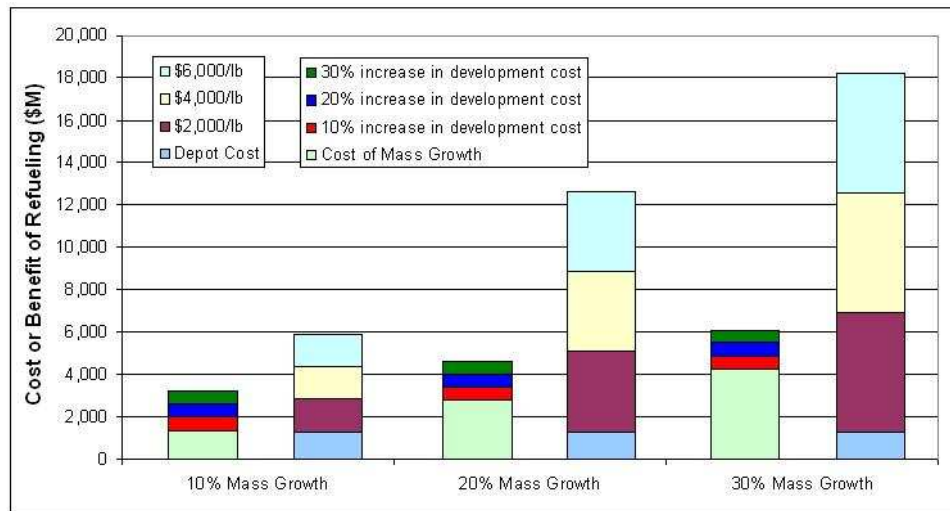


Figure 91: The Costs for Mitigating the Effects of Mass Growth

At a propellant price of \$2,000/lb, the cost of propellant and depot is more than the increase in development and production cost that would result from a 10 – 30 percent increase in system mass. This is because the marginal cost of increasing the size of the CaLV and LSAM is less than the cost of providing propellant to LEO (Figure 86). If the additional development costs are also included (re-design and technologies) than a value of 1 - \$2B can be obtained assuming a propellant price of \$2,000/lb. This represents a small initial estimate of the value and is likely within the uncertainty of this preliminary

estimation. These results suggest that there is little value in utilizing propellant refueling to mitigate architecture mass growth, as the cost of propellant is comparable to the increase in vehicle costs. The primary benefit may not be the ability to reduce the cost of the architecture elements, but rather the ability to limit the development risk to NASA.

There is a small but almost insignificant value that can be obtained by utilizing propellant refueling to mitigate mass growth that results from an increasing in vehicle size. Unless a large increase in additional development cost is experienced, the cost of providing propellant to LEO is more than the increase in the total architecture cost. The true value is not to limit the increase in vehicle cost, but rather to decrease the risk in developing a new complex system. Utilizing propellant refueling to limit the impact that design uncertainty has on the development process potentially provides a greater level of value. This can prevent substantial schedule slip due to additional design and re-design work, and can prevent the design from becoming infeasible or not being able to meet program level requirements. A gap between design capability and program requirements generally leads to the addition of new technologies which increase program cost and risk. If new technologies can not achieve the required increase in performance than a reduction in program requirements may be required. Offloading propellant can eliminate this gap without relying on new technologies and without decreasing the capability of the design. Eliminating this development risk is difficult to quantify, but it provides a high level of value to NASA as it reduces the likelihood that large design changes are needed through the development process.

7.2.2 LIFE CYCLE COST VALUE FOR REFUELING PROPELLANT LOST TO BOILOFF

The second major source of value is related to the dependency of the architecture on the LEO propellant boiloff, and how it affects two major FOMs. The first is an increase in payload capability both to LEO and to the lunar surface, and the second is an improvement in the Loss of Mission (LOM) of the architecture. These architecture improvements have been discussed in great detail, in Chapters 5, 6 and 7. It was shown previously in this chapter how an increase in payload capability can provide value to NASA by lowering the cost and reducing the length of the lunar campaign (section 7.1.2), but how is an improvement in LOM quantified in terms of a total cost or savings to the architecture. The cost of a LOM to NASA includes: the money and time spent on deployed hardware, effects of delays on the exploration program, re-design work needed to prevent future failures, and other political and social factors associated with losing a multi-billion dollar mission. Assuming that a LOM is due to propellant boiloff and not a catastrophic design failure, then the additional re-design work and schedule slip is small. The total cost to the program can then be approximated as the cost of the hardware that was deployed and not salvageable for future missions. This would include the cost of the CaLV and LSAM which are deployed prior to the launch of the crew. The value to NASA is the total cost saved by eliminating this LOM scenario multiplied by the number of times it will occur over the course of the campaign, minus the cost of providing the propellant to the architecture. This is depicted in Equation 8. The probability of a LOM as a function of the designed LEO stay time was provided in Figure 82.

$$V_{\text{Refueling Boiloff}} = C_{\text{hardware}} \times P_{\text{LOM}} - C_{\text{Propellant Refueling}} \quad (8)$$

A summary of this value as a function of the designed LEO loiter period and the launch separation time is provided in Figure 92. It is evident in this chart that the greater the launch separation time, the more value propellant refueling offers NASA. This is because the longer the separation time, the more likely an event will occur that will prevent the launch of the crew from occurring on schedule. In this case, implementing propellant refueling for a mission with a seven day separation has a seven times greater value than for a mission designed with only a 90 minute separation. It also must be noted that if the order of the launch is switched so that the crew are delivered before the cargo then the value of refueling the architecture is greatly reduced. It still has a payload benefit, but no longer a LCC savings. There is also a decrease in the value for missions designed to remain in LEO for longer periods of time. The probability of losing a mission becomes less likely as the LEO stay time increases because more time is available to resolve the issue which caused the delay. Thus the mission could continue within the allowable time. These results do not consider the value gained by increasing the payload capability or decreasing the size of the vehicle due to the reduced mass of propellant that must be carried to LEO, but these have been outlined separately. This would further increase the value for missions with a longer LEO stay time. It is also evident that value is not always provided when utilizing propellant refueling in this manner. In the cases where short separation times and long LEO stay times were considered, a negative value is seen because the costs to the program are greater than the potential benefits.

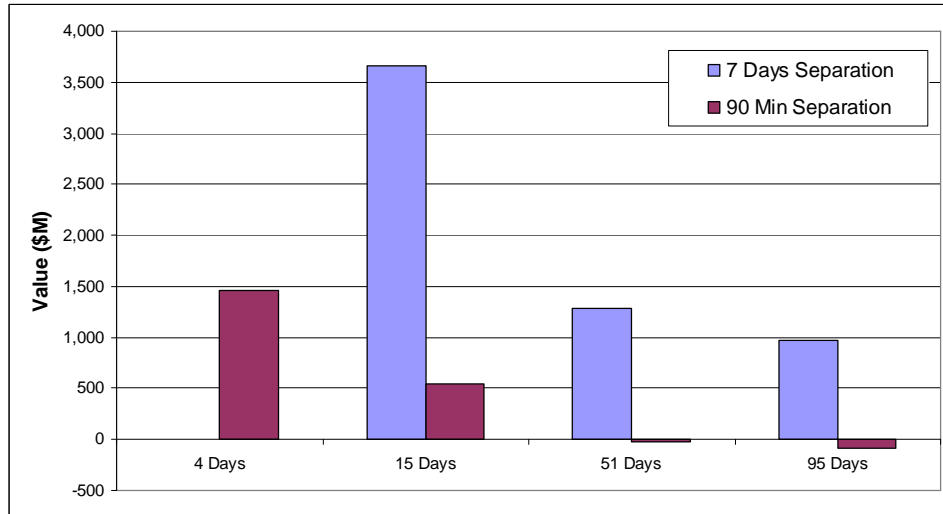


Figure 92: Value of Eliminating the LEO Boiloff LOM Scenario

7.2.3 LIFE CYCLE COST VALUE FOR AN INCREASE IN PAYLOAD CAPABILITY

The total savings achieved through an increase in payload capability was discussed in detail in Section 7.1.2; it improved the deployment of the lunar outpost and the operation of the extended stay missions. The total value, however, includes the cost savings to the lunar campaign, the reduction in campaign time, possible increase in the science capability per mission, a greater payload capability to achieve extensibility to future missions, and risk mitigation through an increase in allowable design margins. The value obtained through an increase in the payload capability extends throughout the design of the entire architecture. The value of the risk mitigation and extensibility are discussed separately as they address a particular design FOM. The value of reducing the length of the campaign enables NASA to either increase the number of missions it can complete within the current schedule or to reduce the time frame before human Mars missions can begin. The ability to increase the science output during the extended lunar

missions also provides value but to a less extent than a reduction in the life cycle cost, because it does not address a particular FOM. A qualitative discussion of the impact that these have on the architecture is provided in Section 1.3. The result of these simplifications is that the total value of an increase in payload capability can be closely approximated as the total savings to the architecture by decreasing the number of missions needed to complete the lunar campaign. A summary of these results is provided in Figure 93. In this case, the total value is represented by the difference between the benefits and costs of implementing propellant refueling. The colored bands correspond to an increase in cost as the price of propellant increases. An increase in propellant price represents a small increase in the total cost and therefore has a small impact on the value. These results again show that an improvement in payload capability always provides value to NASA. It would require a substantial increase in the development cost and the price of propellant in order for these benefits to be erased. These results also show that allowing the EDS to perform the LOI maneuver provides the greatest value since this option provides the greatest improvement in payload without significantly increasing the propellant requirements over the other options.

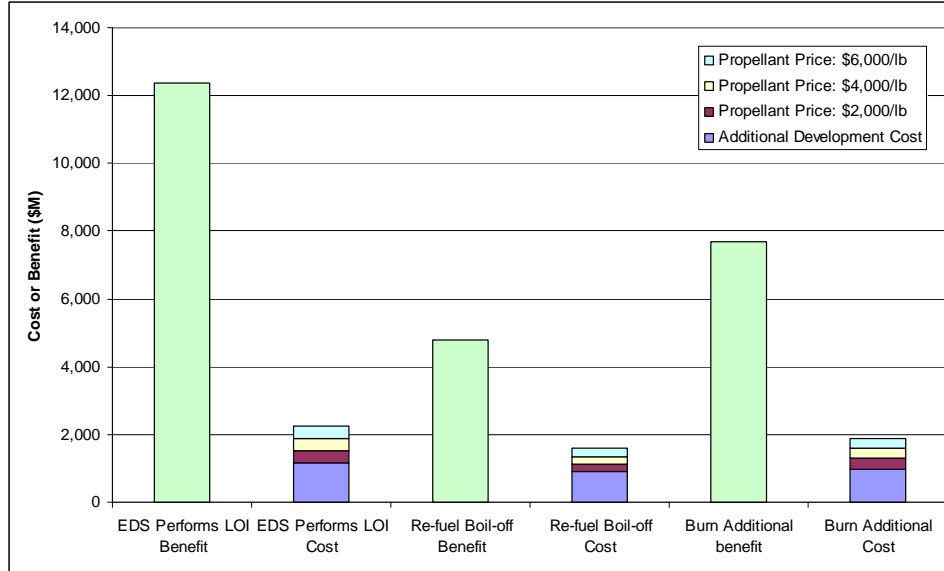


Figure 93: Value of Increasing the Payload Capability of the Architecture

7.2.4 LIFE CYCLE COST VALUE FOR INCREASING EXTENSIBILITY

The introduction of propellant refueling can also provide considerable value to missions designed to go beyond the Moon, specifically a human Mars mission. The biggest change from the lunar campaign to a Mars mission is the quantity of cargo that must be delivered to LEO. The total payload that must be delivered to LEO for Mars DRM 3.0 is in excess of 440,000 lbm of mission payload, plus three 150,000 lb Nuclear Thermal Propulsion (NTP) stages [71]. This totals almost one million pounds of payload that must be delivered to LEO before each Mars mission. The use of propellant refueling can improve these large cargo missions by increasing the amount of payload that can be delivered to LEO on the cargo launch vehicle, and by providing an alternative in-space transfer vehicle. The value is a reduction in the number of launches needed to complete the mission, and thus a large reduction in the total cost of a Mars campaign. The major

issue is that a considerably larger amount of propellant is needed than for the lunar campaign, though the risks would be less assuming the capability had been fully demonstrated during the lunar campaign. The cost versus benefit for introducing propellant refueling for a set of Mars missions is provided in Figure 94. The details for the cost estimation used in this analysis were presented in Section 7.1.4. The value can be interpreted as the difference between the “No Refueling” curve and the three propellant price curves. The benefit is a summation of the savings achieved through a decrease in the number of launches, and the cost is the propellant required to re-fuel each mission plus the development of a larger LEO propellant depot.. The large depot will also have to be delivered to LEO, but would likely require multiple launches as the size of a single propellant depot would be too large to deploy in a single Ares V launch. The number of launches refers to the number of cargo launches required to complete a Mars single mission. The reference mission considered during ESAS called for three cargo missions. The increase in the number of launches represents a growth in the Mars campaign requirements or additional Mars missions. These results show that the value to the Mars architecture increases as the number of cargo launches increases, because a greater number of NTP stages can be replaced with a re-fueled EDS, saving both the launch and production costs of this engine, but the biggest savings is the elimination of the development of the NTP system.

Even with the large quantity of propellant needed to perform the trans-Mars injection maneuver, the cost of propellant is less than the cost of building and delivering a NTP stage to LEO. The total savings of replacing the NTP system with propellant for the EDS is small on a per mission basis, but as the number of required cargo missions

increases, the use of the EDS as the Mars transfer vehicle has the potential to provide a significant value to NASA. An additional benefit is that the development of a NTP system is no longer required for Mars missions, which could save an additional \$5B [69] in development costs. Eliminating the NTP completely from the Mars architecture requires that an additional EDS or CLV Upper Stage be used for the return segment of the Mars mission. This increases the amount of propellant required, but reduces the total cost of the missions. These results show that the use of propellant refueling could provide value to a Mars mission by simply replacing the NTP stage with the already deployed EDS. These results are also not very dependent on the cost of each cargo launch as the majority of the savings comes from the ability to eliminate the need to develop the NTP stage.

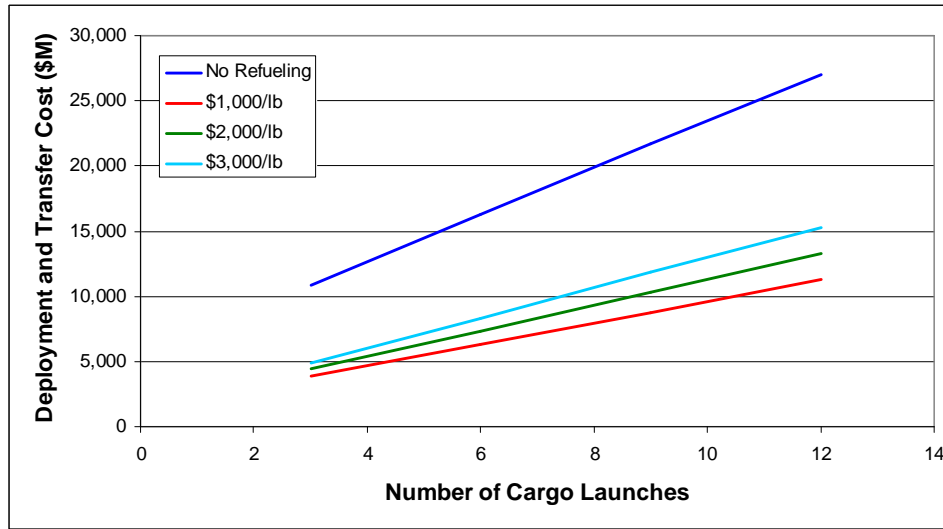


Figure 94: Value to Extending the Architecture to a Mars Mission

A summary of the total value that propellant refueling can provide NASA is provided in Figure 95. This figure illustrates the overall effect of implementing the “best”

refueling strategies into the exploration architecture, under the assumptions in this work. These refueling strategies can help simplify the development of the architecture elements, reduce the effect of program level requirements, and improve the concept of operation on both the lunar and Mars exploration missions.

It is evident that the greatest value to the architecture is the ability to increase the payload capability because it can achieve the greatest benefit by increasing the flexibility of the architecture. In Section 7.1.2 it was shown that this increase in flexibility can decrease the length of the lunar campaign resulting in a decrease in LCC of \$2.6B to \$13B depending on the assumption for the price of propellant and the fixed versus variable cost. By contrast, the use of propellant refueling to help mitigate mass growth has a large cost associated with it because of the amount of propellant that must be provided for each mission. There is still a small benefit to LCC that can be achieved, though generally less than \$500M and only for a lower propellant price and high increase in mass growth. The primary value of this method is the ability to reduce the development risk of the architecture. This method can provide a secondary benefit of introducing propellant refueling to the architecture. Propellant refueling can also help lower the LCC of Mars missions by reducing the number of cargo launches. The total value is dependent on the number of cargo missions and the decrease in savings by eliminating the NTP stage ($\$3.5B + \$1.8B \times \text{Missions}$). These results assume that each of these changes is implemented separately, but all of these options are capable of simultaneously being applied to the architecture. In fact, any number of propellant refueling strategies can be implemented together. This would help further increase the value as the development cost would only need to be accounted for once. The Pareto

frontiers discussed in Chapters 5 and 6 provided evidence that the best propellant refueling strategies utilize a number of propellant refueling techniques to combine the benefits they provide to the architecture. The following section will outline the final value proposition that propellant refueling offers NASA’s exploration program.

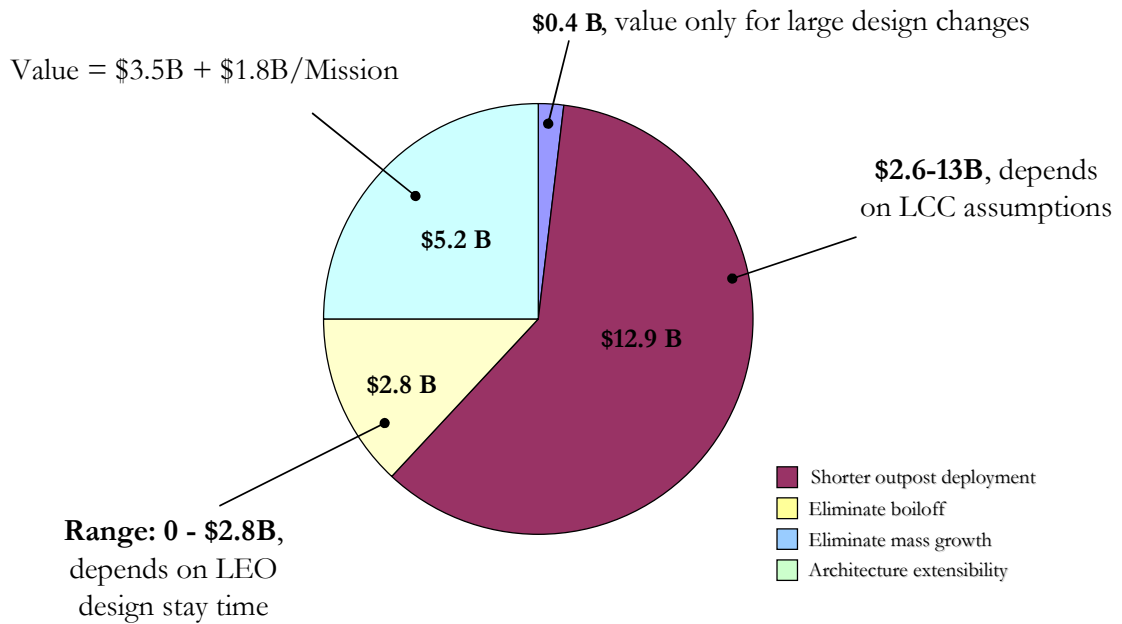


Figure 95: Total Value of Propellant Refueling

7.3 THE VALUE PROPOSITION OF PROPELLANT REFUELING FOR NASA

The work presented in Chapters 5, 6, and the first half of Chapter 7 outlined the effects that various propellant refueling methods have on the baseline architecture. The goals of this thesis are to develop the value proposition of propellant refueling. This requires that the work presented thus far (the characterization of how propellant refueling effects on the baseline architecture) be translated into a set of statements that outline the specific improvements made to the baseline architecture. These statements should

convince NASA of the potential improvements to the baseline architecture that can be achieved by implementing propellant refueling. The value proposition is broken down into five categories that summarize the work presented in this thesis. The categories include: an increase in the LEO payload capability, an increase in the lunar surface payload capability, decoupling the mission reliability from the cryogenic propellant boiloff, increasing the functionality of the EDS, decreasing the size of the architecture elements, and enabling the development of a reusable launch vehicle market.

7.3.1 INCREASED LOW EARTH ORBIT PAYLOAD CAPABILITY

The results presented previously in this thesis discuss three potential means of increasing the LEO payload capability. These options include: eliminating the need to carry additional propellant to LEO to account for boiloff, increasing the EDS propellant used during ascent, and offloading the EDS or LSAM propellant prior to liftoff. The value of increasing the payload that the architecture can deliver to LEO can be broken down into three components. This includes an increase in the lunar surface payload capability, the ability to mitigate mass growth without limiting the capability or changing the design of the architecture elements, and providing a greater capability for high mass exploration missions. The increase in lunar surface payload capability is a direct result of a greater mission payload being delivered to LEO. The additional capability can be used to increase the size of the LSAM, and the payload that can be delivered to the lunar surface. The size of the LSAM is limited by the capability of the CaLV. The addition of propellant refueling can provide a means to improve this capability, thus resulting in a greater lunar surface payload.

One of the most significant improvements that propellant refueling can offer is the ability to mitigate the effect of mass growth on the development of the exploration architecture. The concern with mass growth is that it reduces the capability of the architecture and often results in the design of the architecture temporarily becoming infeasible. In a traditional design problem, an unexpected increase in system mass would result in a number of required design changes. These can include changes to the architecture elements or changes to the requirements placed on the architecture. Design changes to the individual elements lead to an increase in the development cost and often a delay in the program schedule. These can both be particularly detrimental if large technology development programs are required. The other option is to reduce the requirements on the architecture, which will help to eliminate the effect of mass growth. It will also, however, reduce the original objectives of the architecture. The introduction of propellant refueling can increase the amount of payload that can be delivered to LEO without significantly changing the design of the baseline architecture elements. Increasing the payload capability above the baseline requirements provides a payload margin that can be used to account for an increase in system mass. This provides a single solution to mitigate any mass growth that occurs during the development process instead of introducing a number of new technology programs to reduce the mass and improve the capability of the architecture.

The third portion of the value is the ability to improve the capability of future exploration missions by providing a larger LEO payload. Future exploration missions will require a larger payload capability than is required for lunar missions. The ESAS study provided an initial Mars architecture that would require more than one million

pounds of payload to be delivered to Mars before a human mission could be conducted. The ability to provide a greater LEO payload would increase the extensibility of the current architecture, allowing it to better adapt to the needs of future missions. The main result is a reduction in the number of launches required to deliver the exploration payload. This would lead to a reduction in the cost of each mission, and potentially provide a more sustainable architecture.

7.3.2 INCREASED LUNAR SURFACE PAYLOAD CAPABILITY

Throughout this thesis, the discussion has focused on the ability of the propellant refueling to increase the payload delivered to the lunar surface. The results showed that increasing the LEO payload and increasing the functionality of the EDS can result in a greater payload delivered to the lunar surface. The value of increasing the payload capability can be categorized by three potential impacts on the lunar campaign. The improvements include: increasing the capability of each lunar mission (science, length, coverage, etc.), providing alternative solutions to deploy the lunar outpost infrastructure, and offering an additional means to mitigate system mass growth on the LSAM.

Increasing the payload capability that the LSAM can deliver to the lunar surface can increase the number of scientific objectives that are achieved during each lunar mission. A greater payload mass can allow more instrumentation to be used during each mission. This improvement in scientific equipment can provide either a more in-depth analysis or a greater variety of instruments to help understand the lunar environment and better prepare humans for future exploration missions. A greater payload mass can also allow longer lunar missions, especially in the case of the seven day sortie mission. The

length of the sortie mission is limited by the capability of the LSAM and does not utilize any pre-deployed outpost infrastructure. A larger payload capability can increase the capability of the life support systems, allowing the crew to remain on the lunar surface for longer periods. Increasing the length of the sortie missions would allow a greater amount of science to be completed during each mission and potentially reduce the number of mission required to achieve the scientific objectives of the architecture. This could reduce the cost of the lunar campaign because doubling the science completed during each mission requires a lower cost than conducting two lunar missions. A number of other potential improvements to the scientific capability of the architecture can be achieved by increasing the mass that the LSAM can deliver to the lunar surface. The value of this capability can be summarized by the ability to increase the scientific objectives obtained during each lunar mission, allowing NASA to increase its return on the large investment made to develop the exploration architecture.

The analysis in Section 6.1.2 discussed how the LCC of the lunar campaign could be reduced by decreasing the number of missions required to deploy and operate the lunar outpost. One potential outpost manifest, assuming the current architecture capability, requires nine missions to fully deploy the infrastructure needed to begin operating the lunar outpost. Utilizing propellant refueling to increase the payload capability to the lunar surface can potentially reduce the number of missions needed to deploy the lunar outpost to less than four missions. This can save the lunar campaign billions of dollars by eliminating more than half of the outpost deployment missions, which can be done without affecting the scientific missions that begin once the outpost is fully deployed. Considering that budgetary concerns are one of the main limiting factors in conducting

exploration missions, this reduction in cost can provide substantial value to NASA. Another potential improvement, depending on the lunar surface payload capability, is the ability to deliver the crew and cargo needed for each lunar outpost mission in a single launch. The current capability requires that two missions be conducted, the first to deploy a PLM to the outpost and the second to deliver the crew. Utilizing the EDS for the LOI maneuver increases the lunar surface payload capability such that, from mass standpoint, both the crew and cargo can be delivered in a single mission. This would save the architecture the cost of a CaLV and LASM for each outpost mission, further reducing the cost of the lunar campaign. A complete description of these results can be found in Section 6.1.2. The value is summarized as the potential to decrease the cost of the lunar outpost missions by utilizing an increase in lunar surface payload capability to reduce the number of required missions, or by increasing the number of missions that can be conducted over the same time period.

The final impact that a greater lunar surface payload can have on the lunar architecture is to provide another potential means of mitigating mass growth on the CaLV and LSAM. The previous section discussed how mass growth could be mitigated by reducing the amount of propellant that the CaLV delivered to LEO, while keeping the mission payload constant. The mission payload mass is the mass of the LSAM plus the lunar surface payload. It was shown in Section 6.1.1 that propellant refueling can be used to decrease the mass of the LSAM while increasing the lunar surface payload. This allows the mission payload to remain constant while increasing the lunar surface payload. If the mass of the LSAM increases, the lunar surface payload can be decreased without increasing the mission payload the CaLV must deliver to LEO. The additional payload

capability achieved by utilizing propellant refueling provides the architecture with an additional payload margin. This margin can be used to allow an increase in LSAM mass without reducing the original payload requirements of the architecture. In most cases, the mass growth can be mitigated while still achieving a greater lunar surface payload. The value is the ability to accommodate mass growth on the LSAM without increasing the requirements on the CaLV or reducing the lunar surface capability. Without this payload margin, the decision maker would have to reduce the requirements on the LSAM or accept additional growth on the CaLV.

7.3.3 DECOUPLING MISSION RELIABILITY FROM PROPELLANT BOILOFF

One of the major benefits of propellant refueling discovered in this thesis is the ability to replace the propellant lost to boiloff while the EDS and LSAM loiter in LEO. The introduction of this strategy has been shown to provide a greater payload capability and to achieve improved mission reliability. The value of an increase in payload capability was discussed in the two previous sections. This section will outline the value of decoupling the success of each mission from the amount of propellant lost to boll-off.

In the baseline architecture, the crew and cargo are delivered to LEO separately. The EDS and LSAM are designed to be delivered seven days prior to the crew. Based on previous launch systems, it is likely that the CLV will experience a delay that could prevent it from launching on time. The EDS and LSAM are designed to carry additional propellant to account for the boiloff that occurs during this delay. These vehicles may be required to carry enough additional propellant to account for somewhere between fifteen and ninety five days of propellant boiloff. If the CLV is delayed beyond this period, then

the EDS and LSAM will not have sufficient propellant to perform the remaining mission maneuvers. The result in the EDS and LSAM being discarded, and an additional launch is then required to deploy a new set of vehicles. This is a significant increase in cost to the architecture. The introduction of propellant refueling eliminates the dependence of the architecture on the amount of boiloff. The EDS and LSAM are now launched to LEO without any additional propellant, and the propellant lost to boiloff is replaced once the crew is delivered to LEO. In this case, the CLV can be delayed for any period of time and the EDS and LSAM still have sufficient propellant to complete the remaining mission maneuvers. The value to NASA is that the cargo elements of the architecture (EDS and LSAM) are never lost because of a delay in launching the CLV. This has both economic and political value because discarding billion dollar hardware elements would appear to be an insufficient use of public resources.

7.3.4 INCREASING THE FUNCTIONALITY OF THE EARTH DEPARTURE STAGE

The EDS is designed to function as both the 2nd stage of the CaLV and as the in-space transfer stage between Earth and the Moon. This provides the EDS with the capability to hold 500,000 lbm of usable propellant. This stage, once re-fueled, has the potential to provide a very large propulsive maneuver that can be used to transfer large payloads for various exploration missions. It was discussed previously that the EDS can be used to provide the LOI and TLI maneuvers, resulting in an increase in the lunar surface payload capability. It is unlikely that the full potential of the EDS could be used for lunar missions because high mass payloads are not needed. The payload capability for Mars missions, however, is much higher and will require a significant propulsive stage to

meet the estimated demand. The baseline Mars mission requires the development of a new Nuclear Thermal Propulsion (NTP) system to transfer cargo between the Earth and Mars. This new system would require an initial investment between \$4B and \$5B to develop a flight-ready vehicle [69], plus the additional cost to produce and launch the stage to LEO. Utilizing the EDS would require no additional development, production, or launch costs since the EDS is already utilized to deliver the Mars cargo to LEO. The EDS would only need to be re-fueled with sufficient propellant to complete the trans-Martian injection (TMI) maneuver. The baseline Mars mission requires six cargo launches: three to deploy the cargo elements and three to deliver the NTP stages required to transfer the cargo to Mars. The value offered by increasing the functionality of the EDS is the ability to eliminate the development of the NTP system, as well as, a reduction in launch cost because the transfer stage is deployed along with the cargo elements and does not require a separate launch.

7.3.5 DECREASING THE SIZE OF THE ARCHITECTURE ELEMENTS

The work in this thesis has primarily focused on the value of utilizing propellant refueling to improve the payload capability of the architecture. The results in Chapter 6, however, showed how the architecture could be improved by utilizing propellant refueling to directly reduce the LCC by decreasing the size of the architecture elements. This can be accomplished by reducing the amount of propellant delivered to LEO. While this work has primarily focused on the CaLV, reducing the propellant delivered by the CLV can also lower the cost of the architecture. The drawback of this solution is that a reduction in LCC comes at the cost of future extensibility because the LEO payload capability is reduced.

The ability to decrease the size of the architecture elements can offer a number of improvements, and therefore value, to the design of the exploration architecture. The most notable improvement is the ability to decrease the development and production cost of the architecture elements. Chapter 6 discussed how a significant cost savings can be achieved by decreasing the size of the LSAM.

7.3.6 SUMMARY OF NASA VALUE PROPOSITION

Table 49: Summary of Propellant Refueling Value

Effect on Architecture	Value to NASA
Greater LEO payload	<ul style="list-style-type: none"> ○ Provide a greater lunar surface payload ○ Mitigate against potential mass growth during architecture development ○ Provide a greater payload for future exploration missions
Greater lunar surface payload	<ul style="list-style-type: none"> ○ Increase scientific capability for each lunar mission ○ Enable alternative deployment strategies that can reduce cost and length of the lunar campaign ○ Mitigate against potential mass growth during architecture development
Increase mission success	<ul style="list-style-type: none"> ○ Eliminate any missions being lost because the CLV is delayed beyond the design LEO loiter time ○ Remove dependence of the architecture on the propellant boiloff
Increase functionality of EDS	<ul style="list-style-type: none"> ○ Eliminate the need to develop a new NTP system ○ Decrease the number of launches requires for exploration missions ○ Increase usability of current hardware.
Decrease size of vehicles	<ul style="list-style-type: none"> ○ Decrease size and cost of architecture elements ○ Reduce physical constraints on launch vehicles

CHAPTER 8

CONCLUSIONS AND FUTURE WORK

The goal of this research was to develop a thorough understanding of how propellant refueling would impact NASA baseline exploration architecture, providing a more in-depth analysis than is available in the current literature. This goal has been accomplished by developing a parametric architecture model that can be used to evaluate the changes in the architecture FOMs when various propellant refueling strategies are added to the baseline design. A number of refueling strategies have been identified that show an improvement to each FOM, while other strategies have been shown to adversely affect one or more of the FOMs. It was also shown that many propellant refueling strategies have a larger impact on the architecture than other design variables considered (thermal mitigation, LSAM ascent engine, and LEO loiter period). A value proposition was finally presented to summarize why an architecture that utilized propellant refueling was better equipped to meet the goals of the Vision for Space Exploration than the current baseline design. The following will outline the original goals of this thesis and describe how they were accomplished during this work.

8.1 GOALS OF THE DISSERTATION

The objectives of this research were specified in three different goals set out in Section 1.3. These goals are restated below:

- *Goal 1: Develop a lunar architecture model capable of evaluating various propellant refueling techniques.*

This goal was established to provide a foundation for analyzing the effect of propellant refueling on the exploration architecture. During the literature review, it was found that a detailed analysis of propellant refueling had not been performed. Most of the previous work on propellant refueling had been limited to single architecture designs or relied solely on a qualitative discussion. This model provides a means to evaluate a large number of propellant refueling strategies and measure the effects on the design of the entire architecture. While this model specifically focuses on the CaLV and LSAM, it can easily be expanded to include the remaining architecture elements.

A detailed discussion of this model was provided in Chapter 4. This model was developed using the ModelCenter[®] design framework to simplify the integration of the analysis modules and to provide an automated process for evaluating a large number of trade studies. This framework is provided in Figure 96. Any propellant refueling strategy can be selected, and the parameters passed into this simulation environment. The impact on the architecture elements is first determined, and then the FOM can be evaluated and compared against the baseline design. This allows the decision maker to understand how different refueling strategies impact the exploration architecture, and thus which of these strategies provides the greater level of value to NASA.

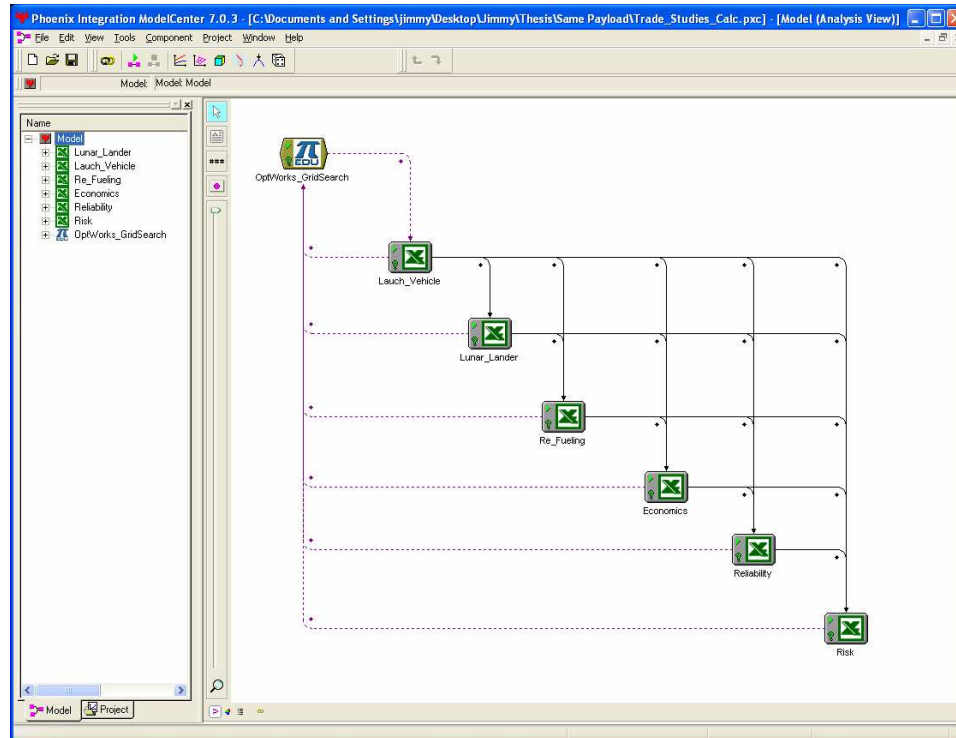


Figure 96: Propellant Refueling Design Space Simulation Environment

- *Goal 2: Explore and understand the effects that propellant refueling have on NASA’s baseline exploration architecture.*

This goal was accomplished by developing a set of design variables that could be used to investigate the impact of a wide variety of propellant refueling strategies on the exploration architecture. These design variables provided the basis for the different refueling strategies that were considered in this thesis. The impact of each was measured against the baseline design and the relative impact of each was compared against the other potential refueling strategies. A Morphological Matrix was used to illustrate these design variables and the respective ranges used in this work. The Morphological Matrices for Scenarios One and Two are provided in Figures 97 and 98.

Additional Ascent Propellant	0	25,000 lbs	50,000 lbs	75,000 lbs	100,000 lbs
EDS Boil-off Mitigation	MLI	MLI+Cryo			
Lander Stage Re-fueled	None	Descent	Ascent	Both	
Lander Propellant	50%	100%			
LSAM Ascent Propellant	LOX/CH4	Hypergols	LOX/LH2 (pressure)	LOX/LH2 (pump)	
Lander Boil-off Mitigation	MLI	MLI+Cryo			
LOI Burn Element	EDS	LSAM DS			
LEO Required Stay Time	95 Days	15 Days			
Re-fuel Boil-off	No	Yes			

Figure 97: Trade Study Morphological Matrix, Scenario One

Offload TLI propellant (LOX)	0	25,000 lbs	50,000 lbs	75,000 lbs	
Offload TLI propellant (LH2)	0	5,000 lbs	10,000 lbs	15,000 lbs	
EDS Boil-off Mitigation	MLI	MLI+Cryo			
Lander Stage Re-fueled	None	Descent	Ascent	Both	
Lander Propellant	50%	100%			
LSAM Ascent Propellant	LOX/CH4	Hypergols	LOX/LH2 (pressure)	LOX/LH2 (pump)	
Lander Boil-off Mitigation	MLI	MLI+Cryo			
LOI Burn Element	EDS	LSAM DS			
LEO Required Stay Time	95 Days	15 Days			
Re-fuel Boil-off	No	Yes			

Figure 98: Trade Study Morphological Matrix, Scenario Two

Five of the design variables directly investigated a particular propellant refueling strategy, and four additional design variables are parameters that could also be affected by the introduction of propellant refueling. The inclusion of both categories of design variables showed the relative impact of propellant refueling compared to other design variables important to the design of the architecture. The propellant refueling design variables were shown to have the largest impact on the architecture FOMs. One of the primary results missing from the propellant refueling literature is a comparison of various refueling strategies with respect to a common architecture design. Having this information would allow a decision maker to understand which refueling strategy could be used to improve a particular FOM and which would help provide the greatest improvement to the design of exploration architecture.

- ***Goal 3: Determine the costs and benefits of adding propellant refueling to the lunar architecture and determine what approach has the greatest effect on the over all design of the architecture.***

The final goal was to utilize the design space and simulation environment developed for Goals 1 and 2 to determine if propellant refueling could improve the baseline lunar architecture. It was also of interest to determine which refueling strategies provided the greatest value to NASA. This was accomplished in two phases. The first was to determine which refueling strategies had the greatest impact on the baseline design. This was achieved by developing a Pareto frontier for LCC and payload capability for both Scenarios One and Two. The LCC and payload capability were the

only two metrics initially considered because the reliability, risk, and extensibility metrics were addressed later as a part of the overall value proposition. The conclusion from the Pareto frontier analysis provided three attractive refueling strategies for Scenario One and two for Scenario Two. These strategies are provided in Table 50.

Table 50: Summary of Preferred Refueling Strategies

Best Strategies	Scenario One	Scenario Two
Re-fuel propellant lost to boiloff	Yes	Yes
Utilize EDS for LOI maneuver	Yes	Yes
Reduce propellant delivered to LEO	Yes	No

The second phase was to determine the value provided by these preferred refueling strategies, measured by their impact on the architecture FOMs. In the case of the LCC, it was shown that two separate effects could improve this metric. An improvement in the lunar surface payload capability was shown to have the potential to reduce the cost of the lunar campaign by reducing the number of missions required to deploy the lunar outpost, and perform the six-month extended stay missions. It was also discussed how the LCC could be reduced by eliminating the dependence of the architecture on the amount of propellant lost to boiloff.

The introduction of propellant refueling can also provide an increase in the LEO and lunar surface payload capability. This increase in payload capability can directly lead to an improvement in the effectiveness of the exploration architecture. The increase in

effectiveness is a result of the ability to perform a wider range of lunar missions. This stems from the ability to use the increase in payload to perform a greater level of science during each mission and to reduce the number of mission required to achieve the objectives of the lunar campaign. The increase in payload capability is also the primary means used to improve the other architecture FOMs. An increase in flexibility provides the architecture with a greater design freedom that allows overall design changes to be made that were not possible with the baseline architecture design.

The reliability of the architecture can also be improved because propellant refueling can be used to decrease the chance that a mission will be lost, although the architecture becomes dependent on achieving a successful propellant transfer. This improvement in reliability is achieved by utilizing propellant refueling to replace the propellant lost to boiloff, and thus eliminating this LOM scenario. Introducing any refueling strategy does impact the reliability of the architecture, but as shown in Section 7.1.3, an overall improvement in reliability can be obtained.

The introduction of propellant refueling has been shown to decrease the development risk associated with the NASA exploration program. This is achieved by providing a means to mitigate unexpected design issues, such as mass growth, without requiring substantial design changes. The current architecture has experienced a number of design changes, especially with the Ares V, that have lead to the addition of a number of advanced technologies. The inclusion of propellant refueling would eliminate the need for a number of these design changes, as well as reduce the need for new technologies to be added to the design of the architecture. There is a level of risk involved with maturing the technologies required for propellant refueling (fluid transfer, long term propellant

storage, and automated docking systems). This risk, however, is likely offset by reducing the number of other advanced technologies that the architecture relies upon. The development of a single technology program has a lower risk and cost than the development of multiple technologies that result in the same closed vehicle design.

The final FOM discussed is the extensibility of the architecture. The introduction of propellant refueling improves this metric by utilizing the EDS for missions beyond the Moon. Section 7.1.4 discussed the payload capability of the EDS, assuming it could be refueling once delivered to LEO. It was shown that this stage could provide large payloads for various missions beyond the Moon without the development of a new NTP system. The extensibility of the architecture is improved because a greater portion of the current lunar architecture can be used for missions in the next phases of the NASA exploration program.

8.2 HYPOTHESES DISCUSSED IN THIS DISSERTATION

The hypotheses outlined in Chapter Two are provided below. These hypotheses have been explored during this dissertation and conclusions for each have been developed. These conclusions are outlined below.

- Propellant refueling can be used to reduce the payload requirements on NASA's baseline launch vehicles.

- Utilizing propellant refueling in LEO can increase the propellant on the EDS, allowing it to perform a wider variety of missions and increase the lunar surface payload capability of the baseline architecture.
- A propellant depot in lunar or Martian orbit can improve the extensibility of NASA's exploration architecture.
- A low cost propellant delivery price is needed to make refueling affordable to NASA's exploration program.

Offloading propellant from the EDS and LSAM has been shown to be an effective means to increase the payload capability of the architecture. It was also established that offloading propellant to reduce the size of the architecture elements only slightly decreased the LCC, while dramatically reducing the extensibility of the exploration architecture.

One of the greatest improvements to the baseline architecture is the ability to utilize the EDS to perform mission maneuvers in addition to the TLI required by the baseline architecture. Utilizing the EDS for the LOI maneuver was shown to greatly increase the lunar surface payload. The EDS can also be used to perform the injection maneuver for other exploration missions, reducing the number of launches required to extend the architecture beyond the Moon.

A propellant depot in Martian orbit can be used to re-fuel the EDS and allow it to provide the Earth return maneuver. This would completely eliminate the need for the development of a Nuclear Thermal Propulsion system. This allows future exploration

mission to rely solely on the current architecture elements, providing an improved extensibility.

The final hypothesis was that low cost propellant delivery was essential to the affordability of propellant refueling. This was a common requirement discussed in much of the literature. It has been shown that even a conservative estimate of the propellant delivery costs can lead to an overall reduction in the LCC of the exploration architecture. This is because, while the introduction of propellant refueling adds additional cost to the architecture (depot development and propellant delivery), it also provides an avenue to lower the cost of other areas of the exploration architecture. The cost of propellant refueling is small compared to the cost of the architecture elements and therefore can help lower the LCC by reducing the number of missions needed to complete the lunar campaign.

8.3 CONTRIBUTIONS

The primary goal of this research was to develop a definitive understating of propellant refueling and how it applied to exploration missions. This goal was established after an extensive investigation of the literature revealed that no comprehensive analysis of propellant refueling existed. The propellant refueling studies found in the literature had three inherent limitations which were addressed in this research. These limitations included a minimal investigation of how propellant refueling can be applied to exploration missions, the use of only a single evaluation criterion, and the lack of a reference baseline architecture from which to make comparable conclusions across multiple studies. These shortcomings have been addressed in this research through the

use of system engineering practices, which allowed a larger design space to be considered, and a number of FOMs to be used to develop overall conclusions about the value of this new capability. The NASA baseline architecture was then used as a non-refueling reference point to access the overall value of propellant refueling. This provided a means of understating how future exploration missions could be improved by implementing this capability, and allowed the determination of the price of propellant needed in order to provide a greater value than the current architecture design.

The contributions of this research were the development of a unified analysis of propellant refueling that went beyond the scope of the previous design work. This resulted in a number of refueling strategies that were shown to improve the design, and thus add value, to the current baseline exploration architecture. This value was achieved by greatly improving the flexibility of the architecture without substantially increasing the mission costs. This improved flexibility was shown to reduce the overall cost of the lunar and Mars campaigns while improving the surface payload capability. As a result of this research, a greater confidence in the application of propellant refueling to future exploration mission has been achieved, and a number of methods have been presented that offer improvements to the design of the current architecture.

APPENDIX A

Lift and Drag Coefficients (APAS)

Table 51: Lift Coefficients, without Solid Rocket Boosters

Mach Number					
alpha (deg)	5	8	10	15	20
-10	-1.2642	-0.8871	-0.7426	-0.6265	-0.5809
-5	-0.5598	-0.3589	-0.2764	-0.2002	-0.1673
0	0	0	0	0	0
5	0.5598	0.3589	0.2764	0.2002	0.1673
10	1.2642	0.8871	0.7426	0.6265	0.5809
15	2.113	1.616	1.4363	1.3049	1.2978
20	3.1013	2.5344	2.3349	2.2539	2.2167

Table 52: Drag Coefficients, without Solid Rocket Boosters

Mach Number					
alpha (deg)	5	8	10	15	20
-10	0.4582	0.6194	1.1054	1.0692	1.0444
-5	0.2784	0.475	0.996	0.9751	0.9568
0	0.2378	0.4599	0.9721	0.9614	0.9457
5	0.2784	0.475	0.996	0.9751	0.9568
10	0.4582	0.6194	1.1054	1.0692	1.0444
15	0.8071	0.9271	1.3628	1.3091	1.1045
20	1.3881	1.4441	1.8316	1.5911	1.491

APPENDIX B

Mass Estimating Relationships

Table 53: Drag Coefficients, with Solid Rocket Boosters

Mach Number								
alpha	0.3	0.6	0.9	1.1	1.5	2	4	5
-10	-1.822	-2.479	-3.819	-4.980	-2.918	-3.626	-1.822	-1.514
-5	-1.497	-2.153	-3.490	-2.534	-1.421	-1.728	-1.497	-0.670
0	0.000	0.000	0.000	0.000	0.000	0.000	0.000	0.000
5	1.497	2.153	3.490	2.534	1.421	1.728	1.497	0.670
10	1.822	2.479	3.819	4.980	2.918	3.626	1.822	1.514
15	2.265	2.914	4.238	7.572	4.418	5.557	2.265	2.534
20	2.788	3.420	4.708	10.092	5.947	7.474	2.788	3.720

Table 54: Drag Coefficients, with Solid Rocket Boosters

Mach Number								
alpha	0.3	0.6	0.9	1.1	1.5	2	4	5
-10	0.711	0.885	1.239	1.497	1.020	1.218	0.614	0.577
-5	0.513	0.629	0.867	0.846	0.618	0.738	0.364	0.361
0	0.377	0.437	0.557	0.650	0.487	0.593	0.299	0.312
5	0.513	0.629	0.867	0.846	0.618	0.738	0.364	0.361
10	0.711	0.885	1.239	1.497	1.020	1.218	0.614	0.577
15	1.013	1.244	1.715	2.658	1.703	2.057	1.092	0.995
20	1.446	1.733	2.317	4.261	2.708	3.275	1.844	1.692

Cargo Launch Vehicle Mass Estimating Relationships

$$\text{Primary Structure} = 1.25(SA_{Stage})^{1.075} * CF$$

$$\text{Secondary Structure} = 2.06 * (2\pi r^2) * CF$$

$$\text{Separation System} = 0.0404 \left(M_{Burnout}^{.7728} \right) * .5 * CF$$

$$\text{TPS} = 317(L/74.6) * CF$$

$$\text{TCS} = 1482 * \frac{M_{inert}}{42645} * CF$$

$$\text{Main Engine} = M_{Engine} * N_{Engines}$$

$$\text{Feed System} = 1.65 \left(\frac{N_{Engines}}{T_{Vac} I_{SP}} \right) * CF$$

$$\text{Thrust Structure} = 0.001908(T_{Vac} N_{Engines})^{1.0657} * CF$$

$$\text{Power} = 793 + 506 \left(\frac{M_{AP}}{1600000} \right) + 0.0000974(T_{vac} N_{Engines}) + 0.405T_{vac} + P_{Cryo-cooler}$$

$$\text{Avionics} = 430 \frac{M_{inert}}{42645}$$

IC124b				S
	<u>Level 2</u>	<u>Level 1</u>	Correction Value	
Structure		121,464		1.
Primary Structure	51,206		0.73	
Ox Tanks	17,236			
Fuel Tanks	39,056			
Secondary Structures	3,815		0.05	
Seperation Systems	4,104		1.29	
TPS	574		1.00	
TCS	5,475		1.00	
Main Propulsion System		60,004		1.00 3
Main	34,500			
Feed System	5,453		1.05	
Thrust Structure	20,052		1.60	
Power		1,265	0.63	4
Avionics and Controls		681		1 6
Growth Margin		14,639		7
Dry Weight		198,053	1.6%	8
Residuals and Reserves		197,124		9
Second Stage		661,805		11
Burnout Weight		880,083		
Main Propellants		2,247,203		12
Fuel	319,659			
Oxidizer	1,927,544			
Strap-on Boosters		3,312,278		2
Payload Fairing		10,552		
Gross Weight		6,450,115		
Startup Losses		6,425,182		
		2,247		
Mazimum Weight		6,452,363	0.91	
Mass Ratio				
Primary Propellant Mass	2,247,203	1.33		
	2,229,286			
T/W	14815			

Figure 99: Example Mass Breakdown of CaLV 1st Stage

Second Stage		<i>Level 2</i>	<i>Level 1</i>	Correction Value
1.0	Structure		25,960	
3	1.1	Primary Structure	7,481	0.608
		O ₂ Tanks	4,820	
		Fuel Tanks	9,047	
1.6	Sec. Structure/Fairing	2,454		1.03
1.7	Seperation Systems	203		0.98
1.8	TPS	316		0.99
1.9	TCS	1,639		1.00
3.0	Propulsion		12,668	1.412
3.1	Main Engines	6,785		
3.2	Feed System	3,032		
	Thrust Structure	2,852		
4.0	Power		2,898	1.66
	Mitigation		2,300	
6.0	Avionics and Controls		476	1.00
7.0	Growth Margin		2,729	
8.0	Dry Weight		47,032	6.4%
9.0	Residuals and Reserves		6,673	
11.0	Payload		101,441	0
	Burnout Weight		155,146	
12.0	Ascent Propellants		268,298	
	Fuel	41,277		
	Oxidizer	227,021		
2	12.5	TLI Propellants		235,794
		Fuel	36,276	
		Oxidizer	199,518	
	Gross Weight		659,238	653343
	Startup Losses		2,567	1283.32969
	Mazimum Weight		661,805	
	Max Propellant	513,332	268,298	
	MECOI propellent	513,332		
	T/W	0.888		

Figure 100: Example Mass Breakdown of CaLV 2nd Stage

Lunar Surface Access Module Estimating Relationships

$$\text{Primary Structure} = 0.07 M_{inert} \frac{L_{mak}}{3.77}$$

$$\text{Secondary Structure} = 0.05 M_{inert}$$

$$\text{Thrust Structure} = 0.000828 (T_{vac} N_{engines})$$

$$\text{Landing Structure} = 0.0576 M_{landed}^{0.9}$$

$$\text{Feed System} = 1.616 \frac{M_{initial}}{I_{SP} T/W}$$

$$\text{Power} = 468 \frac{M_{inert}}{5962}$$

$$\text{Avionics} = 161 \frac{M_{inert}}{5962}$$

Mass breakdown:			
Descent Stage			
ID	Level I	Level II	Value
1.0	Body group		3,201 kg
		Primary structure	479 kg
		Secondary structure	289 kg
		Thrust structure	368 kg
		Landing structure	434 kg
		Oxidizer tanks	625 kg
		fuel tanks	977 kg
		He tanks	29 kg
		Mitigation	0 kg
2.0	Main propulsion		1,103 kg
		Main engines	530 kg
		Pressurization/feed	573 kg
3.0	RCS propulsion		0 kg
		RCS engines	0 kg
		Pressurization/feed	0 kg
4.0	Primary power & distribution		468 kg
5.0			
6.0	Avionics		161 kg
7.0	Margin		839 kg
	Dry Mass		5,772 kg
8.0	Payload to LS		2,268 kg
	Non-cargo		1,033 kg
9.0	Ascent Stage (minus payload to LLO)		9,994 kg
	Cargo		
	Residual/reserves		1,271 kg
		Oxidizer	1,089 kg
		Fuel	182 kg
	Landed Mass		20,338 kg
10.0	RCS propellant		0 kg
		Oxidizer	0 kg
		Fuel	0 kg
11.0	Descent propellant		25,418 kg
		LOI	14,736 kg
		Descent	10,682 kg
		Oxidizer	21,787 kg
		Fuel	3,631 kg
		Boiloff	0 kg
	Outbound Mass		45,529 kg
12.0	Startup Losses		228 kg
	Gross Mass	For Max Crew	45,757 kg

Figure 101: Example Mass Breakdown of LSAM Descent Stage

Ascent Stage			
ID	Level I	Level II	Value
	Body group		1,285 kg
		Primary Structure	978 kg
		Thrust structure	56 kg
		Oxidizer tanks	121 kg
		fuel tanks	119 kg
		He tanks	12 kg
		Mitigation	0 kg
2.0	Main propulsion		257 kg
		Main engines	147 kg
		Pressurization/feed	110 kg
3.0	RCS propulsion		229 kg
		RCS engines	38 kg
		Pressurization/feed	191 kg
4.0	Primary power & distribution		579 kg
6.0	Avionics		385 kg
7.0	Crew Compartment	0.90	1,552 kg
8.0	Margin		729 kg
3	Dry Mass		5,016 kg
9.0	Crew		564 kg
10.0	Payload to LLO		100 kg
11.0	Residual/reserves		205 kg
		Oxidizer	154 kg
		Fuel	51 kg
	MECO Mass		5,884 kg
12.0	RCS Propellant		114 kg
		Oxidizer	89 kg
		Fuel	25 kg
13.0	Ascent propellant		4,097 kg
		Oxidizer	3,072 kg
		Fuel	1,024 kg
		Boiloff	0 kg
3	14.0	Startup Losses	47 kg
7		Ascent (Takeoff) Mass	10,094 kg
		For Max Crew	

Figure 102: Example Mass Breakdown of LSAM Ascent Stage

APPENDIX C

Apollo Reference Reliability Values

Table 55: Lunar Architecture Reliability Estimation

Event	Reliability
Phase 1 - Delivery	0.9861
CaLV	0.9884
CLV	0.9977
Phase 2 - LEO	0.915697
LEO Circulization	0.9863
Orbital Coasting	0.987
Orient for Docking	0.9925
Rendezvous	0.9749
Docking	0.9795
Orient for Injection	0.9925
Phase 3 - Re-Fueling	0.9676
Orient for Docking	0.9925
Rendezvous Maneuver	0.9749
Docking	0.9795
Fuel Transfer and Separation	0.9835
Phase 4 - Transfer	0.7617
LEO to LLO Transfer	0.7617
Phase 5 - LLO	0.9820
Navigate in LLO	0.9990
Separation	0.9907
Orient for Descent	0.9922
Separation	0.9907
Phase 6 - Lunar Mission	0.9551
Lander	0.95515

REFERENCES

-
- 1 O’Keefe, S., “Pioneering the Future.” Administrator Sean O’Keefe at Syracuse University, April 2002.
 - 2 Aldridge, E., “A Journey to Inspire, Innovate, and Discover,” President’s Commission on Implementation of the United States Exploration Policy, June 2004.
 - 3 “Manned Lunar Landing Mode Comparison,” NASA-TM-X-66763, October 1962
 - 4 Rao, P.V., “Exploring the Unknown: 50 Years of NASA History,” 50 years of Space A Global Perspective, University Press, India, 2007, pp. 45-92.
 - 5 Smith, M., “NASA’s Space Shuttle Program: The Columbia Tragedy, the Discovery Mission, and the Future of the Shuttle,” CRS Report for Congress, RS21408, Jan. 2006, pp CRS-5.
 - 6 Stanley, D., et. al. Exploration Systems Architecture Study Final Report, Summer 2006. NASA/TM-2005-214062
 - 7 Bandte, O., “A Probabilistic Multi-Criteria Decision Making Technique for Conceptual and Preliminary Aerospace Design,” Georgia Institute of Technology, Sept. 2006, pp 26-34.
 - 8 Mavris, D., Kirby, M., Qiu, S., “technology Impact Forecasting for High Speed Civil Transport,” SAE/AIAA-98-5547.
 - 9 Malone, B., Papay, M., “ModelCenter: An Integration Environment for Simulation Based Design,” Simulation Interoperability Workshop, Orlando, FL, Mar., 1999.
 - 10 Smith, R.K., *Seventy-Five Years of Inflight Refueling: Highlights, 1923-1998*, Air Force History and Museums Program, Washington, D.C., 1998.
 - 11 Cady, E.C., “Cryogenic Propellant Management Architectures to support the Space Exploration Initiative,” AIAA Space Programs and Technologies Conference, Huntsville, Alabama, 1990.
 - 12 Koelle, H., “Birth, Life, and Death of the Saturn Launch Vehciles,” D-10587, May 2001.
 - 13 “Manned Lunar Landing Mode Comparison,” NASA-TM-X-66763, October 1962

-
- 14 “The Rendezvous That Was Almost Missed: Lunar orbit Rendezvous and the Apollo Program,” December, 1992, NASA Facts Online NF175, 2008. < <http://oea.larc.nasa.gov/PAIS/Rendezvous.html>>
 - 15 Reeves, D., Scher, M., Wilhite, A., Stanley, D., “The Apollo Lunar Orbit Rendezvous Architecture Decision Revisited,” 41st AIAA/ASME/SAE/ASEE Joint Propulsion Conference and Exhibit, Tucson, AZ, July, 2005.
 - 16 Koelle, D.E., “Lunar Space Transportation Systems Options,” 47th International Astronautical Congress, Beijing, China, 1996.
 - 17 Folta, D.C., Vaughn, F.J., westmayer, P.A., Rawistscher, G.S., Bordi, F., “Enabling Exploration Missions Now: Application of On-Orbit Staging,” 2005 AAS/AIAA Astrodynamics Specialist Conference, Lake Tahoe, California., 2005.
 - 18 Chandler, F., Bienhoff, D., Cronick, J., Grayson, G., “Propellant Depots for Earth Orbit and Lunar Exploration,” AIAA-2007-6081, September 2007.
 - 19 Teets, E. H., Ehernberger, J., Bogue, R., Ashburn, C., “In-space Cryogenic Propellant Depot Potential Commercial and Exploration Applications,” NTRS-2007-0003598
 - 20 Troutman, P., “Orbital Aggregation & Space Infrastructure Systems (OASIS),” LaRC Spacecraft a& Sensors Brach, October 2001.
 - 21 Chato, D.J., “Low Gravity Issue of Deep Space Refueling,” 43rd AIAA Aerospace Sciences Meeting and Exhibit, Reno, Nevada, 2005.
 - 22 Griffin, J.W., “Background and Programmatic Approach for the Development of Orbital Fluid Resupply,” AIAA/ASME/SAE/ASEE 22nd Joint Propulsion Conference, Huntsville, Alabama, 1986.
 - 23 Chato, D.J., “Technologies for Refueling Spacecraft On-Orbit,” AIAA Space 200 Conference and Exposition, Long Beach, California, 2000.
 - 24 Boretz, J.E., “Orbital Refueling Techniques,” AIAA 5th Propulsion Joint Specialist Conference, U.S. Air Force Academy, Colorado, 1969.
 - 25 Hastings, L.J., “Marshall Space Flight Center In-Space Cryogenic Fluid Management Program Overview,” 41st AIAA/ASME/SAE/ASEE Joint Propulsion Conference and Exhibit, Tucson, Arizona, 2005.
 - 26 SCHUSTER, J. R., BROWN, N., “ Long Term Orbital Storage of Cryogenic Propellants for Advanced Space Transportation Missions,” AIAA-1987-1498,
 - 27 Plachta, D., “Results of an Advanced Development Zero Boiloff Cryogenic Propellant Storage Test,” NASA/TM-2004-213390, 2004.

-
- 28 Launius, R., Jenkins, D., “Delta The Ultimate Thor,” *To Reach The High Frontier*, The University of Kentucky, pp. 103 – 146.
- 29 Space and Tech, < <http://www.spaceandtech.com/spacedata/index.shtml>.>
- 30 McCartney, F., “National Security Space Launch Report,” RAND Corporation, MG-503, Santa Monica, CA, 2006.
- 31 Wikipedia, “Atlas V,” <http://en.wikipedia.org/wiki/List_of_Atlas_V_launches>
- 32 Musk, E., “Next Falcon I Launch,” Space Exploration Technologies, December 2007, < http://www.spacex.com/updates_archive.php?page=121007>
- 33 Shotwell, G., “The Falcon Launch Vehicle,” IAA.4.11.5.03, Sept. 2004.
- 34 “Falcon Launch Vehicle Lunar Capability Guide,” Space Exploration Technologies, 2008-005a, Rev 2, 2008.
- 35 Woodcock, G., “Re-usable Launch Revisited: Low Cost Potentials,” AIAA-2008-7727, AIAA Space 2008 Conference & Exposition, Sept. 2008, San Diego, CA.
- 36 Dieter, G., “Engineering Design,” 3rd ed, McGraw-Hill Companies, New York, NY. 2000.
- 37 Panzarella, C., Kassemi, M., “Simulations of Zero Boiloff in a Cryogenic Storage System,” AIAA-2003-1159, Jan. 2003, Reno, NV.
- 38 Mosher, D., “Methane Rocket Engine Successfully Tested,” Space.Com, 7 May 2007. <http://www.space.com/business/technology/070507_methane_rocket.html>
- 39 Humble, R., Henry, G., Larson, W., “*Space Propulsion Analysis and Design*,” McGraw-Hill Companies, New York, NY. 1995.
- 40 Cates, G., Cirillo, W., Strongren, C., “Low Earth Orbit Rendezvous for Lunar Missions,” Proceedings of the Winter Simulation Conference 2006, IEEE, Monterey, CA, 2006, pp.1248-1252.
- 41 Malone, B., Papay, M., “ModelCenter: An Integration Environment for Simulation Based Design,” Simulation Interoperability Workshop, Orlando, FL, Mar., 1999.
- 42 Young, D., Olds, J., Hutchinson, V., Krevor, Z., Pimentel, J., Reeves., J., Sakai, T., Young, J., “Centurion: A Heavy-Lift Launch Vehicle Family for Cos-lunar Exploration,” AIAA-2004-3735, July 2004, Fort Lauderdale, FL.
- 43 Sova, G., and P. Divan, “Aerodynamic Preliminary Analysis System II, Part II – User’s Manual,” NASA CR 182077, April 1991.

-
- 44 Brauer, G. L., Cornick D. E., Olson, D., Peterson, F., and Stevenson, R., "Program to Optimize Simulated Trajectories (POST) Formulation Manual," NAS1- 18147, September 1990.
- 45 Rohrschneider, R., "Development of a Mass Estimating Relationship Database for Launch Vehicle Conceptual Design," AE8900 Special Project, School of Aerospace Engineering, Georgia Institute of Technology, April 26, 2002.
- 46 Space and Tech Rocket Engine Database, February 2008,
<http://www.spaceandtech.com/spacedata/engines/r110_specs.shtml>
- 47 Humble, R., Henry, G. , and Larson, W., "*Space Propulsion Analysis and Design*," McGraw-Hill Companies New York, NY. 1995.
- 48 Scher, M., "An Investigation into the Advantages of In-Space Propellant Re-supply," AIAA-2006-4434, July 2006, Sacramento, CA.
- 49 Street, D., Wiltite, A., "A Scalable Orbital Propellant Depot Design," Masters Project, Department of Aerospace Engineering, Georgia Institute of Technology, Atlanta, GA, 2006.
- 50 Chandler, F., Bienhoff, D., Cronick, J., Grayson, G., "Propellant Depots for Earth Orbit and Lunar Exploration," AIAA-2007-6081, September 2007, Long Beach, CA.
- 51 Wertz, J., Larson, W., *Reducing Space Mission Cost*, Microcosm Press, El Sugundo, CA, 1996.
- 52 "NASA System Engineering Handbook" National Aeronautics and Space Administration, SP- 6105, June 1995.
- 53 2008 NASA Cost Estimating Handbook, National Aeronautics and Space Administration, 2008.
- 54 Dieter, G., "Cost Evaluation," *Engineering Design*, 3rd ed., McGraw-Hill, 2000, pp. 697 – 700.
- 55 "Manned Lunar Landing Mode Comparison," NASA-TM-X-66763, October 1962.
- 56 Fragol, J., Maggio, G., "Probabilistic Risk Assessment of the Space Shuttle," Space Applications International Corporation, SAICNY95-02-25, February, 1995.
- 57 Young, D., "An Innovative Methodology for Allocating Reliability and Cost in A Lunar Architecture," Dissertation, Georgia Institute of Technology, May, 2007.

-
- 58 Roth, B., Graham, M., Mavris, D., "Adaptive Selection of Aircraft Engine Technologies in the Presence of Risk," American Society of Mechanical Engineers, Jan. 2004, Vol. 126, pp. 40-44.
- 59 Young, J., Thompson, R., Wilhite, A., "Architecture Options for Propellant Resupply of Lunar Exploration Elements," AIAA-2006-7237, Sept. 2006, San Jose, CA.
- 60 Young, D., "An Innovative Methodology for Allocating Reliability and Cost in A Lunar Architecture," Dissertation, Georgia Institute of Technology, May, 2007.
- 61 Anderson, J., Narus, J., Rossum, W., "Customer Value Propositions in Business Markets," Harvard Business Review, March 2006.
- 62 Anderson, J., Narus, J., Rossum, W., "Customer Value Propositions in Business Markets," Harvard Business Review, March 2006.
- 63 Dorris, C., "Altair Project," 3rd Space Exploration Conference, February 2008, Denver, CO.
- 64 Culbert, C., "Lunar Surface Systems," 3rd Space Exploration Conference, February 2008, Denver, CO.
- 65 "Manned Lunar Landing Mode Comparison," NASA-TM-X-66763, October 1962.
- 66 Wilhite, A., Reeves, D., Stanley, D., Wagner, J., "Evaluating the Impacts of Mass Uncertainty on Future Exploration Architectures," AIAA-2006-7250, AIAA Space 2006 Conference, San Jose, California, 2006.
- 67 Recommended Practice for Mass Properties Control for Satellites, Missiles and Launch Vehicles, ANSI/AIAA, R-020A-1999, August 2000.
- 68 Hoffman, S., Kaplan, D., "Human Mars Exploration: The Reference Mission of the NASA Mars Exploration," NASA Special Publications 6107, July, 1997.
- 69 Howe, S., "Assessment of the Advantages and Feasibility of a Nuclear Rocket for Manned Mars Missions," N87-17794, May 1986.
- 70 Koelle, D., "Handbook of Cost Engineering," TransCostSystems, TCS-TR-168(2000), Germany, November 2000.
- 71 Brothers, B., "Human Mars Mission Weights and Mass properties," Alpha Technology, Inc., H-28653D, Huntsville, AL, September, 1999.
- 72 "Lack of Disciplined Cost-Estimating Processes Hinders Effective Program Management," GAO-04-642, May 2004.

VITA

James Young was born on October 2nd, 1980 to Larry and Kelly Young. He has two younger sisters, Krista and Tiana. He graduated from Highland High School in 1999 as one of the top ten in his class. James attended Arizona State University in Tempe, AZ where he earned a B.S. in Aerospace engineering and graduated at the top of his class. He began his graduate studies at the Georgia Institute of Technology in the Space Systems

Design Lab, where he received a M.S. in Aerospace Engineering in 2005 under the guidance of Dr. John R. Olds. After receiving his masters degree James continued his graduate studies at Georgia Tech under the direction of Dr. Alan White. At the completion of his Ph.D research in 2008, James moved to Houston, TX where he began work with the ARES Corporation. James's fiancée Michelle Kassner also graduated with her Pd.D in 2008 and began working for Chevron.